ADVISORY BOARD

VOLUME FORTY SIX

ADVANCES IN PHYSICAL ORGANIC CHEMISTRY

Edited by

IAN H. WILLIAMS

Department of Chemistry,
University of Bath,
Bath, United Kingdom

NICHOLAS H. WILLIAMS

Department of Chemistry,
University of Sheffield,
Sheffield, United Kingdom

ELSEVIER

Amsterdam • Boston • Heidelberg • London
New York • Oxford • Paris • San Diego
San Francisco • Singapore • Sydney • Tokyo

Academic Press is an imprint of Elsevier

Academic Press is an imprint of Elsevier
The Boulevard, Langford Lane, Kidlington, Oxford, OX51GB, UK
32, Jamestown Road, London NW1 7BY, UK
Radarweg 29, PO Box 211, 1000 AE Amsterdam, The Netherlands
225 Wyman Street, Waltham, MA 02451, USA
525 B Street, Suite 1900, San Diego, CA 92101-4495, USA

First edition 2012

ISBN: 978-0-12-398484-5
ISSN: 0065-3160

Printed and bound in UK
10 11 12 13 10 9 8 7 6 5 4 3 2 1

CONTRIBUTORS

Robin A. Cox
Formerly of the Department of Chemistry, University of Toronto, ON M1R 3Z8, Canada

Matthew P. Meyer
Department of Chemistry and Chemical Biology, University of California, Merced, CA 95343, USA

Michael Novak
Department of Chemistry and Biochemistry, Miami University, Oxford, OH 45056, USA

Yang Zhang
Department of Chemistry and Biochemistry, Miami University, Oxford, OH 45056, USA

PREFACE

This volume of Advances in Physical Organic Chemistry marks a transition as we take over as editors from John Richard. We would like to acknowledge the excellent job that John has done in editing this series for the last decade, producing a series that has been a testament to the diversity of the disciplines that make up the subject that we know of as physical organic chemistry. We shall endeavour to carry on with the same appreciation of the breadth of chemistry in this series, bringing to readers authoritative reviews on the advances in fundamental and applied work leading to the quantitative, molecular level understanding of their properties that is the hallmark of physical organic chemistry. These areas shall no doubt continue to expand, and we aim to provide a valuable source of information for those physical organic chemists who are applying their expertise to both traditional and new problems, and to those chemists across these diverse areas who identify a physical organic component in their approach to their sphere of research.

Although traditionally considered as the study of mechanism, reactivity, structure and binding in organic systems, physical organic chemistry nowadays has expanded to encompass a wider range of contexts than ever before. Physical organic chemistry is being fruitfully applied to supramolecular interactions, aggregation and reactivity; computation of transition states and mechanisms; molecular recognition, reactions and catalysis in biology; materials where molecular structure controls function; structure activity correlations; mechanisms in synthesis and catalysis and interactions and reactivity in organised assemblies and interfaces among others. This issue illustrates both the application of rigorous, detailed analysis of organic reactivity to understanding anti-tumour drugs, the description of fundamental physical phenomena and techniques to understanding organic reactions, and the application of rigorous thinking to probe and question the thinking underpinning some of the most familiar reactions.

In an earlier contribution to volume 36, Novak and Rajagopal comprehensively reviewed the chemistry of nitrenium ions. In this volume, the role of these reactive species as the source of unwanted side effects due to unanticipated metabolism of some drugs is described by Michael Novak and Yang Zhang. This same series of reactions are also thought to explain the

beneficial effects of two classes of emerging anti-tumour drugs, illustrating the delicate balance of metabolic pathways and fundamental selectivity and reactivity in organic chemistry.

Robin Cox provides a challenge to reconsider some of the apparently most familiar and well-recognised mechanisms in organic chemistry. By combining the principle, first formulated by Jencks, that a finite lifetime is a pre-requisite for a putative intermediate to actually exist as such in reaction mechanism, and that the proton in many media does not fulfil this requirement as a localised species, he makes us reconsider the conventional mechanisms of many standard organic reactions. The method of excess acidities, which he has previously described in volume 35, is used to good effect to make a strong case for a much broader view of a proton exchange with solvent and concerted processes. This combination of logical reasoning and accurate quantitative experimental data demonstrates the value that physical organic chemistry brings in providing a practical working model for understanding reactions – but not to be complacent about even familiar explanations.

Isotopic substitution has long been one of the most subtle and unintrusive ways in which mechanism and reactivity can be probed by the organic chemist, and Matt Meyer's chapter provides an excellent review of the recent progress in their measurement, application and interpretation in organic chemistry. New methods and contemporary interpretations and understanding are thoroughly explored, followed by descriptions of the insights they bring to a range of systems. This contribution shows how greater accessibility of accurate methodology and more detailed understanding of the theoretical interpretation of the data are combined to create an even more prominent role for this technique.

Ian H. Williams
Nicholas H. Williams

CHAPTER ONE

Revised Mechanisms for Simple Organic Reactions

Robin A. Cox
Formerly of the Department of Chemistry, University of Toronto
Current address: 16 Guild Hall Drive, Scarborough, ON M1R 3Z8, Canada
E-mail: robin.a.cox@sympatico.ca

Contents

Abstract

The Jencks principle, that postulated mechanistic intermediates have to have a finite lifetime in the reaction medium, has in general not been applied to the mechanisms of organic reactions. In particular, oxygen-protonated species in which the positive charge cannot be delocalized, such as H3O+, R2HO+ and tetrahedral intermediates, and even some of those where it can, such as acylium ions and protonated esters, do not exist in aqueous media that are more dilute than concentrated acid. Nor do primary and secondary carbocations. This has considerable consequences; many accepted organic reaction mechanisms have to be modified. Examples of this are provided, particularly for reactions that take place in acidic solutions. For instance, ether hydrolysis is a general-acid-catalyzed process in which an oxygen-protonated species is not formed,

Advances in Physical Organic Chemistry, Volume 46
ISSN 0065-3160,
http://dx.doi.org/10.1016/B978-0-12-398484-5.00001-8

and nor is a carbocation unless it is stable in the medium. Amide hydrolysis involves a second proton transfer in stronger acid media. Ester hydrolysis involves tetrahedral intermediates which are neutral, not charged, whether the medium is acidic, neutral or basic. Many other reactions are discussed.

1. INTRODUCTION

I am planning a general physical organic chemistry textbook for senior undergraduates and graduate students, dealing with the mechanisms of organic reactions and how these are determined. This should be of moderate length and affordable. I taught this subject for over 30 years in various places, and during all of that time there was no one text that could be used for the entire course; most were too long and too detailed for a one-semester course, and several concentrated, naturally enough, on the author's interests. Currently, many of the available texts are also out of date.

So there is a need, and general concepts to be used as major chapter headings were needed. One of these, first formulated by Jencks[1–4] and consequently referred to as the Jencks principle, states that in order for a species to be a reaction intermediate, it has to have a finite lifetime *in the reaction medium*.[1–4] It has to exist there for more than one molecular vibration and have, say, a lifetime of greater than 10^{-13} s.[5,6] One would have thought that this was obvious, but, amazingly enough, it is seldom if ever taken into consideration in mechanistic studies.

A great deal of valuable work has been performed in recent years concerning the structures, stabilities and reactivities of putative reaction intermediates. For instance, see the excellent review of carbocations by More O'Ferrall in a previous volume in this series.[7] In order to make these species stable enough to observe, to obtain their nuclear magnetic resonance (NMR) and ultraviolet (UV) spectra and so on, the study conditions can hardly the same as those in which they are suspected reaction intermediates. It is hard to visualize a species stable in a frozen argon matrix at 4 K as a stable species in water. Carbocations are often studied in non-aqueous superacid media which do not contain anything nucleophilic;[7] in media such as these their lifetimes are going to be much longer than they would be in water. This work has led, perhaps not surprisingly, to a number of reaction mechanisms being proposed involving intermediates that have not actually been observed under the reaction conditions. Many of these mechanisms are perfectly reasonable, and the proposed intermediates may indeed be involved, but in some cases they are not, as we will see.

It is quite difficult to measure the lifetimes of carbocations and similar species in water, or in the media in which they are suspected to be reaction intermediates, and these measurements often have to be indirect.[7–10] Consequently not very many are accurately known. What information there is does suggest that the lifetimes are very short. For instance, even resonance-stabilized species such as benzyl, phenethyl and cumyl cations only have lifetimes in the nanosecond range in trifluoroethanol and related solvents, as measured by laser flash photolysis.[11] These are quite short, but still long enough to make them perfectly viable reaction intermediates, in S_N1 reactions, for instance. Cations which are not resonance stabilized, however, will have much shorter lifetimes.[9]

In general primary *and secondary* carbocations cannot be reaction intermediates under aqueous conditions (any medium containing 10% water or more);[12] this has been shown experimentally,[13] and a recent re-examination of the original pre-war experimental evidence in favor of S_N1 reactions of secondary substrates[14] has shown it to be spurious.[15] However, as the reaction conditions become more acidic, cations become more stable, due to the decreasing amounts of nucleophilic species available to react with them, and their presence or absence as intermediates can often be inferred from the reaction kinetics. Examples of this will be presented. Similarly, one would expect anions to be stabilized in increasingly basic media, as the concentrations of electrophilic species decrease.

One direct technique that can be utilized has only very recently become available, with the development of the current generation of sensitive high-speed infrared spectrophotometers; if a species is going to exist for more than one molecular vibration it is going to be capable of providing an infrared (IR) or Raman spectrum. The major use of this technique to date has been to study the structure of the proton in aqueous acid media.[16,17] This has been the subject of considerable controversy for several decades now, and remains so today, with the experimentalists and the theoreticians being unable to agree. Proposed have been H_3O^+, usually called the Eigen cation,[18] $H_5O_2^+$, referred to as the Zundel cation,[19] $H_9O_4^+$, first proposed by Bell[20] although often also referred to (mistakenly) as the Eigen cation, and many others.[21] Only very recently has there been any believable experimental evidence for any of them, the proposed $H_{13}O_6^+$,[22] with an IR spectrum obtained using modern instrumentation.[16,17] However, at least one theoretician is against this,[23] with his calculations favoring a modified Zundel structure. The important point for the work under discussion here is that *none* of these structures has a lifetime sufficiently long for it to be a reaction intermediate. The proponents of

$H_{13}O_6^+$ state,[24] "The lifetime of the five central protons is close to the time of their vibrational transitions. In ~70% of these cations it is shorter than the time of normal vibrations and the IR spectrum degenerates to a continuum absorption." Also, modern theoretical calculations on aqueous proton clusters containing several water molecules cannot isolate the positive charge; it is simply "on the cluster" as a whole.[23,25] Thus, as far as the mechanisms of organic reactions is concerned, the actual structure of the solvated proton is unimportant; protons are simply "there when needed". As people have begun to assert in the educational literature, "The solvated proton is *not* H_3O^+!"[26,27] Only when there is insufficient water to solvate all of the protons will H_3O^+ be the only protonated water species present.

Less work has been done on hydroxide species in water, but nevertheless it is becoming apparent that individual HO^- species do not have long enough lifetimes to be viable reaction intermediates either. One recent study has utilized modern ultrafast IR spectroscopy, finding that spectral features in concentrated hydroxide solutions decay on a femtosecond timescale.[28] Hydroxide ion in water is not particularly reactive. Reactions in alcohol solvents, where the hydroxide ion is less solvated, are much faster, and when desolvated in pure dimethylsulfoxide (DMSO) its reactivity is increased by some 12 orders of magnitude.[29]

The reason that these species are so short-lived was first guessed at over 200 years ago by Grotthuss.[30] Water is a highly structured medium,[31] with hydrogen bonds maintaining the structure, and proton transfers along these bonds are going to be very easy. The Grotthuss process[30] cannot be the whole story, though. Liquid water has short-range but not long-range order; if it did one would have ice. Eigen's review[18] gives typical proton transfer rate constants of around 10^{10} M^{-1} s^{-1} (in his Table 4), but he also gives rate constants of 10^{13} M^{-1} s^{-1} for transfer of protons along a hydrogen bond, quite compatible with the recent IR data.[16,17] This value refers to proton transfers in the ordered regions, within which individual protonated water species cannot be said to really exist, but for a proton to move more than a few micrometers requires solvent reorganization at the boundary between ordered regions, leading to the 10^{10} M^{-1} s^{-1} value.

Two factors have not been taken into consideration. Firstly, the presence of the counterion, which must be present for electrical neutrality, means that in practice a proton will not stray too far away from it, and secondly, the medium itself has a nonzero viscosity, which should slow everything down. This is a factor that is not often taken into consideration in mechanistic studies; indeed, there does not seem to be any generally agreed method for

dealing with it. Perhaps the simplest way of thinking about the situation is that, for slow organic reactions, protons or hydroxide ions or water molecules are simply available as needed, and that transfers involving these species take very little activation energy.

Thinking about it, on electronegativity considerations alone undelocalized structures with a whole positive charge on oxygen are rather unlikely to exist in water. Although $^{+}NR_4$ species are common there, $^{+}OR_3$ ones are not, and $^{+}FR_2$ is unknown. ^{-}OH is rather more likely, but even so delocalization of the charge into the medium is going to be highly favorable energetically.

All of this has considerable consequences for the mechanisms of reactions in water, or in aqueous acidic or basic media. For instance, one should perhaps no longer speak of "general" vs. "specific" acid or base catalysis; better to speak of "pre-equilibrium proton transfer" in the case of reactions that involve the formation of a stable protonated or deprotonated intermediate, and "proton transfer as part of the rate-determining step" in the other cases.[32] Every acidic or basic species will contribute to the catalysis, and the strongest will usually contribute the most in cases where they can be differentiated, as we will see. It is recommended that the strongest acid and base species in water be referred to as H^{+}_{aq} or HO^{-}_{aq}, as is done here throughout. Since my research has centered on reactions in acidic media, I will concentrate on them, but certainly much of what I am going to say is going to apply to basic media as well. In all of the reaction schemes that follow, the terminology "aq" will be used to indicate that the aqueous reaction medium is acting as a source or a sink for protons (or hydroxide ions) and water molecules, and "aq" does not appear in the reaction kinetics. Specific H_2O and H^{+}_{aq} (or HO^{-}_{aq}) species indicated in the reaction schemes have the roles indicated, and do indeed appear in the kinetics.

2. ACID SYSTEMS

Most of the work on organic reaction mechanisms in acidic media, much of it involving measuring the rates of reactions as a function of changing acid concentration and reaction temperature, finding out what the reaction products are, and using deuterated media to obtain solvent isotope effects and for exchange studies, has been carried out in aqueous sulfuric acid, aqueous perchloric acid and aqueous hydrochloric acid, with a little work in other aqueous acid media. Each of these systems has its advantages and its drawbacks.

Sulfuric acid is cheap and readily available, and is the only common acid that is usable over the entire acid concentration range, from pure water to 100 wt% acid (and at higher acidities by adding SO_3 to the 100% acid, but this does not concern us here).[33] Consequently it has seen the most use. It is a fairly complex medium, however;[34] the first dissociation into a solvated proton and bisulfate ion is complete as long as there is more water than acid present (the 1:1 acid:water mole ratio point occurs at 84.48 wt% acid), and at low concentrations the bisulfate ion is partially and variably dissociated into sulfate and another solvated proton.[34] Since many organic reactions actually involve two water molecules,[35] another important concentration occurs at the 1:2 acid:water point, 73.13 wt%. At this point an acid species that can be written as $H_2SO_4 \cdot 2H_2O$, or as $HSO_4^- \cdot H_3O^+ \cdot H_2O$, is present at high concentration in the medium[34] and has a long enough lifetime to have a Raman spectrum,[36] but it does not appear to be catalytically active as such. Its presence does, however, ensure easy proton transfer throughout the medium by the Grotthuss mechanism, as indicated below.

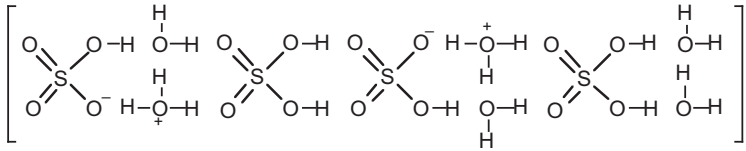

(To avoid overcrowding the structure, dotted hydrogen bonds and electron-flow arrows are not shown, but the easy transfer of protons in such a highly structured medium should still be readily apparent.) Above 84.48 wt% acid there are undissociated sulfuric acid molecules present (but no sulfate, of course),[34] and above about 98 wt% acid the protonated sulfuric acid molecule, $H_3SO_4^+$, from the autoprotolysis of H_2SO_4,[37] is present as well; both of these species can be catalytically active if proton transfer is involved in the rate-determining step of the reaction, as we will see. This is the only common acid system with acid species other than H_{aq}^+ available for catalysis. It has the potential for nucleophilic attack on intermediate species by sulfate and by bisulfate ions, as well as by water, but sulfate attack does not seem to have been reliably observed, and while bisulfate ion can act as a nucleophile[38] it seems to be some 100 times weaker than water.[39]

Aqueous perchloric acid is a much simpler system than is sulfuric acid, and it has also seen extensive use. Only water is available to act as a nucleophile, perchlorate ion being non-nucleophilic. However, it cannot be used over the entire range of acidity. The strongest solution available

commercially is 70 wt%, and by adding the available low-melting solid $H_3O^+ \cdot ClO_4^-$ to this one can reach about 78 wt%, but at higher acidities than this the solution is solid at 25 °C, and it and stronger solutions are too dangerous to use in any case, as strong perchloric acid oxidizes organic compounds explosively. The only acid species present in the usable range is H^+_{aq}; the 1:2 acid:water point occurs at 73.60 wt%, so there is no chance of seeing catalysis by undissociated $HClO_4$ molecules.

Aqueous hydrochloric acid can only be used up to a concentration of about 38 wt%, as the solubility of HCl gas in water is exceeded beyond this point. The 1:2 acid:water concentration would be at 50.30 wt%, were it obtainable. However, there is chloride ion present in solution to act as a nucleophile in addition to water, and reaction with chloride is occasionally observed or can be inferred.[40]

Other aqueous acid systems are used for reactions, but much more rarely. Aqueous HBr is used to cleave ethers all the time in synthesis, but, amazingly, there are no studies of the kinetics of this reaction in the literature.[41] Aqueous nitric acid is not normally used; it is considerably weaker than the other acid systems[42] and it is an oxidizing agent. It can be used for nitrations, and a few studies of these have been reported, but this reaction is more commonly performed in acid mixtures with sulfuric [43] and other acids.[44,45] Aqueous HF is not often used as the dilute solution is very weak and the concentrated solution dissolves glassware. Methanesulfonic acid is weaker than sulfuric acid; although it can also be used over the 0–100 wt% range very few studies using it have been reported. FSO_3H and $ClSO_3H$ cannot be mixed with water. Carboxylic acids are mostly too weak to be useful catalysts, although some work has been done,[46] and trifluoroacetic acid is more of an organic solvent than an acid catalyst. One acid system which is beginning to be used is aqueous trifluoromethanesulfonic acid, triflic acid; unfortunately it is very expensive. Nevertheless its acidity has been studied,[47] and a study of the Beckmann rearrangement of 2,4,6-trimethylacetophenone oxime in the medium is reported.[48] It is a very strong acid,[49] and the pure acid has been used to study the reactions of dications.[50,51]

3. THE EXCESS ACIDITY METHOD

The first method used in media with acidities or basicities outside the normal 0–14 pH range was developed by Louis Hammett, one of the pioneers of physical organic chemistry, in 1932.[52] He extended the pH

range to strongly acidic media by using organic base indicators that were not protonated in the pH range but only became protonated in strong acids. He used these indicators, in the same way that indicators were used in the pH region, to define an "acidity function", which he called H_0, that behaved in the same way that pH did in water.[52]

The problem, of course, is that these concentrated acid media are nonideal, and so molar activities rather than molar concentrations have to be used. Hammett assumed that the molar activity coefficients f for two different primary aromatic amine indicators A and B would be much the same as one another, and thus would cancel out; $\log(f_A f_{BH^+}/f_B f_{AH^+}) = 0$,[52] the Hammett cancellation assumption. However, it was discovered that different types of chemical compound gave rise to different acidity functions, all of them different from H_0.[53,54] At last count there were 58 listed in aqueous sulfuric acid alone,[42] far too many for the concept to be useful any more.

For this reason a less rigorous assumption regarding activity coefficients was conceived, first by Bunnett and Olsen[55] and later by Marziano and her collaborators,[56] and by ourselves.[57,58] This is that activity coefficient ratios in the form $\log(f_B f_{H^+}/f_{BH^+})$ are linear functions of one another. In our case we wrote one for a standard base B*, $\log(f_{B^*} f_{H^+}/f_{B^*H^+}) = X$, and then $\log(f_B f_{H^+}/f_{BH^+}) = m^* X$ with a slope parameter m^*.[57,58] X is called the "excess acidity" because it represents the difference between the acidity according to the log $C_{H^+_{aq}}$ value and the actual, much higher, acidity of the medium.

This technique has been discussed in detail in another volume in this series,[59] so it will only be briefly summarized in this one. Given in that chapter are values of X, log $C_{H^+_{aq}}$ and log a_{H_2O} in molarity units for the three common acid media discussed above.[59] It is also shown there how to modify these values (given at 25 °C) to other temperatures; this modification has been used to obtain standard-state enthalpies and entropies of protonation for many weak bases.[60] Also, for reactions, activation parameters which are a function only of the substrate can be obtained, temperature effects on the medium having been removed;[59] several examples will be given.

Here the technique as it is applied to reaction kinetics is summarized.[59,61,62] The difference is that the activity coefficient of the transition state, $f_{\ddagger}$, takes the place of f_{BH^+} in the equations above, and the slope parameter is $m^{\ddagger}$ rather than m^*. So far, and many hundreds of cases have now been examined, no exceptions to the activity coefficient linearity assumption have been found.[32]

Essentially the log of the rate law is taken and the terms separated.[59] Then the logs of the observed pseudo-first-order reaction rate constants, log k_ψ, measured as a function of the acid concentration, are modified according

to the rate law being tested and the result plotted against X. To find out what if anything is reacting with the substrate S, log k_ψ is modified by subtracting various quantities from it until a linear plot is achieved.[59,61,62] For the pre-equilibrium protonation processes known as A1 reactions, in which a stable protonated intermediate, say a resonance-stabilized acylium ion, is formed, then log k_ψ − log $C_{H^+_{aq}}$ will be linear in X, slope parameter $m^* m^\ddagger$. If protonation is only partial but substantially incomplete at the acid concentrations at which reaction occurs, then a protonation correction term, $\log(C_S/(C_S + C_{SH^+}))$, has to be subtracted as well. If protonation is substantially complete under the reaction conditions (amides, for instance), then it is more convenient to plot $\log k_\psi - \log(C_{SH^+}/(C_S + C_{SH^+}))$ against X, in which case the slope parameter will be $m^*(m^\ddagger - 1)$.[59,61,62]

If something else is reacting with the SH^+ intermediate in an A2 reaction, then it is possible to discover what that is by subtracting (say) the water activity from the log k_ψ term as well. For instance, it is well known now that esters react with two water molecules, and subtracting 2 log a_{H_2O} results in good linearity.[35] It is helpful if the rate constants are measured over a fairly wide range of acidity, one in which the proton concentration and the water activity vary substantially and in different ways, which becomes increasingly apparent above about $X = 4$.[34]

However, as will be seen in some of the examples that follow, many protonated species do not have lifetimes which are long enough for them to be reaction intermediates. In that case proton transfer is part of the rate-determining step, rather than being separate from it. In such cases m^* values and protonation correction terms do not appear in the rate equations, and plots of log k_ψ − log $C_{H^+_{aq}}$ will be linear in X if a stable cation is formed as a reaction product, or log k_ψ − log $C_{H^+_{aq}}$ − log a_{H_2O} will be linear in X if one water molecule is present at the transition state, and so on.[32] Examples follow.

4. MODIFIED REACTION MECHANISMS

4.1. Ether Hydrolysis

Most of the points made above become apparent when this seemingly simple reaction is examined. In fact very little information about the kinetics of the hydrolysis of ethers is available in the literature; very recently all of it that could be found has been examined.[32,40,41] The mechanism, insofar as anyone had thought about it, was assumed to be a pre-equilibrium protonation to give an oxygen-protonated intermediate, followed by the breakup of this to

a carbocation and an alcohol molecule, the carbocation then reacting with solvent to give another alcohol molecule. However, there are at least two things wrong with this. Firstly, if H_3O^+ is incapable of being a reaction intermediate as its lifetime is far too short, RH_2O^+ and R_2HO^+ are not likely to be reaction intermediates either, even with electron-donating R groups present. Neither of these species has ever been directly observed in aqueous solution; their presence has only been inferred. I maintain that they do not in fact exist there; reported NMR observations supposedly leading to pK_{BH^+} determinations for alcohols in aqueous H_2SO_4[63,64] are almost certainly entirely due to medium effects, which are substantial in that medium.[65]

Secondly, only tertiary or resonance-stabilized carbocations are going to have lifetimes long enough that they can be leaving groups in this reaction, at least in dilute acid. Primary carbocations cannot exist there, and secondary ones are only going to be stable enough if the reaction conditions are quite acidic.[41] The actual mechanism for the hydrolysis of diethyl ether is given in Scheme 1.1; as can be seen it is a fully concerted process.[32,41] Remember that "aq" is only a source or a sink for protons and water molecules, and is not involved in the kinetics.

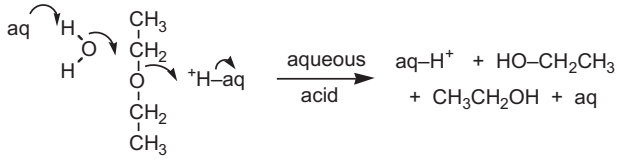

Scheme 1.1

The fact that one, and only one, water molecule is involved in the rate-determining step becomes apparent on an examination of Fig. 1.1. The hydrolysis rate constant data are from Jaques and Leisten,[66] and Fig. 1.1 shows the effect of assuming the involvement of zero, one or two water molecules in the hydrolysis. No water and the graph curves down; two water molecules and the graph curves up; only one water molecule and a beautiful straight line is obtained;[32] correlation coefficient 0.9993.[41] The point at the top right of Fig. 1.1 is off the line because another mechanism involving SO_3 takes over;[66] this point is above the 1:1 acid:water ratio point and there is no water left for the Scheme 1.1 mechanism to use. Data at other temperatures were available;[66] using these gave a $\Delta H^{\ddagger}$ value of 32.8 ± 1.4 kcal mol^{-1} and a $\Delta S^{\ddagger}$ of -12.3 ± 4.6 cal deg mol^{-1} in the aqueous standard state, both of which seem quite reasonable.[41]

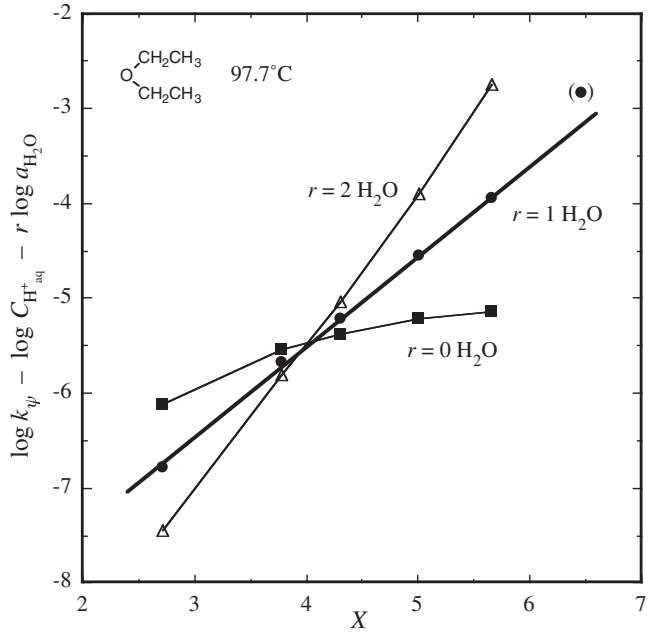

Figure 1.1 Excess acidity plot for the hydrolysis of diethyl ether in aqueous sulfuric acid, showing that only the involvement of one water molecule gives linearity. The number of waters is symbolized as *r*.

Data for many other simple ethers have also been also analyzed,[41] most of it coming from relatively recent studies by the Finnish chemist Lajunen and his group.[67] Summarizing the results: most ethers hydrolyze according to Scheme 1.1. However some, those which are capable of giving tertiary carbocations, or secondary ones if the reaction solution is quite acidic, follow the reaction scheme shown here for methyl *t*-butyl ether as Scheme 1.2. This scheme is quite symmetrical; presumably the observed alcohol products result because water is present in far higher concentration.

The isopropyl cation seems to be stable enough to exist at acidities above about 9 M $HClO_4$, whatever the reason for this may be. Excellent linear plots of just $\log k_\psi - \log C_{H^+_{aq}}$ against X result for the hydrolysis of isopropyl

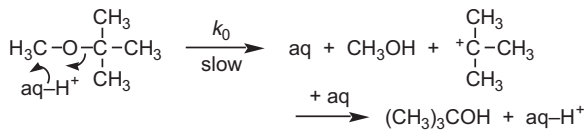

Scheme 1.2

phenyl ether at several temperatures in aqueous perchloric acid,[41] and reaction products resulting from the attack of the isopropyl cation on the reactants and the other reaction products are observed.[68]

Aromatic ethers may react by having water attack at a carbon with a methoxy or other ether group present, and then lose the ether group from that carbon.[41] This is shown in Scheme 1.3; corroborating evidence is that isotope exchange studies show that the bond between the oxygen and the aromatic ring is the one cleaved.[69] There is nothing wrong with positively charged Wheland intermediates, but the one in Scheme 1.3 is shown as being neutral because a water molecule is definitely required in the reaction, according to the kinetic analysis,[41] so this reaction is not a pre-equilibrium protonation.

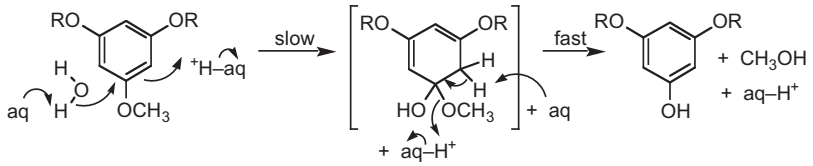

Scheme 1.3

Many of the ethers were also hydrolyzed at a single acidity in $DClO_4$,[67] and the resulting k_H/k_D solvent isotope effects are all around 0.5, plus or minus.[41] Competing effects are at work here. Acids are stronger in D_2O than they are in H_2O, which leads to k_H/k_D values of around 0.3 for equilibrium protonation.[70] However, (1) proton transfer is not complete at the transition state here, and (2) D is heavier than H, which ought to slow down reaction in D_2O as compared to H_2O.[70] The observed values do not seem to be unreasonable, and compounds hydrolyzing according to Scheme 1.2 do seem to have smaller values than those hydrolyzing according to Scheme 1.1.[41]

In several cases it was possible to calculate activation parameters, and for many ethers the observed entropy of activation was slightly positive.[41] On the face of it this might seem improbable, since at least according to Scheme 1.1 several molecules have to come together at the transition state. However, this is somewhat illusory; in these highly structured solutions[31] with everything hydrogen-bonded together and the Grotthuss mechanism[30] at work, all of the water molecules and protons needed are pretty much already there anyway, and do not have to be bought into position first. The only process which really contributes to the entropy change is the formation of two particles from one, which results in the small positive entropy of activation observed in most cases.[32,41]

4.2. Azo-Ethers

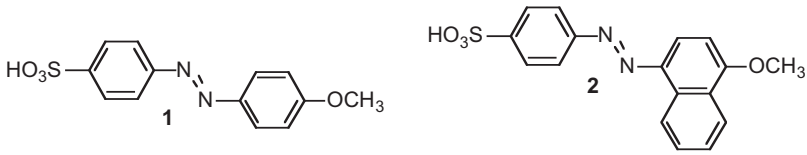

These are considered separately from the other ethers as they have some unique features. They have an azo-group which can be protonated in these acidic solutions, and as this protonation can slow the hydrolysis process down it has to be accounted for in the kinetic analysis.[40] On the other hand, for some azo-ethers it can change the reaction mechanism entirely. Also, compounds **1** and **2** are the only ethers which have been studied in both aqueous HCl and $HClO_4$ media.[71,72]

The excess acidity plots for **1** and **2** are available;[40] the standard-state intercepts for both acid media are the same, as would be expected, but as the acidity increases the reactions are faster in aqueous HCl than they are in aqueous $HClO_4$, as would also be expected, as the good nucleophile Cl^- as well as water is present in the former case. (Methyl chloride was not tested for as one of the reaction products; if formed it might well be hydrolyzed itself, or just lost, at the high reaction temperatures used.)[71,72] This seems to be the only ether hydrolysis that has been studied in more than one medium. A protonation correction term has to be subtracted as the azo-group protonates. Compound **2**, with its naphthyl ring, reacts more quickly than does **1**.[40] Azo-group protonation causes the reaction to slow down[71,72] as the mechanism involves the unprotonated substrate, as shown in Scheme 1.4 for a different molecule, **3**, which reacts in the same way.[40]

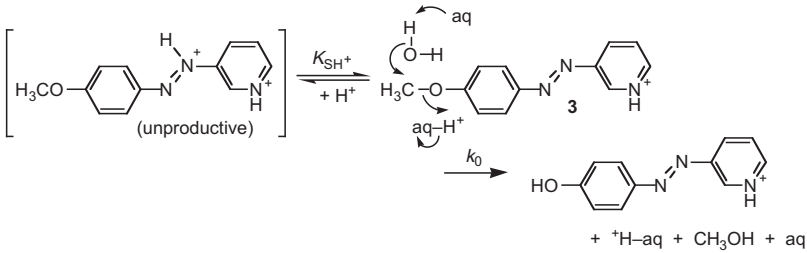

Scheme 1.4

A point of major interest here is that the behavior of compound **3**, which has a pyridinium group in a *meta* orientation and reacts slowly, is quite

different from that of its isomer **4**, which has a pyridinium group situated in a *para* orientation, and reacts quickly by a quite different mechanism, shown in Scheme 1.5.[40,73] In this case the excess acidity plot shows that three water molecules react with the azo-protonated substrate, as Scheme 1.5 predicts; depending on the medium acidity either the k_1 or the k_2 step can be rate determining.[40,73] This type of mechanism, with several water molecules acting together, often cyclically, is quite common.[32] It has recently been referred to in the literature as a "water wire",[74] terminology which may well become more common in the future.

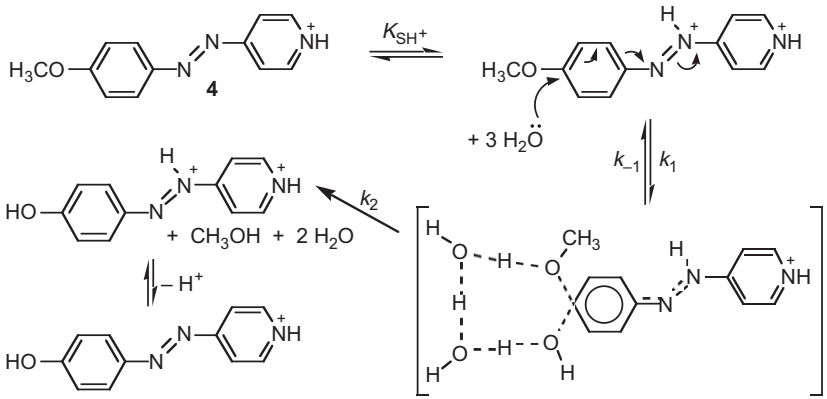

Scheme 1.5

Even more interestingly, when another methoxy group is present in **4**, *ortho* to the one already there, both methoxy groups hydrolyze, but in quite different ways. The *para*-methoxy hydrolyzes quickly according to Scheme 1.5, but the new *meta*-methoxy hydrolyzes much more slowly and by water attack at the *meta*-methoxy position, reminiscent of Scheme 1.3 above.[40,73]

4.3. Acetals

For the first paper on this work[32] the literature data for the hydrolyses of trioxane and paraldehyde in dilute acid media were analyzed. There is quite a lot of this available in all three common aqueous acids.[75] The hydrolysis of the formaldehyde trimer trioxane has been taken by many authors (even by myself)[59] to be a typical A1 process, but it is not. The excess acidity plots are quite clear; $\log k_\psi - \log C_{H^+_{aq}} - \log a_{H_2O}$ is accurately linear in X for all

three acid media.[32] Water is involved in the reaction, and the revised reaction mechanism is shown for paraldehyde in Scheme 1.6.[32] (When the acetaldehyde and acetaldehyde hydrate products are formed they will equilibrate; depending on the acid concentration the equilibrium will almost surely be on the acetaldehyde hydrate side.)[76] The A1 mechanism, pre-equilibrium protonation on oxygen followed by breakup, is not possible because R_2HO^+ species have too short a lifetime to be reaction intermediates, as discussed above. Scheme 1.6 features general acid catalysis, so carboxylic acid buffers and similar systems should also show general acid catalysis for this type of reaction.

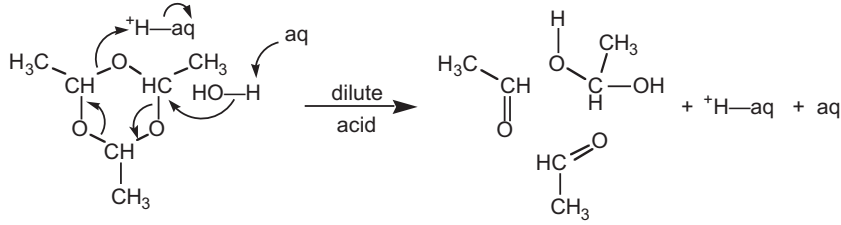

Scheme 1.6

Trioxane hydrolysis is too slow to have been studied in this way, but the similar reaction of paraldehyde (the acetaldehyde trimer) is much faster, and it has been studied in buffers.[46,77] General acid catalysis is indeed observed[46,77] (a fact that seems to have been overlooked (or ignored) since the 1960s), which is good additional evidence for the Scheme 1.1 or the Scheme 1.6 mechanism applying to the hydrolysis of acetals as well as of ethers. Since the reaction of paraldehyde is so fast, the acid range in which reaction rate constants could be obtained is quite narrow, and the experimental scatter is much worse than one would like. Nevertheless, an excess acidity plot according to Scheme 1.6 for paraldehyde at 25 °C in aqueous HCl, $HClO_4$ and H_2SO_4 is given here as Fig. 1.2. The three acid media give three different lines, mainly because the water activity is not known with equal precision in the three media.[32] Nevertheless the slopes and intercepts are, within experimental error, the same; the thick line in Fig. 1.2 combines all of the results in all three media, slope 1.271 ± 0.054, intercept -5.635 ± 0.017, and correlation coefficient 0.97 over 35 points.

Many sugars are acetals, sucrose, for instance, and the hydrolysis of sucrose has been studied by many different research groups over the decades (centuries, even). For this chapter some of the more recent and reliable data on this reaction, obtained at several different temperatures, have been

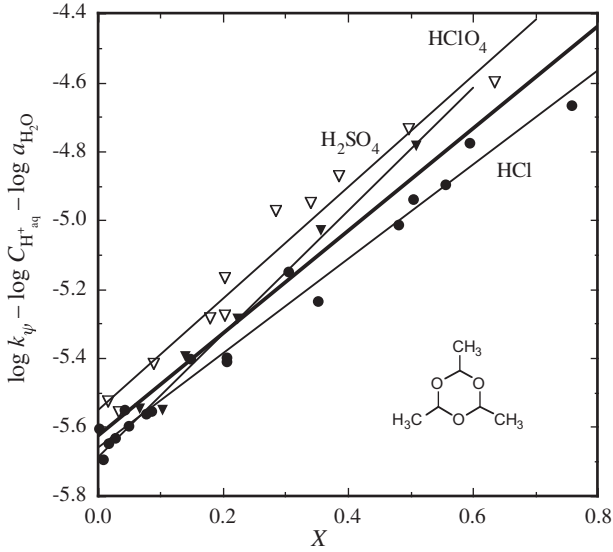

Figure 1.2 Excess acidity plot for the hydrolysis of paraldehyde at 25 °C in three aqueous acid media.

analyzed.[78–80] Not all of the early results have been included, but the consensus is that everybody's results are pretty much in agreement, ancient and modern.[79,80] The analysis is shown in Fig. 1.3, and, unlike the acetals described above, it is apparent that a water molecule is *not* involved in the reaction, since including the water activity results in curves rather than lines.

The likely hydrolysis mechanism is given as Scheme 1.7. Presumably the intermediate with a positive charge on oxygen, **5**, is stable enough to have a finite lifetime because it has a quite highly substituted double bond. Cleavage the other way, from the glucose ring, is less likely because the resulting intermediate does not have this feature. People have always assumed that the cleavage takes place as shown,[80] but there does not seem to be any actual experimental evidence for this. Since **5** is fairly flat, it can presumably be attacked by water on either face; only one fructose anomer is shown in Scheme 1.5 but the other one seems equally likely as a product, if not more so.

Figure 1.3 illustrates several useful features of the excess acidity method. Firstly, since the values of X and log $C_{H^+_{aq}}$ (and log a_{H_2O}) are all corrected to the reaction temperature,[59] the same slope applies regardless of temperature; all of the lines in Fig. 1.3 are parallel. Secondly, since $X = 0$ represents the standard state, the same one as is used for reactions carried out in buffer media,[59] the intercepts and the activation parameters derived from them are

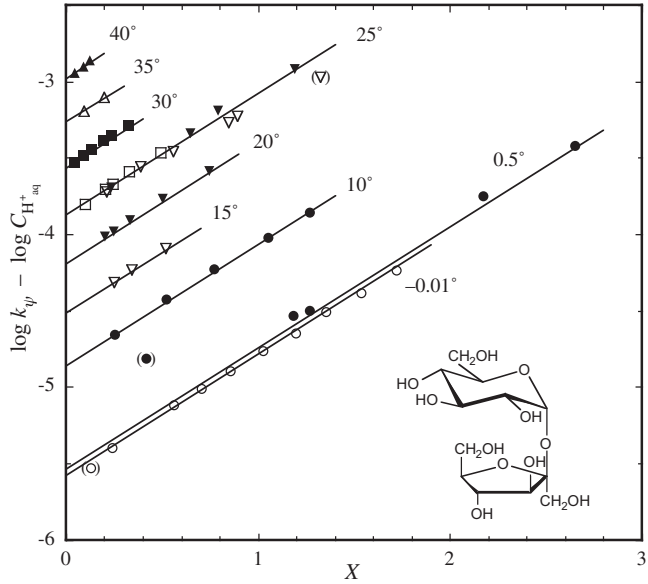

Figure 1.3 Excess acidity plot for the hydrolysis of sucrose in aqueous HCl at several temperatures.

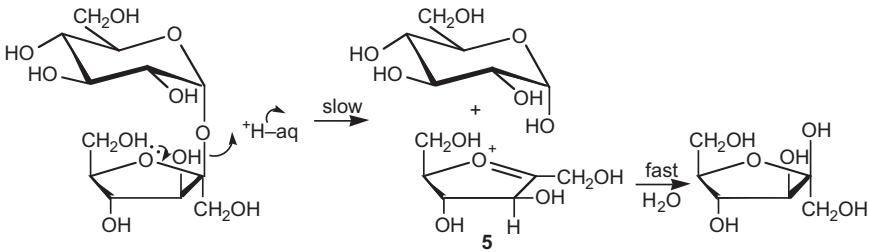

Scheme 1.7

directly comparable to those obtained for other reactions which can be studied in water, or in buffer media, etc. Thirdly, the computer program used for data analysis in this work (double linear regression here) will discard data points that, to 95% confidence, do not form part of the same data set as the rest.[81] This is useful in cases of misreported numbers (typos, etc.), excessive experimental error, wrong temperatures and so on. In the case of sucrose, rather symmetrically one data point from each of the three groups whose data were used[78–80] was rejected; 54 total points, 3 rejected (in parentheses in Fig. 1.3). The multiple correlation coefficient was 0.9993 and the agreement between experimental points and the fitted lines

was ± 0.024. The $m^{\ddagger}$ slope found was 0.7928 ± 0.0082 and the log k_0 (intercept) at 25 °C was -3.8675 ± 0.0051. The activation parameters are: $\Delta H^{\ddagger} = 24.80 \pm 0.14$ kcal mol^{-1}; $\Delta S^{\ddagger} = +6.99 \pm 0.47$ cal deg mol^{-1}. The slightly positive entropy of activation seems to be about what one would expect from Scheme 1.7.

4.4. The Wallach Rearrangement

The parent Wallach rearrangement is that of azoxybenzene **6** to *p*-hydroxyazobenzene **8** in concentrated aqueous sulfuric acid media, see Scheme 1.8. This reaction has been studied by us since the mid-1960s,[34,38,82–90] and it has been extensively reviewed,[91–94] but it is of interest here because the reaction only takes place in strong aqueous sulfuric acid. It was found quite early that the log pseudo-first-order reaction rate constants are not linear functions of H_0 or log $C_{H^+_{aq}}$, but instead were linear functions of the log of the activity of undissociated sulfuric acid molecules up to an acidity of about 98 wt% H_2SO_4, and a linear function of the log $H_3SO_4^+$ concentration above this point.[34] This means that the azoxybenzene, entirely monoprotonated in these media,[82] was reacting with the

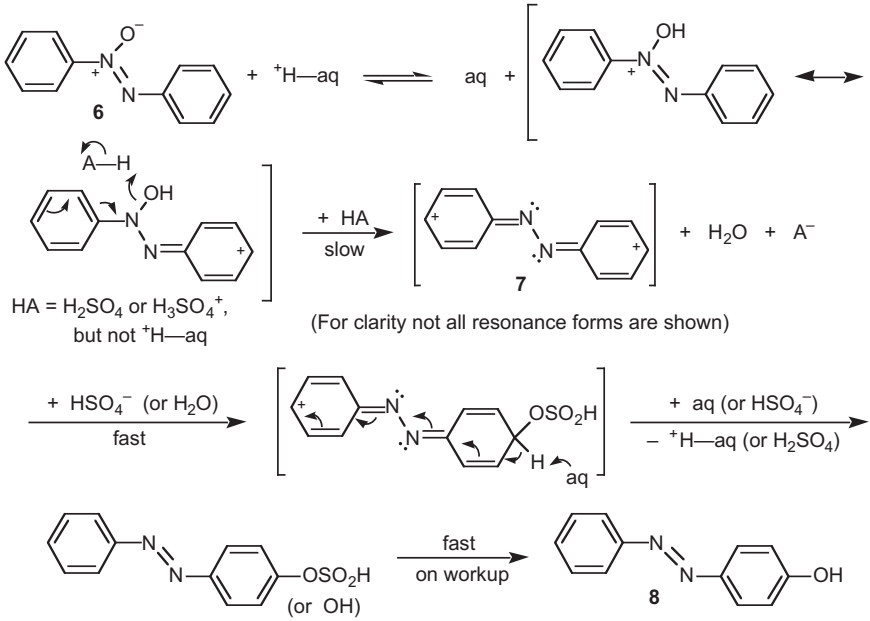

Scheme 1.8

strongest acids available to it in the rate-determining step, giving the dication **7**.[34] The whole mechanism, updated as it stands today,[90] is given here as Scheme 1.8.

We have examined the structure of the dication **7** extensively,[88] and the distribution of positive charge in it is approximately that shown. (For the sake of clarity not all of the resonance forms of the structures in Scheme 1.8 are shown.) Very little positive charge is on the nitrogen atoms, which are sp^2-hybridized with 120° bond angles; the lone pairs are still present. Most of the charge is concentrated on the ring carbons and hydrogens.[88] That makes **7** stable enough to be a reaction intermediate, at least at the high acidities involved. Corroboration comes from the observations that the reaction does proceed in the strongly acidic anhydrous $ClSO_3H$ and FSO_3H media,[95] but *not* in 78% aqueous $HClO_4$.[95] This is a very acidic medium, but the acidity only arises from H^+_{aq}; there are no undissociated $HClO_4$ molecules present, as discussed above, and so the reaction does not go.

This is a clear example of a reaction in which proton transfer to nitrogen or oxygen is involved in the rate-determining step. It has not been found to be necessary to apply the excess acidity approach to this reaction (although it could be done); the simple plots against the undissociated H_2SO_4 activity and the $H_3SO_4^+$ concentration are quite good enough. People do not often think of proton transfer to oxygen or nitrogen as being rate determining, although we have seen several examples here already. Proton transfers to carbon are more readily accepted, however, and we will turn our attention to these next.

4.5. Aromatic Hydrogen Exchange

Quite a number of these processes have been studied using the excess acidity technique.[81] Both deuterium exchange and tritium exchange reaction rate constants obtained in aqueous sulfuric acid, unfortunately not at high enough acidities for undissociated acid molecules to be involved, are available,[96–108] and the molecules involved and the positions of exchange, **9–21**, are indicated in Scheme 1.9.

With both deuterium and tritium exchange data available, it was possible to evaluate all of the rate constants shown in Scheme 1.9, and calculate the isotope effect on the breakup of the Wheland intermediate SH^+ by using the Swain–Schaad relationship.[109] These are given in Table 1.1. Rate constant results at several temperatures were available in some cases, and these enabled calculation of the activation parameters given in Table 1.2.[81] This study is an excellent example of what can be achieved by using the excess acidity analysis

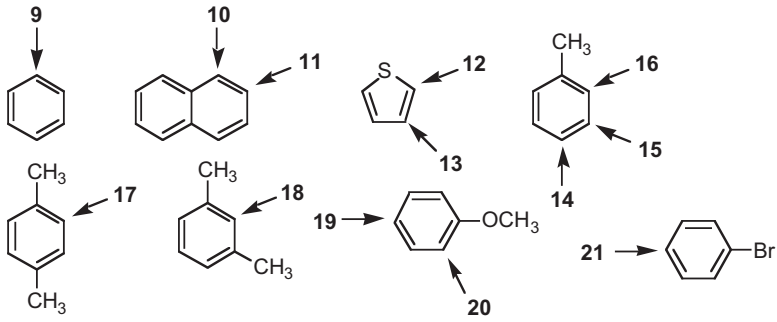

Scheme 1.9

on experimental data which are already in the literature. Combining data, often obtained by different research groups at different times, can lead to results which were not apparent in the original studies.

As might be expected the reactions of the unsubstituted compounds **9–11** are very slow. Attempts to derive a linear free energy relationship, using σ^+, from the log k_1^H values in Table 1.1 lead to two different lines with the same ρ^+ value, -6.5 ± 0.3.[81] The three positions in benzene and naphthalene, **9–11**, form a line of their own some 1.5 log units below that formed by all of the

Table 1.1 Isotope effects on the breakup of the Wheland intermediate SH^+, true protonation rate constants and excess acidity $m^\ddagger$ slope values for **9–21** in Scheme 1.9

Position	k_2^H/k_2^D	$\log k_2^H$	$m^\ddagger$
9	2.4 ± 1.8	-14.36 ± 0.26	0.86 ± 0.01
10	9.8 ± 3.6	-10.76 ± 0.15	0.85 ± 0.02
11	5.4 ± 4.6	-12.38 ± 0.33	0.88 ± 0.04
12	5.9 ± 2.3	-5.31 ± 0.16	0.67 ± 0.02
13	7.5 ± 6.6	-8.48 ± 0.36	0.72 ± 0.04
14	3.3 ± 1.5	-10.65 ± 0.16	0.76 ± 0.01
15	3.5 ± 2.9	-12.20 ± 0.30	0.75 ± 0.02
16	4.4 ± 2.3	-10.47 ± 0.20	0.75 ± 0.01
17	3.9 ± 0.9	-9.93 ± 0.09	0.76 ± 0.01
18	4.1 ± 3.1	-8.09 ± 0.28	0.73 ± 0.03
19	6.8 ± 2.9	-7.45 ± 0.17	0.70 ± 0.02
20	7.5 ± 3.4	-7.71 ± 0.18	0.70 ± 0.02
21	4.7 ± 3.8	-13.79 ± 0.31	0.75 ± 0.02

Table 1.2 Enthalpies of activation (kcal mol^{-1}) and entropies of activation (cal $deg\ mol^{-1}$) for **9–13**

Position	$\Delta H^{\ddagger}$	$\Delta S^{\ddagger}$
9	34.6 ± 0.6	-8 ± 2
10	30.0 ± 0.3	-7 ± 1
11	33.2 ± 0.6	-4 ± 3
12	21.0 ± 0.5	-13 ± 2
13	26.8 ± 1.0	-8 ± 4

other positions, except for the 2-position of thiophene, **12**, which is off on its own, probably because the σ^{+} value used was not suitable for this process.[81]

The $m^{\ddagger}$ values in Table 1.1 are all around 0.75 except, again, for **9–11**, which are higher, more like 0.85. For rate-determining proton transfer reactions at carbon $m^{\ddagger}$ is rather like a Brönsted α, according to Kresge et al.,[110] reflecting the degree of proton transfer at the transition state; about three-quarters transferred in most cases, and more than that for **9–11**. The isotope effects on the Wheland intermediate breakup listed in Table 1.1 are rather error prone; they average out to 5.3 ± 2.1[81] and are probably a combination of both primary and secondary effects. The entropies of activation in Table 1.2 are all more or less the same, -8 ± 3 entropy units, which means that the rate constant differences in Table 1.1 are primarily due to enthalpy differences.

This study has been covered in some detail as a good example of what can be achieved using the excess acidity method in aqueous acid media. In terms of the other mechanisms discussed here, in this one the fact that the rate-determining step is proton transfer, to carbon in this case, is undisputed. There are several other mechanisms where this is true as well, involving double- and triple-bond protonations.

4.6. Alkene and Alkyne Hydrations

A series of 14 substituted styrenes **22**, 8 α-methylstyrenes **23**, 5 α-trifluoromethylstyrenes **24**, and 12 variously substituted *cis*-stilbenes **25**, have been the subject of an extensive excess acidity analysis.[111]

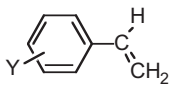

22

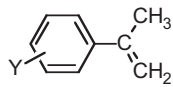

23

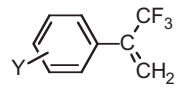

24

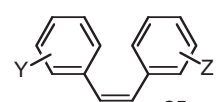

25

The styrenes hydrate and the stilbenes isomerize, but in all cases the rate-determining step is carbon protonation, usually referred to as the A-S_E2 mechanism. The experimental data, again, came from various sources.[112–122] Summarizing the results briefly: the $m^{\ddagger}$ values again indicate that the proton is about three-quarters transferred at the transition state; the reactivities of **22–24** in the aqueous standard state are $1{:}10^3{:}10^{-7}$, as might reasonably be expected; the stilbenes **25** show a good correlation with σ^+, large negative ρ^+, for compounds with substituents in the ring adjacent to the developing positive charge, but with σ, small negative ρ, for compounds with substituents in the other ring.[111] The log k_0 (standard-state intercept) values for **22** and **24** correlate well with σ^+ but those for **23** do not, presumably because the α-CH_3 group twists the molecule enough that the developing positive charge does not overlap well with the ring, an effect not present in **24**, with the strongly deactivating α-CF_3 group, which means that this group must be small enough for the molecule to be planar.[111] The parameters obtained for the styrenes **22** are very similar to those obtained when rate data for phenylacetylenes[123] are treated in the same way, which was taken to mean that reactions with vinyl cation intermediates and those with benzyl cation intermediates can be quite similar.[111]

The hydration reactions of many substituted phenylacetylenes in aqueous sulfuric acid, Y–C_6H_4–C≡C–Z, with Z = CF_3 (eight compounds),[123] H (nine compounds),[113,124–128] COC_6H_4–X (five compounds)[129] and CO_2H (six compounds),[130] have also been studied in this way. Again, summarizing the results: all gave acetophenone-type products consistent with vinyl cation formation; all the compounds have ρ^+ values of −3.8 except those with Z = CF_3, which were more substituent sensitive with a ρ^+ of −5.3; contrary to intuition, proton transfer at the transition state was found to be the most advanced for the fastest reaction, that with Z = H.[123] Several aliphatic alkynes were also examined;[124,131–133] for these, methylacetylene had a log k_0 value of -10.16 ± 0.28 (a very slow reaction), whereas ethylacetylene and *n*-butylacetylene came in at -9.24 ± 0.21 and -8.49 ± 0.01, respectively. Cyclopropylacetylene was much faster, at -3.79 ± 0.03.[123]

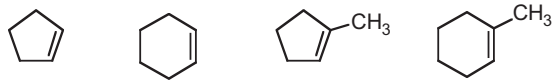

26 **27** **28** **29**

More recently, kinetic data obtained for the hydration of some cyclic alkenes **26–9** have been examined. Compound **26** has been studied at

several temperatures in aqueous perchloric acid, with one measurement in $DClO_4$;[134] **27** at 25 °C in both aqueous H_2SO_4 and aqueous $HClO_4$, plus measurements in the deuterated media;[135] and the methyl derivatives **28** and **29** at 25 °C in aqueous H_2SO_4, with one measurement each in D_2SO_4.[135] The results are presented graphically in Figs 1.4 and 1.5.

Compounds **26** and **27**, which would have to form secondary carbocations if protonation occurred first, apparently do not do that, since secondary carbocations would probably not be stable at these relatively low acidities. Instead they probably react with H^+_{aq} and water in a concerted fashion as shown in Scheme 1.10, in a kind of reverse E2 elimination. In Fig. 1.4 the plots of $\log k_\psi - \log C_{H^+_{aq}} - \log a_{H_2O}$ are perfectly linear.

For the methyl derivatives **28** and **29** the situation is more straightforward; when protonated they form tertiary carbocations, which will be stable enough to be viable reaction intermediates, and so the reaction mechanism will be a two-stage one (reverse E1 rather than reverse E2). In Fig. 1.5 the plots of $\log k_\psi - \log C_{H^+_{aq}}$, without involving the water activity, are linear in X, as would be expected if this were the case. The reactions are slower in D_2SO_4 but not by much, k_H/k_D is 1.22 for **28** and 1.16 for **29**.

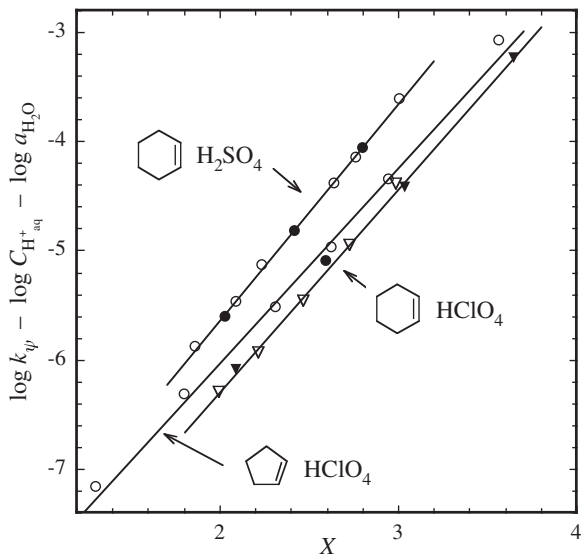

Figure 1.4 Excess acidity plots for the hydrations of cyclopentene in aqueous $HClO_4$, and of cyclohexene in both aqueous H_2SO_4 and $HClO_4$, at 25 °C. The filled points indicate deuterated media.

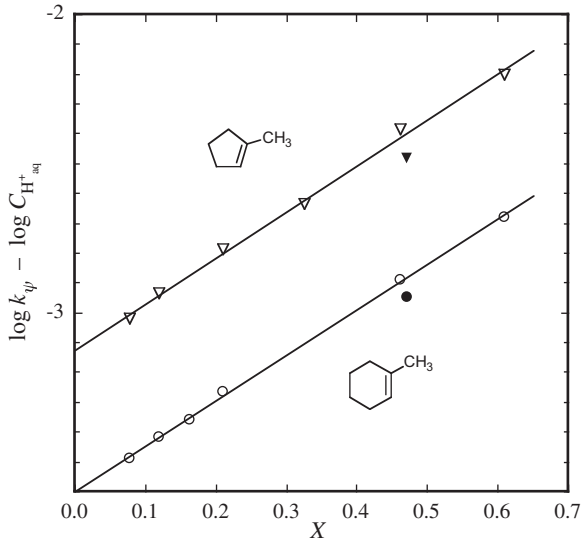

Figure 1.5 Excess acidity plots for the hydrations of 1-methylcyclopentene and 1-methylcyclohexene in aqueous H_2SO_4 at 25 °C. The filled points indicate deuterated media.

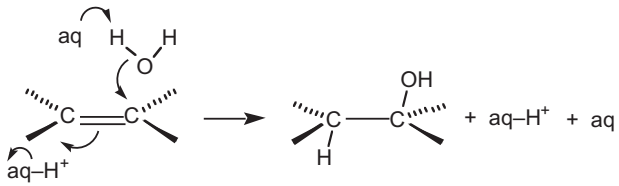

Scheme 1.10

However, puzzles remain; why the lines for **27** in the two different acid media have different intercepts (although the slopes are very similar) is, at present, a complete mystery; for the hydrolyses of trioxane and paraldehyde discussed above, rate constant data in all three common acid systems are more or less coincident. Also the reaction in both media shows no solvent isotope effect at all, the points for H_2SO_4 and D_2SO_4, and those for $HClO_4$ and $DClO_4$, falling on the exact same lines. There are two competing effects at work, as mentioned before, the fact that acids are stronger in deuterated media causing an inverse effect, and the fact that D is heavier than H causing a regular one—but these would have to exactly cancel out, which seems … improbable. Even **26** appears to have only a very small effect, the one point available giving a value of 1.3.

4.7. Cyclic Systems

Cyclic systems often seem to perform in unexpected ways in organic reactions; an example is given above. During a recent examination of the literature for ether hydrolyses[41] very little rate constant data for ring ethers could be found. There seem to be no reliable data for oxirane ring-opening processes, although it might be tucked away under other headings, and the one good recent study of oxetane ring opening[136] does not really fit into any of the categories given above.[41] Even phenyl cyclopentyl ether and phenyl cyclohexyl ether[137] could be reacting by either Scheme 1.1 or Scheme 1.2, as it was not possible to decide between them using the kinetics.[41] Lactams have been studied;[138] these are similar enough to amides that they will not be discussed separately. Also, there is considerable disagreement between the results of the various studies.[139,140] Lactones do not seem to have been studied much at all.

There is, however, a good study available of the ring opening of aziridine in aqueous perchloric acid at several temperatures.[141] This molecule is protonated in the pH region,[141] so it can be assumed to be fully protonated at all acidities in aqueous $HClO_4$. It reacts with water; the plot of $\log k_\psi - \log a_{H_2O}$ is accurately linear at three temperatures, as is shown in Fig. 1.6. Rather amusingly the slope of the graphs is very small, -0.0099 ± 0.0052; for

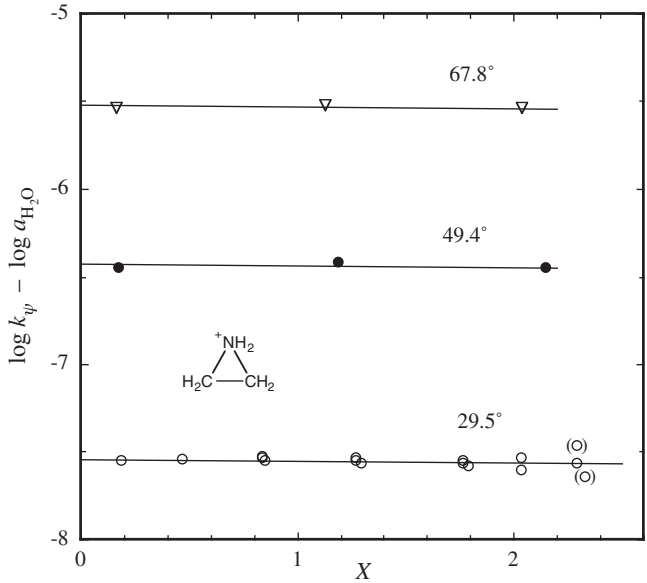

Figure 1.6 Excess acidity plots of $\log k_\psi - \log a_{H_2O}$ against X for the hydration of protonated aziridine in aqueous $HClO_4$ at several temperatures.

reactions of fully protonated substrates the slopes of graphs of this type contain the term ($m^{\ddagger} - 1$) rather than $m^{\ddagger}$, so the latter value is actually 1.01.[59]

The mechanism of this ring opening, probably a rather simple process, is shown in Scheme 1.11. The intercept log k_0 value at 25 °C is -6.0674 ± 0.0080 (on taking account of the log of the water concentration in pure water as being 1.7431), the enthalpy of activation is 24.26 kcal mol^{-1} and the entropy of activation -12.86 ± 0.42 cal deg^{-1} mol^{-1}. Rather a fast reaction compared to some of the others under discussion, which is not surprising as it is the opening of a small ring, but with a negative entropy of activation; a water molecule is being used up.

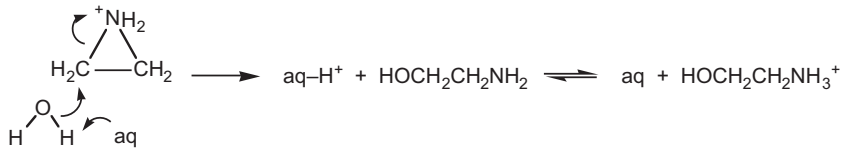

Scheme 1.11

4.8. Substrates Containing Sulfur

Some aromatic sulfonic acids are formed reversibly when the aromatic is treated with sulfuric acid, and if the ring contains electron-donating substituents the reverse hydrolysis process can be quite fast in dilute acid media. One case for which there is a good deal of rate constant information available is the hydrolysis of mesitylene sulfonic acid, **30**. This has been studied at several temperatures in both aqueous sulfuric acid[142] and aqueous hydrochloric acid;[143] the kinetic analysis shows the involvement of both H^{+}_{aq} and a water molecule. Presumably the hydrolysis mechanism is that shown in Scheme 1.12, in which one water molecule is involved; the SO_3 which is the first-formed product would of course quickly hydrolyze to H_2SO_4. In Fig. 1.7, in which are plotted all of the available rate constant measurements for the hydrolysis of **30** at 24.6 °C,[142] despite the experimental scatter it is quite clear that one water molecule is involved in the hydrolysis, the open circles (right axis) clearly indicating a curve.

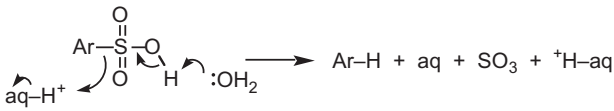

Scheme 1.12

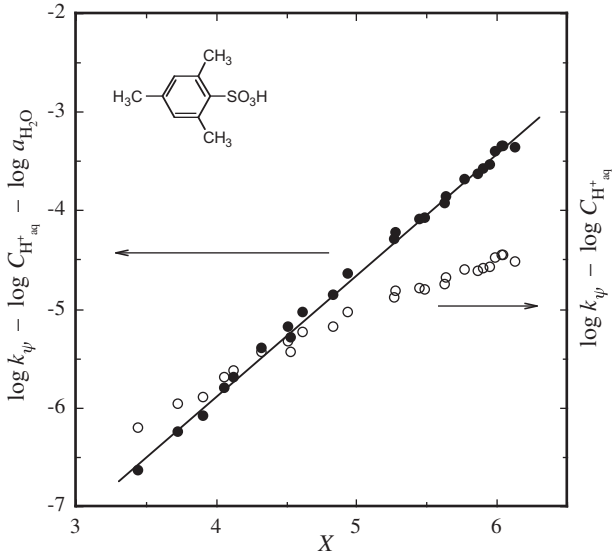

Figure 1.7 Excess acidity plots against *X* for the hydrolysis of mesitylene sulfonic acid **30** in aqueous H_2SO_4 at 24.6 °C, showing the involvement of one water molecule (left axis, line) as compared to no water (right axis, curve).

In Fig. 1.8 all of the other rate constant measurements for **30** are plotted;[142] to make the graph more compact not all of the data from Fig. 1.7 are included. Again all of the lines are clearly parallel, demonstrating that the same $m^{\ddagger}$ value applies at any temperature if the values of *X*, log $C_{H^+_{aq}}$ and log a_{H_2O} are properly corrected to the reaction temperature.[59] This value is 1.490 ± 0.011, and the other numbers obtainable are the standard-state log k_0 value at 25 °C, -10.002 ± 0.045, and the enthalpy and entropy of activation: $\Delta H^{\ddagger} = 28.86 \pm 0.21$ kcal mol^{-1}; $\Delta S^{\ddagger} = -15.40 \pm 0.74$ cal deg^{-1} mol^{-1}, in the aqueous standard state at 25 °C.

Much data were also collected in aqueous HCl,[143] and this is illustrated in Fig. 1.9. The excess acidity analysis gave equivalent results in this medium: $m^{\ddagger} = 1.116 \pm 0.013$; log k_0 at 25 °C $= -9.475 \pm 0.044$; $\Delta H^{\ddagger} = 28.68 \pm 0.31$ kcal mol^{-1}; $\Delta S^{\ddagger} = -13.6 \pm 1.1$ cal deg^{-1} mol^{-1}. It is very interesting that the results in the two media are different from one another, the differences being well outside any possible experimental error (all errors given here are standard deviations).

The slopes are 1.5 and 1.1, certainly a difference worthy of note. The standard-state intercepts show that the reaction is half a log unit faster in HCl, but it is not clear whether this is an enthalpy effect or due to an entropy difference, as these values are the same in the two media, within experimental

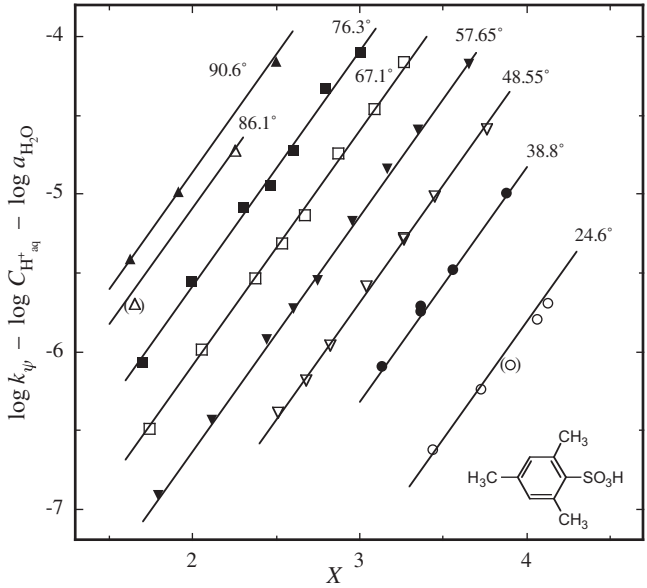

Figure 1.8 All of the rate constant results at several temperatures for the hydrolysis of **30** in aqueous sulfuric acid.

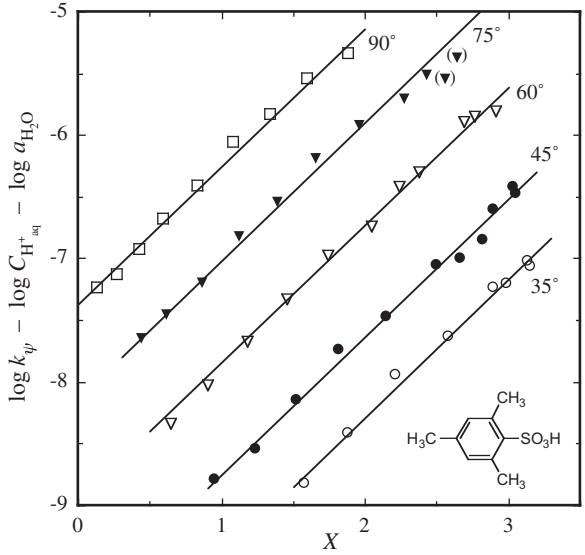

Figure 1.9 All of the rate constant results at several temperatures for the hydrolysis of **30** in aqueous hydrochloric acid.

error. The media are not quite the same in physical terms; aqueous sulfuric acid remains a highly structured medium, with easy Grotthuss proton transfer possible at any acidity, as noted above. Aqueous perchloric acid is probably similar, but in aqueous hydrochloric acid this may not be the case, as the chloride ion, having to be solvated by water itself, is probably a structure breaker.[31] This could well account for the difference in the $m^{\ddagger}$ values noted above—but one would expect a faster reaction in sulfuric acid, opposite to that observed. This is a matter still requiring explanation.

In Scheme 1.12 the proton transfer in the reaction is not actually to the sulfur, but rather to an aromatic carbon. True proton transfer to sulfur is observed in the hydrolysis reactions of some sulfur-containing carboxylic acid derivatives.[144] Some time ago now we used the excess acidity method in an analysis of the hydrolysis rate constants obtained in aqueous sulfuric acid media for some thiobenzoic acids and thioacetic acid[145] and some thiol- and thionbenzoate esters.[146,147]

At high acidities thiolbenzoate esters undergo rate-determining formation of an acylium ion (quite stable as an intermediate in these media) as shown in Scheme 1.13. The major proton transfer agent was found to be the undissociated sulfuric acid molecule;[144] these reactions only have easily measurable rates in quite strong acid, mostly above 70% sulfuric acid, where there are detectable amounts of it.[34] (The Wallach rearrangement takes place in the same acidity region, see above, also utilizing undissociated sulfuric acid molecules.[34]) The thioacids and the thionbenzoate esters mostly hydrolyze like regular carboxylic acid esters, and so will not be considered separately. The thionbenzoates proved to be too reactive to give thioacylium ions.[144] Proton transfer to sulfur, like proton transfer to carbon, can apparently be quite slow, although the reason for this is by no means obvious.

Satchell and his co-workers have used the excess acidity method to study the hydrolyses of thioacetals, among other compounds. They identify cyclic 2-aryl-2-methyl-1,3-dithanes as hydrolyzing in aqueous perchloric acid by an A-S_E2 rather than an A1 mechanism,[148,149] but the diethyl thioacetals of substituted benzaldehydes in the same medium apparently utilize an A1 scheme.[150]

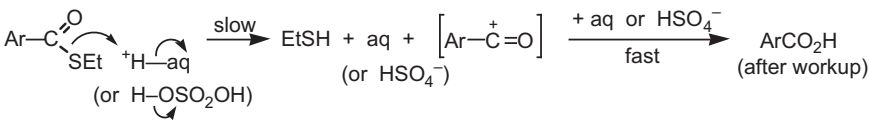

Scheme 1.13

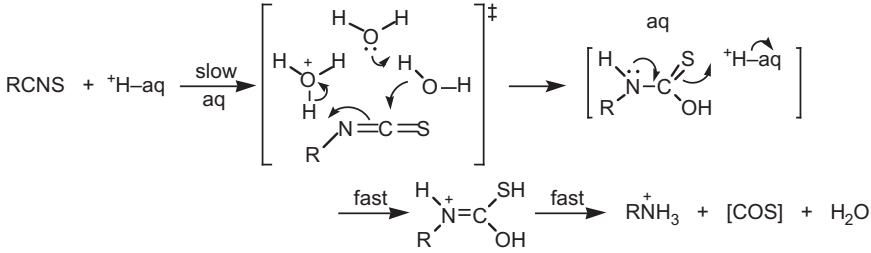

Scheme 1.14

An excess acidity analysis of the hydrolyses of aryl and alkyl isothiocyanates[151] shows that they involve a mechanism with simultaneous proton transfer to nitrogen and nucleophilic attack by water at carbon, in a cyclic transition state, given here as Scheme 1.14. (The authors write a Scheme 1.14 mechanism without the bridging central water molecule,[151] but the one given here has far better bond angles.)

4.9. Amides

We have been studying the mechanism of the hydrolysis of amides in aqueous sulfuric acid, primarily lactams, benzamide and its *N*-methyl and *N*,*N*-dimethyl derivatives, for over 30 years now,[138,152–154] making mistakes along the way; the three mechanisms suggested in 1981[152] all, upon further consideration, proving to be wrong. For instance, the water activity values used in the original work[152] were the original mole-fraction-based values recommended by Bunnett,[155] which later proved to be a poor choice as the mole fraction-based standard state is different from the molarity-based one used by all the other quantities, log $C_{H^+_{aq}}$ and so on.[59] Upon changing to the more appropriate molarity-based water activities[59] it became apparent that rather than the originally proposed[152] three water molecules reacting with the protonated amide, there were actually only two.[154] Also solvent isotope effect results[156] and a multidimensional analysis[157] were only compatible with two water molecules.

However, it was still clear that two different mechanisms were at work, since the rate constants continued to increase with acidity after the first hydrolysis reaction, the two water molecules reacting with the protonated amide, reached its terminal velocity.[154] It is now quite clear that this low-acidity mechanism is the one given in Scheme 1.15.[154]

There is quite a lot of evidence in favor of Scheme 1.15 now; for instance, unlike esters there is essentially no ^{18}O-exchange associated with benzamide

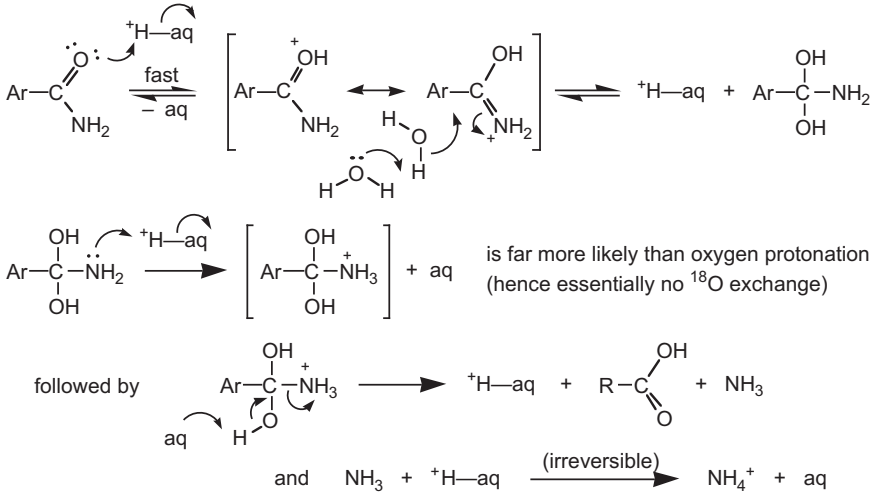

Scheme 1.15

hydrolysis,[158] presumably because the tetrahedral intermediate formed in the rate-determining step is far more likely to protonate on nitrogen and give product than to oxygen protonate and return to starting material. Also unlike esters the reaction is essentially irreversible, since the $^{+}NH_4$ final reaction product is not going to deprotonate in the sulfuric acid reaction medium. Graphs of the plots according to Scheme 1.15 are given for *N*,*N*-dimethylbenzamide in aqueous sulfuric acid at several temperatures in Fig. 1.10; the solid lines are drawn to indicate the limiting behavior according to the scheme.

It is quite clear from Fig. 1.10 that the Scheme 1.15 mechanism is not the only one in operation. Clearly a second one operates at higher acidities, and in the end the only way of finding out what this was involved taking every available rate constant measurement for the benzamides, not only in aqueous H_2SO_4[159–161] but also in $HClO_4$[161–164] and HCl,[161] working out what the rate constants according to the Scheme 1.15 mechanism alone would be, subtracting these from the observed values, and treating the remainder to an excess acidity analysis, subtracting out possible reactants as explained above.[154] This was tedious but it worked, revealing that this high-acidity mechanism involved a previously unsuspected second proton transfer to the already-protonated substrate as part of the rate-determining step, as plots of $\log k_\psi - \log C_{H^+_{aq}}$ proved to be linear.[154] Figure 1.11 illustrates this for *N*,*N*-dimethylbenzamide in aqueous sulfuric acid at several temperatures, and is complementary to Fig. 1.10, with the solid lines again drawn to indicate the limiting behavior, now according to Scheme 1.16.

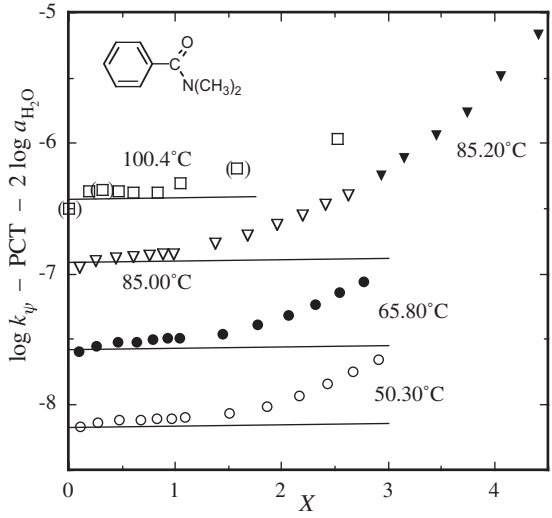

Figure 1.10 Excess acidity plot for the hydrolysis of *N*,*N*-dimethylbenzamide at several temperatures in aqueous sulfuric acid at the lower acidities. PCT stands for the protonation correction term, needed because the substrate is not fully protonated at the lowest acidities; see above.

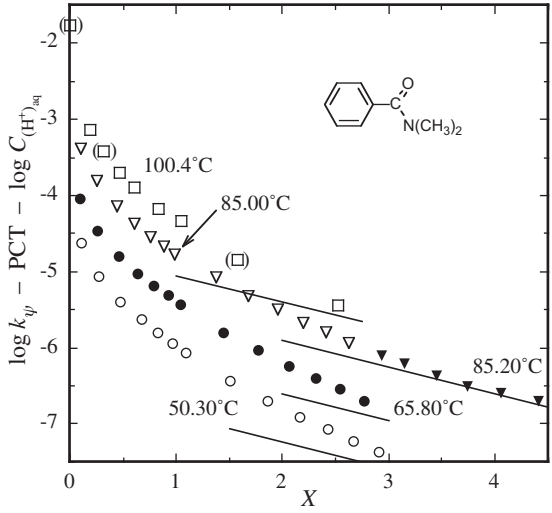

Figure 1.11 Excess acidity plot for the hydrolysis of *N*,*N*-dimethylbenzamide at several temperatures in aqueous sulfuric acid at the higher acidities.

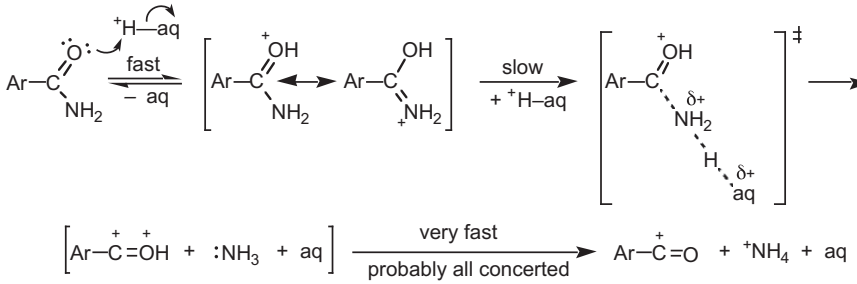

Scheme 1.16

The Scheme 1.16 mechanism is not that easy to draw; the ammonia molecule would almost certainly depart with the proton from the oxygen in the protonated acylium intermediate shown, or it would be lost to the solvent very quickly, and the entire process would almost certainly be concerted. The acylium ion which is the product of Scheme 1.16 would speedily react with the medium to form the carboxylic acid or the protonated carboxylic acid product observed.[154]

However, this is not the only possibility. It was rather difficult to decide whether one or two water molecules should be included in the kinetic analysis or not;[154] the water activity does not change very much over the $X = 1$–4 interval.[59] There is still plenty of water for the reaction to use as the 1:1 acid:water mole ratio point is not reached before about $X = 7$.[59] A "proton wire" cyclic mechanism involving two water molecules has been proposed,[154] but this now looks to be rather improbable. It is possible that water molecules should be included; on looking at Scheme 1.16, it seems most improbable that a dipositive amide species with protons on both oxygen and nitrogen would have a long enough lifetime to exist at all, according to the Jencks principle,[1–4] in these not particularly acidic media.

Amide hydrolysis via the N-protonated form is often proposed,[161,165] and two possibilities are given in Scheme 1.17, one not involving water, and one using one water molecule (a reminder is in order that "aq" in these schemes is simply the solvent acting as a source or sink for protons and water molecules, and does not indicate that "aq" is kinetically involved). It still seems most improbable that the protonated amide would switch from being oxygen protonated, which is a stable resonance-stabilized low-energy structure, to being nitrogen protonated, which is a structure of much higher energy, uphill from the O-protonated one by maybe 7 pK_a units.[166] In any case the kinetics quite definitely show that a second proton is involved,[154]

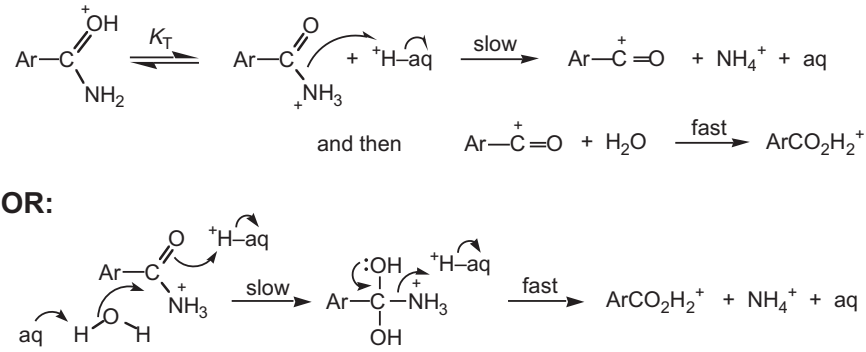

Scheme 1.17

and so ammonia cannot simply leave the N-protonated tautomer directly in an A1 process. If the acidity is high enough in sulfuric acid it is likely that the second proton transfer comes from undissociated sulfuric acid molecules rather than from H^+_{aq}, but with the information available there was only one data point where this could have been the case.[154] The reaction was certainly faster there, but no real conclusions could be drawn from a single data point.[154] In the author's opinion Scheme 1.16 is a more likely mechanism than either of those given in Scheme 1.17, but further experimental information is going to be needed before definitive conclusions can be drawn.

Aliphatic amides are more difficult to deal with than are benzamides, primarily because it is quite difficult to decide what the pK_{BH^+} value of a given amide actually is,[167] which influences the amount of the amide which is protonated at a given acidity and hence the degree of curvature in excess acidity or other graphical analyses. Usually pK_{BH^+} values are determined by measuring the amount of protonated vs. unprotonated forms of the amide present in a given acid solution by UV or NMR spectroscopy.[57–59] Amides, however, are very susceptible to medium effects, the positions of UV or NMR peaks simply being different in different acid media, and separating the effects due to protonation from those due simply to the changing medium is quite difficult.[65,167,168] Quoted values of pK_{BH^+} for amides are often much too negative for this reason; recently some work on acrylamide derivatives (see below) involved finding their pK_{BH^+} values, and the quoted ones of −1.70 and −1.82 for acrylamide and methacrylamide, respectively, at 25 °C[169] seem to be too negative by at least 1.5 log units.[170]

Actually there are not very many reliable, accurate rate constant measurements as a function of acidity for aliphatic amide hydrolyses in the

literature. Also, much of the data consist of very few measurements over a narrow range of acidity, as amide hydrolyses are very slow. Recently a study of the hydrolyses of acetamide, *N*-methylacetamide, *N*,*N*-dimethylacetamide, propionamide, and *N*-*t*-butylacetamide, in aqueous perchloric acid at 80 °C,[164] was examined.[171] The acidities used were high enough that the substrates were almost fully protonated, and no protonation correction term was found to be necessary. For acetamide the plots curved upward slightly, and seemed to resemble Figs 1.10 and 1.11 above, but for the other four amides the plots of $\log k_\psi - 2 \log a_{H_2O}$, and of $\log k_\psi - \log C_{H^+_{aq}}$, against X were both linear. Thus no mechanistic conclusions could be reached from this work. It seems likely, however, that all amides, aliphatic and aromatic, react according to Schemes 1.15 and 1.16 (or Scheme 1.17).[171]

Benzimidate hydrolyses have also been studied.[153] These are essentially the same as protonated benzamides, except that the oxygen is $^+$OR rather than $^+$OH, and they react in the same way as the amides, by Scheme 1.15 above, at the lower acidities.[153] However, for benzimidates where the amidic group is forced out of resonance with the aromatic ring by *ortho*-methyl groups,[172] and for the other benzimidates at higher acidities, an S_N2 attack on the alkyl group by water takes place, as shown in Scheme 1.18. For the benzimidates excess acidity plots of $\log k_\psi - 2 \log a_{H_2O}$ are linear in X, but the graphs have two slopes in those cases where the ring and the amidic group can remain in resonance.[153]

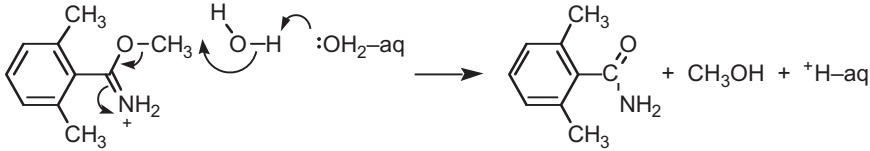

Scheme 1.18

Very recently we have been conducting a study of some of the alkylated derivatives of acrylamide, **31–3**, and of acrylamide itself.[170] These are hydrolyzed in aqueous sulfuric acid, although the first reaction is not actually an amide hydrolysis but rather the simple loss of an alkyl group in an A1 process; all of the alkyl groups in **31–3** can give tertiary carbocations which are stable in the reaction medium and can be isolated as alcohol products. The remaining acrylamide later can undergo hydrolysis itself, but this is a slower reaction.[169] This process is included here to show that A1 reactions in acidic media can still be observed, for those readers who are beginning to have doubts.

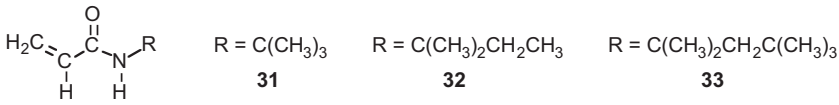

The excess acidity plot for **33** is given here as Fig. 1.12, and the reaction mechanism is given as Scheme 1.19. All of the $m^{\ddagger}$ slopes are around 0.4, less than 1.0, as is characteristic of rate-determining proton transfers,[57–59] with the proton a little less than half-transferred at the transition state.[110] The enthalpies of activation are around 26.4 kcal mol^{-1} and all the entropies of activation are just slightly negative, about -4 cal deg^{-1} mol^{-1}.[170] Two product molecules are being produced from one, but a water molecule is being used up; this seems reasonable. The linearity of the log k_{ψ} − log $C_{H^+_{aq}}$

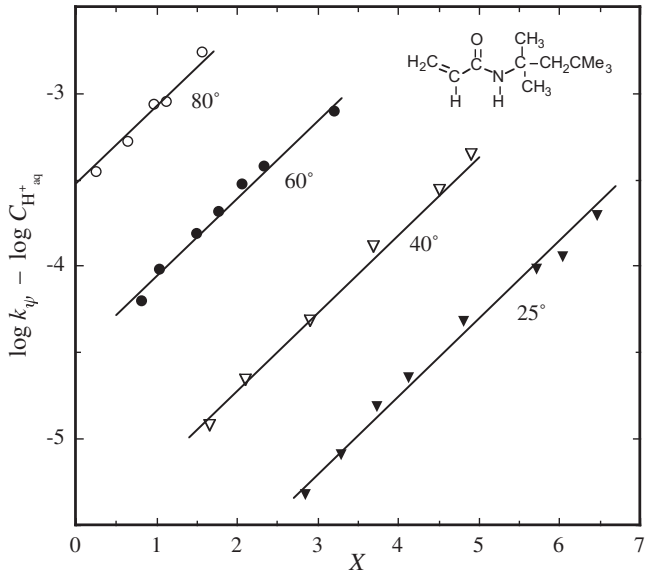

Figure 1.12 Excess acidity plot for the hydrolysis of **33** at several temperatures in aqueous sulfuric acid.

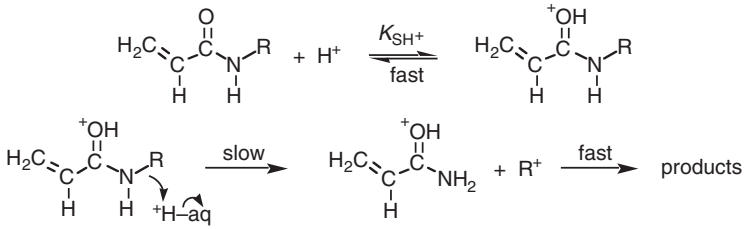

Scheme 1.19

vs. X plot is proof that a second proton transfer is involved in Scheme 1.19, and the linearity also indicates that the first equilibrium protonation on the amide group is essentially complete at these acidities. The pK_{BH^+} values for these molecules and ones like them are thought to be only about -0.3.[170]

Acylhydrazines are interesting amides, having another NH_2 group attached to the amide nitrogen. Several research groups have studied the hydrolyses of some of these,[173,174] and of some benzoylhydrazines,[175–177] in aqueous sulfuric acid at 25 °C and at some other temperatures. They are protonated on the far nitrogen in the pH range,[173] and they undergo hydrolysis by much the same mechanism as do regular amides, except that, since protonation on the carbonyl oxygen is still required, this can be the rate-determining step at low acidities. At higher acidities the attack of two water molecules takes over as the rate-determining step. This is shown in Scheme 1.20 (a slight modification of our original proposal[178] in the light of increased knowledge), and illustrated for acetylhydrazine **34** in Fig. 1.13.

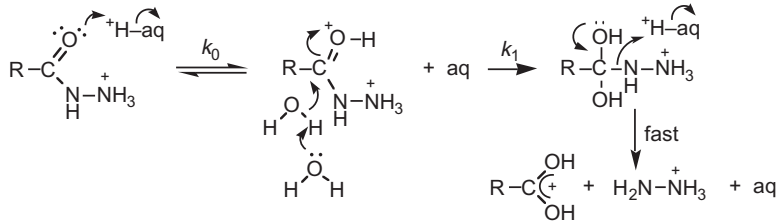

Scheme 1.20

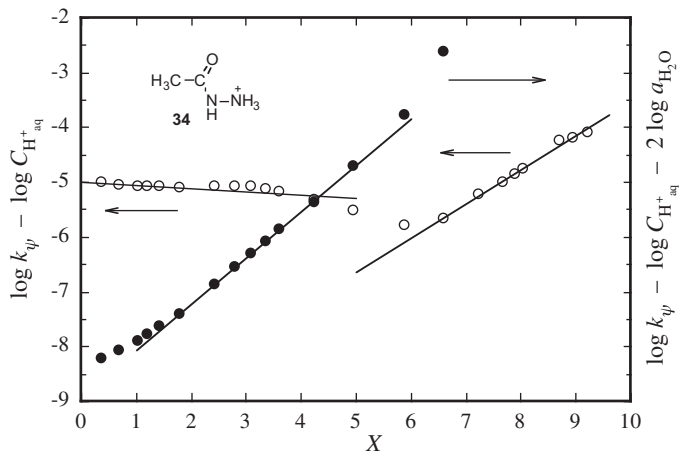

Figure 1.13 Excess acidity plot for the hydrolysis of acetylhydrazine **34** in aqueous H_2SO_4 at 25 °C.

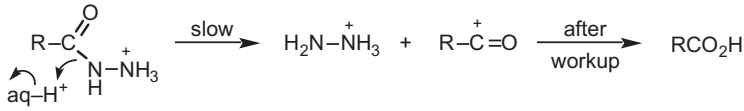

Scheme 1.21

In Fig. 1.13, the open circles refer to the left axis, where linearity indicates slow proton transfer to the carbonyl oxygen, k_0 in Scheme 1.20 (small X values); it is unusual for this to be a slow reaction. The closed circles in the center of the graph refer to the right axis, where the k_1 reaction with two water molecules in Scheme 1.20 is the rate-determining step. Past about $X = 7$ there is too little water present for Scheme 1.20 to be a viable mechanism, and acylium ion formation (open circles, left axis) as shown in Scheme 1.21 takes over, where rate-limiting proton transfer, to nitrogen this time, is again involved.

4.10. Esters and other Carboxylic Acid Derivatives

We have been studying ester hydrolyses for a long time too.[35,153,179,180] Early on it was discovered that two water molecules, rather than one, appeared to be reacting with the protonated ester at low acidities,[179,180] and the mechanism at work was thought to be the one given in Scheme 1.22.[153]

However, in view of the Jencks principle,[1–4] it now seems that protonated esters would not have a lifetime sufficient for them to be intermediates under the reaction conditions. The pK_{BH^+} values for esters are not known with any accuracy, but it is probable that they are much more difficult to protonate than are amides.[181] Attempts to measure these by UV or NMR spectroscopy are problematic, as the spectra are very liable to medium effects.[182] Therefore, it seems that ester hydrolysis is actually a general-acid-catalyzed process, not

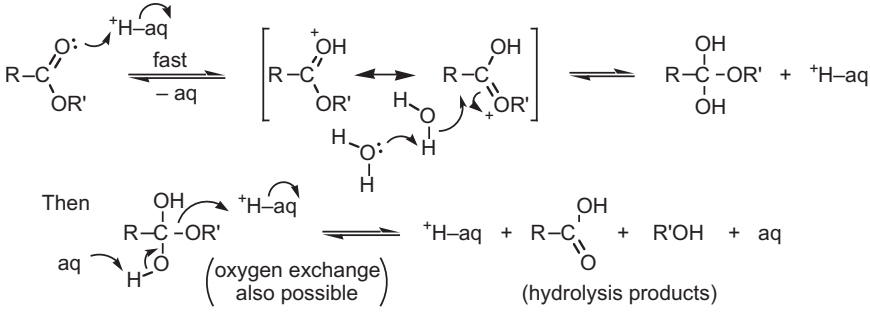

Scheme 1.22

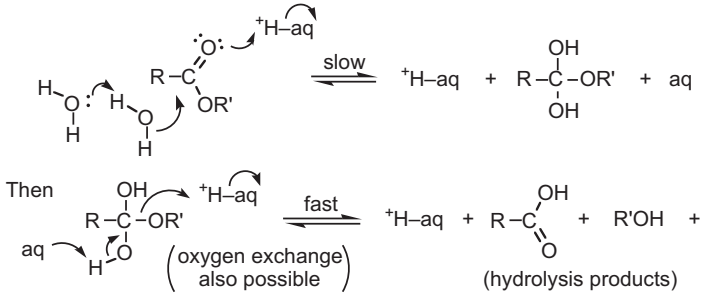

Scheme 1.23

a pre-equilibrium protonation reaction, and a more probable mechanism for ester hydrolysis at low acidities is given in Scheme 1.23.

Schemes 1.22 and 1.23 for esters differ from Scheme 1.15 for amides in that the reaction is reversible. Any one of the three carbon–oxygen bonds in the neutral tetrahedral intermediate has a more or less equal chance of being cleaved, and therefore oxygen exchange into the substrate is likely to occur, as has been observed experimentally.[183]

However, as with amides this is not the only hydrolysis mechanism possible, and other mechanisms can be inferred from the fact that according to Schemes 1.22 and 1.23, the reaction should slow down as acidity increases and the water activity goes down.[34] Often it does,[180] but for many esters the reaction rate increases sharply again in the stronger acids, the changeover often occurring at about the 1:1 acid:water mole ratio point; occasionally in much weaker acids, and for some esters, exclusively.[179,180]

An example of this behavior is given in Fig. 1.14 for *p*-nitrophenyl acetate, using data taken from Yates and McClelland.[179] For these plots the molecule is assumed not to be protonated, as required by Scheme 1.23. If it were partially protonated curvature would be apparent at the lower acidities, which is not the case. The Scheme 1.23 slope, obtained when $\log k_\psi - \log C_{H^+_{aq}} - 2\log a_{H_2O}$ is plotted against X, is 0.818 ± 0.027, and the intercept is -7.735 ± 0.027, quite a slow reaction. Above about 62 wt% H_2SO_4 the graph curves off upward, and the remaining points are linear when $\log k_\psi - \log C_{H^+_{aq}}$ is plotted against X, slope 0.443 ± 0.022. Slope values of less than 1 indicate a mechanism involving rate-determining proton transfer, as expected, see above. The solid lines in Fig. 1.14 represent the extremes of the two mechanisms. The data were curve fitted as a mixture of the two, since it is apparent that both apply in the center of Fig. 1.14; the root-mean-square error between the experimental points and the fitted curve was ± 0.031, excellent agreement.

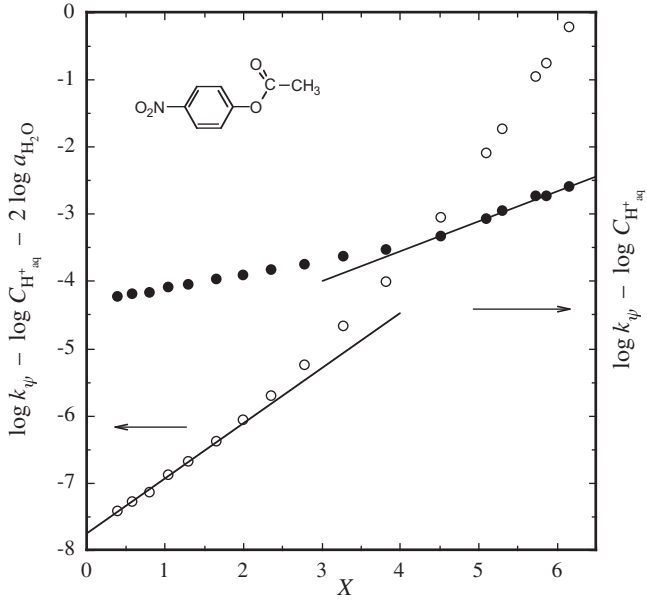

Figure 1.14 Excess acidity plot for the hydrolysis of *p*-nitrophenyl acetate at 25 °C in aqueous sulfuric acid. Left axis, Scheme 1.23 mechanism; right axis, Scheme 1.24 mechanism.

The mechanism in the high-acidity region is given here as Scheme 1.24, quite a simple process; acylium ions will be stable enough to be reaction intermediates at acidities above about $X = 3.5$, but probably not below it. Scheme 1.24 is written as involving H^+_{aq}, but in strong sulfuric acid it may involve undissociated H_2SO_4 molecules. However, this is difficult to establish with certainty using the available reaction rate data. For esters with alcohol groups that can form carbocations that are stable in the reaction medium, benzylic, tertiary, etc., another simple mechanism is possible, Scheme 1.25, an A1 process where the carbocation simply leaves.[179,180]

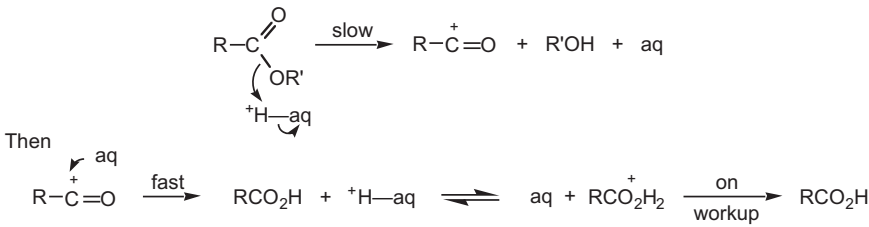

Scheme 1.24

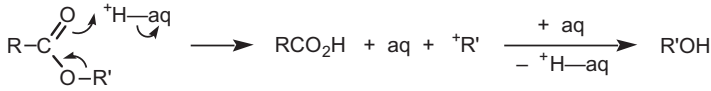

Scheme 1.25

Acylals and thioacylals, $RZCH_2OCOR'$ with $Z = O$ or S, are interesting ester derivatives. A number of acylals, $Y\text{–}C_6H_4OCH_2OCOCH_3$,[184] and thioacylals, $Y\text{–}C_6H_4SCH_2OCOCH_3$,[185] have been studied, along with methoxymethyl acetate and some others;[184,186] methoxythiomethyl acetate[185] and methylene diacetate.[184] Most of the rate constant data for these compounds have been subjected to an excess acidity analysis,[187] and the results are most interesting.

The thioacylals react just as normal esters do at low acidities. The mechanism is given in Scheme 1.26; a general-acid-catalyzed process in which the substrate reacts with two water molecules to give a neutral tetrahedral intermediate; $\log k_\psi - \log C_{H^+_{aq}} - 2\log a_{H_2O}$ is linear in X. The product of the slow step then breaks up to give the observed products shown,[184] perhaps in the cyclic manner shown in Scheme 1.26. This scheme represents an update of our previous mechanistic proposal.[187]

The acylals, however, react with only one water molecule at low acidities;[187] $\log k_\psi - \log C_{H^+_{aq}} - \log a_{H_2O}$ alone is linear in X. We hypothesize that this is because the extra oxygen atom in the molecule is located so that it can hydrogen bond to the incoming water molecule, as shown in Scheme 1.27.[187] This is possible with oxygen in the molecule, which is the right size and has good hydrogen bonding ability. Sulfur is too big and does not hydrogen bond as readily, so the thioacylals react as shown in Scheme 1.26.

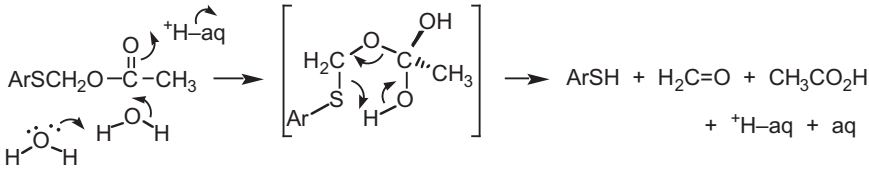

Scheme 1.26

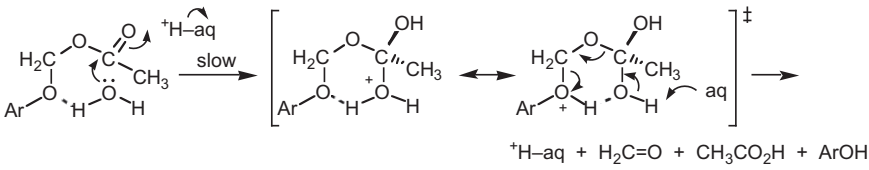

Scheme 1.27

Confirmation of this comes from the excess acidity plot for methylene diacetate, which shows that water is not involved in its low-acidity reaction at all.[187] This, we think, is because the very elegant cyclic internal hydrolysis process shown in Scheme 1.28 is possible for this molecule.[187]

For all of the substrates studied, an A1 process as shown in Scheme 1.29 takes over at higher acidities, where the protonated substrate has a lifetime long enough for it to be an intermediate. For the phenyl-substituted substrates $\log k_{\psi} - \log C_{H^+_{aq}}$ becomes linear in X, at various acidities according to the electron-donating or -withdrawing abilities of the substituent in the phenyl ring.[187] (Acylium and thioacylium cations are resonance stabilized and have lifetimes long enough for them to be viable reaction intermediates at these acidities.) Good linear free energy relationships were obtained for the log k_0 intercept values plotted as a function of σ. For the A2 process ρ is -0.091 ± 0.019 for the acylals and, for the thioacylals, -0.163 ± 0.023; this reaction is little influenced by changing substitution in the phenyl ring, as would be expected. For the A1 reaction ρ is -3.21 ± 0.21 for the acylals and -2.06 ± 0.15 for the thioacylals, much more subject to changing substituent patterns.[187]

The more reactive carboxylic acid derivatives, acid anhydrides, chlorides and fluorides, cannot be said to have established hydrolysis reaction mechanisms at this time. The only ones that have been subjected to the excess

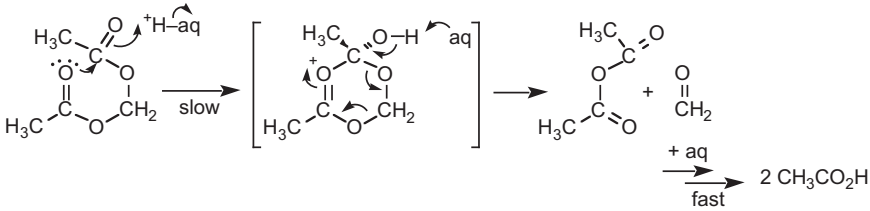

Scheme 1.28

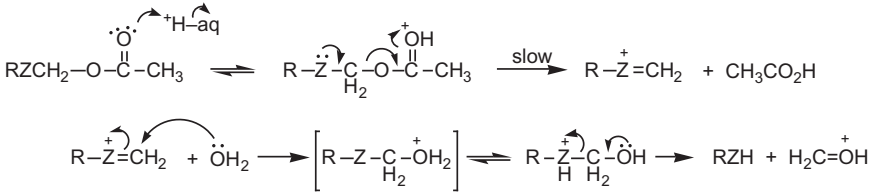

Scheme 1.29

acidity technique are acyl fluorides in aqueous dioxane media,[188,189] two mechanisms being assigned, and benzoic[190] and some other anhydrides[191] in aqueous dioxane and in pure aqueous media, to which two mechanisms were also assigned.

One intriguing mechanism is a concerted S_N2 "water wire" process proposed by Ruff and Farkas,[192] who list references to all of the previous mechanistic proposals for acid chloride hydrolysis.[193] Unfortunately this process is proposed on the basis of theoretical calculation only, in the gas phase and in solution, but the authors feel that is in accordance with published kinetic studies.[192] It is given here as Scheme 1.30.

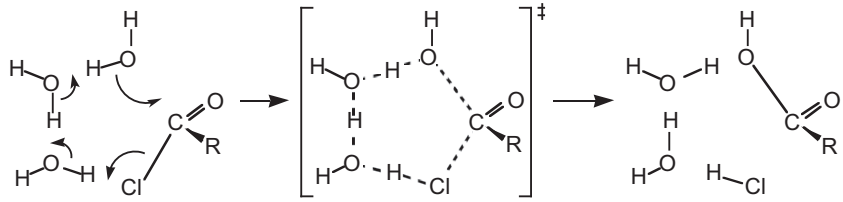

Scheme 1.30

This is interesting because it is not acid catalyzed, only water molecules being involved. Mechanisms involving cyclic chains of water molecules in a "water wire"[74] have been proposed before[32] and would seem to be favored in water because the medium is highly structured already, and oxygen and nitrogen atoms in the substrate are going to be hydrogen-bonded to the solvent as well. Schemes like Scheme 1.30 would appear to be unfavorable entropically because of the number of molecules that have to be brought together in the correct orientation, but this is somewhat illusory as much of the required structure is more or less already there.[32] Scheme 1.30 is a useful lead-in to the next topic:

4.11. Reactions in Water and in Basic Media

Two other mechanisms of the same type as Scheme 1.30 that have been proposed are shown below in Schemes 1.31 and 1.32. Scheme 1.31 is a proposal for the hydrolysis of nitramine (or nitramide) in water; this reaction is acid catalyzed for the most part, but with an additional water term.[194] It was proposed originally on the basis of nothing but its elegance,[194] but later detailed modern calculations, both for the gas phase and also in solution, were found to be in agreement with it.[195]

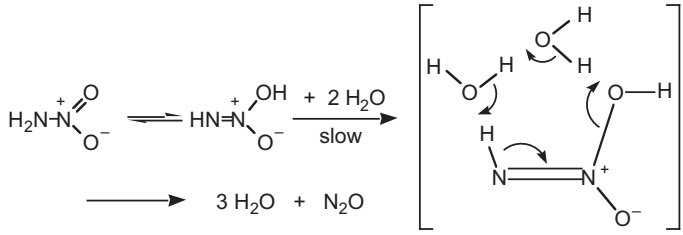

Scheme 1.31

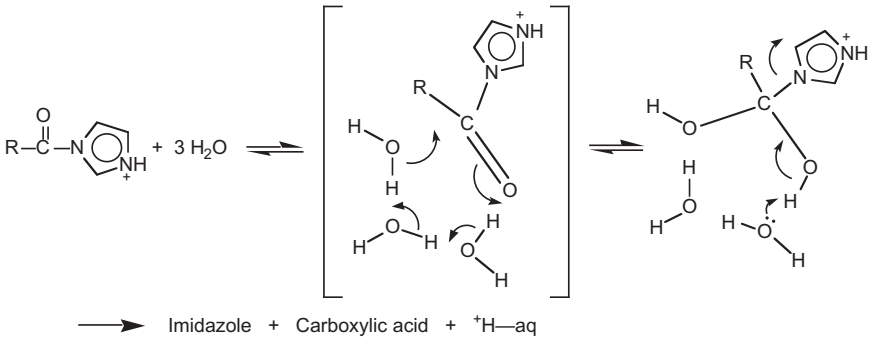

Scheme 1.32

Scheme 1.32 is a proposal for the hydrolysis of acylimidazoles in water.[196] The excess acidity technique was applied to the reactions of acetylimidazole in aqueous $HClO_4$, H_2SO_4 and HCl, and of benzoylimidazole in the latter two. Here the reaction rates decrease with increasing acidity, in fact, but the analysis shows quite clearly that the excess acidity method can be applied in these media even to reactions that are not acid catalyzed.[196]

Basic media have not been studied nearly as much as acid media have, but there are still conclusions that can be drawn. We have made a start at deriving "excess basicities",[197,198] and More O'Ferrall[199] and Bagno, Scorrano and Terrier[200,201] have made contributions as well.

It is, however, becoming plain that hydroxide ions do not add directly to carbonyl groups, in ester hydrolysis, for instance, but rather attack to remove a proton from an adjacent water molecule which then adds to the carbonyl,[202–204] as shown in Scheme 1.33. Heavy-atom isotope effect studies add to the evidence in favor of this.[205]

Note that in Scheme 1.33 the tetrahedral intermediate is neutral, just as in the acid-catalyzed hydrolyses; in general charged tetrahedral intermediates have too short a lifetime in aqueous media to exist.[1–4] In the

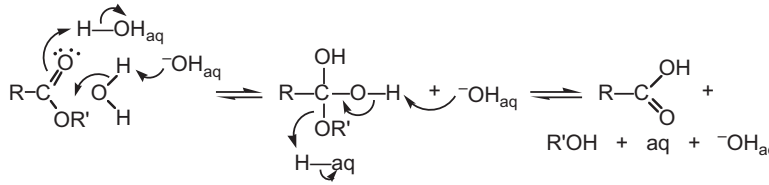

Scheme 1.33

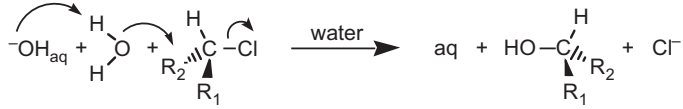

Scheme 1.34

literature tetrahedral intermediates are often mentioned as intermediates in this type of reaction, and there is no doubt that they are. However, the contention made here is that they are almost always *neutral*. The abbreviation used for tetrahedral intermediates is T (or T^0), and the charge believed to be on them is appended as a superscript. One comes across T^+, T^-, $T^{\pm}$, and even T^{2-}, in studies of ester hydrolyses and related processes. It is suggested that authors be quite certain that these exist long enough to be viable reaction intermediates before proposing them in aqueous media.

By analogy, it seems probable that S_N2 substitutions by hydroxide ion on alkyl halides and related substrates would take place as shown in Scheme 1.34. This is the only speculation at present, however; evidence is lacking.

4.12. Other Reactions

Quite a number of nitro-substituted compounds have been studied. The reaction of nitramine (or nitramide) in water has been mentioned above,[194] but this compound has an acid-catalyzed mechanism as well, one that is shared with many other alkylnitramines.[39] As a typical example, an excess acidity plot for the hydrolysis of methylnitramine, which has many reported rate constant measurements as a function of acidity and temperature,[206–208] is given here as Fig. 1.15. The mechanism by which this compound and many other alkylnitramines react is given as Scheme 1.35.[39]

The inferred mechanism, which is followed by all of the nitramines (and nitramine itself)[194] is given in Scheme 1.35.[39] As can be seen from Fig. 1.15, $\log k_\psi - \log C_{H^+_{aq}}$ – the log nucleophile concentration is perfectly linear in X,

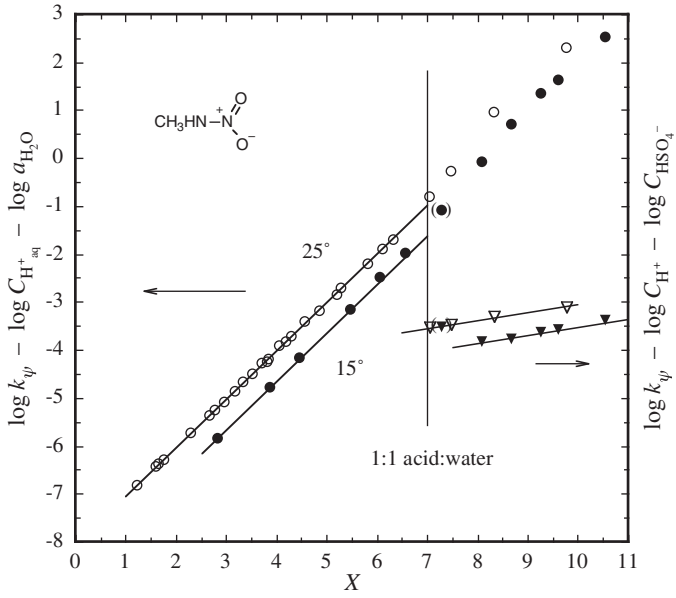

Figure 1.15 Excess acidity plot for the hydrolysis of methylnitramine in aqueous H_2SO_4 at 15 and 25 °C.

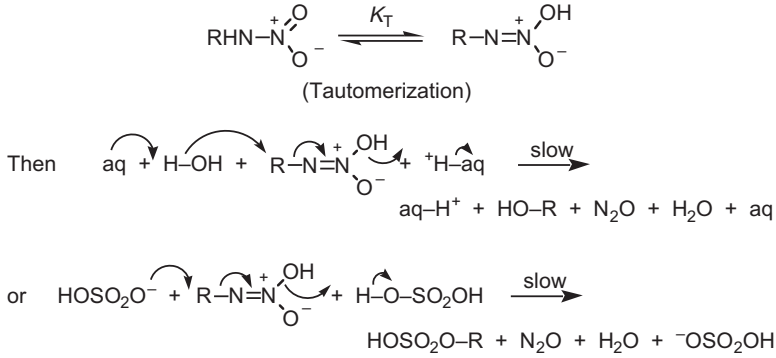

Scheme 1.35

the nucleophile being water as long as there is any present, and bisulfate ion above the 1:1 acid:water mole ratio point. Bisulfate is some 100 times worse as a nucleophile than is water.[39] It is not clear *why* bisulfate is a bad nucleophile; the negative charge it carries is well dispersed and this should make it a "soft" base, and thus a good nucleophile.[209] However, sulfate appears to be even worse, with no reliable reports of it acting as a nucleophile in the literature at all.

The hydrolysis reactions of a number of *N*-nitrobenzenesulfonamides,[210,211] *N*-nitrobenzamides,[212] *N*-methyl-*N*-nitrobenzamides[213] and nitrourea[214] in aqueous sulfuric acid media have also been examined.[215] The former give either $YC_6H_4SO_2^+$ and NH_2NO_2 (electron-donating Y) or $YC_6H_4SO_2NH_2$ and NO_2^+ (electron-withdrawing Y) in two possible A1 processes, depending on whether they are N-protonated or O-protonated, something which is not currently known.[215] *N*-nitrobenzamides behave similarly in strong acid, an A1 reaction following O-protonation, but also have a neutral reaction with water at moderate acidities.[215] In acid nitrourea also undergoes an A1 hydrolysis.[215]

Ketones and aldehydes have been examined briefly. Early on we applied the excess acidity technique to some acid-catalyzed enolization processes, of acetone and some acetophenones,[216] but this work was later shown to be in error because insufficient halogen scavenging in the original experiments on acetophenone itself[217] had not been accounted for.[218] After a correction was made plots of $\log k_\psi - \log C_{H^+_{aq}}$ against X proved to be linear, an unexpected result as the base causing the enolization should appear in the rate law.[59] Further work on this reaction is necessary. The acid-catalyzed aldol condensation of acetaldehyde to an equilibrium mixture of aldol and crotonaldehyde is the only second-order reaction to be examined using the excess acidity technique so far.[219] Interestingly this reaction is base catalyzed; the water activity did appear in the rate law, even in concentrated sulfuric acid.[219]

We have looked at the reactions of some vinyl tosylates, benzoates and 1,1-ditosylates; these hydrate rather than hydrolyze in aqueous acid, undergoing rate-limiting proton transfer to the double bond.[220] Trifluoromethyl- and pentafluoroethyl-substituted vinyl ethers also hydrate rather than hydrolyze.[221] The benzidine disproportionation undergone by some azopyridines[222] and the cyclization of some 2-substituted imidazolines in aqueous sulfuric acid[223] have been reviewed previously.[59]

5. CONCLUSIONS AND GENERAL COMMENTS

A lot of organic reactions have been covered in this chapter. Perhaps the most obvious conclusion to be drawn is that there is much still to be discovered about the mechanisms of simple organic reactions in aqueous media. Research into these reactions is not common today; there are very many systems more complex than the ones discussed here under investigation now, and many more in need of investigation, but perhaps

a reminder about the complexity of apparently simple systems is still in order.

Another, rather surprising, conclusion to which the author has come is that many of the long-accepted mechanisms of organic chemistry actually rest upon a rather narrow base of experimental evidence. This became clear, I think, when a recent study[15] examined the actual experimental evidence for the existence of S_N1 reactions of secondary substrates in aqueous media. This mechanism is still being quoted as a possible one in some[224,225] (but not all[226]) standard texts, and it was found wanting.[15] More recent studies have placed the S_N2 reaction as being the only one possible for secondary substrates, even with quite weak nucleophiles, upon a firm footing,[13] and this should now be in all standard textbooks.

It is clear, certainly from this Chapter, that the Jencks principle, that a postulated reaction intermediate must actually be capable of existing in the reaction medium,[1–4] has already changed the interpretation of many reactions and is going to change the interpretations of many more. Species which are positively, or negatively, charged on oxygen where there is no possibility of delocalizing the charge by resonance, or stabilizing it internally in some other way, are quite unlikely to exist in aqueous media—and, according to recent research, the hydrogen-bonded collective network characteristic of aqueous media is already present in aqueous organic solvents containing more than 10% water.[12,227]

Incidentally, authors who perform theoretical computations on the structures of nonexistent intermediates ought to be aware that they are doing so. There are numerous examples involving implicit aqueous solvation where the solvent is treated as a continuum (e.g. a recent study of glycoside hydrolysis[228]), in which a nonexistent intermediate appears to be stable due to the lack of a nucleophile in the calculated model system. Theoretical results, which are becoming easier and cheaper to obtain all the time, should make sense chemically and not disagree too violently with existing knowledge. For instance, a species that reacts with zero activation energy has to have a lifetime of zero,[228] and a discrepancy of over 12 orders of magnitude between theoretical[229] and experimentally measured species lifetimes is too large to be tolerated.[230]

The water autoprotolysis species H_3O^+ and HO^- do not exist as such in aqueous media, although they are of course well-known species in the solid state and under other circumstances, in superacids or in pure DMSO, for instance. Most likely, nor do RH_2O^+ and R_2HO^+. Tetrahedral intermediates are almost always uncharged, T or T^0 in the terminology used. Species

such as T^+, T^- and $T^{\pm}$, and especially T^{2-}, are quite unlikely to have lifetimes long enough to be intermediates in reactions in aqueous media, although of course this assertion does not preclude their existence in nonaqueous media. With any of these species, it is recommended that authors be very sure that they actually exist under their reaction conditions before proposing them.

Regarding general vs. specific acid catalysis, it appears that the amount of the activation energy for the reaction under consideration which is supplied by the proton transfer is important. For reactions in which this process supplies most of the activation energy, among the reactions cited above these would be proton transfers to carbon in alkene or alkyne hydrations, or to aromatic carbon, or to sulfur, and the Wallach rearrangement; every acid species present will contribute its quota to the reaction. Of the reactions cited this has only actually been seen in the Wallach rearrangement and in the hydrolysis of thiolbenzoate esters, where catalysis by undissociated H_2SO_4 molecules as well as by H^+_{aq}, or by $H_3SO_4^+$, has been observed. However, it is sure to show up in, for instance, alkene hydrations which are slow enough to only take place in sulfuric acid media more concentrated than 84.48 wt%. This is "general acid catalysis".

However, for those processes in which the proton transfer is concerted with the rest of the mechanism and contributes very little to the overall activation energy, it appears not to matter where the proton comes from. Two reactions in which this was found to be the case among those cited above are the hydrolysis of acetylhydrazine **34** at X values higher than 7, see Fig. 1.13, and the hydrolysis of methylnitramine, also at X values higher than 7, see Fig. 1.15, where the log $C_{H^+_{aq}}$ values that gave the best linearity were simply the log of the total sulfuric acid molarity. Undoubtedly other cases will be found; these could still be referred to as "specific acid catalysis".

To end with a plea: the author has never been in a position to conduct his own experiments, having to rely on rate constant and other information already in the literature, or that sent to him to analyze by quite a number of his valued colleagues from all over the world. In recent years the practice of including in papers the numerical experimental data actually obtained in a study has become much less common than it has been in the past. This author urges other authors to make rate constant and other information available; this is quite easy to do nowadays, with the electronic deposition of supplementary data associated with published papers possible for just about all journals, published and electronic. It is a truism that scientific theories change or are updated all the time, and thus are ephemeral; as mentioned

above, three of my own originally proposed amide hydrolysis mechanisms later proved to be wrong, and it looks as if reinterpretation of numerous ester hydrolysis studies is going to be necessary also. However, reliable experimental evidence is there for all time. Some of the experimental rate constant information used in this chapter dates from pre-World War II, but it is still good and reliable. The author's experience with scientific work performed in the former Soviet Union is that all of their experimental data, some of it obtained with considerable difficulty on outdated equipment, is published in their papers, and that it is quite reliable. He has used a lot of it. Some of their interpretations of this data, however, are very strange, coming from elsewhere, perhaps a parallel universe. Please, publish your data!

ACKNOWLEDGEMENTS

Valuable correspondence with Tina Amyes, Andy Bennet, Bill Bentley, Chris Reed and Evgenii Stoyanov is gratefully acknowledged. Peter Guthrie read the original manuscript very carefully and provided a number of very useful suggestions, especially as to where I had not taken my own conclusions far enough! The editors provided some useful suggestions. My friend and colleague Leonid Kuznetsov sent me some of the results discussed above, and general discussions with my colleagues worldwide, and comments by the referees of my papers, have also been of considerable assistance.

REFERENCES

1. Jencks WP. *Chem Rev*. 1972;72:705-718.
2. Jencks WP. *Acc Chem Res*. 1976;9:425-432.
3. Jencks WP. *Acc Chem Res*. 1980;13:161-169.
4. Jencks WP. *Chem Soc Rev*. 1981;10:345-375.
5. Moore WJ. *Physical Chemistry*. 4th ed. Englewood Cliffs, NJ: Prentice-Hall; 1972: p. 769.
6. Whalen DL. *Adv Phys Org Chem*. 2005;40:247-298.
7. More O'Ferrall R. *Adv Phys Org Chem*. 2010;44:19-122.
8. Richard JP, Amyes TL, Toteva MM. *Acc Chem Res*. 2001;34:981-988.
9. Amyes TL, Jencks WP. *J Am Chem Soc*. 1989;111:7888-7900.
10. Richard JP. *J Am Chem Soc*. 1989;111:1455-1465.
11. Cozens FL, Kanagasabapathy VM, McClelland RA, Steenken S. *Can J Chem*. 1999;77:2069-2082.
12. Kalish NB, Shandalova E, Kharlanov V, Pines D, Pines E. *J Phys Chem A*. 2011;115:4063-4075.
13. Bentley TW, Schleyer PvR. *J Am Chem Soc*. 1976;98:7658-7666.
14. See references collected in ref. 15.
15. Murphy TJ. *J Chem Educ*. 2009;86:519-524.
16. Stoyanov ES, Stoyanova IV, Reed CA. *J Am Chem Soc*. 2010;132:1484-1486.
17. Stoyanov ES, Stoyanova IV, Reed CA. *Chem Sci*. 2011;2:462-472.
18. Eigen M. *Angew Chem Int Ed Engl*. 1964;3:1-19.
19. Zundel G. *Adv Chem Phys*. 2000;111:1-217, and many earlier papers.
20. Bascombe KN, Bell RP. *Discuss Faraday Soc*. 1957;24:158-161.

21. Robertson EB, Dunford HB. *J Am Chem Soc.* 1964;86:5080-5089.
22. Jiang J-C, Wang Y-S, Chang H-C, Lin SH, Lee YT, Niedner-Schatteburg G, Chang H-C. *J Am Chem Soc.* 2000;122:1398-1410.
23. Knight C, Voth GA. *Acc Chem Res.* 2012;45:101-109, and earlier papers by Voth.
24. Stoyanov ES, Reed CA 2011. Personal communication.
25. Shevkunov SV. *Zh Obshch Khim.* 2004;74:1585-1592.
26. Silverstein TP. *J Chem Educ.* 2011;88:875.
27. Ault A. *J Chem Educ.* 2010;87:937-941.
28. Roberts ST, Ramasesha K, Petersen PB, Mandal A, Tokmakoff A. *J Phys Chem A.* 2011;115:3957-3972.
29. Dolman D, Stewart R. *Can J Chem.* 1967;45:911-924.
30. Grotthuss CJT. *Ann Chim.* 1806;LVIII:54-74.
31. Marcus Y. *Chem Rev.* 2009;109:1346-1370, and references cited therein.
32. Cox RA. *Int J Mol Sci.* 2011;12:8316-8332.
33. Liler M. *Reaction Mechanisms in Sulfuric Acid*. New York: Academic Press; 1971.
34. Cox RA. *J Am Chem Soc.* 1974;96:1059-1063.
35. Cox RA, Goldman MF, Yates K. *Can J Chem.* 1979;57:2960-2966.
36. Cox RA, Haldna ÜL, Idler KL, Yates K. *Can J Chem.* 1981;59:2591-2598.
37. Gillespie RJ, Robinson EA, Solomons C. *J Chem Soc.* 1960:4320-4326.
38. Cox RA, Dolenko AJ, Buncel E. *J Chem Soc Perkin Trans 2.* 1975:471-478.
39. Cox RA. *Can J Chem.* 1996;74:1774-1778.
40. Cox RA, Buncel E. *Can J Chem.* 2012;90: in press.
41. Cox RA. *Can J Chem* 2012; 90: in press.
42. Cox RA, Yates K. *Can J Chem.* 1983;61:2225-2243.
43. Moodie RB, Schofield K, Taylor PG, Baillie PJ. *J Chem Soc Perkin Trans 2.* 1981: 842-847.
44. Marziano NC, Traverso PG, Cimino GM. *J Chem Soc Perkin Trans 2.* 1980:574-578.
45. Marziano NC, Tortato C, Sampoli M. *J Chem Soc Perkin Trans 2.* 1991:423-429.
46. Bell RP, Brown AH. *J Chem Soc.* 1954:774-778.
47. Marziano NC, Ronchin L, Tortato C, Zingales A, Sheikh-Osman AA. *J Mol Catal A.* 2001;174:265-277.
48. Marziano NC, Ronchin L, Tortato C, Tonon O, Bertani R. *Int J Chem Kinet.* 2004;36:417-426.
49. Cox RA, Krull UJ, Thompson M, Yates K. *Anal Chim Acta.* 1979;106:51-57.
50. Saito S, Sato Y, Ohwada T, Shudo K. *J Am Chem Soc.* 1994;116:2312-2317.
51. O'Connor MJ, Boblak KN, Topinka MJ, Kindelin PJ, Briski JM, Zheng C, Klumpp DA. *J Am Chem Soc.* 2010;132:3266-3267.
52. Hammett LP, Deyrup AJ. *J Am Chem Soc.* 1932;54:2721-2739.
53. Arnett EM, Mach GW. *J Am Chem Soc.* 1966;88:1177-1183.
54. Katritzky AR, Waring AJ, Yates K. *Tetrahedron.* 1963;19:465-469.
55. Bunnett JF, Olsen FP. *Can J Chem.* 1966;44:1899-1916.
56. Marziano NC, Cimino GM, Passerini RC. *J Chem Soc Perkin Trans 2.* 1973:1915-1922.
57. Cox RA, Yates K. *J Am Chem Soc.* 1978;100:3861-3867.
58. Cox RA, Yates K. *Can J Chem.* 1981;59:2116-2124.
59. Cox RA. *Adv Phys Org Chem.* 2000;35:1-66.
60. Cox RA, Yates K. *Can J Chem.* 1984;62:2155-2160.
61. Cox RA, Yates K. *Can J Chem.* 1979;57:2944-2951.
62. Cox RA. *Acc Chem Res.* 1987;20:27-31.
63. Lee DG, Cameron R. *J Am Chem Soc.* 1971;93:4724-4728.
64. Lee DG, Demchuk KJ. *Can J Chem.* 1987;65:1769-1774.
65. Cox RA, Yates K. *Can J Chem.* 1981;59:1560-1567.

66. Jaques D, Leisten JA. *J Chem Soc.* 1964:2683-2689.
67. Lajunen M, et al. References collected in ref. 41.
68. Lajunen M, Laine R, Aaltonen M. *Acta Chem Scand.* 1997;51:1155-1161.
69. Schubert WM, Quacchia RH. *J Am Chem Soc.* 1963;85:1284-1289.
70. Ruff F, Csizmadia IG. *Organic Reactions: Equilibria, Kinetics and Mechanism*. Amsterdam: Elsevier; 1994. pp. 215 and 222.
71. Bunnett JF, Buncel E. *J Am Chem Soc.* 1961;83:1117-1123.
72. Bunnett JF, Buncel E, Nahabedian KV. *J Am Chem Soc.* 1962;84:4136-4140.
73. Cox RA, Onyido I, Buncel E. *J Am Chem Soc.* 1992;114:1358-1363.
74. Kwon O-H, Mohammed OF. *Phys Chem Chem Phys.* 2012;14:8974-8980.
75. Bell RP, Bascombe KN, McCoubrey JC. *J Chem Soc.* 1956:1286-1291.
76. Bell RP. *Adv Phys Org Chem.* 1966;4:1-29.
77. Hamer D, Leslie J. *J Chem Soc.* 1960:4198-4202.
78. Leininger PM, Kilpatrick M. *J Am Chem Soc.* 1938;60:2891-2899.
79. Vinnik MI, Kislina IS, Bushmakin LG. *Kinet Katal.* 1991;32:282-290.
80. Barnett JW, O'Connor CJ. *J Chem Soc B.* 1971:1163-1165.
81. Cox RA. *J Phys Org Chem.* 1991;4:233-241.
82. Buncel E, Lawton BT. *Can J Chem.* 1965;43:862-875.
83. Buncel E, Cox RA. *J Chem Soc Chem Commun.* 1972:1259-1260.
84. Cox RA, Buncel E. *Can J Chem.* 1973;51:3143-3149.
85. Buncel E, Cox RA, Dolenko AJ. *Tetrahedron Lett.* 1975:215-218.
86. Cox RA, Buncel E. *J Am Chem Soc.* 1975;97:1871-1875.
87. Cheon K-S, Cox RA, Keum S-R, Buncel E. *J Chem Soc Perkin Trans 2.* 1998:1231-1239.
88. Cox RA, Fung DYK, Csizmadia IG, Buncel E. *Can J Chem.* 2003;81:535-541.
89. Buncel E, Keum S-R, Rajagopal S, Kiepek E, Cox RA. *Can J Chem.* 2008;86:298-304.
90. Buncel E, Keum S-R, Rajagopal S, Cox RA. *Can J Chem.* 2009;87:1127-1134.
91. Buncel E. *Mech Mol Migrat.* 1968;1:61-119.
92. Buncel E. *Acc Chem Res.* 1975;8:132-139.
93. Cox RA, Buncel E. In: Patai S, ed. *The Chemistry of the Hydrazo, Azoxy and Azo Groups.*, vol. 1. New York: John Wiley; 1975;Chapter 18: 775–859.
94. Cox RA, Buncel E. In: Patai S, ed. *The Chemistry of the Hydrazo, Azoxy and Azo Groups.*, vol. 2. New York: John Wiley; 1997;Chapter 15: 569–602.
95. Cox RA, Buncel E, Bolduc R. 1971. Unpublished observations.
96. Banger J, Johnson CD, Katritzky AR, O'Neill BR. *J Chem Soc Perkin Trans 2.* 1974: 394-398.
97. Eaborn C, Taylor R. *J Chem Soc.* 1960:3301-3307.
98. Olsson S, Russell M. *Ark Kemi.* 1969–70;31:439-453.
99. Stevens CG, Strickler SJ. *J Am Chem Soc.* 1973;95:3918-3922.
100. Butler AR, Hendry JB. *J Chem Soc B.* 1970:852-854.
101. Greig CC, Johnson CD, Rose S, Taylor PG. *J Org Chem.* 1979;44:745-753.
102. Olsson S. *Ark Kemi.* 1970;32:89-103.
103. Baker R, Eaborn C, Taylor R. *J Chem Soc.* 1961:4927-4930.
104. Gold V, Satchell DPN. *J Chem Soc.* 1956:2743-2746.
105. Russell M, Olsson S. *Ark Kemi.* 1969–70;31:455-466.
106. Satchell DPN. *J Chem Soc.* 1956:3911-3918.
107. Olsson S. *Ark Kemi.* 1970;32:105-110.
108. Gold V, Satchell DPN. *J Chem Soc.* 1955:3609-3618.
109. Swain CG, Stivers EC, Reuwer JF, Schaad LJ. *J Am Chem Soc.* 1958;80:5885-5893.
110. Kresge AJ, Mylonakis SG, Sato Y, Vitullo VP. *J Am Chem Soc.* 1971;93:6181-6188.
111. Cox RA. *Can J Chem.* 1999;77:709-718.

112. Durand J-P, Davidson M, Hellin M, Coussemant F. *Bull Soc Chim Fr.* 1966:43-51.
113. Ellis GWL, Johnson CD. *J Chem Soc Perkin Trans 2.* 1982:1025-1027.
114. Allen AD, Rosenbaum M, Seto NOL, Tidwell TT. *J Org Chem.* 1982;47:4234-4239.
115. Simandoux J-C, Torck B, Hellin M, Coussemant F. *Bull Soc Chim Fr.* 1972:4402-4409.
116. Schubert WM, Lamm B, Keeffe JR. *J Am Chem Soc.* 1964;86:4727-4729.
117. Schubert WM, Lamm B. *J Am Chem Soc.* 1966;88:120-124.
118. Schubert WM, Keeffe JR. *J Am Chem Soc.* 1972;94:559-566.
119. Deno NC, Kish FA, Peterson HJ. *J Am Chem Soc.* 1965;87:2157-2161.
120. Koshy KM, Roy D, Tidwell TT. *J Am Chem Soc.* 1979;101:357-363.
121. Noyce DS, Hartter DR, Miles FB. *J Am Chem Soc.* 1968;90:4633-4637.
122. Noyce DS, Hartter DR, Miles FB. *J Org Chem.* 1968;33:4260-4261.
123. Cox RA, Grant E, Whitaker T, Tidwell TT. *Can J Chem.* 1990;68:1876-1881.
124. Modena G, Rivetti F, Scorrano G, Tonellato U. *J 9Am Chem Soc.* 1977;99: 3392-3395.
125. Noyce DS, Schiavelli MD. *J Am Chem Soc.* 1968;90:1020-1022.
126. Noyce DS, Schiavelli MD. *J Am Chem Soc.* 1968;90:1023-1026.
127. Chokotho NCJ, Johnson CD. *Isr J Chem.* 1985;26:409-413.
128. Banait N, Hojatti M, Findlay P, Kresge AJ. *Can J Chem.* 1987;65:441-444.
129. Noyce DS, DeBruin KE. *J Am Chem Soc.* 1968;90:372-377.
130. Noyce DS, Matesich MA, Peterson PE. *J Am Chem Soc.* 1967;89:6225-6230.
131. Noyce DS, Schiavelli MD. *J Org Chem.* 1968;33:845-846.
132. Allen AD, Chiang Y, Kresge AJ, Tidwell TT. *J Org Chem.* 1982;47:775-779.
133. Cramer P, Tidwell TT. *J Org Chem.* 1981;46:2683-2686.
134. Lajunen M, Laaksonen R. *Acta Chem Scand.* 1988;42:254-255.
135. Chwang WK, Nowlan VJ, Tidwell TT. *J Am Chem Soc.* 1977;99:7233-7238.
136. Lajunen M, Koskinen J-M. *Acta Chem Scand.* 1994;48:788-791.
137. Lajunen M, Kähkönen M. *Acta Chem Scand.* 1992;46:726-731.
138. Cox RA. *Can J Chem.* 1998;76:649-656.
139. Wan P, Modro TA, Yates K. *Can J Chem.* 1980;58:2423-2432.
140. Vinnik MI, Moiseev YV. *Izv Akad Nauk SSSR.* 1983:777-786.
141. Bunnett JF, McDonald RL, Olsen FP. *J Am Chem Soc.* 1974;96:2855-2861.
142. Vinnik MI, Abramovich LD. *Izv Akad Nauk SSSR.* 1972:833-840.
143. Vinnik MI, Smirnov AI. *Kinet Katal.* 1991;32:600-607.
144. Cox RA, Yates K. *Can J Chem.* 1982;60:3061-3070.
145. Edward JT, Welch G, Wong SC. *Can J Chem.* 1978;56:935-940.
146. Edward JT, Wong SC. *J Am Chem Soc.* 1977;99:7224-7228.
147. Edward JT, Wong SC, Welch G. *Can J Chem.* 1978;56:931-934.
148. Ali M, Satchell DPN. *J Chem Soc Chem Commun.* 1991:866-867.
149. Ali M, Satchell DPN. *J Chem Soc Perkin Trans 2.* 1992:219-221.
150. Ali M, Satchell DPN. *J Chem Soc Perkin Trans 2.* 1991:575-578.
151. Joseph VB, Satchell DPN, Satchell RS, Wassef WN. *J Chem Soc Perkin Trans 2.* 1992:339-341.
152. Cox RA, Yates K. *Can J Chem.* 1981;59:2853-2863.
153. Cox RA. *Can J Chem.* 2005;83:1391-1399.
154. Cox RA. *Can J Chem.* 2008;86:290-297.
155. Bunnett JF. *J Am Chem Soc.* 1961;83:4956-4967.
156. Bennet AJ, Slebocka-Tilk H, Brown RS, Guthrie JP, Jodhan A. *J Am Chem Soc.* 1990;112:8497-8506.
157. Guthrie JP. *Can J Chem.* 2005;83:1-8.
158. McClelland RA. *J Am Chem Soc.* 1975;97:5281.
159. Smith CR, Yates K. *J Am Chem Soc.* 1971;93:6578-6583.

160. Rysman de Lockerente S, van Brandt P, Bruylants A, de Buyl-Gaudissart M, Hubert D. *Acad Roy Belg Bull Cl Sci.* 1972;58:180-186.
161. Bunton CA, Farber SJ, Milbank AJG, O'Connor CJ, Turney TA. *J Chem Soc Perkin Trans 2.* 1972:1869-1875.
162. Leisten JA. *J Chem Soc.* 1959:765-768.
163. Shingare MS, Ingle DB, Khanolkar DD. *J Indian Chem Soc.* 1975;52:599-601.
164. Yamana T, Mizukami Y, Tsuji A, Ikuta M. *Chem Pharm Bull.* 1972;20:1778-1784.
165. Liler M. Ref. 30, pp. 189–96.
166. Fersht AR. *J Am Chem Soc.* 1971;93:3504-3515.
167. Rochester CH. *Acidity Functions.* New York: Academic Press; 1971. pp 132–135.
168. Cox RA, Druet LM, Klausner AE, Modro TA, Wan P, Yates K. *Can J Chem.* 1981;59:1568-1573.
169. Markovic DA. *J Serb Chem Soc.* 1994;59:943-948.
170. Cox RA, Kuznetsov LL. 2012; Work in progress.
171. Cox RA. 2012; Work in progress.
172. McClelland RA. *J Am Chem Soc.* 1975;97:3177-3181.
173. Mashima M, Ikeda F. *Bull Chem Soc Jpn.* 1973;46:1366-1371.
174. Mashima M, Ikeda F, Doi T, Nishikawa S. *Bull Chem Soc Jpn.* 1981;54:3659-3664.
175. Zarakhani NG, Borisova EN, Nechaev PP, Zaikov GE. *Izv Akad Nauk SSSR Ser Khim.* 1981:2476-2478.
176. Jagdale MH, Nimbalkar AY. *Acta Cienc Indica.* 1976;2:336-340.
177. Jagdale MH, Nimbalkar AY. *Gazz Chim Ital.* 1979;109:51-54.
178. Cox RA, Yates K. *Can J Chem.* 1984;62:1613-1617.
179. Yates K, McClelland RA. *J Am Chem Soc.* 1967;89:2686-2692.
180. Yates K. *Acc Chem Res.* 1971;4:136-144.
181. Rodima TK, Haldna ÜL. *Org React.* 1975;11:777-784.
182. Siigur JR, Mägi M, Haldna ÜL, Lippmaa E. *Reakts Sposobn Org Soedin.* 1971;8: 267-276.
183. Bunton CA, James DH, Senior JB. *J Chem Soc.* 1960:3364-3367.
184. McClelland RA. *Can J Chem.* 1975;53:2763-2771.
185. McClelland RA. *Can J Chem.* 1975;53:2772-2780.
186. Salomaa P. *Acta Chem Scand.* 1957;11:132-140.
187. Cox RA, Yates K. *J Org Chem.* 1986;51:3619-3624.
188. Motie RE, Satchell DPN, Wassef WN. *J Chem Soc Perkin Trans 2.* 1992:859-860.
189. Motie RE, Satchell DPN, Wassef WN. *J Chem Soc Perkin Trans 2.* 1993:1087-1090.
190. Satchell DPN, Wassef WN. *J Chem Soc Perkin Trans 2.* 1992:1855-1856.
191. Satchell DPN, Wassef WN, Bhatti ZA. *J Chem Soc Perkin Trans 2.* 1993:2373-2379.
192. Ruff F, Farkas Ö. *J Phys Org Chem.* 2011;24:480-491.
193. See references collected in Ref. 192.
194. Cox RA. *Can J Chem.* 1996;74:1779-1783.
195. Eckert-Maksic M, Maskill H, Zrinski I. *J Chem Soc Perkin Trans 2.* 2001:2147-2154.
196. Cox RA. *Can J Chem.* 1997;75:1093-1098.
197. Cox RA, Stewart R. *J Am Chem Soc.* 1976;98:488-494.
198. Cox RA, Stewart R, Cook MJ, Katritzky AR, Tack RD. *Can J Chem.* 1976;54: 900-904.
199. More O'Ferrall RA. *J Chem Soc Perkin Trans 2.* 1972:976-982.
200. Bagno A, Scorrano G, Terrier F. *J Chem Soc Perkin Trans 2.* 1990:1017-1027.
201. Bagno A, Scorrano G, Terrier F. *J Chem Soc Perkin Trans 2.* 1991:651-655.
202. Mata-Segreda JF. *J Am Chem Soc.* 2002;124:2259-2262.
203. Haeffner F, Hu C-H, Brinck T, Norin T. *J Mol Struct (Theochem).* 1999;459:85-93.
204. Hori K, Hashitani Y, Kaku Y, Ohkubo K. *J Mol Struct (Theochem).* 1999;461-462:589-596.
205. Marlier JF. *J Am Chem Soc.* 1993;115:5953-5956.

206. Astrat'ev AA, Vorob'eva EN, Kuznetsov LL, Gidaspov BV. *Zh Org Khim*. 1979;15:1136-1138.
207. Vorob'eva EN, Kuznetsov LL, Gidaspov BV. *Zh Org Khim*. 1983;19:698-704.
208. Glukhov AA, Kuznetsov LL, Gidaspov BV. *Zh Org Khim*. 1983;19:704-707.
209. Pearson RG, Songstad J. *J Am Chem Soc*. 1967;89:1827-1836.
210. Leiman SN, Astrat'ev AA, Kuznetsov LL, Selivanov VF. *Zh Org Khim*. 1979;15: 2259-2263.
211. Drozdova OA, Astrat'ev AA, Kuznetsov LL, Selivanov VF. *Zh Org Khim*. 1982;18:2335-2340.
212. Drozdova OA, Astrat'ev AA, Kuznetsov LL, Selivanov VF. *Zh Org Khim*. 1983;19:761-766.
213. Challis BC, Rosa E, Iley J, Norberto F. *J Chem Soc Perkin Trans 2*. 1990:179-183.
214. Dewhurst F, Lamberton AH. *J Chem Soc B*. 1971:788-789.
215. Cox RA. *J Chem Soc Perkin Trans 2*. 1997:1743-1750.
216. Cox RA, Smith CR, Yates K. *Can J Chem*. 1979;57:2952-2959.
217. Zucker L, Hammett LP. *J Am Chem Soc*. 1939;61:2791-2798.
218. Chiang Y, Kresge AJ, More O'Ferrall RA, Murray BA, Schepp NP, Wirz J. *Can J Chem*. 1990;68:1653-1656.
219. Baigrie LM, Cox RA, Slebocka-Tilk H, Tencer M, Tidwell TT. *J Am Chem Soc*. 1985;107:3640-3645.
220. Cox RA, McAllister MA, Roberts KA, Stang PJ, Tidwell TT. *J Org Chem*. 1989;54:4899-4902.
221. Bégué J-P, Benayoud F, Bonnet-Delpon D, Allen AD, Cox RA, Tidwell TT. *Gazz Chim Ital*. 1995;125:399-402.
222. Cox RA, Cheon K-S, Buncel E. *Can J Chem*. 1998;76:896-906.
223. Cox RA, Moore DB, McDonald RS. *Can J Chem*. 1994;72:1910-1914.
224. Bruice PY. *Organic Chemistry*. 5th ed. Upper Saddle River, NJ: Pearson Prentice-Hall; 2007. pp. 372–375.
225. Ingold CK. *Structure and Mechanism in Organic Chemistry*. 2nd ed. Ithaca, NY: Cornell University Press; 1969.
226. Solomons TWG, Fryhle CB. *Organic Chemistry*. 7th ed. New York: Wiley; 2007. p. 242.
227. Luong TQ, Verma PK, Mitra RK, Havenith M. *J Phys Chem A*. 2011;115:14462-14469.
228. Beck JM, Miller SM, Peczuh MW, Hadad CM. *J Org Chem*. 2012;77:4242-4251.
229. Tulub AA. *Phys Chem Chem Phys*. 2006;8:2187-2192.
230. Harvey JN, Zurek J, Pentikäinen U, Mulholland AJ. *Phys Chem Chem Phys*. 2006;8:3566-3567.

CHAPTER TWO

New Applications of Isotope Effects in the Determination of Organic Reaction Mechanisms

Matthew P. Meyer
Department of Chemistry and Chemical Biology, University of California, Merced, CA 95343, USA
Current address: 5200 N. Lake Rd., Merced, CA 95343
E-mail: mmeyer@ucmerced.edu

Contents

Abstract

Our understanding of the basic physical processes that govern chemical reactions has put us at the cusp of beginning to understand, in stark detail, the way in which reactivity and selectivity are determined in organic reactions. Recent efforts at new

Advances in Physical Organic Chemistry, Volume 46
ISSN 0065-3160,
http://dx.doi.org/10.1016/B978-0-12-398484-5.00002-X

experimental design coupled with the advent of enabling technologies have created a target-rich environment for the physical organic chemist. Additionally, computational chemistry has continued to develop apace of experiment in a manner that has facilitated the integration of experimental and computational efforts in the study of reaction mechanism. Few endeavors demonstrate the synergy of experiment and theory more convincingly than the study of isotope effects. This review will begin by introducing isotope effects using both mathematical and conceptual constructs. The second major section of this review will cover recent experimental and computational advancements in isotope effect methodologies. The third section of this review will take a systems approach that will highlight areas of chemical and biochemical mechanism in which isotope effects are advancing those fields. Finally, this review will look forward to the major challenges in chemical mechanism and identify areas where isotope effects may be critical to achieving vertical advancements.

1. SCOPE AND PURPOSE FOR THIS REVIEW

Isotope effects find application in diverse fields spanning nearly all of the physical sciences. This chapter aims to review recent progress in the measurement, application, and interpretation of kinetic and equilibrium isotope effects (EIEs) as they are utilized in organic and biological chemistry. A monograph[1] and textbook[2] that explore methods of isotope effect measurement and systems in which their study has played a decisive role have been published recently. This review seeks to be largely complementary to those texts and seeks to approach the subject of isotope effects in two ways: (1) a methods approach and (2) a systems approach. Method development has been one of the most important aspects of isotope effect measurement that has helped to maintain vitality in the field. As new hypotheses develop in both emerging and established fields, new methods must often be developed to test them. This feature has made isotope effect measurement a key tool in the exploration of both small molecule and enzyme-catalyzed reactions. Complementary and synergistic with method development is the identification of systems in which isotope effects can shed new light on misunderstood phenomena. Examples taken from the literature will be utilized to demonstrate concepts. This is done partially to calibrate the reader quantitatively and to place examples in the concrete so that the reader can seek out the original publications for more in-depth information.

Although physical organic chemistry has enabled a much greater understanding of entire classes of reaction mechanisms, mechanistic organic chemistry remains a largely explicative (rather than predictive) endeavour. Recent efforts have brilliantly illustrated the capacity of isotope effect measurements to

elucidate mechanism in reactions as simple as small molecule gas-phase reactions and as complex as enzyme-catalyzed reactions occurring in solution. As isotope effect measurements continue to augment our understanding of the physical processes that underlie chemical reactivity and selectivity, our abilities to predict chemical behaviour will necessarily increase – leading to more successful rational efforts in new reaction development and the study and manipulation of complex biochemical phenomena.

The purpose of the present review is threefold: The first goal is to provide an introduction to isotope effects to the nonspecialist. Kinetic isotope effect (KIE) studies can be immensely useful in constructing models of transition structures and conferring information regarding rate and product determination. Ancillary to the first goal of this review is the goal of illustrating how traditional and recently developed methods of measuring isotope effects can accelerate efforts in more applied fields, such as the development of asymmetric synthetic methodology. Finally, this review is intended as something of an update for practitioners of isotope effect measurement. While it is likely that many specialists will be aware of developments in the field, it is a strange trick of coincidence that isotope effect studies in chemistry tend to partition into three categories (enzyme mechanism, small molecule organic reaction mechanism, and quantum phenomena), and communication between specialists in those fields tends to be imperfect.

2. GENERAL INTRODUCTION AND BACKGROUND

Experimental mechanistic studies typically fall into one or more of four classes of measurements: (1) structural studies, (2) measurements of the separation of energy levels (spectroscopy), (3) absolute kinetics, and (4) relative (or comparative) kinetics. Under the simplest interpretation (see below), isotope effects reflect changes in the force constants of bonds. As such, KIEs reflect the manner in which structure determines energetics and therefore occupy the interface of structural and energetic studies. KIE measurements are perhaps the finest exemplum of the fourth class of measurement as isotopic substitution can alter kinetics without affecting the potential energy surface that describes the reaction. Interpretation of KIEs, via reactant and transition structure calculations, confers detailed structural information about the transition structure and the energy required to achieve the rate-limiting transition state. As a consequence, KIE studies are one of the most informative mechanistic methods in the physical organic toolbox.

A KIE is simply the ratio of rate constants for two isotopologs (compounds of identical chemical composition but which differ only in isotopic composition) or isotopomers (isomers having the same number of each isotopic atom but differing in their positions).[3] KIEs are typically reported as k_{light}/k_{heavy}, where k_{light} is the rate constant for conversion of the light (or less massive) isotopolog, and k_{heavy} is the corresponding rate constant for conversion of the heavy (or more massive) isotopolog. KIEs are also typically classified as being either primary (1°) or secondary (2°). Primary KIEs arise at positions where bond breaking or bond forming occurs. Secondary KIEs reflect the effect of isotopic substitution at positions excluding those at which bonds are broken or formed. Simple E2 reactions can be used to explain key differences between 1° and 2° KIEs. Figure 2.1 illustrates a 1°-^{2}H KIE. Following a discussion of primary KIEs, Fig. 2.3 is used to illustrate a 2°-^{3}H KIE in an E2 reaction.

As a first approximation, primary KIEs can be thought of in the following way: Bonds that are broken (or formed) in an elementary reaction step have no restoring force at the transition state. As a consequence, the zero-point energy contained in the intact bond in the reactant is not present in the transition state. The ultimate consequence of this situation is that the difference in zero-point energy between the light and heavy reactant isotopologs determines the difference in free energy of reaction between the two isotopologs, with the light isotopolog having a lower free energy of

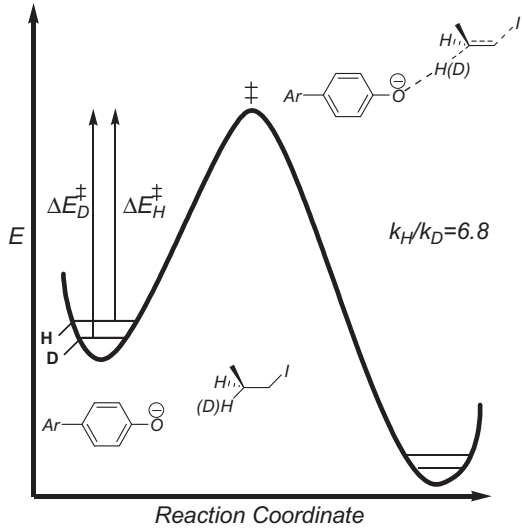

Figure 2.1 Simplistic model for the origins of a 1°-^{2}H KIE in an E2 reaction.

activation (Fig. 2.1). If one considers bond breaking in a typical sp^3 C—H bond with a frequency of 3000 cm^{-1}, the corresponding zero-point energies for the C—H and C—D are approximately 4.29 and 3.03 kcal mol^{-1}. Assuming contributions from zero-point energy only, the resulting KIE at 25 °C is $k_H/k_D = 8.35$. The above model is a gross approximation. In bimolecular reactions, the transition structure possesses five vibrational modes (of real frequency) in addition to those contained in the reactants. Westheimer developed a model to take these considerations into account in bimolecular proton transfers.[4] The essence of the Westheimer model is that the compensatory symmetric vibration (Fig. 2.2) is the strongest for strongly exoergic or endoergic reactions. This effect leads to retention of zero-point energy in vibrations in which the transferred hydrogen atom participates, thus reducing the resultant primary KIE. This concept can be envisioned structurally, as well. Consider a model system where D—H represents the hydrogen donor and A represents the hydrogen acceptor. For an extremely exoergic reaction, the transition state is nearest in identity to the reactant. The symmetric vibration consequently retains much of the force constant present in the D—H bond in the reactant. For ergoneutral reactions, a balance in D—H breaking and A—H formation is achieved. As a consequence, the symmetric vibration can be approximated as involving little hydrogenic motion, removing the isotopic dependence upon the zero-point energy contained in this vibration at the transition state. To summarize Westheimer's conclusions: Compensatory vibrational modes contribute minimally for fundamental reaction steps for which $\Delta G^\circ = 0$, making primary KIEs a maximum for ergoneutral reactions (Fig. 2.2).

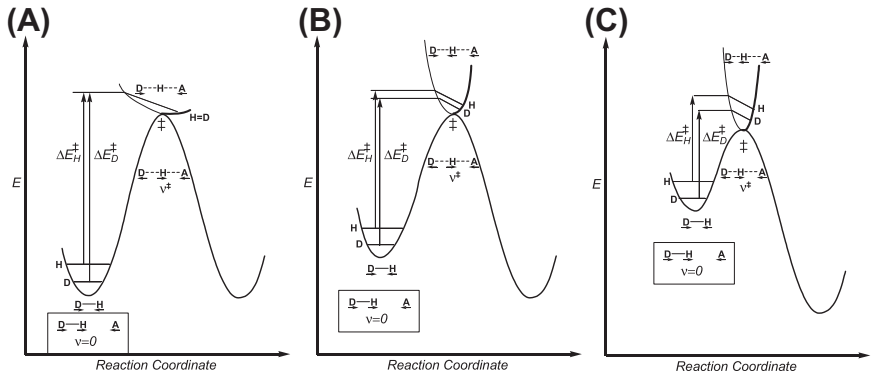

Figure 2.2 Illustration of the Westheimer model for 1°-^{2}H KIEs and its prediction of maximal KIEs for isoergic hydrogen transfers.

The Westheimer model is rooted in what is most commonly termed, 'semiclassical transition state theory'.[5] Although semiclassical transition state theory typically works well for reactions excluding those in which hydrogen transfer is involved, it is really a conflicted model, allowing bound vibrations to be considered quantum mechanically, while the imaginary mode that defines the reaction coordinate at the first-order saddle point is treated classically. This can be best understood by considering the expression for KIEs derived from semiclassical rate theory (Eqn 2.1a–d). The expression for KIEs can be further simplified by invoking the Teller–Redlich[6] product rule (Eqn 2.2) to yield the Bigeleisen–Mayer[7,8] equation (Eqn 2.3). The imaginary frequency prefactor arises as a result of the Teller–Redlich rule. The $3N^{\ddagger}$-7-bound vibrational modes in the transition structure and the $3N$-6 vibrational modes in the reactant(s) are treated as quantized with zero-point energy arising as a consequence of the Heisenberg uncertainty principle. Contributions from the molecular masses and moments of inertia can be collected into a single product which is designated as MMI in Eqn 2.1b. The zero-point energy (ZPE) and excitation (EXC) terms arise from the quantization of the bound vibrational states (Eqn 2.1c and d). The imaginary frequency term, when framed completely within the Bigeleisen–Mayer equation, reflects the effects of isotopic substitution upon the reduced mass of the imaginary mode associated with a first-order saddle point.

$$\frac{k_1}{k_2} = \mathrm{MMI} \times \mathrm{EXC} \times \mathrm{ZPE} \tag{2.1a}$$

$$\mathrm{MMI} = \left(\frac{M_1^{\ddagger}}{M_2^{\ddagger}} \times \frac{M_2}{M_1}\right)^{3/2} \left(\frac{I_{\mathrm{A},1}^{\ddagger} I_{\mathrm{B},1}^{\ddagger} I_{\mathrm{C},1}^{\ddagger}}{I_{\mathrm{A},2}^{\ddagger} I_{\mathrm{B},2}^{\ddagger} I_{\mathrm{C},2}^{\ddagger}} \times \frac{I_{\mathrm{A},2} I_{\mathrm{B},2} I_{\mathrm{C},2}}{I_{\mathrm{A},1} I_{\mathrm{B},1} I_{\mathrm{C},1}}\right)^{1/2} \tag{2.1b}$$

$$\mathrm{EXC} = \prod_{i-1}^{3N^{\ddagger}-7} \frac{1-\exp(-h\nu_{i,2}^{\ddagger}/kT)}{1-\exp(-h\nu_{i,1}^{\ddagger}/kT)} \prod_{i-1}^{3N-6} \frac{1-\exp(-h\nu_{i,1}/kT)}{1-\exp(-h\nu_{i,2}/kT)} \tag{2.1c}$$

$$\mathrm{ZPE} = \prod_{i-1}^{3N^{\ddagger}-7} \frac{\exp(h\nu_{i,2}^{\ddagger}/2kT)}{\exp(h\nu_{i,1}^{\ddagger}/2kT)} \prod_{i-1}^{3N-6} \frac{\exp(h\nu_{i,1}/2kT)}{\exp(h\nu_{i,2}/2kT)} \tag{2.1d}$$

$$\left(\frac{M_1}{M_2}\right)^{3/2} \left(\frac{I_{\mathrm{A},1} I_{\mathrm{B},1} I_{\mathrm{C},1}}{I_{\mathrm{A},2} I_{\mathrm{B},2} I_{\mathrm{C},2}}\right)^{1/2} = \prod_{j=1}^{3N-6} \frac{\nu_{j,1}}{\nu_{j,2}} \prod_{i-1}^{N} \left(\frac{m_{i,1}}{m_{i,2}}\right)^{3/2} \tag{2.2}$$

$$\left(\frac{k_1}{k_2}\right)_{\text{semiclassical}} = \frac{\nu^{\ddagger}_{im,1}}{\nu^{\ddagger}_{im,2}} \frac{\prod_{i-1}^{3N^{\ddagger}-7} \frac{\nu^{\ddagger}_{i,1}}{\nu^{\ddagger}_{i,2}} \frac{\exp(h\nu^{\ddagger}_{i,2}/2kT)}{\exp(h\nu^{\ddagger}_{i,1}/2kT)} \frac{1-\exp(-h\nu^{\ddagger}_{i,2}/kT)}{1-\exp(-h\nu^{\ddagger}_{i,1}/kT)}}{\prod_{i-1}^{3N-6} \frac{\nu_{i,1}}{\nu_{i,2}} \frac{\exp(h\nu_{i,2}/2kT)}{\exp(h\nu_{i,1}/2kT)} \frac{1-\exp(-h\nu_{i,2}/kT)}{1-\exp(-h\nu_{i,1}/kT)}} \tag{2.3}$$

Very early in the history of primary KIEs, Bell recognized that tunneling could have profound effects upon both the magnitude and temperature dependence of primary KIEs. He developed a multiplicative tunnel correction (Eqn 2.4a) based on Wentzel-Kramers-Brillouin theory[9] that approximated a correction for tunneling based on the permeability of a truncated (Eqn 2.4b)[10] or infinite parabolic barrier (Eqn 2.4c).[11] The barrier height, $V_1^{\ddagger}$, is the difference between the zero-point energy and the first-order saddle point and is therefore isotope dependent.[12] Bell's treatment, as developed, was only intended as a correction. The limitations in any model are rooted in the assumptions or approximations inherent to the model. The general problem with Bell's approach is that it is a 'zero-curvature' approximation. In other words, Bell's approach assumes that the tunneling event penetrates the barrier along the reaction coordinate. This is, in general, only a good approximation for reactions that are not profoundly affected by tunneling. It has long been recognized that tunneling, which is omnipresent in chemical reactions, can have profound effects upon the reaction pathway itself. When the dividing surface between the reactant(s) and product(s) is crossed at a point that differs significantly from the first-order saddle point, it can be expected that the Bigeleisen–Mayer equation will no longer yield quantitative agreement with experimentally determined KIE measurements. Below, recent developments in theoretical treatments of tunneling are briefly summarized in the context of recent experimental efforts. Dynamical effects, which result from semiclassical deviations from the minimum energy path (MEP) and effects that arise from a shift in the surface that divides reactant(s) and product(s), are treated in a later section.

$$\left(\frac{k_1}{k_2}\right)_{\text{quantum}} = \left(\frac{Q_{t,1}}{Q_{t,2}}\right)\left(\frac{k_1}{k_2}\right)_{\text{semiclassical}} \tag{2.4a}$$

$$Q_{t,1} = \frac{h\nu^{\ddagger}_{im,1}/2kT}{\sin(h\nu^{\ddagger}_{im,1}/2kT)} - \sum_{n=1}^{\infty}(-1)^n \frac{\exp\left(\frac{(h\nu^{\ddagger}_{im,1}/kT - 2n\pi) \times (V_1^{\ddagger}/kT)}{h\nu^{\ddagger}_{im,1}/kT}\right)}{\frac{h\nu^{\ddagger}_{im,1}/kT - 2n\pi}{h\nu^{\ddagger}_{im,1}/kT}} \tag{2.4b}$$

$$Q_{t,1} = \frac{h\nu^{\ddagger}_{im,1}/2kT}{\sin(h\nu^{\ddagger}_{im,1}/2kT)} \tag{2.4c}$$

Primary KIEs have held a prominent place in the study of reaction mechanism. One of the most common uses of primary KIEs is in the testing of mechanistic hypotheses.[13–19] Intermolecular isotopic fractionation is determined by the rate-determining step in a chemical reaction. The presence of a substantial ^{2}H or ^{3}H KIE or a significant ^{13}C KIE ($^{12}k/^{13}k \geq 1.010$) is often accepted as evidence of rate-limiting bond breaking or bond formation at a given position. Other heavy-atom isotope effects have also proven important in identifying rate-determining steps, including ^{12}C/^{14}C, ^{14}N/^{15}N, ^{16}O/^{17}O, ^{16}O/^{18}O, or ^{35}Cl/^{37}Cl.[20–24] The magnitudes of primary KIEs are also used to make assertions regarding the position of the transition state along the reaction coordinate. In irreversible reactions, early transition states are traditionally assumed to yield smaller KIEs than late transition states; however, as shall be discussed below, numerous caveats must be considered in interpreting the magnitudes of KIEs in the absence of a reliable structural model. One class of reactions in which the magnitudes of 1°-^{2}H KIEs are particularly telling are C—H activations. Insertions are generally assumed to yield diminutive 1°-^{2}H KIEs, while proton-coupled electron transfer and hydrogen atom abstraction are assumed to yield sizable KIEs – often exceeding the semiclassical limit of $k_H/k_D \approx 7$. As will be discussed below, insight into a host of mechanistic nuances involved in C—H bond breaking can be gained using KIEs.

KIEs have been the most useful observables in the study of tunneling. Historically, 1°-^{2}H and 1°-^{3}H KIEs have been the principal metrics by which the importance of hydrogen tunneling is estimated;[25] however, over the past several years new ways of looking at this interesting phenomenon have arisen (see below). Conventional interpretations of 1°-^{2}H KIEs have placed somewhat arbitrary bounds upon what is considered behavior indicative of tunneling and that which is explicable via transition state theory. It is somewhat unfortunate that, because of historical influence, the lingua franca used to describe tunneling phenomena utilizes parameters from the Arrhenius equation. Patently quantum mechanical behavior can yield isotope effects whose temperature dependence is well within the accepted 'semiclassical' boundaries defined by isotope effects upon Arrhenius parameters. Stern and Weston, who delineated the boundaries for semiclassical and quantum Arrhenius behavior, noted that reactions in which tunnelling has profound effects upon reactivity can exhibit isotope effects

upon Arrhenius parameters that are within the semiclassical regime.[26] Giagou and Meyer recently provided an example of this behavior in the *syn*-β-elimination step in the Swern oxidation.[27]

Although the distinction between 1° and 2° KIEs is often somewhat arbitrary, in general 2° KIEs are taken to be changes in rate due to isotopic substitution at positions at which bonds are neither broken nor formed. Historically, 2°-^{2}H KIEs have been those most often measured, and they have been classified by how far they are removed from the primary bond-breaking or bond-forming process, i.e. α, β, γ, etc. The vast majority of 2°-^{2}H and ^{3}H KIEs that have been measured are α (attached to the atom at which bond making or bond breaking occurs) or β (attached to the atom which is adjacent to the position of bond making or bond breaking). Customarily, 2°-^{2}H KIEs are commonly ascribed to one or more of several physicochemical processes: (1) hybridization change, (2) hyperconjugation, (3) steric repulsion, (4) inductive effects, and (5) conformational change. Needless to say, the putative origins of 2°-^{2}H KIEs are not mutually exclusive, and observed KIEs can result from a combination of the physicochemical origins listed above.[28,29]

Perhaps exploring 2° KIEs using a positional progression will help to highlight the various origins of these isotope effects. Secondary ^{2}H and ^{3}H KIEs occurring at the α-position have been most commonly utilized in addition to multiple bonds (e.g. carbonyl additions, olefin hydrogenations, etc.), eliminations to form multiple bonds (e.g. oxidations, eliminations, etc.), and both unimolecular and bimolecular substitutions. In general, α-2° KIEs are dominated by hybridization changes. Partial conversion of a carbon center from sp^2 to sp^3 at the transition state results in a generally tighter manifold of vibrations, yielding an inverse ($k_{light}/k_{heavy} < 1.0$) ^{2}H or ^{3}H KIE. Conversely, partial conversion of a carbon center from sp^3 to sp^2 at the transition state results in a generally looser manifold of vibrations, yielding a normal ($k_{light}/k_{heavy} < 1.0$) ^{2}H or ^{3}H KIE (Fig. 2.3).[30] Vibrational manifolds that give rise to KIEs under these scenarios are often described as being dominated by contributions from out-of-plane vibrations.[31] However, changes in the force constants of C—H stretching modes can also contribute substantially or even dominate the observed effect.[32–34] Separately, Halevi[35] and Streitweiser[36] suggested that, in reactions where an electron-poor center is generated in the rate-limiting step, normal ($k_H/k_D > 1.0$) contribution to the KIE can originate from the more electropositive nature of deuterium. This effect is described as originating from the anharmonicity associated with the C—H(D) bond. The more closely associated C—D bond places electrons

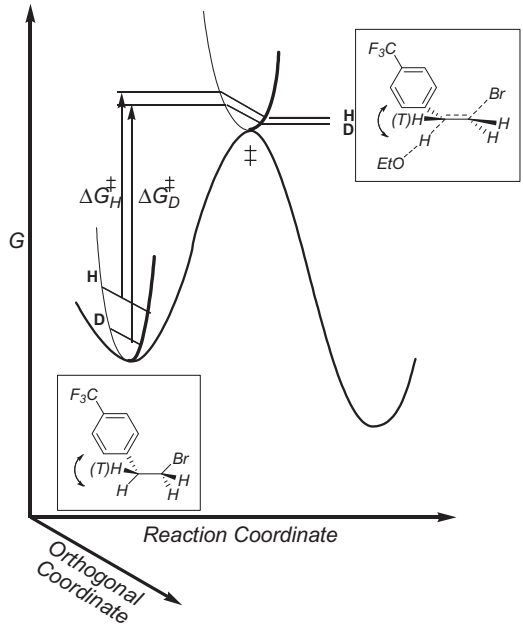

Figure 2.3 Illustration of a normal α-2°-^{3}H KIE in an E2 reaction.

closer to the carbon atom. The net influence of this effect would act in opposition to hybridization effects in α- or β-2° KIEs that result from hybridization change or hyperconjugation, respectively. Upon closer inspection, however, it must be conceded that, if anharmonicity were responsible for what have been termed electrostatic isotope effects, computed estimates of 2°-^{2}H KIEs would deviate systematically from measured values. This has not been borne out by comparisons of experimental and computed 2°-^{2}H KIEs. The first report of these conflicting contributions to observed KIEs was reported by Williams.[32]

Here we will highlight concrete examples to illustrate the utility of secondary KIEs. In Scheme 2.1A, the normal α-2°-^{2}H KIEs associated with Lewis acid promoted formation of dialkyl ethers from methoxymethyl ethers suggest that the rate-limiting step involves the formation of an oxacarbenium intermediate.[37] In Scheme 2.1B, the normal α-2°-^{2}H KIE results from the partial conversion of the reactive carbon center from sp^3 to sp^2.[28] In carbonyl additions to aldehydes, partial conversion of the α-center from sp^2 in the reactant to an sp^3 center at the transition state results in a higher force constant associated with R-C-H(D) bending vibrations. Tighter vibrations at the transition state, relative to those present in the reactant, result in an inverse ^{2}H

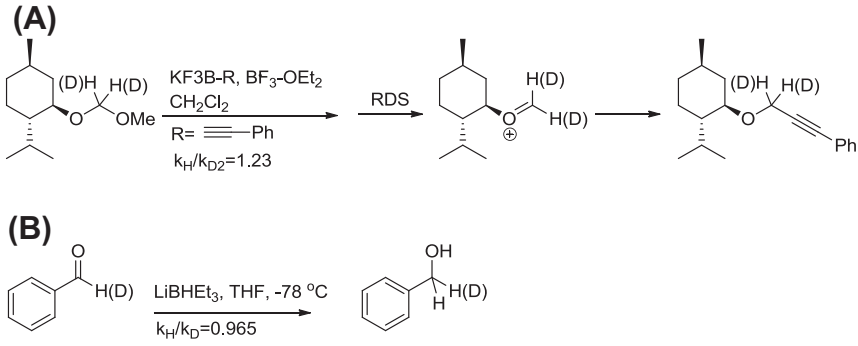

Scheme 2.1 Examples of α-2° ^{2}H KIEs: (A) normal α-2°-^{2}H KIE associated with rate-limiting conversion of an sp^{3} centre to an sp^{2} centre. (B) Inverse α-2°-^{2}H KIE associated with rate-limiting conversion of an sp^{2} centre to an sp^{3} centre.

KIE. An explicit example of this is shown in Scheme 2.1B.[38] In addition to supporting mechanistic scenarios, α-2° KIEs can be used to gain quantitative information regarding the transition structure. In a recent study, Kim et al. used variational transition state theory in conjunction with a small curvature tunneling (SCT) correction and implicit solvent model to predict the 1°-^{2}H, 2°-^{2}H, and 1°-^{18}F/^{19}F KIEs for the elimination of HF from 4-fluoro-4-(4′-nitrophenyl)butane-2-one by acetate and imidazole in 75% aqueous ethanol. Various computational metrics of reaction progress are compared to substantially different 2°-^{2}H KIEs observed when imidazole ($k_H/k_D = 1.014 \pm 0.0017$) or acetate ($k_H/k_D = 1.038 \pm 0.0013$) is utilized as the base.[39] As will be discussed below, α-2° KIEs have also been useful in the study of tunneling in hydride transfer reactions.

Because the magnitude of β-2°-^{2}H KIEs can often be correlated with geometric features of the transition structure, they are arguably the most informative class of secondary ^{2}H effects. For the majority of cases, β-2°-^{2}H KIEs result from changes in hyperconjugation that, in turn, result from hybridization changes at the adjacent α-position.[40–44] Hyperconjugation can most easily be conceptualized as the energetically favorable donation from a filled C—H sp^{3} orbital into an empty (or partially filled) p-orbital (Fig. 2.4A). As is shown in Fig. 2.4A, donation of the filled σ(C—H) orbitals into the nascent empty p-orbital weakens the C—H stretching force constant, making the zero-point energy difference between the C—H versus the C—D bond smaller. In reactions where hyperconjugative donation increases in the transition state, this interaction results in a normal ($k_H/k_D > 1$) isotope effect. Conversely, transition states that result in attenuated hyperconjugation result in an inverse isotope ($k_H/k_D < 1$) effect. Adjacent orbital overlap depends

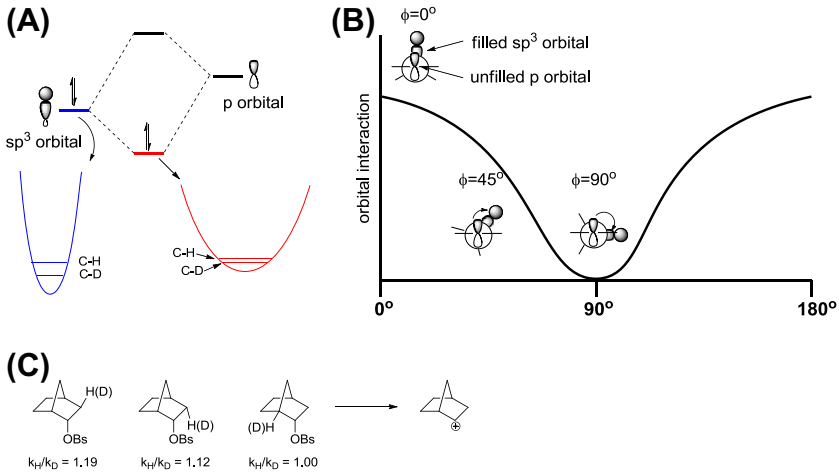

Figure 2.4 Illustration of (A) β-2°-^{2}H KIEs in an S_N1 reaction, (B) a pictorial description of orbital overlap dependence that makes β-2° KIEs useful in determining transition structure geometry, and (C) an exemplum employing β-2°-^{2}H KIEs arising during the solvolysis of norbornyl brosylates. For color version of this figure, the reader is referred to the online version of this book.

upon $\cos^2\varphi$, where φ is the angle between donor and acceptor p-orbitals (Fig. 2.4B), yielding maximal KIEs for 0° and 180°, while an angle of 90° yields a minimal KIE.[45–47] Perhaps the clearest expression of the angular dependence of hyperconjugation and its effect upon observed β-2°-^{2}H KIEs have been demonstrated on solvolyses of *exo*-2-norbornyl brosylates. Because of this angular dependence, the ^{2}H KIE at the bridgehead position of *endo*-norbornyl brosylate in Fig. 2.4C is negligible, while *endo*- or *exo*-labeling of the 2-position yields a sizable effect. Abundant examples of β-2°-^{2}H KIEs can be found in the extensive solvolysis literature. It is worth noting that β-2°-^{2}H KIEs that reflect isotopic substitution at methyl positions are conformationally independent within the framework of the above model under the assumption of 120° H–C–H dihedral angles within the methyl rotor.

The simple paradigm for understanding the effect of hyperconjugation upon ^{2}H and ^{3}H KIEs is that hyperconjugation weakens sp^3 C—H bonds via the mechanism shown in Fig. 2.4A. For this reason, increased hyperconjugation in the transition state leads to a normal ($k_H/k_{D,T} > 1.0$) KIE, while decreased hyperconjugation in the transition state leads to an inverse ($k_H/k_{D,T} < 1.0$) KIE. In Scheme 2.2A, the inverse β-2°-^{2}H KIE expressed on the bimolecular rate constant for the *Drosophila melanogaster* acetylcholinesterase-catalysed hydrolysis of acetylcholine, $^D(k_{cat}/K_M)$, is likely due to the partial conversion of the thioester carbonyl into an sp^3 center at the transition state for

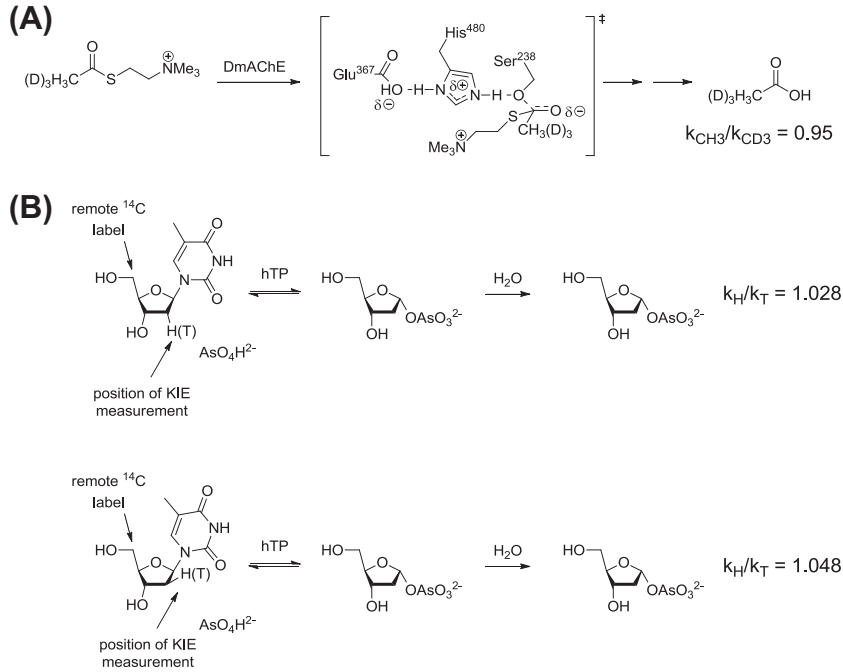

Scheme 2.2 Examples of β-2°-^{2}H KIEs: (A) inverse β-2°-^{2}H KIE associated with rate-limiting conversion (at low substrate concentration) of an sp^2 centre to an sp^3 centre. (B) Normal β-2°-^{2}H KIE associated with rate-limiting conversion of an sp^3 centre to a centre possessing modest sp^2 character.

attack of Ser upon the carbonyl center.[48] Attenuation of hyperconjugative donation of the CH_3/CD_3 into the π^* orbital of the carbonyl occurs upon partial conversion of the carbonyl carbon into an sp^3 center, increasing the sp^3 C—H stretch force constants. By contrast, arsenolysis of thymidine by human thymidine phosphorylase yields a modest normal β-2°-^{2}H KIE for both 2′-β-positions on thymidine. Transition structure modeling suggests that an associative rate-limiting S_N2-like transition state with much less oxacarbenium character than would be expected from a formal S_N1 mechanism.[49] At the simplest level, it appears that hyperconjugative weakening of C—H bonds at the 2′-position on thymidine results in the observed normal KIEs of $k_H/k_T = 1.028$ and $k_H/k_T = 1.048$ (Scheme 2.2B). Although β-2°-^{2}H KIEs are often interpreted solely in terms of hyperconjugation, it has been shown computationally that inductive effects can operate in opposition to hyperconjugation in gas-phase models of heterolysis.[50]

More remote secondary KIEs, such as γ-2°-^{2}H KIEs, have been measured on systems where through-space orbital interactions have been

thought to be important. Scheme 2.3A shows normal γ-2°-^{2}H KIEs associated with the solvolyses of *exo*-2-norbornyl brosylates.[51] These isotope effects are considered indicative of nonclassical ion behavior and are some of the most compelling evidence for through-space orbital interactions in the 2-norbornyl cation system. It should be noted that γ-2°-^{2}H KIEs are not observed in the solvolyses of *endo*-2-norbornyl brosylates. In other systems, the remote ^{2}H KIE is thought to reflect changes in going from reactant to the rate-limiting transition state that are distinct from bonding or electronic changes (Scheme 2.3B). In an interesting example, Ko and Robertson report an inverse γ-2°-^{2}H KIE for the solvolysis of dimethylsulfamoyl chloride that is thought to be due to the interaction of the solvent shell with the methyl groups.[52] There is substantial support for an S_N1 mechanism in this reaction. The presence of an inverse ^{2}H KIE suggests that any influence from hyperconjugative donation is overwhelmed by a competing effect. It is plausible that the observed inverse KIE results from repulsive interactions with solvent or the formation of an ion pair with its additional requirements upon solvent structure. However, an alternative explanation might be the attenuation of hyperconjugative donation of the nitrogen lone pair into σ*(C—H) orbitals on the *N*-methyl groups as the nitrogen lone pair stabilizes the formation of an adjacent positive charge on the sulfur center. The net effect of strengthening C—H stretching vibrations in the partially cationic transition state would also yield an inverse ^{2}H KIE.

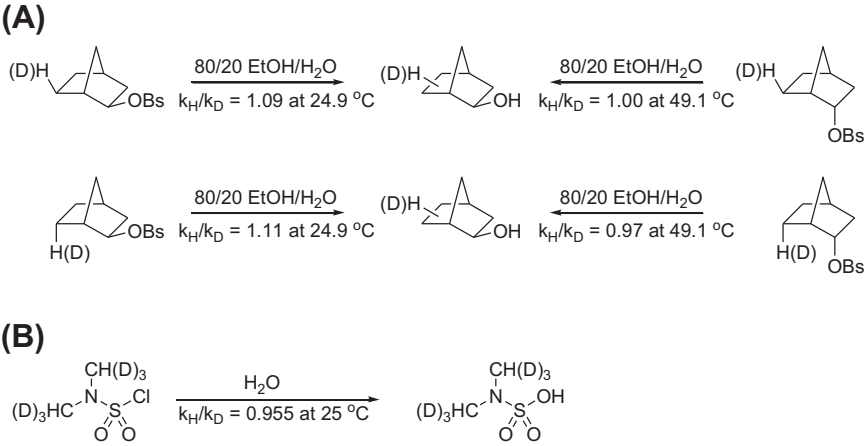

Scheme 2.3 Examples of γ-2°-^{2}H KIEs: (A) normal γ-2°-^{2}H KIE associated with putative through-space orbital interactions during the formation of the nonclassical norbornyl cation. (B) Inverse γ-2°-^{2}H KIE associated with putative repulsive interactions between the labelled methyl groups and the highly structured solvent shell.

Secondary KIEs are typically characterized either positionally or according to their origins. A somewhat distinct type of 2°-^{2}H KIE is the steric KIE, which arises as the result of the steric compression of positions interrogated by isotopic labeling. The origin of steric ^{2}H KIEs was identified by Bartell in 1960.[53–56] Following this work, Mislow, Carter, Melander, and others constructed systems based upon axial chirality that would have to pass through a sterically compressed transition state to stereochemically invert. Scheme 2.4 shows three of the original systems in which the inverse ^{2}H KIEs measured for stereochemical inversion were postulated to have their origins in steric repulsion.[57–60] Each of the compounds shown in Scheme 2.4 could be enantiomerically resolved or prepared enantiomerically pure. Stereochemical inversion (and ultimate conversion to the racemate) was measured using polarimetry carried out at temperatures exceeding those at which the pure enantiomer was resolved or synthesized. As Bartell predicted, the reactions in Scheme 2.4 proceed with significant inverse ^{2}H KIEs in accordance with the expectation that C–D bonds are more sterically diminutive than C–H bonds. Steric KIEs can most reasonably be thought of as originating from two quantum effects: (1) greater C–H bond length due to greater vibrational wave function dispersion and (2) greater average C–H bond length due to influences from anharmonicity (Fig. 2.5). Because the zero-point energy associated with the C–D bond is substantially lower than that associated with the C–H bond, the C–D bond experiences a part of the C–H(D) potential that is less anharmonic than that sampled by the C–H bond. The model first proposed by Bartell ignored the second factor listed above. This is important as the often accepted estimate of the C–D bond being 0.005 Å shorter than the C–H bond is based upon the Bartell model. In reality, the inherent anharmonicity present in C–H bonds is likely to make the disparity between C–H and C–D bonds larger.

Steric ^{2}H KIEs have also been important to our understanding of the internal dynamics of cyclophanes, the energetic characteristics of solvolyses, and the steric demands of carbonyl additions, among other interesting

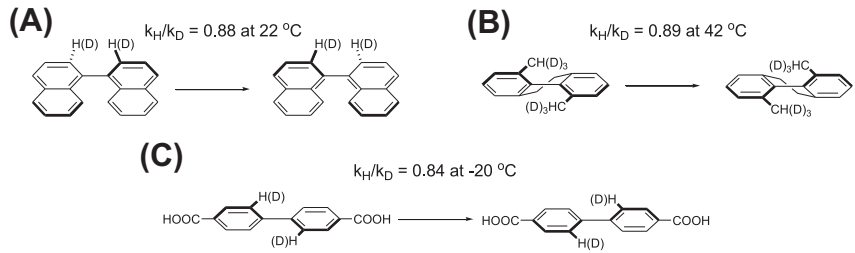

Scheme 2.4 Examples of steric ^{2}H KIEs measured in systems containing axial chirality.

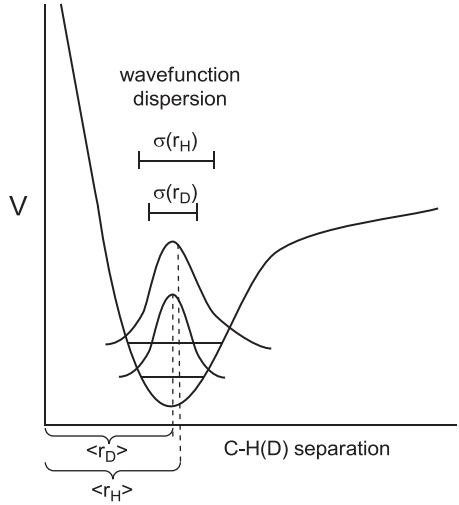

Figure 2.5 Anharmonicity of the C–H potential energy surface and differences in wave function dispersion associated with C–H and C–D stretching vibrations make C–D bonds effectively shorter than C–H bonds.

phenomena. Scheme 2.5 illustrates some examples of interesting manifestations of steric isotope effects. The rate of internal rotation in the cyclophane shown in Scheme 2.5A was measured using a double irradiation NMR technique.[61] It is likely that the steric repulsion that develops in the transition state for internal rotation is mitigated to some degree by attractive C—H–π interactions. While the inverse ^{2}H KIE in Scheme 2.5B has been ascribed entirely to attenuated hyperconjugation in the transition state, it is likely that there is some contribution from increased steric interaction in the transition state, as well.[62] The isotope effect in Scheme 2.5C is quite small on a per deuterium basis and is thought to result from increased planarization in the transition state as positive charge develops at the benzylic position.[63] Of course, part of the reason for the smaller per deuterium KIE is likely steric impact upon only four C—H(D) bonds of the 27 positions labeled. Although bromination is typically quite rapid and is often thought to proceed upon a potential with little or no potential energy barrier, the reaction shown in Scheme 2.5D proceeds with a substantial inverse ^{2}H KIE.[64] Although this isotope effect was measured using the [D_{20}]-labeled isotopolog, the resulting isotope effect is likely to result from interactions between only a few positions. Finally, Scheme 2.5E shows a reaction that yields a normal ($k_H/k_D > 1.0$) ^{2}H KIE because of the release of steric repulsion upon partial formation of the carbocationic intermediate.[65] Though it might be tempting

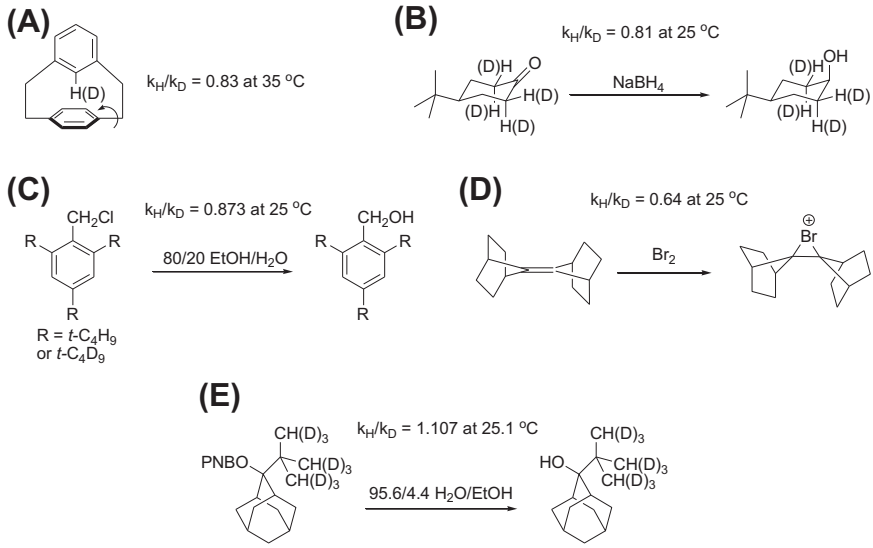

Scheme 2.5 Examples of steric ^{2}H KIEs measured in (A) internal rotation of cyclophanes and (B–E) various reactions in which substantial steric strain is developed or released during bond breakage or formation.

to ascribe the solvolysis reaction in Scheme 2.5E to a propagated hyperconjugative effect, this seems doubtful, given the distance of the labeled positions from the nascent carbocationic center in the transition structure. While substantial weakening of one C—CH_3 bond will have an overall loosening effect upon the vibrational manifold of the affected methyl group, it is unlikely that this would result in the magnitude of isotope effect observed.

Steric ^{2}H KIEs continue to be important today and have been applied to problems of recent relevance, like understanding complex host–guest interactions[66] and the dynamical behaviors of large molecular structures, such as corannulenes[67] and rotaxanes.[68] Another recent computational study explored the ^{2}H EIE associated with the conformational bias of d_3-1,1,3,3-tetramethylcyclohexane. Density functional calculations (B3LYP/6-311G*), utilizing a harmonic oscillator model for vibrational wave functions, yielded a ratio of axial to equatorial preference for the CD_3 group of 1.0417, which is in excellent agreement with previous NMR measurements, which yielded a value of 1.042.[69,70] While it may be tempting to take such excellent agreement to mean that steric ^{2}H KIEs are not affected by anharmonicity, agreement between computed and measured steric ^{2}H KIEs under the harmonic approximation is variable with computed values often yielding artificially more inverse effects.[71,72]As will be discussed below, steric

KIEs have begun to play a role in quantitatively understanding how nonbonding interactions influence stereoselection. Steric ^{2}H KIEs have almost exclusively been considered to arise because of zero-point energy differences between isotopologs. As will be discussed below, this conceptual view is being refined to address some of the more complex behaviors that accompany steric interactions.

Secondary KIEs have also been used in the context of EIEs to infer transition state position. According to the Hammond–Leffler postulate, the transition state corresponding to a fundamental reaction step is a structural interpolation of the reactant(s) and product(s), resembling the stable species to which it is energetically proximal.[73,74] Application of this postulate to the study of KIEs implies that the magnitude of the secondary KIE relative to the EIE reflects the position of the transition state relative to the product state.[75–80] A corollary of this concept is that the maximal secondary KIE cannot exceed the corresponding EIE. One of the most elegant applications of this idea was Gajewski's notion that secondary KIEs could be used to compute the degree of bond making or bond breaking in pericyclic transition states.[81–83] Of course, the notion that the EIE is the maximum bound for KIEs rests upon two assumptions that are not always applicable: (1) structural changes occur monotonically in the progression from reactants to products and (2) tunnelling does not have an appreciable effect upon the observed KIE.[84] The first assumption is potentially relevant in reactions where the KIE results largely from hybridization changes and/or continuous changes in hyperconjugation. The first assumption is not applicable to reactions where the reactants and products are similar, such as S_N2 reactions.[85] It is well known that tunneling can profoundly inflate 1° KIEs relative to values that might be expected from transition state theory. We often refer to tunneling in reactions where it has an obvious and tangible effect upon observables as 'hydrogen tunneling'. This label is misleading. During the tunneling process, numerous atoms in the reactant reposition in the act of crossing the dividing surface between reactants and products. Because tunneling inherently involves the motion of atoms other than the transferred entity in a reaction, it can reasonably be expected that tunneling will inflate secondary KIEs as well. The laboratories of Kreevoy,[86] Saunders,[87] and Schowen[88] were instrumental in demonstrating this principle. It follows that, even in reactions where structural changes from reactant to product are monotonic, the observed 2°-^{2}H or ^{3}H KIE may exceed the EIE. This phenomenon has been observed in a number of studies.[89–94] In several reactions of this type, researchers have posited that tunneling is exerting

a significant influence upon the observed KIE measurements. In summary, the correspondence of 2° KIEs with transition state position is a powerful tool, but it is based upon the Hammond–Leffler postulate, which assumes the validity of semiclassical transition state theory and monotonic geometric changes along the reaction coordinate.

Secondary ^{2}H and ^{3}H KIEs have also been used extensively in the study of tunneling. The Swain–Schaad exponent, described in Eqn 2.5, was originally developed as a means of relating the magnitudes of 2°-^{2}H and ^{3}H KIEs.[95,96] Under assumptions of the harmonic approximation for vibrational frequencies, and semiclassical transition state theory, this exponent is assumed to be near 3.34. Of course, the Swain–Schaad exponent contains other assumptions that are more worrisome. Among them is the assumption that the mass dependence of the frequencies responsible for the KIE is equivalent to the mass dependence exhibited by C—H, C—D, or C—T stretches. For this principle reason, extension of Swain–Schaad exponents to 2° KIEs can be troublesome.

$$\frac{k_{\mathrm{H}}}{k\mathrm{T}} = \left(\frac{k_{\mathrm{H}}}{k_{\mathrm{D}}}\right)^{\mathrm{EXP}} \tag{2.5}$$

Use of Swain–Schaad exponents is a source of some contention. First pointed out by Stern and Vogel in 1971, Swain–Schaad exponents can deviate strongly from 3.34, especially for reactions that exhibit strong coupling between motions of the primary and secondary positions in at the transition state. Regarding 2°-^{2}H and ^{3}H KIEs, one might expect α-2° KIEs to exhibit substantial anomalous Swain–Schaad exponents, even under semiclassical transition state theory. Kohen and Jensen recently explored this notion using a model system that was expected to be representative of the addition to hydride to aldehydes and serve as a point of connection to studies upon the various alcohol dehydrogenase enzymes. In the context of the model system they explore, a new upper bound of EXP = 4.8 is tendered. Another report, by Hirschi and Singleton, illustrates that for many reactions exhibiting inherently small 2° EIEs, the Swain–Schaad exponents appear to be, for all intents and purposes, boundless.[97] The use of Swain–Schaad exponents to describe tunneling phenomena remains an active field and a source of some contention. The work of Stern and Vogel, Kohen and Jensen, and Hirschi and Singleton does not preclude the use of Swain–Schaad exponents as diagnostics of tunneling; however, they bolster the notion that experimentally determined Swain–Schaad exponents should not be used as prima facie evidence for the importance of tunneling unless done so in the context of transition

structure calculations of the expected Swain–Schaad exponent. Huskey has shown that inflated Swain–Schaad exponents are associated with violations of the rule of the geometric mean.[98] The rule of the geometric mean is expected to fail for reactions in which tunneling is important. As a consequence, Swain–Schaad and related exponents have been used to identify reactions in which tunneling has a significant effect upon the reaction rate.

3. NEW METHODS

3.1. Competitive Kies Using Continuous ^{13}C NMR Measurement

Numerous analytical techniques have been leveraged toward the measurement of competitive KIEs. Polarimetry,[99] scintillation counting, and mass spectrometry[100] provide superior sensitivity but are limited molecular scope or require labeling that can sometimes be onerous and is often quite difficult to apply to the whole of a molecule of interest. While significantly less sensitive, NMR (^{2}H, ^{13}C, and ^{17}O) has been used effectively to measure KIEs at natural abundance in a number of small molecule reactions. Pascal first utilized ^{2}H NMR to measure ^{2}H KIEs at natural abundance.[101] Singleton then applied NMR as an analytical tool to measure ^{2}H, ^{13}C, and ^{17}O fractionation in the measurement of KIEs.[102] Since the first report of Singleton and Thomas of using ^{13}C NMR to measure KIEs, this technique has seen widespread application.[103] The requirement of large amounts of reisolated starting material from high-conversion reactions or product from low-conversion reactions is the primary limitation of this technique. In spite of this limitation, natural abundance ^{13}C KIEs have been measured in enzyme-catalyzed reactions using NMR as an analytical tool.[104,105]

Recent advancements in the design of cryogenically cooled NMR probes have rendered approximately fivefold signal-to-noise enhancements over conventional NMR probes, reducing acquisition time by a factor of 25. The research group of Andrew Bennet recently applied this technology, in conjunction with isotopic labeling, to the measurement of competitive ^{13}C and ^{18}O KIEs using continuous ^{13}C NMR monitoring of the *Vibrio cholerae* sialidase-catalysed hydrolysis of **1** (Fig. 2.6).[106] Bennet's work has advantages over the technique developed independently by Pascal and Singleton in that fractionation can be measured continuously over a range of conversions during the course of the reaction, providing a statistically averaged value for the KIE from one experience. This approach, however, does require the synthesis of costly isotopologs.

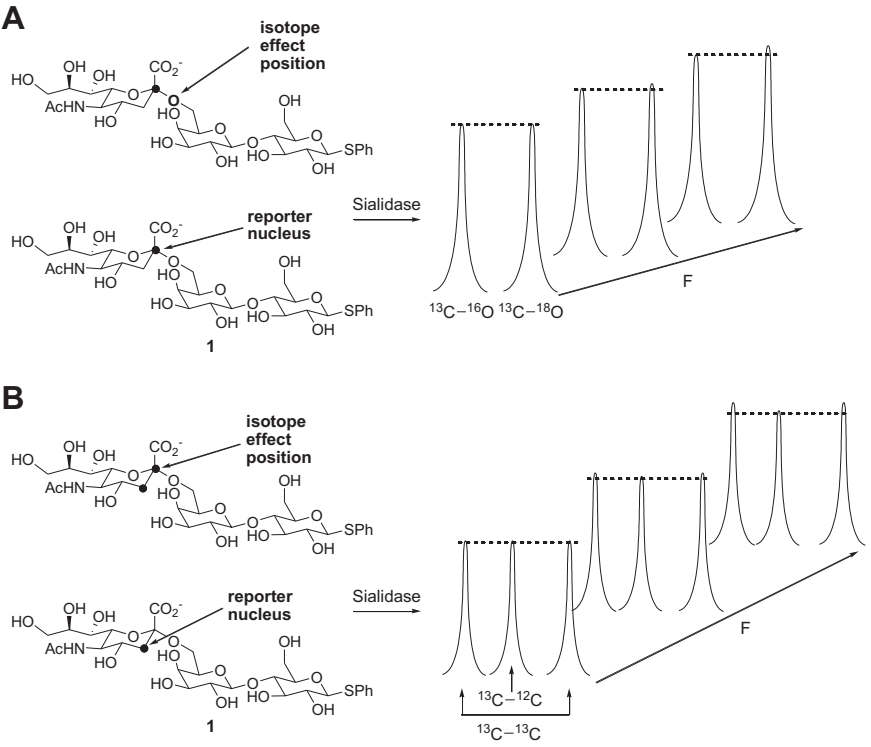

Figure 2.6 Illustration of Bennet's technique for the continuous measurement of (A) ^{18}O and (B) ^{13}C KIEs during the course of a reaction, taking advantage of heavy-atom isotope effects upon or 1-bond couplings with ^{13}C NMR chemical shifts and cryogenically cooled NMR probe technology.

Bennet's technique uses quantitative ^{13}C labeling at a 'reporter' position to reflect isotopic ratios at adjacent ^{13}C or ^{18}O sites. As is shown in Fig. 2.6, the NMR-active ^{13}C nucleus at the anomeric carbon can report upon the isotope effect at the exocyclic or exocyclic oxygen linkage. The same reporter nucleus can be used to report upon the isotope effect at the endocyclic position, as well. The $^{18}O/^{16}O$ isotope effect upon the ^{13}C chemical shift separates the resonances for the heavy and light isotopologs – allowing a constant measurement of the relative concentrations of both isotopologs, R. The relationship of this continuously measured ratio, as compared to the initial ratio, R_0, yields the isotope effect according to Eqn 2.6. A ^{13}C reporter nucleus can also be used to report $^{12}C/^{13}C$ ratios at an adjacent position. While the isotope effect upon the ^{13}C NMR resonance itself is substantially less than that for adjacent $^{16}O/^{18}O$ positions, an adjacent ^{13}C nucleus splits the reported resonance into a well-resolved doublet, as is shown in Fig. 2.6B. Because of this splitting, the relative

amounts of ^{13}C label can be quantified at an adjacent position. KIEs at the exocyclic oxygen reflect substantial bond breaking: $^{16}k/^{18}k = 1.0400$ (14), 1.0388 (17), and 1.0393 (38) at the cleaved glycosidic C–O bond. The endocyclic position reflects a net tightening in the transition state: $^{16}k/^{18}k = 0.9747$ (17), 0.9749 (31), and 0.9743 (25). This isotope effect is indicative of an overall increase in bonding – indicating an oxacarbenium-like transition state. The ^{13}C KIE at the anomeric position was found to be substantial and normal: $^{12}k/^{13}k = 1.0224$ (27), 1.0229 (16), and 1.0211 (19). This KIE contradicts the notion of an oxacarbenium intermediate and is interpreted as resulting from the formation of a transition structure where the anomeric carbon is pentacoordinate in nature with bond breaking at the leaving group compensating for the formation of a partial double bond with the endocyclic oxygen. Hydrolysis of 4-nitrophenyl-α-D-sialoside yields an isotope effect of $^{16}k/^{18}k = 1.046$ upon the exocyclic oxygen.[107] Because the leaving group in this instance has a much lower pK_a than the lactoside leaving group used by Bennet's group yet yields a similar exocyclic $^{16}O/^{18}O$ KIE, it is believed that general acid catalysis does not activate the leaving group. The proposed qualitative transition structure model is shown below:

$$R/R_0 = (1 - F)^{[(1/\mathrm{KIE})-1]} \tag{2.6}$$

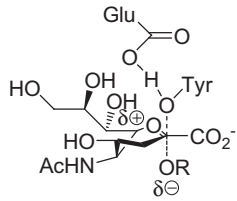

In summary, Bennet's technique exploits the inherently high chemical shift dispersion associated with ^{13}C NMR, isotope effects upon chemical shifts, modern NMR technologies, and clever labeling strategies to gain high precision estimates of KIEs for enzymatically catalysed reactions. This technique should be of intense interest to researchers exploring the enzyme-catalyzed conversions of polysaccharides and nucleic acids.

3.2. Methods for Inquiry into Asymmetric Reactions

The development of stereoselective reactions has remained an incredibly active field for over 30 years. While mechanistic studies and the information derived from them have accelerated asymmetric reaction development, a fundamental

understanding of the physical processes that govern stereoselection is lacking. In all existing models for stereoselection, steric repulsion is posited as a dominant influence.[108–118] However, quantifying steric bulk has been difficult. Winstein and Holness introduced the *A*-value as a measure of steric bulk.[119] Taft, Charton, and others approached the question of relative steric bulk using linear free energy relationships.[120–125] With one notable exception,[126] these methods were not applied to the study of asymmetric reactions until recently. The Sigman group has applied linear free energy relationships toward understanding enantiofacial selection in novel allylation reactions developed in their laboratory and an organocatalytic desymmetrization developed in Scott Miller's laboratory.[127–129] Sigman's group has also applied a Charton parameter analysis to regioselectivity in a recently reported hydroarylation.[130] Zhu et al. have also reported a ^{13}C NMR method for the simultaneous measurement of relative rates for use in linear free energy relationships.[131] These methods are complementary to recently developed KIE methodologies discussed below that enable quantification of steric interactions at the transition state.[132]

Standard methodologies for probing mechanism are blind to the essential feature of enantioselective reactions, namely symmetry breaking. Symmetry breaking between enantiofacial faces or enantiotopic position defines enantioselectivity. Nonbonding interactions, including steric repulsion, are essential to this process. A recently developed method reports ^{2}H KIEs at enantiotopic groups as a probe of enantiofacial selection.[133] Rather than attempting the resolution or synthesis of stereoselectively labelled substrates, this method employs two competition reactions and the rule of the geometric mean[134] to extract the ^{2}H KIE at each enantiotopic methyl group (Fig. 2.7). Kinetic competition between isotopomeric enantiomers, (*R*)-d_3-**1** and (*S*)-d_3-**1** yields the ratio of isotope effects at the prochiral positions, KIE_R (Eqn 2.7). The relative rates are determined by analyzing the amounts of (*R*)-d_3-**1** and (*S*)-d_3-**1** in starting material reisolated from a high-conversion (~90%; $F \sim 0.9$) reaction using ^{1}H NMR. However, because the isotopic labeled groups are enantiotopic, the reisolated starting material must be desymmetrized in a deterministic way using a highly stereoselective reaction. The desymmetrization process uses a highly stereoselective process to establish a chiral center near the enantiotopic groups at which KIEs are being measured. Usually, this process is the stereoselective reaction being studied. However, in the first report of this methodology, the Corey-Bakshi-Shibata reduction was used to desymmetrize the reisolated starting material due to the relative ease of work-up and the observation that this reaction yields the product resulting from *Si*-attack with greater than 99:1

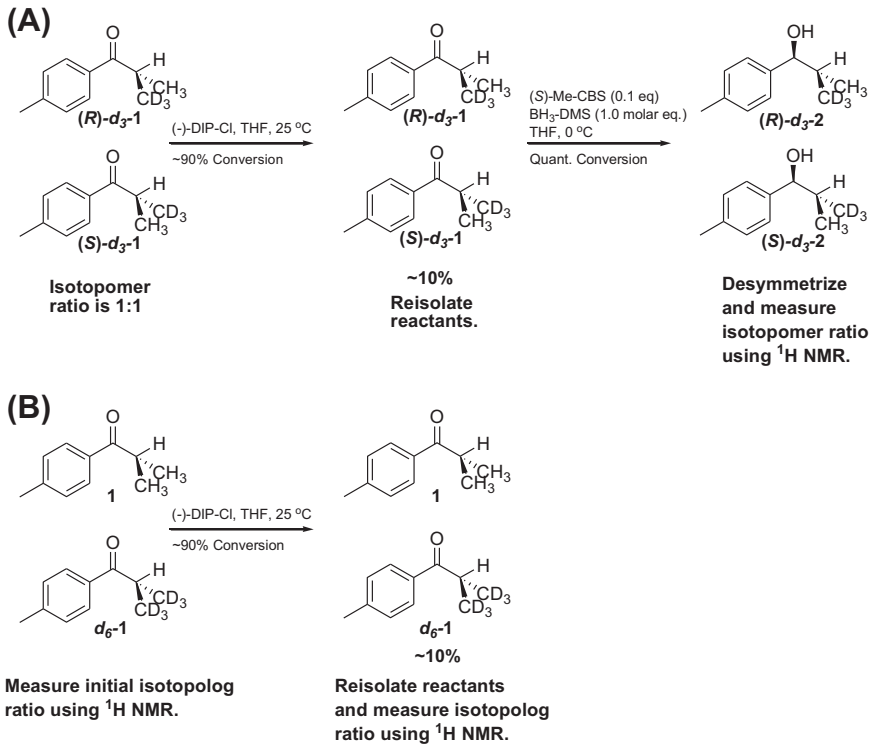

Figure 2.7 Method for measuring enantiotopic ^{2}H KIEs at enantiopic groups using (A) a competition reaction between enantiomeric isotopomers and (B) a competition between perprotiated substrate and the isotopolog labeled at each of the enantiotopic groups. For color version of this figure, the reader is referred to the online version of this book.

enantioselectivity. Desymmetrization converts the enantiomeric isotopically labeled groups into diastereotopic groups and allows relative quantification of reisolated (*R*)-d_3-**1** and (*S*)-d_3-**1** to yield the ratio of the two isotopomers, *R*, from which the KIE is computed (Eqn 2.8). Kinetic competition between **1** and d_6-**1** yields the relative rates for the conversion of these two isotopologs. The resulting ratio of rates is referred to as the product KIE, KIE_P (Eqn 2.9). Relative rates are determined in by taking the reaction to high conversion (~90%; $F = 0.9$) and comparing the ratio of reisolated **1** and d_6-**1** (*R*) to the ratio that existed prior to reaction (R_0). The resulting product KIE is computed using Eqn 2.10. Finally, the KIEs at each enantiotopic group can be computed from KIE_R and KIE_P using Eqn 11a and b.

$$\frac{k_{S-d_3-1}}{k_{R-d_3-1}} = \frac{k_1}{k_{R-d_3-1}} \Big/ \frac{k_1}{k_{S-d_3-1}} = \mathrm{KIE}_R \tag{2.7}$$

$$\frac{k_{S-d_3-1}}{k_{R-d_3-1}} = \frac{\ln[2(1-F)/(1+1/R)]}{\ln[2(1-F)/(1+R)]} \tag{2.8}$$

$$\frac{k_1}{k_{d_6-1}} = \frac{k_1}{k_{R-d_3-1}} \times \frac{k_1}{k_{S-d_3-1}} = \mathrm{KIE}_P \tag{2.9}$$

$$\frac{k_1}{k_{d_6-1}} = \frac{\ln[(1+1/R_0)(1-F)/(1+1/R)]}{\ln[(1+R_0)(1-F)/(1+R)]} \tag{2.10}$$

$$\frac{k_1}{k_{R-d_3-1}} = \sqrt{\mathrm{KIE}_P \times \mathrm{KIE}_R} \tag{2.11a}$$

$$\frac{k_1}{k_{S-d_3-1}} = \sqrt{\mathrm{KIE}_P / \mathrm{KIE}_R} \tag{2.11b}$$

The limitations of the method described above are that only highly stereoselective reactions, those which proceed almost exclusively via one transition state, are amenable to study by this technique. It should also be mentioned that the above approach is not the only way that these isotope effects could be measured. This measurement could be performed by measuring fractionation in the products in a low conversion reaction using a mixture of **1**, (*R*)-d_3-**1**, and (*S*)-d_3-**1** and using ^{1}H NMR to obtain the ratio of **1** to (*R*)-d_3-**1** and (*S*)-d_3-**1** and using ^{2}H NMR to obtain the ratio of (*R*)-d_3-**1** to (*S*)-d_3-**1**. This technique was not chosen in initial studies because the size of the observed ^{2}H KIEs was expected to be small, and fractionation is larger in remaining reactants in a high-conversion reaction than in products obtained from low-conversion reactions.[9]

The data obtained from measurements of ^{2}H KIEs at enantiotopic methyl groups suggest that the resulting ^{2}H KIEs largely result from increased steric repulsion in the transition state. One of the primary motivations for measuring ^{2}H KIEs at enantiotopic methyl groups in the DIP-Cl (*B*-chlorodiisopinocampheylborane) reduction was that the qualitative transition structure used to explain stereoselection in this system was well established, and from this highly probable qualitative transition structure, it was reasonable to expect the pro-*S* and pro-*R* methyl groups in 4′-methylisobutyrophenone to experience significant but disparate degrees of steric repulsion. Figure 2.8A shows the qualitative transition structure model that was put forth by Brown adapted to the substrate used in the isotope effect measurements.[135] Figure 2.8B shows the corresponding optimized [B3LYP/6-31G*] transition structure.

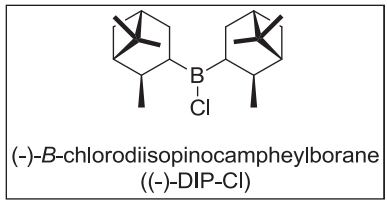

Oxazaborolidine catalysts have been found to catalyze an extremely broad array of reactions, ranging from stereoselective reductions to stereoselective cycloadditions.[136–140] Measurements of ^{2}H upon the enantiotopic groups of 2′,5′-dimethylisobutyrophenone as a substrate in the Corey–Bakshi–Shibata reduction have contributed to our understanding of how oxazaborolidine catalysts enforce stereoselectivity in enantioselective reductions. The oxazaborolidine catalysts collectively known as CBS catalysts are modular. The effects of changes in the geminal diaryl groups, the boroalkyl group, and the stoichiometric reductant upon the enantiomeric ratio of 1-phenylethanol resulting from the reduction of acetophenone have been explored extensively. Alterations in the modular CBS catalyst have provided some insight into how oxazaborolidine catalyst–reductant complexes create a steric environment. While changes in the geminal diaryl groups and the stoichiometric reductant appear to have substantial influence upon stereoselection,[141–143] the boroalkyl group can be varied from H to *n*-butyl with no observable change in selectivity in the reduction of acetophenone.[144,145] In the simplest paradigm for the stereoselective reduction of prochiral ketones, the chiral catalyst–reductant complex distinguishes the *Re* and *Si* faces via size discrimination between the small (R_S) and large (R_L) substituents on the ketone. Presumably, this discrimination process involves

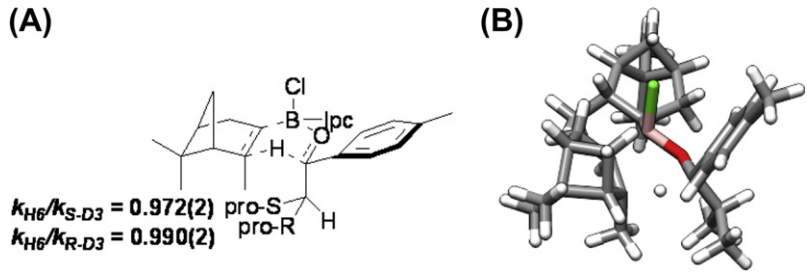

Figure 2.8 A) Qualitative and (B) optimized transition structures for the DIP-Cl reduction of 4′-methylisobutyrophenone. ^{2}H KIEs on prochiral groups are indicated to the left of the qualitative transition structure. For color version of this figure, the reader is referred to the online version of this book.

Figure 2.9 A) Qualitative and (B) optimized [B3LYP/6-31+G(d,p)] transition structures for the CBS reduction of 2′,5′-dimethylisobutyrophenone. ^{2}H KIEs on prochiral groups are indicated to the right of the qualitative transition structure.

avoiding placement of R_L in the more sterically constrictive environment. By inference, it might be expected that steric interactions could be measured at the small group (R_S) in a prochiral ketone. To test this hypothesis and to better understand interactions between the catalyst–reductant complex and the ketone substrate in the transition state, Meyer measured the ^{2}H KIEs at the enantiotopic groups on 2′,5′-dimethylisobutyrophenone.[146] These measurements, in conjunction with transition structure modeling, suggest that the substrate makes steric contact with both the stoichiometric BH_3 reductant and the boroalkyl group (Fig. 2.9). These results, in the context of the studies mentioned earlier, suggest that oxazaborolidine catalysts are in fact quite flexible in the manner in which they provide steric constraints upon selectivity. This, in fact, may be part of the reason for the substantial substrate range exhibited by the most often utilized CBS catalyst, (*S*)-1-methyl-3,3-diphenyl-tetrahydro-pyrrolo[1,2c][1,3,2]oxazaborole (**2**). Alagona et al. have proposed an opposing viewpoint, suggesting that the CBS is an extraordinarily rigid catalyst.[147] They further suggest that this is the reason for high stereoselectivity observed in a number of CBS reductions. Further work on this system is currently being prepared for publication and promises to resolve this disagreement.

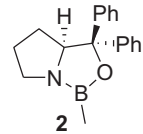

2

Steric ^{2}H KIEs (see below) are often viewed as arising from an increase in zero-point energy difference between protiated and deuterated isotopologs at the first-order saddle point. By analogy, one should expect to see inverse ^{13}C KIEs in methyl groups upon which steric ^{2}H KIEs are substantial. It

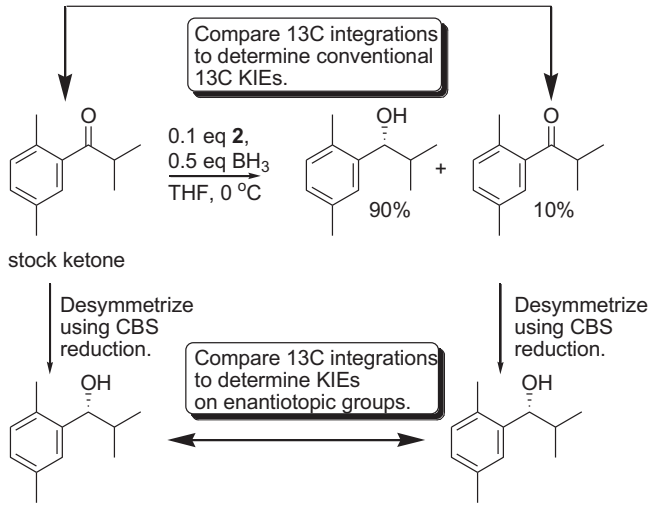

Figure 2.10 Illustration of the method for measuring ^{13}C KIEs at enantiotopic groups for the CBS reduction of 2′,5′-dimethylisobutyrophenone.

follows that the systems described above (DIP-Cl and CBS reductions) should yield measurable steric ^{13}C KIEs at the prochiral methyl groups on 4′-methylisobutyrophenone and 2′,5′-dimethylisobutyrophenone, respectively. To test this hypothesis, the Singleton method for measuring ^{13}C KIEs at natural abundance was adapted to study asymmetric reactions (Fig. 2.10).

Global ^{13}C KIEs at natural abundance have been measured for both the DIP-Cl and CBS reductions of 4′-methylisobutyrophenone and 2′,5′-dimethylisobutyrophenone, respectively. These measurements,

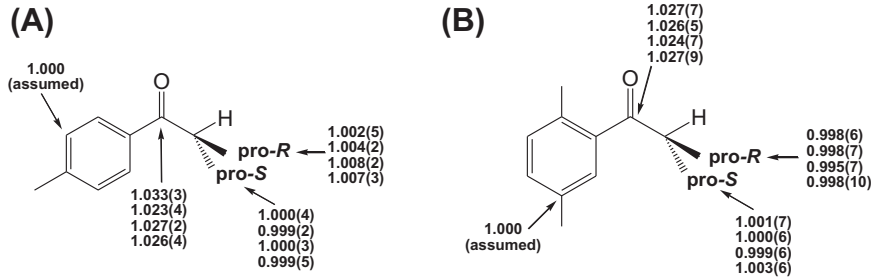

Figure 2.11 Global ^{13}C KIEs measured at natural abundance for (A) the DIP-Cl reduction of 4′-methylisobutyrophenone and (B) the CBS reduction of 2′,5′-dimethylisobutyrophenone. KIEs for all positions were measured. KIEs for positions not shown were within experimental error of unity.

carried out according to the method outlined in Fig. 2.10, yielded surprising results that we are only starting to understand now (Fig. 2.11). By analogy with observed inverse ^{2}H KIEs observed in these reactions, one would have anticipated small but measurable inverse ^{13}C KIEs on the pro-*S* methyl group on 4′-methylisobutyrophenone and both prochiral groups on 2′,5′-dimethylisobutyrophenone in the DIP-Cl and CBS reductions shown in Figs 2.8 and 2.9, respectively. Instead, the observed ^{13}C KIEs at the prochiral positions where an inverse effect might be expected did not deviate significantly from unity.[148,149] The possibility remains that steric ^{13}C KIEs are not, in general, large enough to be observed.

Global ^{13}C KIEs sensitive to the process of enantioselection, in a curious twist of fate, did provide substantial insight into the proline-catalyzed intramolecular aldol reaction.[150] It was previously held that C−C bond formation was at least partially rate limiting in this reaction.[151] The triketone (**3**) possesses two prochiral carbonyls. For this reason, the technique shown in Fig. 2.10 appeared to be an excellent means of understanding the physical origins of stereoselection in proline-catalyzed reactions. To our surprise, neither carbonyl exhibited a substantial ^{13}C KIE. This result meant that the turnover-limiting step occurs prior to C−C bond formation (Scheme 2.6). This finding was further motivated by computed estimates of ^{13}C KIEs for carbinolamine formation (**TS1**), iminium formation (**TS2**), and C−C formation (**TS3**). Deprotonation of the iminium to yield the nucleophilic enamine was eliminated from consideration, given that no significant ^{13}C KIE was observed at the nucleophilic carbon. KIEs computed [B3LYP/6-31+G(d,p)] using a polarizable continuum model for the dimethylformamide solvent are shown in Fig. 2.12. Predicted KIEs for carbinolamine and iminium formation, as computed from **TS1** and **TS2**, were in excellent agreement with measured KIEs; however, the precise turnover-limiting step was unable to be identified using KIEs alone. Further kinetics studies, which have resolved this uncertainty, will be published in the near future.

In summary, new approaches to measuring both ^{2}H and ^{13}C KIEs in asymmetric reactions are providing information about the precise mechanisms of stereocontrol and the inherent nature of nonbonding forces. Inverse ^{2}H KIEs that appear to arise from steric repulsion yield important information about the steric requirements imposed upon the transition state by asymmetric catalysts. As will be discussed below,

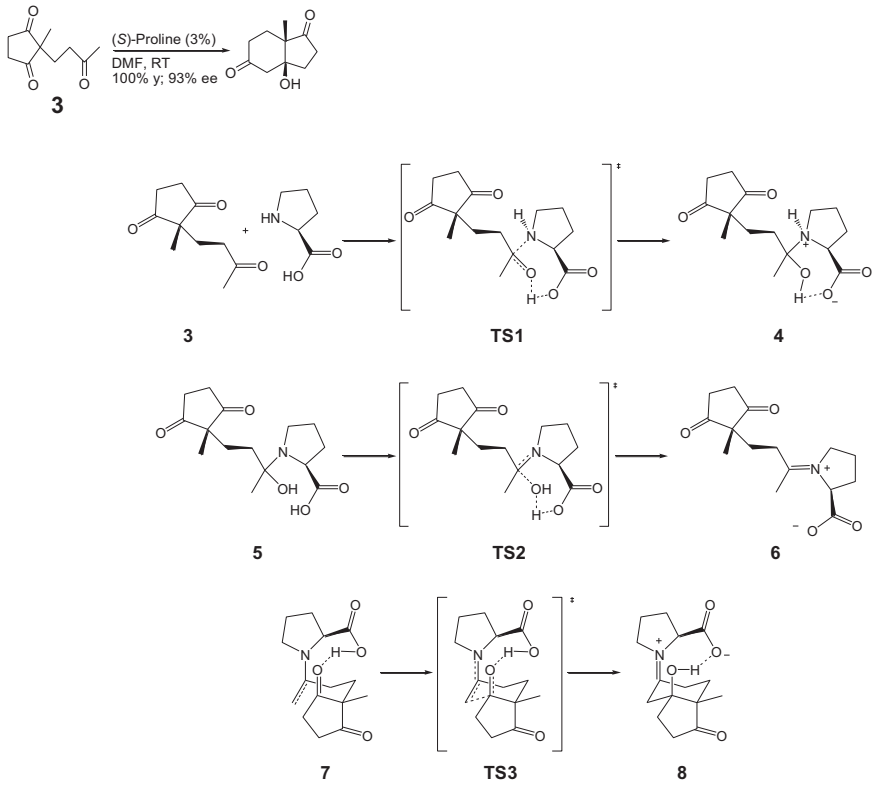

Scheme 2.6 Candidate rate-limiting reaction steps in the intramolecular proline-catalysed aldol reaction.

repulsive nonbonding interactions yield ^{2}H KIEs that appear to have substantial normal entropic contributions to the KIE accompanied by the expected inverse enthalpic contribution. These recent findings may shed light on the origins of the normal to insubstantial ^{13}C KIEs observed in the DIP-Cl and CBS reductions at positions that yielded substantial inverse ^{2}H KIEs. Finally, ^{13}C KIEs measured at the prochiral carbonyls in **3** have been used to deduce that C—C bond formation is not turnover limiting in the proline-catalyzed intramolecular aldol reaction. It is obvious that KIEs can yield a substantial amount of information in the context of experimentally validated transition structure models. This approach yields direct information about how these catalysts accelerate chemical reactions while simultaneously controlling product distributions. It seems likely that these techniques will be useful in the rational design and optimization of asymmetric catalysts in the future.

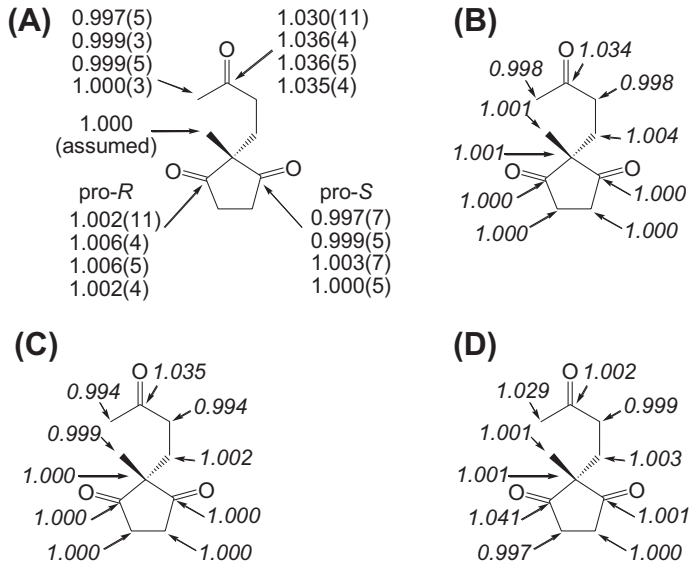

Figure 2.12 A) Experimentally determined ^{13}C KIEs. Computed [B3LYP/6-31+G(d,p)] ^{13}C KIEs corresponding to turnover-limiting (B) carbinolamine formation, (C) iminium formation, and (D) C–C bond formation.

3.3. Dynamical Deviations from Transition State Theory

From the preceding sections of this review, it is evident that transition state theory often plays a substantial role in interpreting KIEs. Carpenter's research group has been instrumental in showing that a number of reactions possess features on the potential energy surface, known as valley ridge inflections (VRIs), that can influence product ratios in a manner that cannot be predicted using transition state theory.[152,153] A VRI can be thought of as the point along a MEP where restoring force in an orthogonal coordinate disappears, resulting in a bifurcation of the MEP. While this definition conveys the essence of the concept and is easily visualized in potential energy surfaces like that in Fig. 2.13, a more rigorous definition has been provided.[154] Singleton's research group has explored a number of reactions possessing bifurcated potential energy surfaces that can influence KIEs and other observables in ways that cannot be accurately described using transition state theory. The ene reaction of singlet ($^1\Delta_g$) oxygen ($^1O_2$) with [D_6]-**9** yields a substantial intramolecular ^2H KIE, whereas, competition between **9** and [D_{12}]-**9** yields a much smaller intermolecular KIE (Scheme 2.7).[155,156] Grdina et al. reasonably took this to indicate that the reaction involved a rate-determining initial transition state followed by an intermediate and

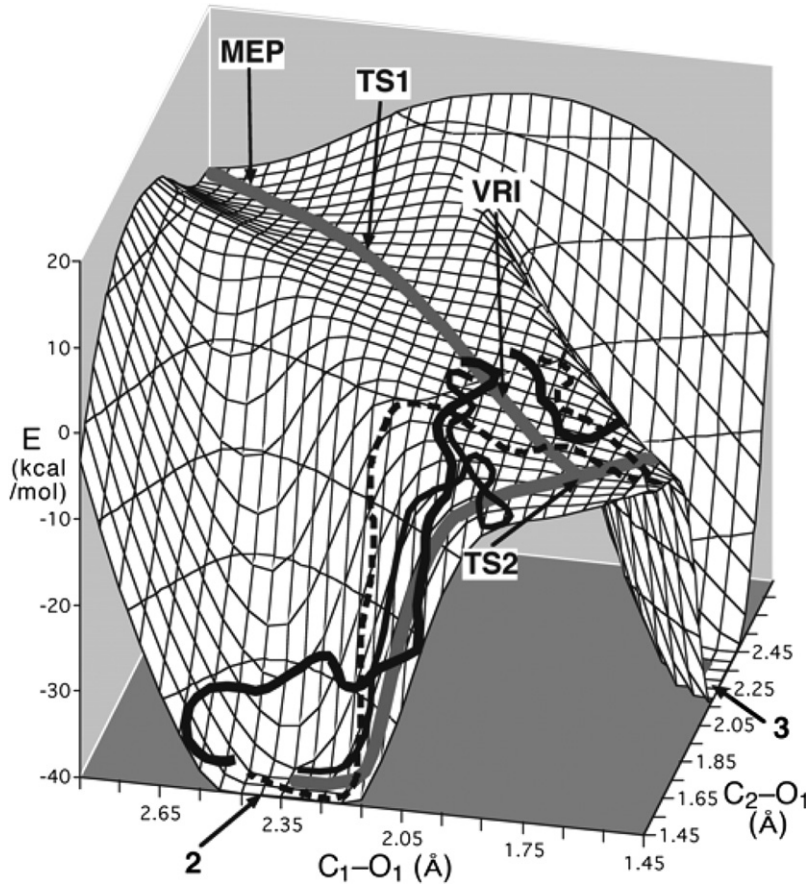

Figure 2.13 Potential energy surface (B3LYP/6-31G*) for the reaction of $^1O_2$ with 2-butene. For color version of this figure, the reader is referred to the online version of this book.

a product-determining transition state. Computational efforts to locate such an intermediate met with failure.

Singleton et al. constructed a B3LYP/6-31G* surface shown in Fig. 2.13. Using trajectories starting in an area between the points labeled 'TS1' and 'VRI', Singleton et al. were able to demonstrate an intramolecular ^{2}H KIE of $k_H/k_D = 1.38 \pm 0.17$ for the reaction of $^1O_2$ with [D_3]-2-butene, which agrees quite closely with the measured effect of between 1.38 and 1.41.[157] This result seems counterintuitive at first because we tend to think of potential energy surface as being independent of isotopic identity. If, however, we consider using mass-weighted coordinates, then the side of the

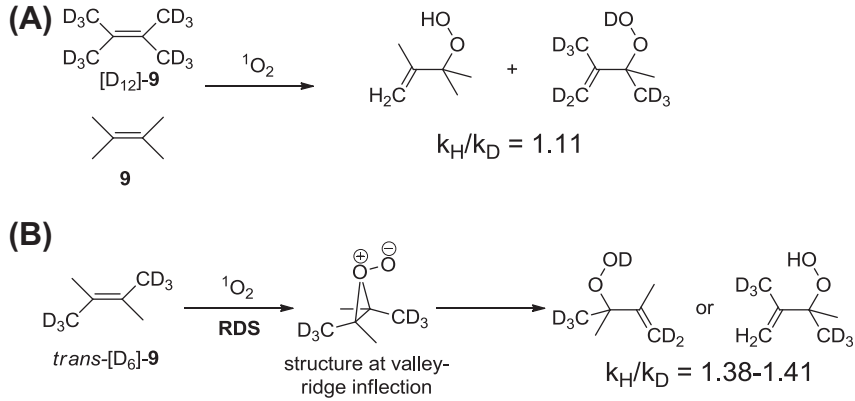

Scheme 2.7 (A) Intermolecular and (B) intramolecular ^{2}H KIEs for the ene reaction between $^{1}O_2$ and 2,3-dimethylbutene.

potential energy surface corresponding to deuterium abstraction becomes broader than the side corresponding to protium abstraction. As a result, smaller oscillations perpendicular to the MEP are required to commit the trajectory to protium abstraction. This work has been expanded to other systems to yield results that challenge some of the most fundamental assumptions in mechanistic organic chemistry.

Perhaps one of the most cogent examples of the effects of dynamical influences upon mechanistic outcomes can be found in a recent report by Kelly et al., which describes both computed and experimental intramolecular ^{13}C KIEs for the pericyclic dimerization of cyclopentadiene.[158] Computationally, it had been shown that a minimum energy pathway connecting two cyclopentadiene molecules to the dimer possesses a transition structure of C_2 symmetry (Fig. 2.14A).[159] An identity Cope rearrangement pathway connects the two equivalent product pathways. The cyclopentadiene dimer (Fig. 2.14B) possesses five pairs (a/a′, b/b′, c/c′, d/d′, and e/e′) of inequivalent carbon positions that are equivalent by the C_2 symmetry axis in the C_2 transition structure. Thus, the only transition structure that is located upon either of the bifurcated minimum energy pathways cannot yield the intramolecular ^{13}C KIEs reported (Fig. 2.14B). In this report, the development of an extrapolation methodology for computing 'Newtonian isotope effects' is disclosed.

Isotopic replacement of one of the carbon atoms in the C_2 transition structure breaks the C_2 symmetry. The product formation path that involves the greatest motion (action) of the heavy isotope becomes longer. As

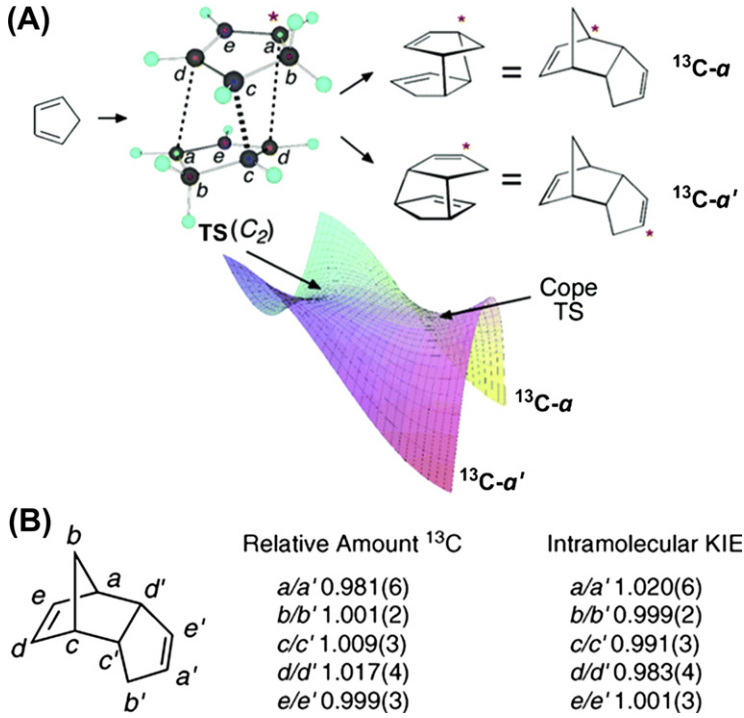

Figure 2.14 The cyclodimerization of cyclopentadiene occurs on (A) a bifurcated PES and yields (B) intramolecular KIEs that are due entirely due to mass-sensitive dynamically influenced product lineages. For color version of this figure, the reader is referred to the online version of this book.

a consequence, dynamical dividing surfaces that yield two distinct isotopomers, have different effective dividing surfaces that define the decision point at which a trajectory is committed to a product lineage. Kelly et al. make use of this fact to generate classical trajectories of isotopically labelled C_2 transition structures with a Boltzmann distribution of vibrational energy and random vibrational phases. However, replacing the light ^{12}C nuclei individually with ^{13}C nuclei and running trajectories in order to elicit the preference for one product pathway over another would require a tremendous number of trajectories to generate intramolecular KIEs with suitably low statistical error. Instead, Kelly et al. ran a smaller number of trajectories with fictional ^{140}C, ^{76}C, ^{44}C, ^{28}C, and ^{20}C isotopologs labeled at one position among the five distinct pairs of positions. The intramolecular ^{140}C KIE at the a/a' position, for example, was simply the ratio of pathways yielding the ^{140}C nucleus in the a' position versus the a position in the

product. In this case, 420 trajectories yielded 269 trajectories resulting in label at the *a* position, while 151 trajectories yielded the label at the *a′* position, yielding an intramolecular ^{140}C KIE of 1.80 ± 0.28. Intramolecular KIEs computed using successively less massive 'carbon' isotopes were then extrapolated to the value expected for ^{13}C. This method yielded exceptional agreement with experiment (a/a': 1.018 ± 0.008; c/c': 0.988 ± 0.004; d/d': 0.982 ± 0.004). This approach and result are exceptional in that they have challenged the traditional view that KIEs originate largely from zero-point energy differences. Instead, a classical set of decoupled harmonic oscillators, i.e. a completely classical description of a molecular system, yielded valid estimates of intramolecular ^{13}C KIEs on a bifurcated PES.

Over the past decade, Singleton's work has demonstrated how dynamical effects, once considered curious nuances, can have profound effects upon product distributions and mechanistic interpretations. One of the principal lessons from Singleton's recent work is that attempts to represent a dividing surface in terms of a single transition structure can lead to qualitatively incorrect predictions of product distributions and other mechanistic metrics, like KIEs. For reactions that are poorly treated by conventional or variational transition state theory, the structures that would define a dividing surface between reactant(s) and product(s) can be (1) structurally diverse and (2) yield structurally distinct products. A very recent report from the Singleton group highlights a related surprising phenomenon: the presence of entropic intermediates on the free energy surface that describes the [2 + 2] cycloaddition of dichloroketene to 2-butene.[160] Whereas, traditional optimizations of transition structures yield only the first transition structure on the reaction pathway,[161] free energy calculations along reaction paths[162] demonstrate the presence of an intermediate. The second barrier, which arises in part due to increased zero-point energy and in part due to decreased entropy, is actually higher in free energy than the first free energy barrier, which corresponds closely to a saddle point on the potential energy surface.

3.4. EIEs upon Substrate Binding

Perhaps the most durable and compelling notion of how catalysis is achieved was posited by Pauling in 1948, when he put forth the hypothesis that catalysts bind the transition state for the uncatalyzed reaction, thus lowering its energy through stabilizing interactions.[163] Of course, since

1948, a number of refinements, addenda, and improvements have been tendered.[164–172] Wolfenden recognized that Pauling's model for enzyme catalysis could be applied to the design of competitive enzyme inhibitors.[173,174] This method has been applied with considerable success, as transition structure mimics have proven to be extraordinarily potent inhibitors. Vern Schramm's research group has had great success in using KIE measurements to construct transition structure models for enzymatic reactions.

Recently, Schramm's group has developed an innovative method for probing multiple interactions between enzyme and substrate using equilibrium ^{3}H-binding EIEs.[175] This work follows upon an earlier study by LaReau et al. which reported the first EIEs for substrate binding in the lactate dehydrogenase enzyme.[176] Lewis and Schramm report binding EIEs for glucose binding to human brain hexokinase. They also explored the effect of the binding of β-γ-CH_2-ATP upon the ^{3}H-binding EIEs. β-γ-CH_2-ATP is a competitive inhibitor designed to have allosteric properties analogous to the other natural substrate of hexokinase, ATP. Centrifugal ultrafiltration is employed to separate free glucose from bound glucose upon incubation with the hexokinase. Mutarotase was included to rapidly equilibrate between α- and β-anomers of glucose. Remotely labeled [2-^{14}C]- and [6-^{14}C]-glucose was used to quantify the relative concentrations of glucose in the enzyme-containing and enzyme-free compartments of the ultrafiltration apparatus. Comparison of tritium counts in the enzyme-containing and enzyme-free compartments of the ultrafiltration apparatus were used to compute the ^{3}H-binding EIEs. EIEs for the binding of glucose to hexokinase (binary complex) and to hexokinase with β-γ, CH_2-ATP and Mg^{2+} bound (ternary complex) are reported in Table 2.1.

A computational effort to explain the effects shown in Table 2.1 explored the geometric dependence and the effects of hydrogen bonding upon equilibrium ^{3}H EIEs.[177] Normal effects at H1, H3, and H4 can be explained large by the presence of hydrogen bond acceptor sites on hexokinase effectively raising the energy of oxygen lone pairs [n(O)] such that donation to β-hydrogen σ*(C–H) is enhanced, providing a weaker C–H bond when glucose is bound (Fig. 2.15A). Steric compression at H2 and H5 are thought to result in the observed inverse KIEs (Figs. 2.15B and 2.15C). The situation at H6 is slightly more complicated and is thought to arise from three different contributions: the above n(O) → σ*(C–H) is

Table 2.1. Experimental ^{3}H-binding EIEs for the glucose/human brain hexokinase system

Position of ^{3}H label	Binding EIE (binary complex)	Binding EIE (ternary complex)
[1-*t*]Glucose	1.027 ± 0.002	1.013 ± 0.001
[2-*t*]Glucose	0.927 ± 0.0003	0.929 ± 0.002
[3-*t*]Glucose	1.027 ± 0.004	1.031 ± 0.0009
[4-*t*]Glucose	1.051 ± 0.001	1.052 ± 0.003
[5-*t*]Glucose	0.988 ± 0.001	0.997 ± 0.0009
[6,6-t_2]Glucose	1.065 ± 0.003	1.034 ± 0.004

expected to dominate. Restriction of the hydroxyl rotor to geometries expected to enhance the above interaction are also thought to be responsible for an augmented normal EIE. A small inverse contribution is expected from a restriction in the torsion about the C5–C6 bond. Aside from the possibility of understanding the geometry and strength of enzyme–substrate interactions, a larger message is contained within Schramm's work: observed ^{3}H and ^{2}H KIEs measured in enzymatic systems may have substantial contributions from enzyme–substrate binding interactions. This point is important, as most KIEs in enzymatic systems are explained only within the context of bond-breaking and bond-forming processes. Given the often unique complementarity between enzymes and their natural substrates, it is not surprising that enzyme–substrate binding should affect vibrational frequencies in the process of using binding to release catalytic power.

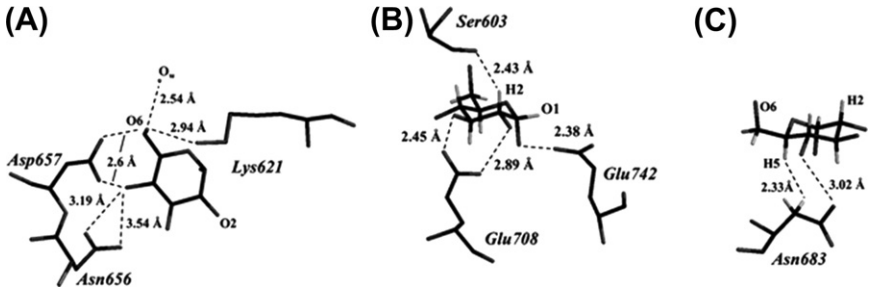

Figure 2.15 Attractive and repulsive interactions thought to be responsible for the ^{3}H-binding EIEs corresponding to the hexokinase/glucose interaction.

As an extension of the above work, Schramm's group recently extended the use of ^{3}H-binding EIEs to study the interactions between enzymes and competitive inhibitors. This work follows upon what is thought to be the first report of equilibrium binding isotope effects for enzyme–inhibitor binding.[178] The Pauling/Wolfenden model for enzyme catalysis and competitive inhibition states that competitive inhibitors that are better transition structure analogs will bind more tightly to their enzyme target. Purine nucleoside phosphorylase catalyzes the cleavage of purine nucleotides into the component phosphorylated ribose and nucleoside. Purine nucleoside phosphorylase (PNP) inhibitors, ImmH+ and DADMe-ImmH+ (Fig. 2.16), are picomolar inhibitors that approximate the geometry and charge distribution in the largely dissociative transition structure for the displacement of the nucleoside moiety from ribonucleotides by phosphate. DADMe-ImmH+ binds PNP more strongly than ImmH does. One would, therefore, expect a larger binding EIE for DADMe-ImmH+ than for ImmH. That is, in fact, what is observed when the binding ^{3}H EIE is measured at the 5′-position of the ribose ring. As a point of comparison, the ^{3}H EIE is what is surprising is that the binding isotope effect for DADMe-ImmH+ is greater than twice the effect observed for the less potent inhibitor, ImmH+. The fact that the isotope effect is quite distant from the point of bond cleavage and formation makes this observation even more surprising. This observation lends further

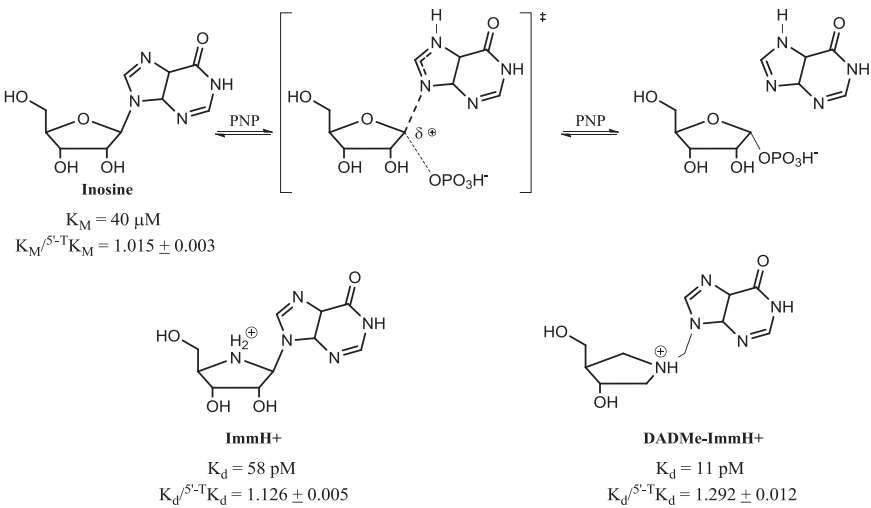

Figure 2.16 Attractive and repulsive interactions thought to be responsible for the ^{3}H-binding EIEs corresponding to the hexokinase/glucose interaction. For color version of this figure, the reader is referred to the online version of this book.

credence to the notion that enzymes make full use of enzyme–substrate complementarity to leverage catalytic power.

Further insight can be garnered when binding EIEs are compared with KIEs at the same position. Binding EIEs report upon interactions that develop in the formation of the Michaelis complex. Intrinsic KIEs report upon changes in force constant that occur during the rate-limiting step. Orotate phosphoribosyltransferases (OPRTs) cleave or form the C—N bond between the ribosyl and pyrimidine moieties in orotidine (or orotidine monophosphate). Recent measurements of α-2°-^{3}H KIEs for the OPRT-catalyzed cleavage of 1′-^{3}H-orotidine and 1′-^{3}H-orotidine phosphate suggest a largely dissociative transition state with significant conversion of the sp^3 C1 position to an sp^2 center.[179] In the context of Schramm's earlier work on binding EIEs, it might seem likely to expect a significant contribution to the expressed KIE from enzyme–substrate binding. Zhang and Schramm recently showed that the binding EIE for formation of the Michaelis complex is strongly dependent upon the degree of phosphorylation of orotidine.[180] Where half of the expressed α-2°-^{3}H KIE is due to binding for orotidine 5′-monophosphate, there is almost no EIE for binding expressed for the orotidine substrate (Table 2.2). This makes sense in the context of both K_M and k_{cat}/K_M estimates for the unphosphorylated and phosphorylated substrates. The K_M for the cleavage of orotidine by human OPRT is 91 ± 37 μM; whereas that for orotidine 5′-monophosphate is 1.6 ± 0.6 μM. The first-order rate constant is also affected. The k_{cat}/K_M value associated with orotidine is

Table 2.2. Experimental ^{3}H-binding EIEs and intrinsic KIEs for human OPRT

Measurement	OPRT·OMP (binary complex)	OPRT·OMP·SO_4^{2-} (ternary complex)
BIE*	1.108 ± 0.003	1.096 ± 0.004
K_d (μM)	2.5 ± 1.2	4.1 ± 2.5
KIE**	1.199 ± 0.015	1.330 (computed)
Measurement	**OPRT·orotidine (binary complex)**	**OPRT·orotidine·SO_4^{2-} (ternary complex)**
BIE*	0.999 ± 0.003	0.991 ± 0.005
K_d (μM)	140 ± 27	150 ± 22
KIE**	1.209 ± 0.004	1.411 (computed)

* Binding equilibrium isotope effect.
** Intrinsic KIE.

240-fold lower than that for orotidine 5′-monophosphate for the human enzyme. These results suggest that enzyme–substrate interactions that occur at the 5′-position have significant impact upon the enzyme's ability to deform the C1 center, which experiences substitution, from sp^3 hybridization to a geometry that is more representative of sp^2 hybridization.

One final note on Yang and Schramm's work on OPRT concerns measurements of binding EIEs and KIEs for the binary versus the ternary complex. The ternary complex is approximated using sulfate as a metaphosphate mimic. It is surprising that binding EIEs and Michaelis constants are very nearly equal for the binary and ternary complexes. This suggests one of two things: either sulfate is a poor approximation to metaphosphate, or metaphosphate binding does not affect enzyme geometry upon binding. If the latter scenario is true, it implies that OPRT exerts the bulk of its catalytic power in distorting orotidine 5′-monophosphate and is rather insensitive to the binding of a substrate bearing considerable charge.

3.5. Born–Oppenheimer Enzymes

The Pauling view of enzyme catalysis suggests a rather static role for the enzyme, as the active site of the enzyme essentially serves as a template for the transition state of the uncatalyzed reaction. While many of the origins of catalytic power in enzymes can reasonably be relegated to static sources, a number of reports over the past 15 years suggest a significant role for dynamics in enzyme catalysis.[181–184] Some recent elegant work by the Schramm laboratory indicates a role for dynamics in purine nucleoside phosphorylase catalysis. The report by Silva et al. explores the steady-state and single-turnover rates for unlabeled recombinant PNP and recombinant PNP that is expressed using heavily ^{13}C-, ^{15}N-, and ^{2}H-enriched nutrient sources.[185] Labeling of the PNP enzyme results in an enzyme that is 109.9% of the mass of PNP expressed in unlabeled media. Steady-state kinetic parameters for the phosphorolysis of inosine and guanosine were nearly identical for both 'heavy' and 'light' PNP. However, forward commitments to catalysis, measured using the isotope trapping method,[186] differed by a statistically significant amount for 'heavy' and 'light' PNP. As is shown in Table 2.3, the forward commitment to catalysis is smaller for 'heavy' PNP. These data are further bolstered by single-turnover rate constants (k_{chem}) for phosphorolysis measured using stopped-flow kinetics. The pseudo-first-order rate constant is approximately 20% smaller for 'heavy' PNP than for

Table 2.3. Kinetic parameters for phosphorolysis of inosine and guanosine catalysed by light and heavy PNP isotopologs

Kinetic parameter	Light PNP	Heavy PNP
	Inosine	
K_M (μM)	13 ± 2	12 ± 2
k_{cat}	7.5 ± 0.8	7.2 ± 0.9
K_{chem}	69 ± 3	55 ± 2
C_f	0.163 ± 0.010	0.139 ± 0.009
	Guanosine	
K_M (μM)	42 ± 6	45 ± 8
k_{cat}	10.0 ± 1.0	9.5 ± 0.9
K_{chem}	26 ± 1	19 ± 1
C_f	0.173 ± 0.013	0.122 ± 0.015

'light' PNP for the phosphorolysis of inosine. The effect is even greater for the phophorolysis of guanosine (27%).

The most mundane interpretation of the above results is that the enzyme is, of course, involved in the reaction coordinate and *should* exhibit an isotope effect. However, the exchangeable positions on PNP are not labeled, so the isotope effect cannot be attributed to deuterium versus protium transfer. The isotope effect, expressed as $k_{light\text{-}PNP}/k_{heavy\text{-}PNP}$ can be calculated from single turnover experiments to be 1.25 for inosine and 1.37 for guanosine. To attribute these effects to traditional heavy-atom KIEs, one would have to have approximately five large ($k_{light}/k_{heavy} = 1.050$) ^{13}C or ^{15}N effects acting in concert. Such an effect, requiring five bond-breaking or bond-forming processes that directly involve the enzyme, seems difficult to rationalize, especially considering that PNP does not appear to utilize covalent catalysis.[187] Another possibility is that the high isotopic enrichment of the 'heavy' PNP alters its structure in a way that makes it a less efficient catalyst. This notion is contradicted by the observation that six intrinsic KIEs measured for the arsenolysis of inosine (1′-^{14}C, 9-^{15}N, 1′-^{3}H, 2′-^{3}H, 5′-$^{3}H_2$, and 4′-^{3}H) are statistically indistinguishable for both 'light' and 'heavy' PNP. The only cogent hypothesis that remains is that isotopic labeling of PNP creates a dynamically distinct enzyme, referred to as a Born–Oppenheimer enzyme by Silva et al. In light of recent experimental work that highlights the importance of what might be called catalytically important motions, it seems reasonable to assume that

Table 2.4. Kinetic parameters for HIV-1 protease-catalysed cleavage of a model peptide

Kinetic parameter K_M (μM)	Light enzyme 8.7 ± 0.7	Heavy enzyme 14.0 ± 1.2
k_{cat} (s^{-1})	3.28 ± 0.08	2.75 ± 0.08
v_{ss} (FU min^{-1})	5.00 ± 0.04	4.47 ± 0.05
k_{burst} (s^{-1})	142 ± 5	90 ± 4

Schramm's work is yet another important indicator that enzyme catalysis is a dynamic process. Silva et al. explain these dynamic effects as being manifest in the isotopically induced changes in the femtosecond vibrations that are important to exploring phase space in the conversion of the Michaelis complex to the transition structure.

HIV-1 protease has also been isotopically enriched in ^{13}C, ^{15}N, and ^{2}H to yield a 'heavy' isotopolog that is 111.6% as massive as the enzyme expressed in media that is not isotopically enriched.[188] Unlike PNP, whose steady-state kinetics are dominated by product release, differences in heavy and light HIV-1 protease manifest themselves directly in steady-state kinetic parameters. Kipp et al. explored both pre-steady-state and steady-state kinetics using fluorescence as a spectroscopic handle. The pre-steady-state rate constant, referred to as k_{obs}, likely reflects the formation of the hydrate which results from attack of the nucleophilic water molecule upon the amide carbonyl. The first-order rate constant, k_{cat}, is thought to be dominated by the microscopic rate constant that corresponds to scission of the C–N bond of the peptide substrate. Table 2.4 illustrates isotope effects upon both k_{obs} and k_{cat} for heavy HIV-1 protease. Once again, the detailed mechanism for HIV-1 protease catalysis does not appear to involve direct formation of bonds to the enzyme, so the observed effect that results from isotopic labeling of the enzyme does not correspond to a traditional KIE that is dominated by zero-point energy contributions.

The isotope effect upon the pre-steady-state rate constant is substantially larger than that for k_{cat}. This implies a greater role for dynamics in the formation of the hydrate than for bond scission. This is not surprising. Most of the evidence that suggests a role for dynamics in enzyme catalysis is rooted in hydrogen transfer reactions. Hydrogen transfers, especially those for which tunneling is extremely important, are very sensitive to transfer distance. Formation of the hydrate involves simultaneous deprotonation of

the nucleophilic water molecule and general acid catalysis provided by a nearby aspartate residue. While rate-limiting C—N bond cleavage has been shown to involve the simultaneous transfer of two or more protons, the associated solvent isotope effect on k_{cat} is 2.2–3.2, depending upon the peptide substrate at high pH.[187] The solvent isotope effect indicates the compound effect of two small KIEs or one dominant KIE of normal magnitude. It seems possible that the reaction coordinate for formation of the hydrate contains a greater net contribution from the motion of hydrogen atoms. Consequently, it is reasonable to expect this fundamental reaction step to be more sensitive to dynamic effects than C—N bond scission.

Schramm's work with isotopically labeled enzymes adds credence to the idea that enzyme catalysis is not merely the result of pre-organized residues capable of providing a template to the transition structure of the uncatalyzed reaction. While the static view of enzyme catalysis has yielded high-affinity transition structure analog inhibitors, a number of isotope effect measurements in enzymes that specifically catalyze hydrogen transfers have been difficult to fit within the Pauling model for enzyme catalysis. Schramm's work provides another experimental tool capable of quantifying the importance of dynamical effects in enzyme catalysis and expands the discussion beyond hydrogen transfer.

3.6. Other Methods and Approaches

3.6.1. High-Performance Liquid Chromatography as a Means of Measuring KIEs

Thornton and others have noted that perdeuterated compounds can be separated from their perprotiated isotopologs with baseline resolution using reverse-phase high-performance liquid chromatography (HPLC).[189–193] Large hydrophobic molecules, like fatty acids, tend to be separated with better resolution than small molecules, especially those bearing numerous heteroatoms. This phenomenon was exploited by Holman's laboratory to use HPLC as a means of measuring competitive ^{2}H KIEs for the oxidation of linoleic acid to 13-hydroperoxy-9,11-(*Z,E*)-octadecadienoic acid (HPOD) catalyzed by human 15-lipoxygenase.[194] Holman's group used quantitative HPLC to measure isotopic fractionation in the product of a reaction taken to low (~5%) conversion. Quantitative HPLC analysis of a full conversion (100%) reaction was used to analyze the initial ratio or HPOD to d_{31}-HPOD. The report by Lewis et al. applied this convenient methodology to

measure ^{2}H KIEs for the human 15-lipoxygenase-catalyzed oxidation of linoleic acid at two starting concentrations of linoleic acid over a range of temperatures. This method is an incredibly convenient method that should be broadly applicable to the analysis of large KIEs in enzyme-catalyzed conversions of fatty acids.

3.6.2. KIEs upon Multiple Reaction Steps Using Global Kinetic Analysis

Kinetic complexity, the absence of a single predominating rate-determining step, is frequently a complicating factor in attempts to measure KIEs in enzyme-catalyzed reactions. Recently, Spies and Toney reported a methodology that utilizes isotope washout, isotopic equilibrium perturbation, and reaction progress curves to arrive at intrinsic 1° and 2° KIEs and EIEs for alanine racemase.[195] Using only circular dichroism as a spectroscopic handle, Spies and Toney collected reaction progress curves and performed isotope washout[196] and equilibrium perturbation[197] experiments to constrain parametric assignments of the rate constants shown in Fig. 2.17. Additional rate constants for isotope washout were included but were assumed to be large and had no reversible component. Intrinsic equilibrium and KIEs in the context of the experimentally supported mechanism are shown in Fig. 2.17. From individual estimates of rate constants and the isotope effects upon those rate constants, Spies and Toney generated a free energy profile for the racemization of alanine. There are a couple of interesting observations that can be made concerning alanine racemase catalysis. First, the EIEs for the formation of the external aldimines in both directions are large, considering that the isolated enzyme and substrate are nearly ergoneutral with the external aldimine intermediate. This suggests that alanine racemase, much like PNP (*vide supra*), achieves catalysis, at least in part, by deforming the C_α position from sp^3 hybridization to sp^2 in preparation for transferring the labile proton. The free energy profile generated from global kinetic analysis is insensitive to the free energy of the quinonoid intermediate, but the rather diminutive 1°-^{2}H KIE for both directions is rather small and is especially small in the direction of D → L. This suggests that the quinonoid intermediate is rather high in energy since 1°-^{2}H KIEs for proton transfer are largest for ergoneutral processes. In total, the approach taken here by Spies and Toney is powerful in two ways: it (1) yields intrinsic KIEs and (2) reports KIEs from multiple reaction steps. While racemases are special in that they catalyze a reaction whose equilibrium constant is identically 1, it seems reasonable

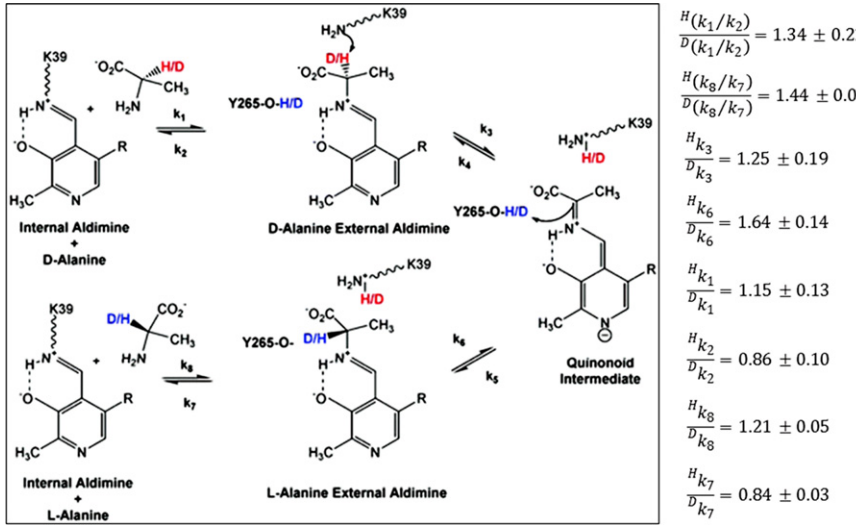

Figure 2.17 Experimentally validated mechanism for alanine racemase with associated intrinsic kinetic and EIEs.

to expect that a modified form of this approach could be applied to other enzymes that operate under equilibrium conditions.

3.6.3. Analysis of KIEs Arising from Nonbonding Interactions

Steric ^{2}H KIEs, as discussed above, rely upon the simple and satisfying expectation from well-understood quantum mechanical models that C–D bonds are shorter than C–H bonds. Dunitz and Ibberson recently reported measurements that challenge this simple model.[198] Neutron diffraction measurements of the size of the unit cell for C_6H_6 and C_6D_6 over a temperature range from 5 to 280 K indicate that C_6D_6 is smaller than C_6H_6 below 170 K and larger than C_6H_6 above this temperature. Dunitz and Ibberson explain their results in terms of low-frequency modes that make entropic effects outweigh enthalpic effects above 170 K. Gelabert et al. computationally explored the gas-phase molecular volumes of C_6H_6 and C_6D_6 from near 0 to 2000 K.[199] Over this temperature range, C_6D_6 always possesses a smaller molar volume than its lighter isotopolog. They conclude, as did Ibberson and Dunitz, that low-frequency extended crystalline modes are likely responsible for the size inversion of C_6H_6 and C_6D_6 in the solid phase. Ibberson and Dunitz relate their results to one of the first attempts by Mislow's laboratory to measure steric ^{2}H KIEs. The stereochemical inversion of **5** as compared to d_8-5 gave rise to a ^{2}H KIE of 1.06, in

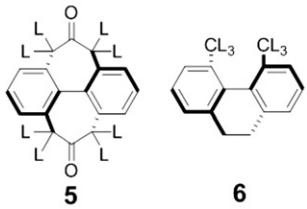

k_H/k_D	**5** vs. $[D_8]$-**5**	**6** vs. $[D_6]$-**6**
Experimental	1.06	0.880
Bigeleisen-Mayer	1.075	0.888
ZPE	1.026	0.755
EXC	1.050	1.182
MMI	0.998	0.995
ΔΔG≠	1.075	0.888
ΔΔH≠	0.973	0.743
-TΔΔS≠	1.105	1.193

Figure 2.18 Computed ^{2}H KIEs resulting from the development of nonbonding interactions in stereoinversions of **5** and **6**.

direct conflict with the expectations of Bartell's theory.[200–202] Following upon the questions raised by the work of Dunitz and Ibberson's, O'Leary et al. have used density functional calculations to decompose steric KIEs into their enthalpic and entropic components.[203] As is shown in Fig. 2.18, density functional calculations (B3LYP/6-31+G**) do well in replicating the measured KIE. This is somewhat surprising, given that the B3LYP functional has not been parameterized like the B97D or M06-2X functionals to account correct for correlation-mediated nonbonding interactions. What is perhaps more surprising is that there is a substantial inverse enthalpic H/D KIE of 0.973 which is masked by a much larger entropic H/D KIE of 1.105. A similar effect can be seen in the stereoinversion of **6**, where the enthalpic KIE outweighs the entropic KIE. The opposing entropic and enthalpic contributions can be extended to the consideration of a crossover temperature for KIEs that result from essentially repulsive nonbonding interactions. The physical origins and meaning of the crossover temperature can be interpreted in the context of the vibrational modes that are perturbed by the nonbonding interactions. However, another aspect of the report by O'Leary et al. is the notion that the enthalpic contribution to the KIE is not the same as the zero-point contribution. Here, once again, one must go beyond a simple zero-point energy view to capture the essence of the KIEs reported.

4. AREAS OF CURRENT INTEREST: A SYSTEMS VIEW

KIEs remain relevant to understanding the unique behaviors of fundamental organic reactions, reactions catalyzed by small organic or organometallic catalysts, reactions catalyzed by enzymes, and interesting

reaction phenomena. In this section, we explore three areas of intense current interest and rapid development. Applications of KIEs toward understanding new reactions have increased in recent years due to the robust and convenient method published by Singleton. While it is not always the case, useful organic reactions catalysed by relative small organic or organometallic catalysts often have one fundamental reaction step that is turnover limiting. Typically, this reaction step is the step of greatest interest. This aspect of small molecule reactions makes the application of KIEs toward understanding mechanism quite straightforward. In the quite recent past, the use of KIE measurements to identify rate- and product-determining steps in useful new reactions has become more common. It seems reasonable that this trend will continue and grow. Here, we outline some recent applications of KIEs toward understanding the mechanistic details behind recently developed synthetic methods.

The vanguard of the development of new methods for determining KIEs (and EIEs) has largely resided in enzymology. The seminal work by Cleland and others in formulating methods for measuring and interpreting KIEs in enzyme-catalyzed reactions established KIEs as one of the most powerful tools in the mechanistic toolbox. This is somewhat surprising, considering that KIE determinations in enzyme-catalyzed reactions are often much more difficult to interpret. Part of the difficulty associated with the measurement of KIEs in enzyme-catalyzed reactions is associated with the fact that enzyme-catalyzed reactions frequently have more than one partially rate-limiting step. In spite of these challenges, work by Schramm, Toney, and others continues to expand the borders of what is possible. Here we survey some recent applications of KIE measurement to enzyme catalysis. It seems likely that isotope effect measurement will remain one of the primary mechanistic tools in the enzymologists' toolbox. This is all the more likely as enzymologists strive not only to arrive at detailed mechanistic schemes for individual enzymes but try to understand the very origins of catalytic power.

The conventional view of isotope effects holds that they report directly upon vibrational force constant changes in proceeding from reactant to transition state (or product). Work described in the previous section showed that this is not always the case; KIEs can report upon dynamic phenomena that are affected by isotopic substitution by virtue of how mass impacts the sampling of phase space. Quantum mechanical tunneling is another phenomenon for which KIE studies are ideal mechanistic probes; however, the influence of tunneling upon 1° KIEs is not directly and uniformly related

to changes in force constants. The standard Bigeleisen–Mayer expression for the determination of KIEs is rooted in Eyring theory. There is something of a paradoxical nature to the Bigeleisen–Mayer expression: Bound motions, those for which real frequencies exist at the transition state, are treated quantum mechanically in the context of the harmonic oscillator approximation. The unbound motion, that which describes reaction coordinate motion at the first-order saddle point, is treated classically. KIEs are ideal mechanistic observables capable of testing the degree to which this assumption, rooted in Eyring theory, is valid. Here we survey some recent reports of isotope effect measurement used to further elucidate tunneling phenomena.

4.1. Mechanism in Synthetic Methodology

Synthetic methodology and mechanism have always developed symbiotically. Perhaps now more than ever, KIEs are being used to gain insight into C—H activation and catalytic enantioselective reactions. However, it is rare for KIEs to be used to elicit detailed mechanistic information in newly reported reactions. Often times, KIEs are used to identify the rate-determining step but are not coupled with transition structure modeling or additional analyses. Wu et al. recently reported a measurement of ^{13}C KIEs for the asymmetric olefin isomerization of butenolides catalyzed by a cinchona alkaloid.[204] The results are shown in Fig. 2.19. The only significant ^{13}C KIE resides at the C_γ position, indicating a candidate mechanism which involves deprotonation at C_α followed by rate-limiting enantioselective protonation of the vinylogous enolate at C_γ.

The coupling of C—C and C—N bonds in conjunction with C—H activation is perhaps the most active area of current synthetic methodology. A recently developed methodology that allows the coupling of activated alkenes with alcohols using a cationic ruthenium hydride catalyst, $[(C_6H_6)(PCy_3)(CO)RuH]^+BF_4^-$, represents a significant advancement in methodologies that involve C–H activation.[205] While it is somewhat rare for synthetic methodology groups to report significant mechanistic work upon the report of a new reaction, it is becoming more common. Yi's group often utilizes KIE studies to better understand the mechanistic underpinnings of their reactions. Figure 2.20 shows Yi's application of a variant[206] of Singleton's original method for measuring ^{13}C KIEs to their coupling reaction of indene and 1-(4-methoxyphenyl)ethanol. The only significant

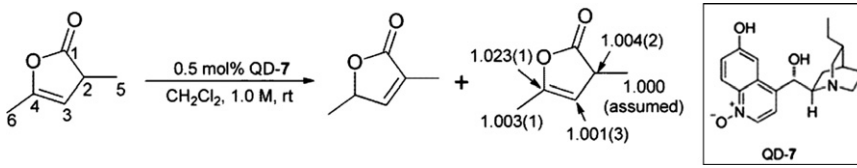

Figure 2.19 Experimentally determined ^{13}C KIEs measured for the stepwise cinchona alkaloid-catalysed asymmetric isomerization of butenolides.

KIE resides at the activated position on the indene substrate. Yi attributes this to rate-limiting C—C bond formation; however, it seems reasonable to consider initial C—H activation as an alternative rate-limiting step. This ambiguity highlights the importance of combined computational modeling and experimental KIE determination. An alternative approach would be to combine ^{2}H KIE measurements. The absence of a ^{2}H KIE at the activated position would indicate that the rate-limiting step is indeed C—C bond formation/reductive elimination step.

A general trend in the synthetic methodology community seems to be developing. As new reactions are developed, mechanistic studies are beginning to be used to gain a deeper understanding of steps which are turnover and product determining in catalytic reactions. The two examples above are representative of this trend, though a partial sampling of the recent integration of KIE studies and reaction discovery can be found in references 207-212.[207–212]

4.2. Tunneling

The application of KIEs to the study of hydrogen transfer is an intensely active field. The simultaneous involvement of both experimental and theoretical approaches to tunneling phenomena has fomented explosive growth in our understanding of hydrogen tunneling in both enzymatic and small molecule systems. A number of excellent reviews that treat tunneling

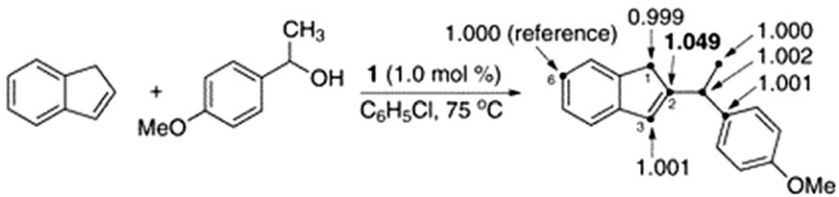

Figure 2.20 Experimentally determined ^{13}C KIEs measured for the coupling of indene and 1-(4-methoxyphenyl)ethanol catalysed by $[(C_6H_6)(PCy_3)(CO)RuH]^{+}BF_4^{-}$.

in the context of hydrogen transfer are available.[213–221] Here, we will primarily treat recent work upon systems that illustrate the effects of tunneling upon observed KIEs.

Soybean lipoxygenase 1 exhibits extremely large 1°-^{2}H KIEs ($k_H/k_D \approx 80$) and yields an essentially temperature-independent Arrhenius plot.[222,223] As such, soybean lipoxygenase has served as a sort of laboratory in which to study a reaction that is profoundly affected by hydrogen tunneling. A recent report by Meyer and Klinman used the Singleton method for measuring KIEs to measure 2°-^{2}H and ^{13}C KIEs at the vinylic positions (C9, C10, C12, and C13) for the soybean lipoxygenase-catalyzed oxidation of both 11,11-[D_2]-linoleic acid and linoleic acid.[224] Surprisingly, substantial β- and γ-^{2}H KIEs were found for both isotopologs of linoleic acid (Figs 2.21A and B). What is even more surprising is the presence of substantial ^{13}C KIEs at the vinylic positions for the oxidation of 11,11-[D_2]-linoleic acid (Fig. 2.21C). As Schramm's work showed, it can be expected that some of the ^{2}H isotope effects observed are likely to have contributions from binding, but it is unlikely that binding alone can explain the results in Fig. 2.19. Instead, it is well known that hydrogen tunneling has a profound effect upon the 1°-^{2}H KIE in soybean lipoxygenase 1. Applying a quantum transition state theory view, it seems reasonable for tunneling to have a significant effect upon 2° KIEs. Shifts in the positions of nuclei associated with hydrogen tunneling are not isolated to the transferred nucleus. Atomic motions at nearby locations are involved in the tunneling event. It seems reasonable to assume that these motions are a part of the tunneling coordinate and can exhibit 2° KIEs in excess of those seen in reactions that can largely be treated using Eyring theory. Tunneling phenomena can also be modeled using a Marcus theory view. In this view, the tunneling event is considered as involving distinct contributions from motion of the primary nucleus and the reorganization of nearby nuclei to resemble the product. In other

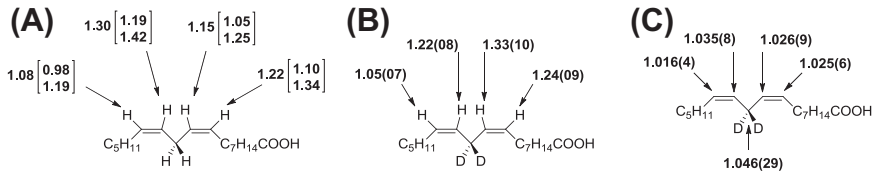

Figure 2.21 Experimentally determined 2°-^{2}H KIEs measured for the soybean lipoxygenase 1-catalysed oxidation of (A) linoleic acid and (B) 11,11-[D_2]-linoleic acid and (C) ^{13}C KIEs measured at vinylic positions for the oxidation of 11,11-[D_2]-linoleic acid.

words, motion of the transferred hydrogen atom is artificially decoupled from secondary nuclear motion. The application of a Marcus-like model tendered by Kuznetsov and Ulstrup was applied by Knapp et al. to model the temperature dependence of the 1°-^{2}H KIE in oxidations catalysed by soybean lipoxygenase 1.[225,226] In this model, tunneling in the primary coordinate depends upon a static electronic overlap and vibrational wave function overlap between donor and acceptor hydrogenic wave functions modulated by dynamical motions within the enzyme. The Kuznetsov–Ulstrup model, however, is only germane to modeling the 1°-^{2}H KIE. Meyer and Klinman used a model by Buhks et al. to demonstrate that tunneling effects upon reorganization energy could also help to explain the significant magnitudes of the 2°-^{2}H KIEs.[227] These data serve as an example of how tunneling can have profound effects upon 2°-^{2}H and ^{13}C KIEs and serve as a challenge to theoreticians to develop models that can compute 2° KIEs that are heavily influenced by tunneling.

The work described above demonstrates that tunneling can manifest itself in exalted 2°-^{2}H and ^{13}C KIEs. Recent calculations by the Borden group utilizing canonical variational transition state theory (CVT) with a SCT correction predicted a substantial inverse ^{2}H KIE at C1 (Fig. 2.22) for the rearrangement of the cyclopropylcarbinyl radical to the 3-butenyl radical. This is surprising because the rearrangement proceeds with substantial contributions from tunneling to the reaction. Borden's calculations, however, were performed at a temperature of 20 K (−253.15 °C), which significantly increases the magnitude of isotope effects substantially over what would be expected at room temperature. If tunneling corrections are not applied to the calculation of the ^{2}H KIE at C1, the inverse KIE is very substantial ($k_H/k_D = 0.0023$). The semi-classical origins of this isotope effect can be found in the conversion of the sp^{2} hybridized C1 from a radical centre to an alkene that results from the rearrangement of the cyclopropylcarbinyl radical to the 3-butenyl radical. Restriction of torsional motions tighten the force constants associated with vibrational modes that involve the terminal CH_2 group, leading to a substantial inverse ^{2}H KIE. Tunneling yields a normal contribution to the ^{2}H KIE, which raises the effect to $k_H/k_D = 0.37$. Singleton's group then measured intramolecular ^{13}C KIEs [$^{12}k/^{13}k$ for C4]/[$^{12}k/^{13}k$ for C3] over the temperature range −100 to 80 °C (Table 2.5). Borden's calculated intramolecular KIEs matched the experimental KIEs exceedingly well using the CVT/SCT approach. These results demonstrate two things: (1) While tunneling always contributes a normal component to

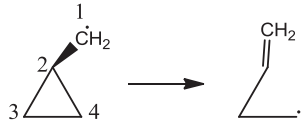

Carbon	k(^{12}C/^{13}C)	k(^{1}H/^{2}H)
C1	0.96	0.37
C2	1.77	1.49
C3	1.12	0.85
C4	2.42	6.47

Figure 2.22 KIEs predicted for the rearrangement of the cyclopropylcarbinyl radical using CVT and an SCT correction. For color version of this figure, the reader is referred to the online version of this book.

KIEs, the composite KIE can still be inverse and (2) the CVT/SCT can be an effective means of computing KIEs that result in large part from tunnelling contributions.

KIEs have served as one of the most useful probes of mechanism for many reasons. One of the most compelling aspects of KIEs as observables is their amenability to computational efforts. Using quantum chemical software packages to optimize saddle points as approximations to the transition state and using frequency calculations as inputs to the Bigeleisen–Mayer equation has been a suitable approach for the vast majority of reactions for which KIEs have been measured. New computational methodologies offer a means of developing cogent physical models to augment experimental work. As has been indicated above, tunnelling provides one of the greatest challenges to computational efforts. Recent work by Wong et al. demonstrates the use of an approximate Feynman path integral technique, second-order Kleinert perturbation theory, to compute the 1°-^{2}H KIE associated

Table 2.5. Comparison of experimental and computed (CVT/SCT) intramolecular ^{13}C KIEs for the rearrangement of the cyclopropylcarbinyl radical

Temperature (°C)	Experimental KIE	Computed KIE
80	1.062 ± 0.003	1.057
22	1.079 ± 0.002	1.073
0	1.085 ± 0.003	1.082
−78	1.131 ± 0.002	1.138
−100	1.163 ± 0.004	1.169

with the protonation of α-methoxystyrenes by acetic acid analoges.[228–230] Resulting comparisons between experiment and theory are quite promising. Wong et al. found that vibrational anharmonicity and tunneling contribute substantially to the isotope effect.

5. AREAS OF FUTURE EXPLORATION

Previous mention has been made of a number of sensitive and versatile methods for the experimental measurement of KIEs. Likewise, we have explored classes of systems where KIEs and EIEs have helped contribute a deeper physical understanding of pervasive phenomena. There is little doubt that isotope effects will continue to contribute to our understanding of interesting chemical and biological systems. Below, we will explore some areas of current interest that are ripe for experimental and theoretical development in which isotope effect measurements are likely to contribute to forward progress.

5.1. Solvation

Numerous researchers have demonstrated that solvent can have a profound effect upon experimentally determined KIEs. However, explanations of the origins of solvent effects upon observed KIEs remain speculative. Great strides have been made that incorporate some of the effects due to solvation in transition structure calculations. Among these advancements are continuum models for solvent influence. Polarizable continuum models provide an adequate means of modeling solvent effects when solvent serves only to screen charge.[231] Recent algorithmic developments have facilitated the application of polarizable continuum models to transition structure calculations.[232] Continuum models are especially important to reactions that proceed in polar aprotic solvents. In these solvents, the differences between structures computed in the gas phase and those computed using a polarizable continuum model can be profound.

Solvation is frequently complicated owing to directional interactions like hydrogen bonding and coordination. To appropriately model the coordinating effects of solvent, hydrogen bonding effects, or the effects of solvent friction, an explicit model is often necessary. To some extent, this problem has been addressed in systems of interest to the organic chemistry community by using molecular dynamics in conjunction with transition structure optimizations; however, accounting for all relevant phase space at

the transition state, given the microstates due to solvation, is still an unsolved problem. Car–Parrinello molecular dynamics may prove very useful in future efforts to simulate reactions for which solvation has a profound, yet nonintuitive, influence upon reactivity or selectivity.[233,234] Two examples that merit study are an asymmetric allylboration reported by Lou et al. and the general field of micellar catalysis. In the former study, the use of toluene as solvent results in only moderate yields, but the use of α,α,α-trifluorotoluene as a solvent nearly doubles the reported yield and improves selectivity slightly.[235] It seems reasonable to assume that solvent microstructure plays a key role in defining the transition structure for this reaction. Other similar effects have been demonstrated in the partitioning of products between C—H activation and cyclopropanation lineages for Rh-catalyzed additions of vinylcarbenoids when using α,α,α-trifluorotoluene as opposed to more conventional solvents.[236] The use of α,α,α-trifluorotoluene as a solvent may be analogous to the use of amphiphilic cosolvents to form micelles that solvate organic reactions. A recent review of the developments in micellar catalysis cataloges many of the recent developments in applying this technology to metal-catalyzed reactions.[237] Isotope effects, especially $2°$-^{2}H KIEs, may be instrumental in understanding differences in solvent environments between micelles and bulk solvent. It seems reasonable to expect that a micelle environment may exert an effect that can be mimicked by pressure. Combined computational and experimental studies will be crucial in developing a mechanistic understanding for solvent when it plays an active role in influencing reaction outcomes.

5.2. Ion Pairing

Reaction selectivity can be thought of in broad terms as being the result of making one reaction channel overwhelmingly energetically favorable. Of course, in the context of an enantioselective reaction where selectivity results from the relative free energies of two diastereomeric transition states, energy differences as low 2.2 kcal mol^{-1}mol give rise to what is considered a highly enantioselective reaction (>95% e.e.) at room temperature. Even less of an energy difference is needed at low temperatures to yield high selectivity. Ion pairs involving chiral ions can have substantial effects in stereoselective reactions. This idea was first explored in the context of phase transfer catalysis.[238] Chiral phase transfer catalysts continue to be of great interest today.[239] Presumably, KIEs and EIEs could yield insight into the structure of ion pairs both at the transition state and as stable complexes.

Previous work in the Meyer laboratory (vide supra) demonstrated the capacity of ^{2}H KIEs arising from nonbonding interactions to report on transition structure. A similar approach to the one used by the Meyer laboratory could be used to extract information about chiral ion pairing in phase transfer catalysis.

Ion pairing can also have tremendous influence upon organometallic structure. This influence can have substantial downstream effects on catalyst performance. An example of a profound difference in ion pair structure has been reported by Zuccaccia et al.[240] They report that cationic adducts between cationic Au(I) complexes and 4-methylstyrene have distinct placements of the BF_4^- cation depending upon the nature of the ligand. Triphenylphosphine ligands yield a structure that sandwiches the alkene between Au(I) and BF_4^-. By contrast, *N*-heterocyclic carbene ligands yield a complex that sandwiches the ligand between Au(I) and the tetrafluoroborate counterion (Fig. 2.23). In agreement with these findings, it is noted that Au(I)-catalyzed activation of alkenes and alkynes demonstrate greater counterion sensitivity when phosphines are used as ligands. This idea has recently been applied to the development of new Au(I)-catalysed hydroalkoxylation strategies.[241] It seems reasonable to expect this strategy to become more common in a diverse array of ionic organometallic catalysts.

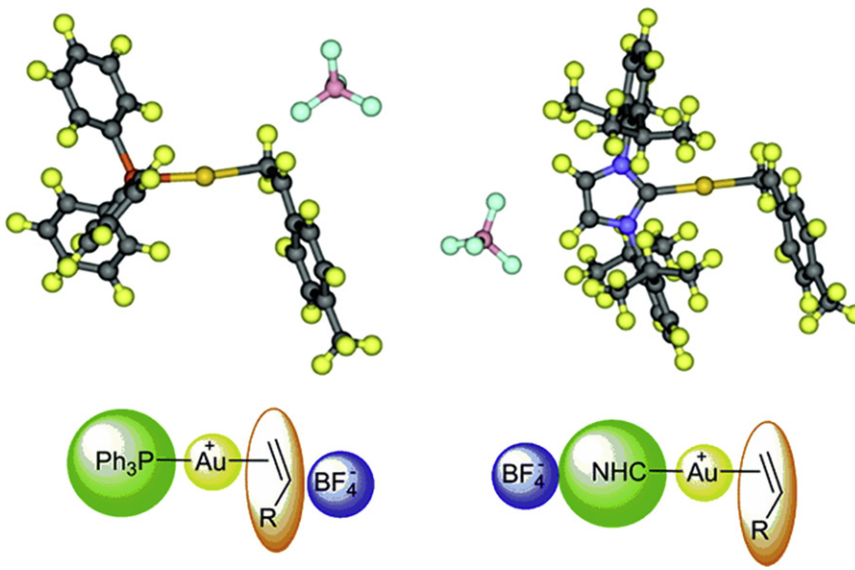

Figure 2.23 Differences in anion position depend upon the nature of the ligand in Au(I)–alkene complexes.

KIEs offer a means of exploring nonbonding interactions that arise in the transition states of these reactions.

5.3. Mechanisms of Catalysis

The development of catalytic asymmetric reactions continues to occupy a significant portion of the organic chemistry community. Of primary interest are the interactions between the catalyst and the substrate(s) at the transition state that determines product distribution. Currently, we rely upon computational models and KIEs measured upon substrate molecules to infer these interactions. Measurement of KIEs upon the catalyst itself will yield information about the turnover-limiting step. In most current catalytic asymmetric reaction mechanistic hypotheses, it is assumed that the turnover-limiting, rate-determining, and product-determining steps are equivalent. In such cases, the measurement of rates resulting from isotopologs of the catalyst have the capacity to confer detailed structural knowledge relating the manner in which stereoselection occurs. This idea is analogous to Schramm's Born-Oppenheimer enzymes but aims toward a very different scientific goal. In cases where catalyst turnover is limited by off-cycle processes, KIEs resulting from isotopic substitution upon the catalyst could be used in conjunction with techniques such as reaction progress kinetics analysis developed by the Blackmond laboratory, yielding a comprehensive approach to identifying potential improvements to existing catalysts in efforts to increase turnover frequency.

5.4. Asymmetric Reactions

Enantioselective catalysis remains an active area of development in synthetic methodology. However, the development of new mechanistic tools for the exploration of asymmetric reactions poses some unique challenges. For all but the most robust reactions, either selectivity, yield, or both can be limited. Of course, it is this stage in reaction development where mechanistic information is most crucial. One of the principal limitations of measuring intermolecular KIEs is the essential requirement that essentially one reaction channel be responsible for isotopic fractionation. Intramolecular KIEs, where applicable, circumvent this requirement. As mechanistic work becomes an ever more frequent complement to synthetic methodology, it is likely that new methods will be developed to meet the challenges of understanding reactions that proceed by more than one reaction channel.

5.5. C–H Activation

Mechanisms that govern C–H activation span a broad continuum.[242–244] KIEs have been tremendously useful in understanding mechanism at the level of arrow pushing in these reactions,[245] but the fundamental physical behavior of recently developed C–H activation reactions is not well understood. Of course, some of the most interesting examples of C–H activation exist in enzymatic systems. Enzymes with heme and nonheme iron centers, quinone cofactors, and putative radical cofactors have diverse ways of cleaving both activated and unactivated C–H bonds in a very selective fashion. Enzymes as diverse as cytochrome P450s, lipoxygenases, desaturases, and oxidases have KIEs that vary over nearly two orders of decade magnitude and have extremely diverse Arrhenius behavior. It seems reasonable to expect similar disparities in C–H activations catalyzed by man-made catalysts. Practices, methodologies, and accumulated mechanistic ideas will likely flow from both enzymology and tunneling subfields to aid in understanding the physics behind potentially useful C–H activation reactions over the next several years. Detailed mechanistic pictures capable of yielding a nuanced picture of how hydrogen moves in C–H activations will likely yield understanding crucial to the development of future C–H activation methods.

6. CONCLUDING COMMENTS

KIE measurement and interpretation continues to be one of the most often employed means of mechanistic inquiry. New analytical methods, innovative experimental design, increased computational power, improved computational algorithms, and an ever-growing set of intriguing mechanistic questions guarantees that KIEs will continue to supply physical insight into chemical mechanism and structure. The measurement and interpretation of KIEs is one of the happiest marriages of experiment and theory. As new experimental methods allow insight into previously unapproachable questions, theory will play an important role in elucidating the physical origins of isotope effects. In fact, it may have gone largely unnoticed, but mechanistic organic chemistry has been turning a corner since the early 2000s. Due to the efforts of Singleton and others, KIE measurements have become accessible to the nonspecialist. Apace of these developments has been the advent of complementary mechanistic methods, like reaction progress kinetics analysis[246,247] and recent adaptations of linear free energy

relationships.[121–124,248,249] These factors promise a more prominent role for physical organic chemistry in the development of new reactions and the elucidation of biochemical reactions important to life processes.

ACKNOWLEDGEMENTS

The author gratefully acknowledges past support from the Petroleum Research Fund (48060-G4) and the National Institute of General Medical Sciences (GM87706-01) and the National Science Foundation (CHE-1058483) for current support. The author would also like to acknowledge the mentorship of three pioneers in the measurement and interpretation of KIEs: Richard L. Schowen, Daniel A. Singleton, and Judith P. Klinman.

REFERENCES

1. Kohen A, Limbach H-H, eds. *Isotope Effects in Chemistry and Biology*. Boca Raton, FL: Taylor & Francis; 2006.
2. Wolfsberg M, van Hook WA, Paneth P. *Isotope Effects in the Chemical, Geological, and Bio Sciences*. New York: Springer; 2010.
3. Muller P. *Pure Appl Chem*. 1994;66:1077-1084.
4. Westheimer FH. *Chem Rev*. 1961;61:265-273.
5. Eyring H. *J Chem Phys*. 1935;3:107-115.
6. Redlich O. *Z Phys Chem B*. 1935;28:371-382.
7. Bigeleisen J. *J Chem Phys*. 1949;17:675-678.
8. Bigeleisen J, Wolfsberg M. *Adv Chem Phys*. 1958;1:15-76.
9. Fröman N, Fröman PO. *JWKB Approximation: Contributions to the Theory*. Amsterdam: North-Holland Publishing Company; 1965.
10. Many references include typographical errors in this equation. Northrop provides the typographically correct expression here: Northrop DB *J Am Chem Soc*. 1999;121:3521-3524.
11. Bell RP. *Trans Faraday Soc*. 1959;55:1-4.
12. Melander L, Saunders WH Jr. *Reaction Rates of Isotopic Molecules*. Malabar, FL: Robert E. Krieger Publishing Co.; 1987. 15.
13. Toth K, Amyes TL, Wood BM, Chan K, Gerlt JA, Richard JP. *J Am Chem Soc*. 2010;132:7018-7024.
14. Mundle SOC, Lacrampe-Couloume G, Sherwood Lollar B, Kluger RJ. *J Am Chem Soc*. 2010;132:2430-2436.
15. Cannon JS, Kirsch SF, Overman LE, Sneddon HF. *J Am Chem Soc*. 2010;132:15192-15203.
16. Seo SY, Yu X, Marks TJ. *J Am Chem Soc*. 2009;131:263-276.
17. Rousseaux S, Gorelsky SI, Chung BKW, Fagnou K. *J Am Chem Soc*. 2010;132:10692-10705.
18. Deprez NR, Sanford MS. *J Am Chem Soc*. 2009;131:11234-11241.
19. Gaweska H, Henderson Pozzi M, Schmidt DMZ, McCafferty DG, Fitzpatrick PF. *Biochemistry*. 2009;48:5440-5445.
20. $^{15}N/^{14}N$ KIE example: Marlier JF, Fogle EJ, Cleland WW *Biochemistry*. 2008;47:11158-11163.
21. $^{18}O/^{16}O$ KIE example: Humphreys KJ, Mirica LM, Wang Y, Klinman JP *J Am Chem Soc*. 2009;131:4657-4663.
22. $^{14}C/^{12}C$ KIE example: Schwartz PA, Vetticatt MJ, Schramm VL *Biochemistry* 2011; 50: 1412–1420.

23. $^{35}Cl/^{37}Cl$ KIE example: Lewandowicz A, Rudziński J, Tronstad L, Widersten M, Ryberg P, Matsson O, Paneth P *J Am Chem Soc.* 2001;123:4550-4555.
24. $^{35}Cl/^{37}Cl$ KIE example: Westaway KC, Fang YR, MacMillar S, Matsson O, Poirier RA, Islam SM *J Phys Chem A.* 2007;111:8110-8120.
25. Bell RP. *The Tunnel Effect in Chemistry*. London: Chapman and Hall; 1980.
26. Stern MJ, Weston RE Jr. *J Chem Phys.* 1974;60:2808-2814.
27. Giagou T, Meyer MP. *J Org Chem.* 2010;75:8088-8099.
28. Creary X, Keller M, Dinnocenzo JP. *J Org Chem.* 1978;43:3874-3878.
29. Siehl HU, Walter H. *J Am Chem Soc.* 1984;106:5355-5356.
30. Amin M, Price RC, Saunders WH Jr. *J Am Chem Soc.* 1990;112:4467-4471.
31. Streitweiser A Jr, Jagow RH, Fahey RC, Suzuki S. *J Am Chem Soc.* 1958;80:2326-2332.
32. Williams IH. *J Am Chem Soc.* 1984;106:7206-7212.
33. Zhao XG, Tucker SC, Truhlar DG. *J Am Chem Soc.* 1991;113:826-832.
34. Wolfe S, Kim CK. *J Am Chem Soc.* 1991;113:8056-8061.
35. Halevi EA, Secondary Isotope Effects. Chap. 4. In: Cohen SG, Streitweiser Jr A, Taft Jr. RW, eds. *Progress in Physical Organic Chemistry.*, Vol. 1. New York: Interscience; 1963.
36. Streitweiser A Jr, Klein HS. *J Am Chem Soc.* 1963;85:2759-2763.
37. Mitchell TA, Bode JW. *J Am Chem Soc.* 2009;131:18057-18059.
38. Gajewski JJ, Bocian W, Harris NJ, Olson LP, Gajewski JP. *J Am Chem Soc.* 1999;121:326-334.
39. Kim Y, Marenich AV, Zheng J, Kim KH, Kołodziejska-Huben M, Rostkowski M, et al. *J Chem Theory Comput.* 2009;5:59-67.
40. Streitwieser A Jr, Nair PM. *Tetrahedron.* 1959;5:149-165.
41. Lewis ES. *Tetrahedron.* 1959;5:143-148.
42. Shiner VJ Jr. *Tetrahedron.* 1959;5:243-247.
43. Servis KL, Borčić S, Sunko DE. *Tetrahedron.* 1968;24:1247-1253.
44. Meot-Ner M. *J Am Chem Soc.* 1987;109:7947-7950.
45. DeFrees DJ, Hehre WJ, Sunko DE. *J Am Chem Soc.* 1979;101:2323-2327.
46. Shiner VJ Jr, Jewett JG. *J Am Chem Soc.* 1964;86:945-946.
47. Sunko DE, Szele I, Hehre WJ. *J Am Chem Soc.* 1977;99:5000-5005.
48. Tormos JR, Wiley KL, Wang Y, Fournier D, Masson P, Nachon F, Quinn DM. *J Am Chem Soc.* 2010;132:17751-17759.
49. Schwartz PA, Vetticatt MJ, Schramm VL. *Biochemistry.* 2011;50:1412-1420.
50. Williams IH. *Chem Comm.* 1985:510-511.
51. Murr BL, Nickon A, Swarz T, Werstuik HN. *J Am Chem Soc.* 1967;89:1730-1732.
52. Ko ECF, Robertson RE. *J Am Chem Soc.* 1972;94:573-575.
53. Bartell LS. *Tetrahedron Lett.* 1960:13-16.
54. Bartell LS. *Iowa State J Sci.* 1961;36:137-146.
55. Bartell LS. *Tetrahedron.* 1961;17:177-190.
56. Bartell LS. *J Am Chem Soc.* 1961;83:3567-3571.
57. Carter RE, Kahlgren L. *Acta Chem Scand.* 1969;23:504-514.
58. Mislow K, Graeve R, Gordon AJ, Wahl GH Jr. *J Am Chem Soc.* 1964;86:1733-1741.
59. Mislow K, Graeve R, Gordon AJ, Wahl GH Jr. *J Am Chem Soc.* 1963;85:1199-1200.
60. Melander L, Carter RE. *J Am Chem Soc.* 1964;86:295-296.
61. Sherrod SA, da Costa RL, Barnes RA, Boekelheide V. *J Am Chem Soc.* 1974;96:1565-1577.
62. Geneste P, Lamaty G. *Tetrahedron Lett.* 1965:4633-4638.
63. Barclay LRC, Mercer JR, MacAulay PJ. *Can J Chem.* 1975;53:3171-3174.
64. Nagorski RW, Slebocka-Tilk H, Brown RS. *J Am Chem Soc.* 1994;116:419-420.
65. Badger RC, Fry JL. *J Am Chem Soc.* 1979;101:1680-1687.

66. Mugridge JS, Bergman RG, Raymond KN. *Angew Chem Int Ed*. 2010;49:3635-3637.
67. Hayama T, Baldridge KK, Wu TT, Linden A, Siegel JS. *J Am Chem Soc*. 2008;130:1583-1591.
68. Felder T, Schalley CA. *Angew Chem Int Ed*. 2003;42:2258-2260.
69. Saunders M, Wolfsberg M, Anet FAL, Kronja O. *J Am Chem Soc*. 2007;129:10276-10281.
70. Anet FAL, Basus VJ, Hewett APW, Saunders M. *J Am Chem Soc*. 1980;102:3945-3946.
71. Zhu H; O'Leary DJ; Meyer MP. To be submitted.
72. Fong AYW; O'Leary DJ; Meyer MP. To be submitted.
73. Hammond GS. *J Am Chem Soc*. 1955;77:334-338.
74. Leffler JE. *Science*. 1953;117:340-341.
75. Hogg JL. Secondary Hydrogen Isotope Effects. In: Goundour RD, Schowen RL, eds. *Transition States of Biochemical Processes*. New York: Plenum; 1978:201-224.
76. Shiner VJ Jr. Deuterium Isotope Effects in Solvolytic Substitution. In: Collins CJ, Bowman NS, eds. *Isotope Effects in Chemical Reactions*. New York: Van Nostrand Reinhold; 1970:90-159.
77. Pohl ER, Hupe DJ. *J Am Chem Soc*. 1980;102:2763-2768.
78. do Amaral L, Bastos MP, Bull HG, Ortiz JJ, Cordes EH. *J Am Chem Soc*. 1979;101:169-173.
79. Kirsch JF. Secondary Kinetic Isotope Effects. In: Cleland WW, O'Leary MH, Northrop DB, eds. *Isotope Effects on Enzyme-Catalyzed Reactions*. Baltimore, MD: University Park Press; 1977:100-121.
80. Kovach IM, Elrod JP, Schowen RL. *J Am Chem Soc*. 1980;102:7530-7534.
81. Gajewski JJ, Conrad ND. *J Am Chem Soc*. 1979;101:6693-6704.
82. Gajewski JJ. *Acc Chem Res*. 1980;13:142-148.
83. Gajewski JJ, Jurayj J, Kimbrough DR, Gande ME, Ganem B, Carpenter BK. *J Am Chem Soc*. 1987;109:1170-1186.
84. Ostović D, Roberts RMG, Kreevoy MM. *J Am Chem Soc*. 1983;105:7629-7631.
85. Poirier RA, Wang Y, Westaway KC. *J Am Chem Soc*. 1994;116:2526-2533.
86. Kim Y, Kreevoy MM. *J Am Chem Soc*. 1992;114:7116-7123.
87. Amin M, Price RC, Saunders WH Jr. *J Am Chem Soc*. 1988;110:4085-4086.
88. Huskey WP, Schowen RL. *J Am Chem Soc*. 1983;105:5704-5706.
89. Cook PF, Oppenheimer NJ, Cleland WW. *Biochemistry*. 1981;20:1817-1825.
90. Welsh KM, Creighton DJ, Klinman JP. *Biochemistry*. 1980;19:2005-2016.
91. Kurz LC, Frieden C. *J Am Chem Soc*. 1980;102:4198-4203.
92. Hermes JD, Morrical SW, O'Leary MH, Cleland WW. *Biochemistry*. 1984;23:5479-5488.
93. Pudney CR, Hay S, Sutcliffe MJ, Scrutton NS. *J Am Chem Soc*. 2006;128:14053-14058.
94. Karsten WE, Hwang CC, Cook PF. *Biochemistry*. 1999;38:4398-4402.
95. Streitwieser A, Jagow RH, Fahey RC, Suzuki F. *J Am Chem Soc*. 1958;80:2326-2332.
96. Swain CG, Stivers EC, Reuwer JF Jr, Schaad LJ. *J Am Chem Soc*. 1958;80:5885-5893.
97. Hirschi J, Singleton DA. *J Am Chem Soc*. 2005;127:3294-3295.
98. Huskey WP. *J Phys Org Chem*. 1991;4:361-366.
99. Schimerlik MI, Rife JF, Cleland WW. *Biochemistry*. 1975;14:5347-5354.
100. Roth JP. *Acc Chem Res*. 2009;42:399-408.
101. Pascal RA, Baum MW, Wagner CK, Rodgers LR, Huan D-S. *J Am Chem Soc*. 1986;108:6477-6482.
102. Singleton DA, Thomas AA. *J Am Chem Soc*. 1995;117:9357-9358.
103. Yoshikai N, Matsuda H, Nakamura E. *J Am Chem Soc*. 2009;131:9590-9599.

104. Lee JK, Bain AD, Berti PJ. *J Am Chem Soc.* 2004;126:3769-3776.
105. Meyer MP, Klinman JP. *J Am Chem Soc.* 2011;133:430-439.
106. Chan J, Lewis AR, Gilbert M, Karwaski MF, Bennet AJ. *Nat Chem Biol.* 2010;6:405-407.
107. Guo X, Sinnott ML. *Biochem J.* 1993;294:653-656.
108. Cram DJ, Elhafez FAA. *J Am Chem Soc.* 1952;74:5828-5835.
109. Evans DA, Dart MJ, Duffy JL, Yang MG. *J Am Chem Soc.* 1996;118:4322-4343.
110. Reetz MT, Kesseler K, Jung A. *Tetrahedron Lett.* 1984;25:729-735.
111. Leitering TJ, Cram DJ. *J Am Chem Soc.* 1968;90:4019-4026.
112. Leitering TJ, Cram DJ. *J Am Chem Soc.* 1968;90:4011-4018.
113. Cornforth JW, Cornforth MRH, Mathew KK. *J Chem Soc.* 1959:112-127.
114. Chérest M, Felkin H, Prudent N. *Tetrahedron Lett.* 1968;9:2199-2204.
115. Zimmerman HE, Traxler MD. *J Am Chem Soc.* 1957;79:1920-1923.
116. Roush WR. *J Org Chem.* 1991;56:4151-4157.
117. Vittorelli P, Winkler T, Hansen H-J, Schmid H. *Helv Chim Acta.* 1968;51:1457-1461.
118. Evans DA, Vogel E, Nelson JV. *J Am Chem Soc.* 1979;101:6120-6123.
119. Winstein S, Holness NJ. *J Am Chem Soc.* 1955;77:5562-5578.
120. Taft RW. *J Am Chem Soc.* 1952;74:3120-3128.
121. Taft RW. *J Am Chem Soc.* 1952;74:2729-2732.
122. Taft RW. *J Am Chem Soc.* 1953;75:4538-4539.
123. Charton M. *J Am Chem Soc.* 1969;91:615-618.
124. Charton M. *J Am Chem Soc.* 1975;97:1552-1556.
125. Charton M. *J Org Chem.* 1976;41:2217-2220.
126. Wu JH, Zhang G, Porter NA. *Tetrahedron Lett.* 1997;38:2067-2070.
127. Sigman MS, Miller JJ. *J Org Chem.* 2009;74:7633-7643.
128. Miller JJ, Sigman MS. *Angew Chem Int Ed.* 2008;47:771-774.
129. Gustafson JL, Sigman MS, Miller SJ. *Org Lett.* 2010;12:2794-2797.
130. Liao L, Sigman MS. *J Am Chem Soc.* 2010;132:10209-10211.
131. Zhu H, Reyes NS, Meyer MP. *Tetrahedron Lett.* 2009;50:6803-6806.
132. Giagou TG, Meyer MP. *Chem Eur J.* 2010;16:10616-10628.
133. West JD, Stafford SE, Meyer MP. *J Am Chem Soc.* 2008;130:7816-7817.
134. Decius JC, Wilson EB Jr. *J Chem Phys.* 1951;19:1409-1412.
135. Brown HC, Chandrasekharan J, Ramachandran PV. *J Am Chem Soc.* 1988;110:1539-1546.
136. Corey EJ, Helal CJ. *Angew Chem Int Ed.* 1998;37:1986-2012.
137. Liu D, Hong S, Corey EJ. *J Am Chem Soc.* 2006;128:8160-8161.
138. Zhou G, Corey EJ. *J Am Chem Soc.* 2005;127:11958-11959.
139. Corey EJ. *Angew Chem Int Ed.* 2002;41:1650-1667.
140. Corey EJ. *Angew Chem Int Ed.* 2009;48:2100-2117.
141. Corey EJ, Link JO. *Tetrahedron Lett.* 1990;31:601-604.
142. Jones DK, Liotta DC, Shinkai I, Mathre DJ. *J Org Chem.* 1993;58:799-801.
143. Wang X, Du J, Liu H, Du D-M, Xu J. *Heteroatom Chem.* 2007;18:740-746.
144. Corey EJ, Bakshi RK, Shibata S. *J Am Chem Soc.* 1987;109:5551-5553.
145. Corey EJ, Link JO. *Tetrahedron Lett.* 1992;33:4141-4144.
146. Meyer MP. *Org Lett.* 2009;11:4338-4341.
147. Alagona G, Ghio C, Persico M, Tomasi S. *J Am Chem Soc.* 2003;125:10027-10039.
148. Saavedra J, Stafford SE, Meyer MP. *Tetrahedron Lett.* 2009;50:1324-1327.
149. Stafford SE, Meyer MP. *Tetrahedron Lett.* 2009;50:3027-3030.
150. Zhu H, Clemente FR, Houk KN, Meyer MP. *J Am Chem Soc.* 2009;131:1632-1633.
151. Clemente FR, Houk KN. *Angew Chem Int Ed.* 2004;43:5766-5768.
152. Newman-Evans RH, Carpenter BK. *J Am Chem Soc.* 1984;106:7994-7995.

153. Carpenter BK. *Acc Chem Res*. 1992;25:520-528.
154. Basilevsky MV. *Chem Phys*. 1977;24:81-89.
155. Grdina B, Orfanopoulos M, Stephenson LM. *J Am Chem Soc*. 1979;101:3111-3112.
156. Gollnick K, Hartmann H, Paur H. On the Mechanism of the Ene-reactions with Singlet Oxygen O2(1Δg): Dependance of Rates on Solvent Polarity and Structure. In: Rodgers MAJ, Powers EL, eds. Oxygen and Oxy-Radicals in Chemistry and Biology. New York: Academic Press; 1981:379-395.
157. Singleton DA, Hang C, Szymanski MJ, Meyer MP, Leach AG, Kuwata KT, et al. *J Am Chem Soc*. 2003;125:1319-1328.
158. Kelly KK, Hirschi JS, Singleton DA. *J Am Chem Soc*. 2009;131:8382-8383.
159. Caramella P, Quadrelli P, Toma L. *J Am Chem Soc*. 2002;124:1130-1131.
160. Gonzalez-James OM, Kwan EE, Singleton DA. *J Am Chem Soc*. 2012;134:1914-1917.
161. Xu L, Doubleday CE, Houk KN. *J Am Chem Soc*. 2010;132:3029-3037.
162. Gonzalez-Lafont A, Moreno M, Lluch JM. *J Am Chem Soc*. 2004;126:13089-13094.
163. Pauling L. *Nature*. 1948;161:707-709.
164. Schowen RL. Catalytic Power and Transition-State Stabilization. In: Goundour RD, Schowen RL, eds. *Transition States of Biochemical Processes*. New York: Plenum; 1978:77-114.
165. Nagel ZD, Klinman JP. *Nature Chem Bio*. 2009;5:543-550.
166. Kuntz E, Chen A, Sharp KA, Kollman PA. *Proc Natl Acad Sci U S A*. 1999;96:9997-10002.
167. Bruice TC. *Acc Chem Res*. 2002;35:139-148.
168. Jencks WP. *Adv Enzymol Relat Areas Mol Biol*. 1975;43:219-410.
169. Benkovic SJ, Hammes-Schiffer S. *Science*. 2003;301:1196-1202.
170. Warshel A. *J Biol Chem*. 1998;273:27035-27038.
171. Garcia-Viloca M, Gao J, Karplus M, Truhlar DG. *Science*. 2004;303:186-195.
172. Zhang X, Houk KN. *Acc Chem Res*. 2005;38:379-385.
173. Wolfenden R. *Annu Rev Biophys Bioeng*. 1975;5:271-306.
174. Radzicka A, Wolfenden R. *Methods. Enzymol*. 1995;249:284-312.
175. Lewis BE, Schramm VL. *J Am Chem Soc*. 2003;125:4672-4673.
176. LaReau RD, Wan W, Anderson VE. *Biochemistry*. 1989;28:3619-3624.
177. Lewis BE, Schramm VL. *J Am Chem Soc*. 2003;125:4785-4798.
178. Gawlita E, Paneth P, Anderson VE. *Biochemistry*. 1995;34:6050-6058.
179. Zhang Y, Luo M, Schramm VL. *J Am Chem Soc*. 2009;131:4685-4694.
180. Zhang Y, Schramm VL. *Biochemistry*. 2011;50:4813-4818.
181. Benkovic SJ, Hammes-Schiffer S. *Science*. 2003;301:1196-1202.
182. Klinman JP. *Nat Chem Biol*. 2010;2:907-909.
183. Schramm VL. *Annu Rev Biochem*. 2011;80:703-722.
184. Nagel ZD, Klinman JP. *Chem Rev*. 2006;106:3095-3118.
185. Silva RG, Murkin AS, Schramm VL. *Proc Natl Acad Sci USA*. 2011;108:18661-18665.
186. Rose IA. *Methods Enzymol*. 1980;64:47-59.
187. Hyland LJ, Tomaszek TA Jr, Meek TD. *Biochemistry*. 1991;30:8454-8463.
188. Kipp DR, Silva RG, Schramm VL. *J Am Chem Soc*. 2011;133:19358-19361.
189. Turowski M, Yamakawa N, Meller J, Kimata K, Ikegami T, Hosoya K, et al. *J Am Chem Soc*. 2003;125:13836-13849.
190. Cartoni GP, Ferreti I. *J Chromatogr*. 1976;122:287-291.
191. Tanaka N, Thornton ER. *J Am Chem Soc*. 1977;99:7300-7307.
192. Tanaka N, Thornton ER. *J Am Chem Soc*. 1976;98:1617-1619.
193. Lockley WJS. *Chromatography*. 1989;483:413-418.
194. Lewis PR, Johansen E, Holman TR. *J Am Chem Soc*. 1999;121:1395-1396.
195. Spies MA, Toney MD. *J Am Chem Soc*. 2007;129:10678-10685.

196. Bahnson BJ, Anderson VE. *Biochemistry*. 1991;30:5894-5906.
197. Schimerlik MI, Rife JE, Cleland WW. *Biochemistry*. 1975;14:5347-5354.
198. Dunitz JD, Ibberson RM. *Angew Chem Int Ed*. 2008;47:4208-4210.
199. Gelabert R, Moreno M, Lluch JM. *J Phys Chem A*. 2009;113:14161-14169.
200. Mislow K, Simon E, Hopps HB. *Tetrahedron Lett*. 1962:1011-1014.
201. Bartell LS. *Tetrahedron Lett*. 1960;6:13-17.
202. Bartell LS. *J Am Chem Soc*. 1961;83:3567-3571.
203. O'Leary DJ, Rablen PR, Meyer MP. *Angew Chem Int Ed*. 2011;50:2564-2567.
204. Wu Y, Singh RP, Deng L. *J Am Chem Soc*. 2011;133:12458-12461.
205. Lee DH, Kwon KH, Yi CS. *Science*. 2011;333:1613-1616.
206. Frantz DE, Singleton DA, Snyder JP. *J Am Chem Soc*. 1997;119:3383-3384.
207. Lee D-H, Kwon K-H, Yi CS. *J Am Chem Soc*. 2012;134:7325-7328.
208. Švenda J, Myers AG. *Org Lett*. 2009;11:2437-2440.
209. Moore JL, Silvestri AP, de Alaniz JR, DiRocco DA, Rovis T. *Org Lett*. 2011;13:1742-1745.
210. Rathbun CM, Johnson JB. *J Am Chem Soc*. 2011;133:2031-2033.
211. Ryan SJ, Stasch A, Paddon-Row MN, Lupton DW. *J Org Chem*. 2011;77:1113-1124.
212. Bartelson KJ, Singh RP, Foxman BM, Deng L. *Chem Sci*. 2011;2:1940-1944.
213. Nagel ZD, Klinman JP. *Chem Rev*. 2006;106:3095-3118.
214. Nagel ZD, Klinman JP. *Nat Chem Biol*. 2009;5:543-550.
215. Kohen A. Probes for Hydrogen Tunneling and Coupled Motion in Enzymatic Systems. In: Hynes JT, Klinman JP, Limbach HH, Schowen RL, eds. *Hydrogen Transfer Reactions.*, Vol. 4. Weinheim, Germany: Wiley; 2006:1311-1340.
216. Hay S, Pang J, Monaghan PJ, Wang X, Evans RM, Sutcliffe MJ, et al. *Chem Phys Chem*. 2008;9:1536-1539.
217. Klinman JP. *Chem Phys Lett*. 2009;471:179-193.
218. Hammes-Schiffer S. *Acc Chem Res*. 2006;39:93-100.
219. Klinman JP. *Philos Trans R Soc Lond B Biol Sci*. 2006;361:1323-1331.
220. Northrop DB. *Philos Trans R Soc Lond B Biol Sci*. 2006;361:1341-1349.
221. Kohen A, Klinman JP. *Chem Biol*. 1999;6:R191-R198.
222. Jonsson T, Glickman MH, Sun S, Klinman JP. *J Am Chem Soc*. 1996;118:10319-10320.
223. Rickert KW, Klinman JP. *Biochemistry*. 1999;38:12218-12228.
224. Meyer MP, Klinman JP. *J Am Chem Soc*. 2011;133:430-439.
225. Kuznetsov AM, Ulstrup J. *Can J Chem*. 1999;77:1085-1096.
226. Knapp MJ, Rickert K, Klinman JP. *J Am Chem Soc*. 2002;124:3865-3874.
227. Buhks E, Bixon M, Jortner J. *J Phys Chem*. 1981;85:3763-3766.
228. Wong K-Y, Richard JP, Gao J. *J Am Chem Soc*. 2009;131:13963-13971.
229. Kleinert H. *Path Integrals in Quantum Mechanics, Statistics, Polymer Physics, and Financial Markets*. 3rd ed.). River Edge, NJ: World Scientific; 2004.
230. Kleinert H. *Phys Lett A*. 1993;173:332-342.
231. Tomasi J, Mennucci B, Cammi R. *Chem Rev*. 2005;105:2999-3094.
232. York DM, Karplus M. *J Phys Chem A*. 1999;103:11060-11079.
233. Car R, Parrinello M. *Phys Rev Lett*. 1985;55:2471-2474.
234. Jezierska A, Panek JJ, Koll A, Mavri J. *J Chem Phys*. 2007;126:205101.
235. Lou S, Moquist PN, Schaus SE. *J Am Chem Soc*. 2006;128:12660-12661.
236. Davies HML, Jin Q. *Proc Natl Acad Sci U S A*. 2004;101:5472-5475.
237. Lipshutz BH, Ghorai S. *Aldrichim Acta*. 2012;45:3-16.
238. Dolling UH, Davis P, Grabowski EJJ. *J Am Chem Soc*. 1984;106:446-447.
239. Hong S, Lee J, Kim M, Park Y, Park C, Kim M, et al. *J Am Chem Soc*. 2011;133:4924-4929.
240. Zuccaccia D, Belpassi L, Tarantelli F, Macchioni A. *J Am Chem Soc*. 2009;131:3170-3171.

241. LaLonde RL, Wang ZJ, Mba M, Lackner AD, Toste FD. *Angew Chem Int Ed*. 2010;49:598-601.
242. Kwon K-H, Lee DW, Yi CS. *Organometallics*. 2010;29:5748-5750.
243. Bromberg SE, Yang H, Asplund MC, Lian T, McNamara BK, Kotz KT, et al. *Science*. 1997;278:260-263.
244. Ryabov AD. *Chem Rev*. 1990;90:403-424.
245. Parkin G. *Acc Chem Res*. 2009;42:315-325.
246. Blackmond DG. *Angew Chem Int Ed*. 2005;44:4302-4320.
247. Mathew JS, Klussmann M, Iwamura H, Valera F, Futran A, Emanuelsson EAC, et al. *J Org Chem*. 2006;71:4711-4722.
248. Harper KC, Sigman MS. *Proc Natl Acad Sci U S A*. 2011;108:2179-2183.
249. Harper KC, Sigman MS. *Science*. 2011;333:1875-1878.

CHAPTER THREE

Antitumor Drugs and Nitrenium Ions

Michael Novak* **and Yang Zhang**
Department of Chemistry and Biochemistry, Miami University, Oxford, OH 45056, USA
*Corresponding author: E-mail: novakm@miamioh.edu

Contents

Abstract

The metabolism of arylamines (AAs) into reactive metabolites giving rise to *N*-arylnitrenium ions that are ultimately responsible for the carcinogenic activity of the amines has been thoroughly investigated for over 50 years. The metabolic activation pathways are now well understood, as are the properties of the nitrenium ions involved. It is less well known that nitrenium ions, generated by unanticipated metabolic processes, have been implicated in the unwanted side effects of certain drugs such as clozapine. It is even less well known that nitrenium ions appear to be the cytotoxic warheads of two emerging classes of antitumor drugs, 2-(4-aminophenyl)benzothiazoles and 5,4′-diaminoflavones, that owe their selectivity to some of the same metabolic paths that are responsible for the activation of carcinogenic AAs. In this chapter, the evidence for the involvement of nitrenium ions in chemical carcinogenesis is briefly reviewed, but more emphasis is placed on the involvement of nitrenium ions in drug side effects and in antitumor drugs. Clozapine and aristolochic acid are presented as two examples in which the evidence for the involvement of nitrenium ions in dangerous drug side effects is particularly strong. The last half of the chapter is devoted to the two classes of antitumor drugs, 2-(4-aminophenyl)benzothiazoles and 5,4′-diaminoflavones, that

Advances in Physical Organic Chemistry, Volume 46
ISSN 0065-3160,
http://dx.doi.org/10.1016/B978-0-12-398484-5.00003-1

appear to use nitrenium ions to exert their cytotoxic effects. The evidence for the involvement of nitrenium ions in the mode of action of these two classes of drugs is presented with emphasis on the metabolic activation pathways for the drugs that are responsible for the specificity of these drugs and the nitrenium ion chemistry that has been examined carefully for the 2-(4-aminophenyl)benzothiazoles.

1. INTRODUCTION

The involvement of *N*-arylnitrenium ions as the active reactive intermediates in chemical carcinogenesis caused by arylamines (AAs) and food-derived heterocyclic arylamines (HAAs or HCAs) has been well established by over 50 years of biochemical and chemical research.[1–20] Representative examples of well-known carcinogens in both classes are shown in Chart 3.1. The most well-studied carcinogenic AA is 2-aminofluorene (**2-AF**) and its *N*-acetylated derivative *N*-acetyl-2-aminofluorene (**2-AAF**).[1–6] Other well-known AA carcinogens include 2-aminonapthalene (**2-NA**), 4-aminobiphenyl (**4-ABP**), and benzidine (**BZ**).[1–6] Over 20 mutagenic and carcinogenic HAAs including 2-amino-3-methylimidazo[4,5-*f*]quinoline (**IQ**), 2-amino-1-methyl-6-phenylimidazo[4,5-*b*]pyridine (**PhIP**), and 2-amino-6-methyldipyrido[1,2-*a*:3′,2′-*d*]imidazole (**Glu-P-1**) have been isolated over the years from cooked meats and fish and meat-derived sauces.[12–16] These materials are procarcinogens that are metabolized in two steps by oxidation to a hydroxylamine or hydroxamic acid derivative, followed by esterification to the ultimate carcinogen, a reactive ester metabolite (Scheme 3.1).[7–10] Heterolysis of the N–O bond of the ester metabolites generates *N*-arylnitrenium ions that react with DNA and proteins.[1–4,17–20]

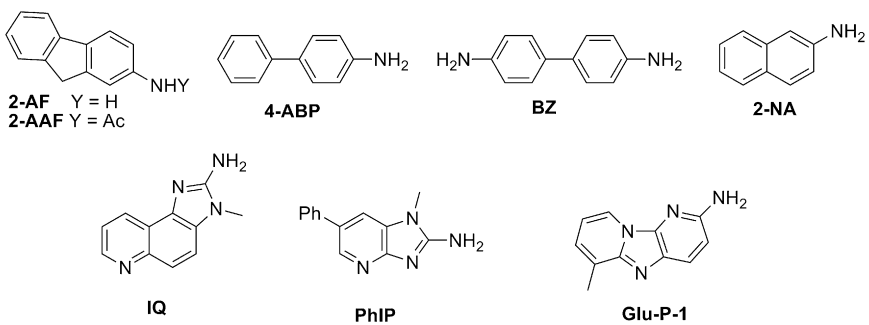

Chart 3.1 Representative carcinogenic AAs and HAAs.

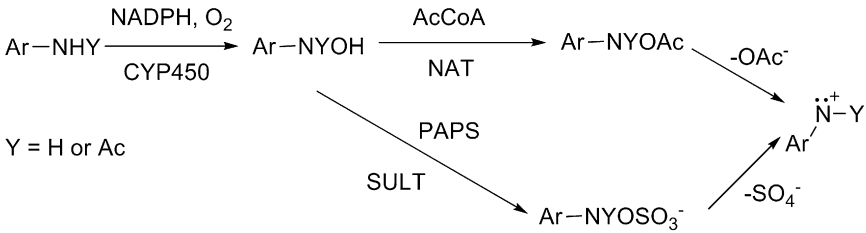

Scheme 3.1 Simplified metabolic activation pathway for AAs and HAAs.

Although many of the details of the metabolism of carcinogenic AAs and HAAs and the subsequent reactions of the nitrenium ions have been known for decades, it has only recently been appreciated that nitrogen-containing drugs may be metabolized to form similar reactive intermediates leading to deleterious drug side effects.[21–26] Clozapine (**1**, Chart 3.2) is a more effective treatment for refractory schizophrenia than standard antipsychotic drugs.[22,23] Its use has been limited because it leads to agranulocytosis, a lowering of the white blood cell count, particularly among neutrophils, that leads to serious risk of infection, in about 1% of patients treated with the drug.[23] It has been shown that **1** is oxidatively metabolized by human neutrophils to form a long-lived nitrenium ion that binds irreversibly to the neutrophils.[23] The detailed mechanism for the development of agranulocytosis is not completely understood, but the involvement of the nitrenium ion appears to be well established.[23]

Aristolochic acid is an extract of *Aristolochia* species used in herbal medicines.[24–26] The two major components (**2**, Chart 3.2) are known carcinogens in rodents.[24] They are also associated with renal fibrosis and urothelial cancer in humans treated with herbal remedies containing aristolochic acid.[24,25] It has been shown that these compounds are subject to reductive metabolism leading to *N*-hydroxyaristolactams that appear to

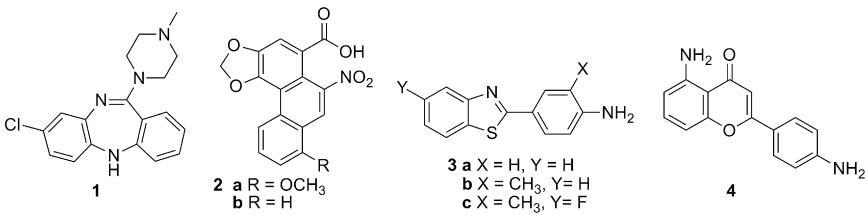

Chart 3.2 Clozapine (**1**), aristolochic acids (**2**), and antitumor 2-(4-aminophenyl)benzothiazoles (**3**) and 5,4′-diaminoflavone (**4**).

generate reactive nitrenium ions responsible for the formation of DNA adducts.[26]

The involvement of nitrenium ion chemistry in the development of side effects of certain drugs is now established, but very recently, evidence has been presented that the activity of two new classes of antitumor drugs based on 2-(4-aminophenyl)benzothiazole (**3a**, Chart 3.2) and 5-amino-2-(4-aminophenyl)-4*H*-1-benzopyran-4-one, better known as 5,4′-diaminoflavone (**4**, Chart 3.2) is mediated by nitrenium ions generated as a result of oxidative metabolism of both classes of drug.[27–31] The evidence for benzothiazole derivatives of **3** is particularly strong because the nitrenium ion in that case has been generated by laser flash photolysis (LFP), directly observed, and its reactions characterized.[29,30] The evidence for derivatives of **4** is based largely on results concerning the metabolic activation of the drug.[31] The evidence that nitrenium ion generation is actually critical to the mechanism of drug action is unique and reverses previous examples in which nitrenium ions are responsible only for deleterious health effects.

In this chapter, the pertinent evidence for the involvement of nitrenium ions in the carcinogenic activity of AAs and HAAs is briefly reviewed. A discussion of nitrenium ion involvement in the deleterious side effects of **1** and **2**, and related drugs, follows. The chapter closes with a presentation of the evidence for the interesting conclusion that nitrenium ions can serve a useful medical purpose in antitumor drugs.

2. CARCINOGENIC AAs AND HAAs

Research on carcinogenic AAs and HAAs has been reviewed in recent years, so only the results most pertinent to understanding the data concerning the drugs will be presented.[9–11,15,19,20] Data from studies of metabolic activation, characterization of DNA adducts, and experiments on *N*-arylnitrenium ion chemistry provide a coherent picture of the basis of AA carcinogenesis.

2.1. Metabolism

The metabolic pathway illustrated in Scheme 3.2 is a considerable oversimplification of the metabolism of AAs and HAAs. The first step, *N*-hydroxylation, catalyzed by the microsomal enzyme cytochrome P-450 (CYP450) can also lead to ring hydroxylation which is a detoxification process.[10,32,33] Most AAs are preferentially *N*-hydroxylated by two isozymes

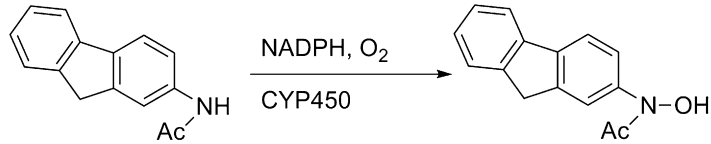

2-AAF **5**

Scheme 3.2 Metabolic *N*-hydroxylation of **2-AAF**.

of rat CYP450: 1A1 and 1A2.[10,32] Since several isozymes of rat CYP450 (including 1A1 and 1A2) are also involved in detoxification, and the activity of each isozyme for *N*-hydroxylation/ring hydroxylation is dependent on the individual AA, the balance between activation/detoxification varies considerably for each particular AA.[10,32,33] The level and activity of each CYP450 isozyme also vary from species to species, adding more complexity to the picture.[32,33] Initial mutagenesis studies of HAAs in *Salmonella typhimurium* showed that these compounds were mutagenic only in the presence of mammalian liver homogenates or purified CYP450 indicating that they follow the same activation pathway as AAs.[12–15,34,35] Studies with recombinant human CYP450 isozymes have concluded that human CYP4501A1 and 1A2 are the dominant activators of AAs and HAAs.[10,33,36,37]

Historically, *N*-hydroxylation was first demonstrated in 1960 by the isolation of *N*-hydroxy-**2-AAF**, **5** (Scheme 3.2), from the urine of rats fed a diet containing **2-AAF**.[38] The importance of **5** to the carcinogenic activity of **2-AAF** was indicated by its decreased formation in rats fed 3-methylcholanthrene, a specific inhibitor of **2-AAF** carcinogenicity.[38] The involvement of CYP450 in the *N*-hydroxylation was demonstrated in 1973.[39] Prior treatment of mice with $CoCl_2$ decreased the amount of CYP450 and the rate of *N*-hydroxylation of **2-AAF** in liver microsomes. Partially purified immune γ-globulin against microsomal NADPH–cytochrome c reductase also inhibited the *N*-hydroxylation reaction.[39]

The second step of activation, conversion of the *N*-arylhydoxylamine or *N*-arylhydroxamic acid into a reactive ester, was first demonstrated for **2-AF** and **2-AAF**.[1,2,4,10,40–45] Since these esters are reactive, and not directly isolatable from a biological environment, the evidence was indirect and was based on the effect of inhibitors, activators, and cofactors for the suspected enzyme systems on the observed carcinogenicity of, or formation of DNA adducts from, **2-AF** and **2-AAF**.

In humans, there are two isozymes of the *N*-acetyltransferases, NAT1 and NAT2. NAT1 is distributed ubiquitously throughout the body, while

NAT2 is most highly expressed in the liver and intestine.[8,9,46–52] Both enzymes are highly polymorphic.[46,47] Both AAs and their hydroxylamine metabolites are substrates of NAT1 and NAT2 with the hydroxylamines undergoing *O*-acetylation.[48–52] The *N*-acetylation of an AA into the corresponding amide is a detoxification process for most AAs since the amide is generally a poorer substrate for CYP450-catalyzed hydroxylation than the parent amine.[8,46,47]

The involvement of sulfotransferases (SULTs) in the activation of AAs has been known since 1970.[41–43] Early studies confirmed that cytosolic SULTs were involved in the activation.[53] Human cytosolic SULTs are a super family of enzymes that are grouped into four families: SULT1, SULT2, SULT4, and SULT6.[7,54] The SULT1A enzymes have received the most attention as activators of *N*-hydroxy-AAs and *N*-hydroxy-HAAs.[55,56] SULT1A1 is the major SULT present in human liver.[54] It is also found in the brain, gastrointestinal tract, platelets, and placenta.[54] The SULTs also play a role in detoxification of some AAs and HAAs, by *N*-sulfonation.[57,58] The dominant form of activation via NAT or SULT is dependent on the organism and on the individual *N*-hydroxy-AA or *N*-hydroxy-HAA.[59,60]

2.2. DNA Adducts

The major adducts derived from in vivo and in vitro studies of **2-AF**, **2-AAF**, **4-ABP**, **IQ**, and **PhIP** and from chemical studies of the reactions of synthetic activated esters with DNA or monomeric nucleosides are summarized in Chart 3.3.[3,4,61–64] These structures are representative of adducts derived from other carcinogenic AAs and HAAs.[3,4,65] For all

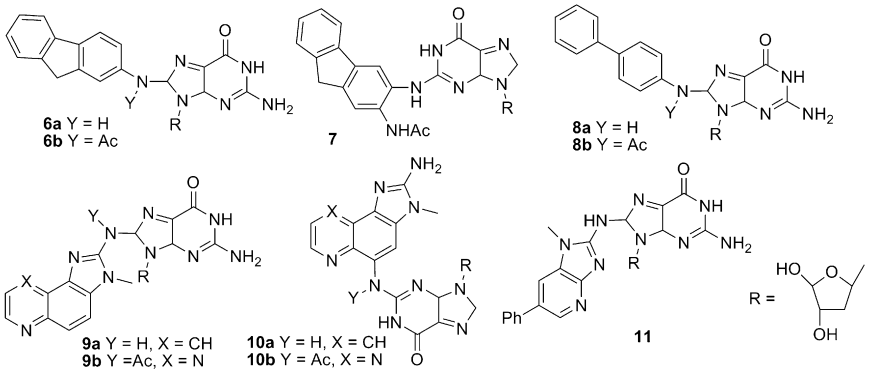

Chart 3.3 Structures of representative DNA adducts of AAs and HAAs.

polycyclic AAs and HAAs, 2′-deoxyguanosine (**d-G**), whether in DNA or present as the monomeric nucleoside, is the major target, and C-8 adducts such as **6**, **8**, **9**, and **11** are the most common adducts.[3,4,61–65] The N-2 adducts such as **7** and **10** are less commonly observed. The **2-AAF** N-2 adduct **7** has only been observed during in vivo studies or from the reaction of a synthetic ester with native DNA.[66–68] The **IQ** N-2 adduct **10a** is a minor product (10–15%) of the reaction of a synthetic **IQ** ester with either native DNA or **d-G**.[69,70] The major C-8 adduct **9a** is the only other observed adduct.[69] The acetylated adducts **9b** and **10b** were isolated as the major and minor adduct, respectively, of a model study discussed in more detail below.[71]

In cases in which both the C-8 and N-2 adducts have been generated from the same carcinogen in vivo, the C-8 adduct is always the major initially formed DNA adduct, but the N-2 adduct is more resistant to DNA repair enzymes, so it becomes the major observable DNA adduct after a period of time.[66–70]

2.3. Nitrenium Ion Chemistry

After the general outline of metabolic activation and the structures of the DNA adducts became known, James and Elizabeth Miller proposed that the reactive intermediate responsible for the carcinogenic activity of AAs was an electrophilic nitrenium ion, **12** (Scheme 3.3).[1,2] The nitrenium ion hypothesis was an attractive proposal, but the known properties of *N*-arylnitrenium ions at the time indicated that their lifetimes in water were too short (≤2 ns) for them to be able to react selectively with the DNA bases.[72–76] All data that were available had been collected for monocyclic *N*-arylnitrenium ions, so the Novak group began a study of the polycyclic ions proposed to be the intermediates in carcinogenesis.[77]

Hydrolysis of the two synthetic esters **13a** and **13b**, ultimately derived from **4-ABP**, led to the major product, quinol **17** (Scheme 3.4).[77] The

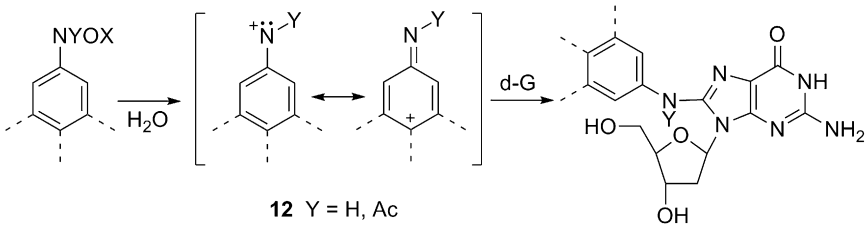

Scheme 3.3 The nitrenium ion hypothesis for DNA adduct formation.

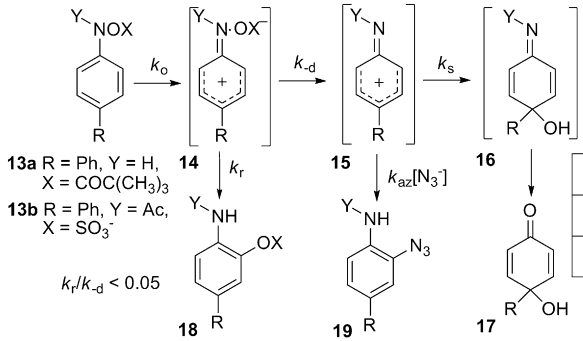

ion	k_{az}/k_s (M^{-1})	$1/k_s$ (μs)
15a	2.9×10^3	0.6
15b	1.0×10^3	0.2

Scheme 3.4 Competitive azide and solvent trapping of the 4-biphenylylnitrenium ions **15a** and **15b**.

quinolimines **16a** and **16b** that decomposed into **17** could be detected by UV–vis spectroscopy, and the kinetics of their decomposition into **17** were monitored by UV–vis spectroscopy and high-performance liquid chromatography (HPLC).[77,78] The *N*-acetylated imine **16b** was also characterized by nuclear magnetic resonance.[78] The only other products observed in aqueous solution in the absence of additional nucleophiles were the rearrangement products **18a** and **18b** and a product derived from intramolecular rearrangement of **18a**.[77] The yield of the rearranged products was <5% in both cases indicating that intramolecular recombination of the tight ion pair (k_r) did not compete significantly with diffusional separation of the ion pair (k_{-d}) to form the free ions, **15a** and **15b**. This result indicated that the biphenylyl ions were significantly different from previously investigated monocyclic *N*-arylnitrenium ions for which k_r was always a major process.[72–75] For example, the 4-Me analog of **14b** yielded 15% of the rearrangement product analogous to **18b** under identical reaction conditions.[75] The ions **15a** and **15b** were competitively trapped by low concentrations (<10 mM) of N_3^- to generate **19a** and **19b** with no change in the rate of disappearance of **13a** and **13b**.[77] Application of the 'azide clock' equations[79,80] to the product yield data obtained in the presence of N_3^- led to the azide/solvent selectivity ratios, k_{az}/k_s, shown in Scheme 3.4. The estimated lifetimes, $1/k_s$, of the two ions shown in Scheme 3.4 are lower limits based on the assumption that k_{az} is diffusion limited at ca. $5 \times 10^9\ M^{-1}\ s^{-1}$. These lifetimes are at least two orders of magnitude longer than those previously measured for monocyclic nitrenium ions and they do show that these ions have sufficient lifetimes in an aqueous environment to be selectively trapped by biological nucleophiles at millimolar

concentrations.[77] The results also show that the *N*-acetyl group of a *N*-acetyl-*N*-arylnitrenium ion is only moderately destabilizing.[77]

Subsequent direct measurements of k_{az} and k_s for **15a**, **15b**, and the corresponding 2-fluorenyl ions **20a** and **20b** generated by LFP (Scheme 3.5) confirmed azide clock measurements for **15a**, **15b**, and **20b** and showed that k_{az} is at or near the diffusion limit for these ions.[81,82]

Although the biphenylyl and fluorenylnitrenium ions were shown to be long lived, this did not prove that they were involved in the reactions that formed the **d-G** adducts. The Novak group showed by kinetics measurements and competitive trapping with **d-G** and solvent that **d-G** had no effect on the hydrolysis rate of the precursors to **15a**, **15b**, and **20b** under conditions in which formation of the adduct predominated.[83,84] They established rate constants for reaction of these nitrenium ions with **d-G** based on the product yield data and the known values of k_s for these ions (Scheme 3.6).[83,84] The rate constants were subsequently confirmed by direct measurements on the ions generated by LFP in the presence of **d-G**.[17,85,86] These results confirm that the **d-G** adducts are derived from the nitrenium ions and that trapping of the ions by **d-G** is very efficient. On the other hand, adenosine traps **15a** with a much smaller rate constant of $3.1 \times 10^7\ M^{-1}\ s^{-1}$ and **15b** with a rate constant of $1.4 \times 10^8\ M^{-1}\ s^{-1}$.[84] Trapping with cytidine was at least another order of magnitude slower. The single-stranded DNA oligomer d-ATGCAT was shown to trap **20b** with an

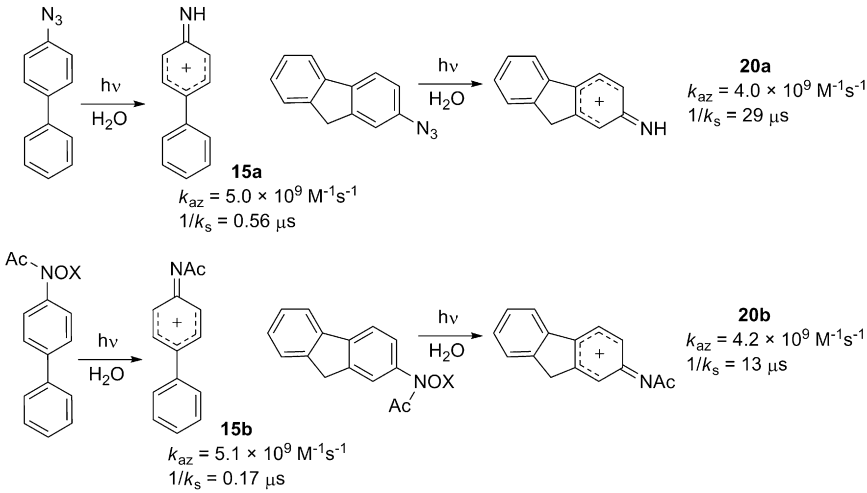

Scheme 3.5 Nitrenium ions obtained by LFP, with directly measured k_{az} and k_s.

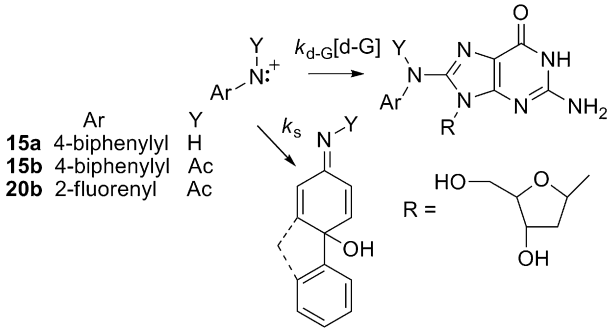

cation	$k_{d\text{-}G}$ ($M^{-1}s^{-1}$)
15a	1.9×10^9
15b	1.9×10^9
20b	6.2×10^8

Scheme 3.6 Competitive trapping of nitrenium ions by solvent and **d-G**.

efficiency 27% of that of **d-G** confirming that the reaction efficiency was not significantly altered by the DNA backbone.[87] In the same study, it was shown that the double-stranded form of the self-complementary oligomer trapped **20b** at only 2% of the efficiency of **d-G**, demonstrating that intact double-helical DNA is fairly resistant to attack by nitrenium ions.[87]

Similar results have been found in studies on the chemistry of synthetic esters derived from HAAs.[19,71,88,89] For example, **21** (Scheme 3.7), derived from the HAA **IQx** (2-amino-3-methylimidazo[4,5-*f*]quinoxaline), generates a heterocyclic ion **22**, that yields **23** in water in the absence of other nucleophiles.[71] The cation is competitively trapped by N_3^- to yield **24** with the azide/solvent selectivity shown in Scheme 3.7. If k_{az} is diffusion limited at $5 \times 10^9\ M^{-1}\ s^{-1}$, the lifetime of **22** in water is about 10 μs,

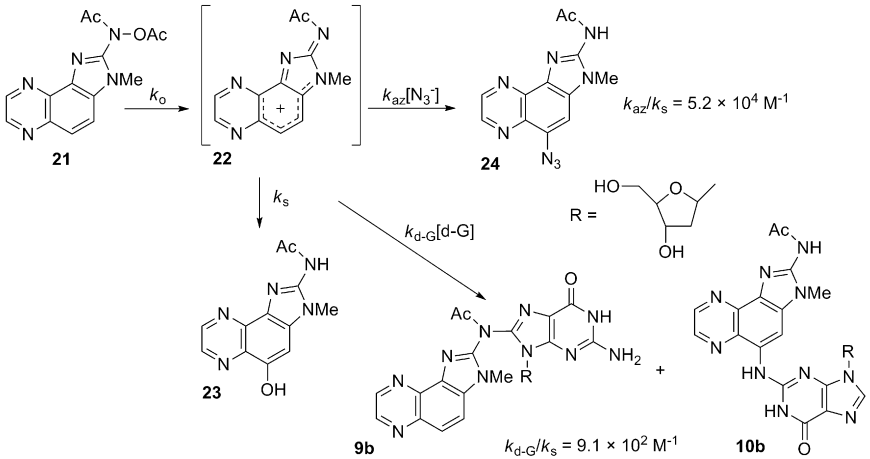

Scheme 3.7 Chemistry of the *N*-acetyl-IQx nitrenium ion, **22**.

comparable to **20b** under the same conditions.[71] Trapping with **d-G** is also efficient. The minor N-2 adduct **10b** accounts for about 20% of the **d-G** products with the C-8 adduct **9b** accounting for the rest.[71] This is similar to the N-2/C-8 product ratios obtained in studies with synthetic ester derivatives of **IQ** mentioned earlier.[69,70]

The detailed mechanisms of how DNA adducts lead to tumor growth are not fully elucidated, but the early stages of the process, including metabolic activation of the carcinogens and formation of DNA adducts, are now well understood.[1–20] Considerable progress is being made in understanding how the structures and conformations of DNA adducts lead to specific mutations.[11,90] The rest of this chapter will examine how the metabolic processes and characteristic nitrenium ion chemistry lead to unanticipated drug side effects and how the metabolism and chemistry can be harnessed to generate useful drugs.

3. NITRENIUM-MEDIATED DRUG SIDE EFFECTS

In recent years, it has become apparent that a significant number of drug side effects are not caused by the drug itself, but by drug metabolism that leads to a variety of electrophilic or radical intermediates including epoxides, iminium ions, diazonium ions, nitroso compounds, quinones, quinone imines, carbocations, nitrenium ions, and various carbon- and nitrogen-centered radicals.[21–26,91–93] We will examine two cases of drug side effects in which nitrenium ion intermediates have been implicated.

3.1. Clozapine

Clozapine, **1**, represented a significant advance in the treatment of schizophrenia because of its effectiveness in many patients resistant to other drug treatments and its lack of motor side effects that are common to other neuroleptic drugs.[94–98] Unfortunately, the drug leads to life-threatening agranulocytosis in about 1% of patients and is associated with toxic hepatitis in isolated cases.[97,99–102] This has led to curtailed use of the drug and the requirement for regular blood tests to monitor white blood cell counts in patients treated with clozapine.[96,97] Because of clozapine's effectiveness, further research on the drug proceeded in two complementary areas. The first was a search for analogs of **1** that did not exhibit the agranulocytosis side effect. Clozapine and some of its important analogs that do not cause agranulocytosis, and are now in clinical use, are shown in Chart 3.4.[92,103,104]

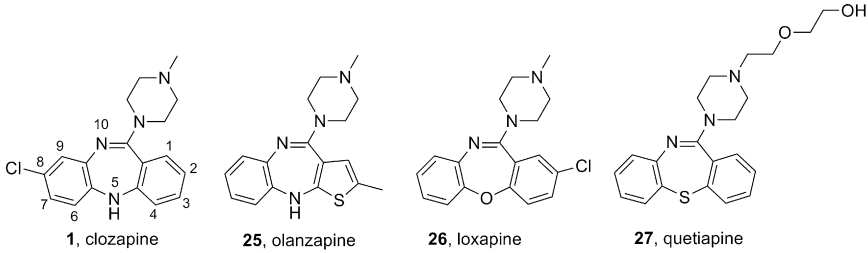

Chart 3.4 Clozapine and some of its analogs.

The second line of clozapine research was an investigation into the molecular mechanisms underlying the agranulocytosis side effect. Major results of that research are outlined in Scheme 3.8.

Oxidation of **1** by HOCl occurs rapidly at a rate first order in both [**1**] and [HOCl] to generate a reactive intermediate with a λ_{max} of 460 nm and a lifetime of ca. 60 s in water.[105] The intermediate was detected by mass spectrometry (MS) and shown to be a cation with a mass of 325, one unit less than **1**. The intermediate was efficiently trapped by glutathione, GSH, to generate two major adducts with structures **30** and **31**.[105] The cation was

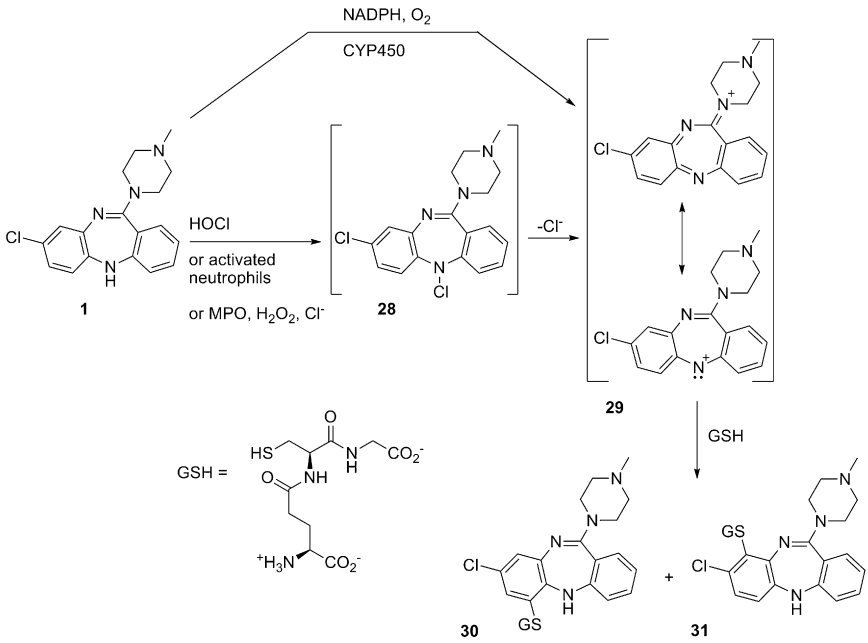

Scheme 3.8 Evidence for the generation of the nitrenium ion **29** from clozapine.

assigned the highly delocalized nitrenium ion structure **29**, reminiscent of the delocalized nitrenium ions derived from HAAs.[105] It was assumed that the cation was generated by heterolysis of the chloramine **28**, but that material was not directly detected. In the absence of GSH, the intermediate decayed into several products detected by liquid chromatography–mass spectrometry (LCMS) with m/z 343, consistent with the protonated molecular ions of phenols derived from the reaction of **29** with water.[105] Purified myeloperoxidase, the most abundant enzyme present in neutrophils, generated the same products with m/z 343 in the presence of H_2O_2 and Cl^-.[105] Oxidatively activated neutrophils also metabolize **1** to generate **30** (major) and **31** (minor) in the presence of GSH. Metabolism of **1** by neutrophils in the absence of GSH led to significant covalent binding of **1** to the cells. About 7% of **1** was irreversibly bound to the cells at therapeutic doses (0.5 μM).[105] The binding was significantly reduced in the presence of GSH.[105]

Oxidation of **1** by human liver cells in vitro was decreased dramatically by CYP450 inhibitors. Metabolism led to about 1–2% of **1** irreversibly bound to protein. That binding was inhibited by GSH.[106] The same major GSH conjugate, **30**, with lesser amounts of **31**,was detected in experiments in which **1** was incubated with human, rat, and mouse liver cells, human neutrophils, and bone marrow cells in the presence of GSH.[107] The GSH adducts were also detected during in vivo experiments with rats and mice.[107] In the presence of horseradish peroxidase and/or H_2O_2, **1** was significantly cytotoxic to neutrophils, but GSH, *N*-acetylcysteine, and ascorbic acid protected the cells.[108] Cytotoxicity was not observed in the absence of horseradish peroxidase and/or H_2O_2.[108] It appears that the same reactive intermediate, identified as **29**, is generated in all these cases.[105–108]

The lack of observable agranulocytosis for **26** and **27** is understandable if oxidative metabolism to a nitrenium ion is responsible for development of agranulocytosis. Consistent with the lack of this side effect for **26** and **27**, studies with analogues of **1** showed that a reactive intermediate could only be generated by HOCl treatment of analogues containing N at position 5.[109] On the other hand, **25** does have N at a position that should allow it to be oxidized to a nitrenium ion. Indeed, **25** is oxidized by HOCl to an intermediate with properties very similar to **29**.[103,104] However, **25** exhibits significantly less covalent binding to neutrophils than **1** under the same conditions.[103,104] This result, coupled with the almost 50-fold smaller therapeutic dose of **25** compared to **1**, may explain why **25** does not lead to agranulocytosis during treatment.[103,104]

Human glutathione *S*-transferases appear to catalyze the reaction of GSH with the nitrenium ion.[110] In vivo studies in rabbits show that **1** has a significant effect on neutrophil kinetics, increasing the rate of release of neutrophils from bone marrow and decreasing the lifetime of neutrophils in the blood stream.[111] Although the mechanism of the induction of agranulocytosis by **1** is not fully understood, it does appear that the nitrenium ion **29** plays a critical role in the process.[22,23,112–114]

3.2. Aristolochic Acid

Aristolochic acid is a plant extract of *Aristolochia* species that has been used in traditional medicine in many parts of the world for centuries to treat snake bites and open wounds and in obstetrics.[115] It is a mixture of nitrophenanthrene carboxylic acids containing primarily aristolochic acid I (**2a**) and aristolochic acid II (**2b**) (Chart 3.2 and Scheme 3.9).[116,117] Because of its uses in traditional medicine, purified components of the mixture, primarily **2a**, were examined for potential use in modern medicine, including use as an antitumor drug.[118,119] This work was largely abandoned after Mengs'

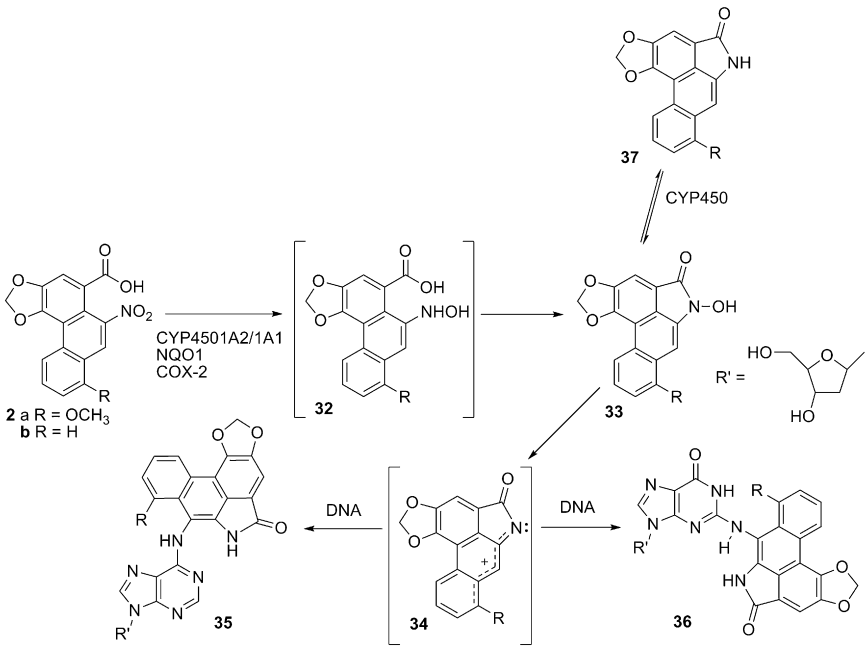

Scheme 3.9 Metabolism of aristolochic acids **2a** and **2b** and structures of their DNA adducts.

demonstration that aristolochic acid containing 77% **2a** and 21% **2b** is strongly carcinogenic in rats and mice.[120,121]

Mutagenicity tests in *S. typhimurium* TA100 and TA1537 confirmed that purified **2a** and **2b** were direct acting mutagens in both strains, requiring no additional activating enzymes.[122] Both compounds had little to no mutagenicity in a nitroreductase-deficient strain of TA100 indicating that reductive metabolism of the nitro group was essential to mutagenicity.[122] A well-known case of long-term human exposure to aristolochic acid inadvertently included in a diet pill formulation in Belgium, and similar cases related to herbal medicines in the United States, Europe, and Asia have linked aristolochic acid consumption to a progressive renal fibrosis documented in approximately 300 patients.[123–126] The disease has required kidney transplantation in about half of the cases and has culminated in several cases of renal and urinary tract cancer.[123–126] Pharmaceutical preparations containing aristolochic acid have been withdrawn in many countries, and in the United States the FDA issued a warning in 2001 that consumers stop using all botanical preparations, sold as traditional medicines or dietary supplements, that contain aristolochic acid.[127]

In vitro studies with rat liver homogenates and in vivo studies in rats led to the detection and characterization of DNA adducts **35a** and **36a** (Scheme 3.9) from treatment with **2a** and smaller amounts of **35b** and **36b** from treatment with **2b**.[128–132] In single feeding studies in rats the adenosine adduct **35a** was formed in greater amounts than the guanosine adduct **36a** and was more persistent.[133] The adducts **35a**, **35b**, and **36a** have also been detected by ^{32}P-postlabelling methods in the kidneys and ureters of Belgian kidney transplant patients suffering from aristolochic acid-induced renal fibrosis.[134,135] The adducts **35a** and **36a** have recently been detected by ultraperformance liquid chromatography/mass spectrometry (UPLC/MS) in patients suffering from upper urinary tract carcinoma in Taiwan where the highest incidence rates of this uncommon cancer are found.[136]

The major metabolites of **2a** and **2b** recovered from urine and faeces of laboratory animals are the aristolactams **37a** and **37b** (Scheme 3.9), indicating an overall reductive metabolism.[137] The *N*-hydroxyaristolactams **33a** and **33b** had been suspected metabolites for some time, but have only recently been isolated from rat urine.[138] The likely precursors to **33a** and **33b**, **32a**, and **32b** have not been detected. Several redox enzymes have been implicated in the reductive metabolic activation of **2a** and **2b**, including the microsomal enzymes CYP4501A2, and 1A1 to a lesser extent,

and the cytosolic enzymes NAD(P)H: quinone oxidoreductase (NQO1) and cyclooxygenase-2 (COX-2), among others.[26,139–146] The reversible formation of **37** is suggested by the mutagenicity of **37a** and **37b** to *S. typhimurium* in the presence of rat liver homogenate S-9 and the isolation of the DNA adducts **35a** and **36a** from **37a** activated by CYP450 or horseradish peroxidase/H_2O_2.[147,148] It should be noted that pathways leading to detoxification have not been included in Scheme 3.9. The involvement of the nitrenium ions **34a** and **34b** is suggested by the structures of the DNA adducts and the expected stability of the ions.[24–26] The guanosine adduct **36** is reminiscent of the minor N-2 adducts **7** and **10** (Chart 3.3) isolated from experiments involving the carcinogens **2-AAF**, **IQ**, **IQx**, and related HAAs.[66–71] The ions **34a** and **34b** should be significantly stabilized by resonance throughout the phenanthrene ring system, and the lactam structure should only be moderately destabilizing to a nitrenium ion.[77]

These examples show that the use of a drug with an unanticipated metabolic pathway to generation of a nitrenium ion can lead to devastating effects. The significant cytotoxic effects of nitrenium ions could be put to use in certain situations, but the most important challenge to the development of such a drug would be the proper targeting of the drug to the desired tissue.

4. ANTITUMOR DRUGS MEDIATED BY NITRENIUM IONS

The cytotoxic effects of *N*-arylnitrenium ions have been amply demonstrated through research on AA carcinogens and on the limited number of drugs that have been shown to be metabolized to nitrenium ions. Nitrenium ions have been demonstrated to be more efficient at targeting single-stranded DNA than native double-stranded DNA.[87] Since actively growing cells, such as tumor cells and stem cells in their mitotic phase, are more susceptible to anticancer drugs that attack DNA because a significant portion of their DNA is unwound and in a single-stranded form,[149] nitrenium ions could be utilized as the warheads for appropriately designed antitumor drugs. The nitrenium ion itself cannot distinguish the DNA of a tumor cell from that of a healthy cell in its mitotic phase, so the targeting of the drug must be provided by another mechanism. Two examples of nitrenium ion-based antitumor drugs that are under development and appear to have a specific targeting mechanism for certain tumor cells are presented below.

4.1. 2-(4-Aminophenyl)benzothiazoles

Since 1996, a series of benzothiazole derivatives based on the lead compound 2-(4-aminophenyl)benzothiazole, **3a** (Chart 3.5), have been under development as antitumor agents.[150] Complexes incorporating the 2-(4-aminophenyl)benzothiazole moiety, **38**, are being developed as radiopharmaceuticals for imaging (**38a**) and targeted radiotherapy (**38b**,^{186}Re, ^{188}Re) of breast cancer.[151,152] Other derivatives of **3a**, including **39–41**, are being investigated as radiopharmaceuticals for binding and in vivo imaging of Aβ-plaques, one of the earliest pathological processes in the development of Alzheimer's disease.[153–157] Still other derivatives of **3a** are under investigation as antimicrobial and antifungal agents,[158–161] so the 2-(4-aminophenyl)benzothiazole moiety is finding its way into a significant number of drug candidates.[162]

The discovery of the antitumor activity of **3a** and its derivatives was serendipitous.[150] Originally, **3a** was generated as a synthetic intermediate in a study of the biological activities of polyhydroxylated 2-phenylbenzothiazoles related to genistein and quercetin, but it was found to have remarkable activity against two human breast cancer cell lines (MCF-7 and MDA 468) with IC_{50} values of 0.3–0.8 nM for MCF-7 and 1.6 nM for MDA 468.[150] Structure–activity studies showed that the 4′-NH_2 was essential to activity, and replacement of the S in the thiazole ring of **3a** with O or N led to decreased activity by a factor of 10 or 1000.[150] Substitution at the 3′-position by methyl or halogens led to enhanced activity against the original cell lines and a broader spectrum of activity against certain colon, lung, ovarian, and renal cancer cell lines, although other cell lines were insensitive to the drugs demonstrating that these drugs did have some

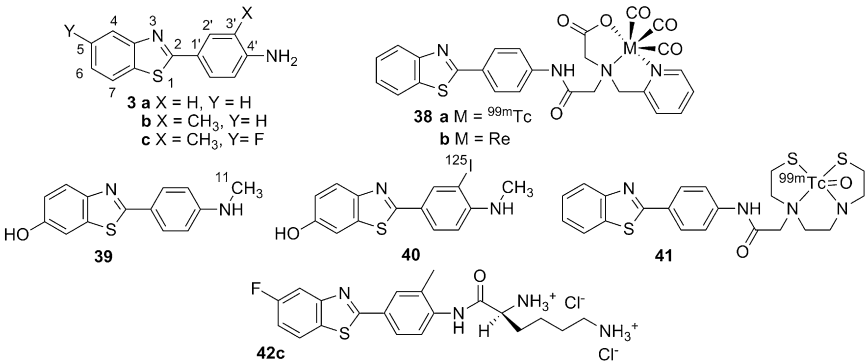

Chart 3.5 Drug candidates derived from 2-(4-aminophenyl)benzothiazole.

selectivity.[150,163] The 3′-methyl derivative, **3b**, outperformed all other derivatives in initial in vivo tests on six human derived breast tumors xenografted to female mice and in human ovarian cancer cells cultured in hollow fibers and implanted in the peritoneal cavity of mice, so further developments concentrated on this derivative.[150,164] Metabolism of 2-(4-aminophenyl)benzothiazoles into the active antitumor metabolite in sensitive breast cancer cell lines requires the constitutive presence of CYP4501A1.[165] That enzyme is also induced by the drug in sensitive cells.[165] Cell lines that contain neither constitutive nor inducible CYP4501A1 are insensitive to these drugs.[165] This enzyme also leads to detoxification since CYP4501A1 hydroxylates the drug at the 6-position, leading to an inactive metabolite.[166] Metabolism of these compounds is associated with binding to the aryl hydrocarbon receptor (AhR) in the cytosol, active translocation of the AhR–benzothiazole complex to the nucleus caused by a binding-induced conformational change in the AhR, and induction of CYP4501A1.[167] Metabolism is significantly attenuated in AhR-deficient MCF-7 cells.[168] The involvement of AhR binding in CYP4501A1 induction by other xenobiotics is well known.[169,170] This induction occurs because the AhR complex interacts with specific DNA sequences called the xenobiotic response elements (XREs).[169,170] Genes that have XREs in their promoter sequence can be activated by the AhR complex.[169,170] Both CYP4501A1 and CYP4501A2 have been shown to be induced by such a mechanism with other xenobiotics.[169,170]

Fluorination at C-5 preserves induction of CYP4501A1 and activity against sensitive cell lines, but suppresses the C-6 hydroxylation that leads to detoxification.[171] Finally, the low water solubility of the 3′-methyl-5-fluoro derivative, **3c**, could be circumvented by conjugation to lysine to form **42c**, the prodrug that was approved for Phase 1 clinical trials in the UK in 2004.[27,172] This compound, named Phortress, is readily metabolized into the active drug, **3c**.[172–174] Gene expression profiling in sensitive and insensitive cells treated with **3c** has been studied extensively to probe the detailed mechanism of cytotoxicity and as a potential marker for patient sensitivity.[175–179] The range of cell lines sensitive to **3c** has been thoroughly investigated,[180] and other thiazoles of related structure are being investigated for anticancer activity.[181–184]

Based on the available data, the mechanism of action of **3a** and its simple ring-substituted derivatives is thought to involve selective uptake into sensitive cells mediated by AhR binding and translocation into the nucleus, induction of CYP4501A1, oxidation and conversion of the drug into an

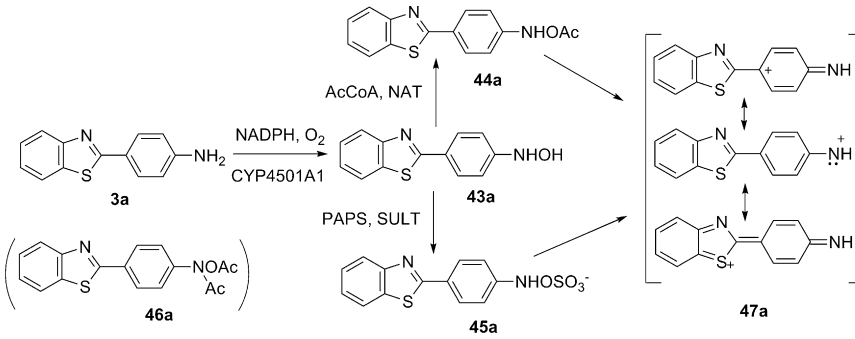

Scheme 3.10 Proposed metabolism of 2-(4-aminophenyl)benzothiazole.

electrophilic reactive intermediate, and formation of extensive DNA adducts resulting in cell death.[27] It is suspected that the active metabolite of **3a** is the hydroxylamine **43a** (Scheme 3.10) or, more likely, based on the metabolism of AAs and HAAs, an ester derivative, **44a** or **45a**, but none of these compounds have been detected during metabolic studies.[27,28] The diacetylated derivative **46a** has been synthesized and shown to be active against some of the same cell lines as **3a**.[166] It was not studied further in part because its high reactivity makes conclusions from bioassay studies difficult to interpret.[166] DNA adducts are known to be formed, and single and double DNA strand breaks have been reported, but the structures of DNA adducts were not determined.[185–188] It has been proposed that the nitrenium ion **47a** and its ring-substituted derivatives are responsible for the antitumor activity of **3a** and its ring-substituted derivatives such as **3b** and **3c**.[27,28,189,190]

The proposed metabolic path for **3a** and its derivatives is consistent with the requirement of CYP4501A1 for activation of the drug and with the well-known metabolism of carcinogenic AAs and HAAs.[1–10] Evidence for the subsequent generation of nitrenium ions from the carcinogenic metabolites and their reactions with DNA and other nucleophiles was described above. Recently, the Novak group has studied the chemistry of the putative reactive metabolite **44a** to determine if the nitrenium ion mechanism is viable for this class of drugs.[29,30]

At first glance, it does not appear that the benzothiazol-2-yl substituent should stabilize a cation. Indeed, σ_p for this substituent has been measured as 0.29 based on the substituent effect for the ionization constant of 4-(benzothiazol-2-yl)benzoic acid.[191,192] On the other hand, the group could stabilize a positive charge by the extensive π–resonance interaction

shown for **47a** in Scheme 3.10. From previous work on substituted *N*-arylnitrenium ions, it has become clear that resonance effects are more important than inductive effects for stabilization of nitrenium ions compared to carbocations.[18,20,77,193,194]

Synthesis of **44a** was accomplished in two steps from 2-(4-nitrophenyl) benzothiazole.[29] Hydrolysis of **44a**, monitored by UV–vis methods, showed that the compound decomposes in water via two consecutive pseudo-first-order process.[29,30] Monitoring the reaction by HPLC shows that the larger of the two rate constants, k_o, governs the decay of **44a**, while the smaller rate constant, k_1, governs the rate of formation of the final quinol hydrolysis product **49a** by way of the quinolimine **48a** (Scheme 3.11).[29] This process has been observed previously for other nitrenium ion precursors (see Scheme 3.4, for example), but it does not require the involvement of a nitrenium ion. The rate constant k_o that governs the decomposition of **44a** is pH dependent and is governed by Eqn (3.1).[30]

$$k_o = k'_o\left(K_a/\left(\left[H^+\right]K_a\right)\right) \tag{3.1}$$

The pH dependence is consistent with spontaneous decomposition of the conjugate base (**44a**) of a conjugate acid base pair (**44aH**$^+$/**44a**, Scheme 3.11). The kinetic (1.47 ± 0.04) and spectrophotometric (1.45 ± 0.13) pK_a values are in good agreement,[30] and the observation of this rate law is consistent with that determined for ester derivatives of *N*-hydroxy-HAAs containing a basic ring nitrogen.[19,21,88,89]

Hydrolysis of **44a** in the presence of N_3^- leads to the competitive trapping of **47a** by N_3^- and the aqueous solvent that is detected by the $[N_3^-]$-dependent competitive formation of the products **50a** and **51a** and the quinol **49a** with no change in the rate of decomposition of **44a**.[29,30]

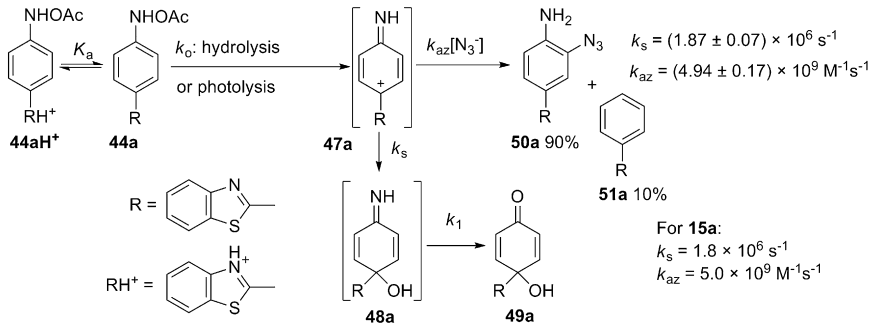

Scheme 3.11 Generation and characterization of the benzothiazole nitrenium ion **47a**.

The standard 'azide clock' treatment leads to the measurement of k_{az}/k_s of $(2.6 \pm 0.3) \times 10^3\ M^{-1}$.[29] If k_{az} is diffusion limited, the lifetime of the cation, $1/k_s$, is ca. 520 ns. The major (90%) azide adduct **50a** is an expected product based on precedent with other nitrenium ions, but **51a** is unusual because it contains no azide moiety.[30] It is not formed in the absence of N_3^- and kinetically it behaves like an N_3^--derived product. A potential mechanism involving **47a** has been proposed and some evidence for the proposal has been presented.[30]

Photolysis of **44a** also generated **49a** through the intermediacy of **48a** indicating that photolysis may lead to the same intermediates as hydrolysis.[29] LFP of **44a** at 308 nm led to the generation of a transient absorbance with λ_{max} 570 nm that decayed in an $[N_3^-]$-dependent pseudo-first-order fashion.[29] Direct measurement of k_{az} and k_s (Scheme 3.11) provided k_{az}/k_s, of $(2.64 \pm 0.13) \times 10^3\ M^{-1}$, identical, within experimental error, to the value obtained from the classical trapping study.[29] The kinetic behavior of the transient, the correspondence between the LFP kinetics and classical trapping experiments, and the red-shifted λ_{max} of the transient are consistent with its identification as **47a**.[29,30] Direct comparisons of k_{az} and k_s for **47a** and the 4-biphenylylnitrenium ion **15a** obtained under the same conditions (30 °C, 5 vol% CH_3CN/H_2O, $\mu = 0.5$) are shown in Scheme 3.11.[29,30,77] The two ions behave very similarly with apparently diffusion-controlled reactions with N_3^- and nearly identical aqueous solution lifetimes ($1/k_s$) of 530 ns for **47a** and 560 ns for **15a**.[29,30,77] The rate constants for ionization of the carboxylic acid ester precursors of **47a** and **15a** at neutral pH are considerably different though. For **44a**, k'_o is $2.3 \times 10^{-3}\ s^{-1}$ at 30 °C,[30] while k_o for **13a**, the precursor to **15a** (Scheme 3.4), is $0.13\ s^{-1}$ at 0 °C.[77] This difference is probably due to the large electron-withdrawing inductive effect of the benzothiazol-2-yl substituent that is more dominant in the transition state for N–O bond cleavage before the electron donating resonance effect is fully realized.[30]

The ion **47a** is also trapped efficiently by **d-G**. Competition experiments (Scheme 3.12) show that **d-G** competes with solvent for the cation to generate a C-8 adduct, **52a**, whose structure is analogous to the C-8 adducts derived from AA and HAA nitrenium ions (Schemes 3.6 and 3.7).[30] The rate constant $k_{d\text{-}G}$ was determined from the [**d-G**] dependence of the yields of **49a** and **52a** that provides $k_{d\text{-}G}/k_s$, and the known value of k_s.[30] The value is comparable to $k_{d\text{-}G}$ determined for the biphenylyl and fluorenylnitrenium ions **15a**, **15b**, **20a**, and **20b**.[17–20,83–86] A direct comparison of $k_{d\text{-}G}$ with **15a** is provided in Scheme 3.12.[30,83,84]

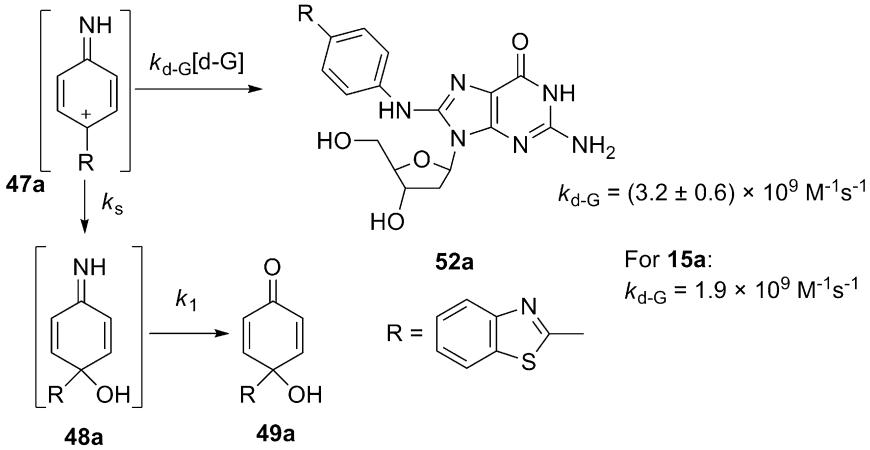

Scheme 3.12 Competitive trapping of **47a** by solvent and **d-G**.

Kinetic and trapping studies have shown that nitrenium ions derived from polycyclic AAs and HAAs are very selective for reactions with d-G compared to the other DNA bases.[83,84] The same is true for **47a**.[195] Chart 3.6 shows the reaction products and rate constants for the reaction of **47a** with adenosine, and the uncommon bases xanthosine and inosine, with comparisons to the equivalent reactions of **15a**.[84,195]

Inosine and xanthosine react with comparable rate constants with both ions (Chart 3.6).[84,195] The rate constants for xanthosine are similar in magnitude to $k_{d\text{-}G}$ for both ions. Inosine reacts with both ions with a much smaller rate constant. Both bases generate C-8 adducts that in all cases represent at least 50% of the purine adduct yield.[84,195] In two of the four cases (inosine with **15a** and xanthosine with **47a**) an additional adduct was isolated and characterized.[84,195] Adenosine generates considerably different adducts with the two cations, a hydrazine derivative with **47a** and a benzene imine adduct with **15a**.[84,195] Both ions behave similarly in that no C-8 adduct was detected with adenosine, and the selectivity for reaction with adenosine is at least an order of magnitude smaller than for reaction with **d-G**.[84,195]

The biphenylyl ion **15a** shows very little selectivity for reaction with any of the common pyrimidine bases found in DNA or RNA.[84] Rate constants for the reaction of **15a** with cytidine, uridine, and thymidine were $\leq 1.0 \times 10^7\ M^{-1}\ s^{-1}$.[84] Reaction products were not isolated. The reaction of **47a** with cytosine was examined in some detail.[195] Although the reaction is inefficient, it is somewhat faster than the reactions of **15a** with

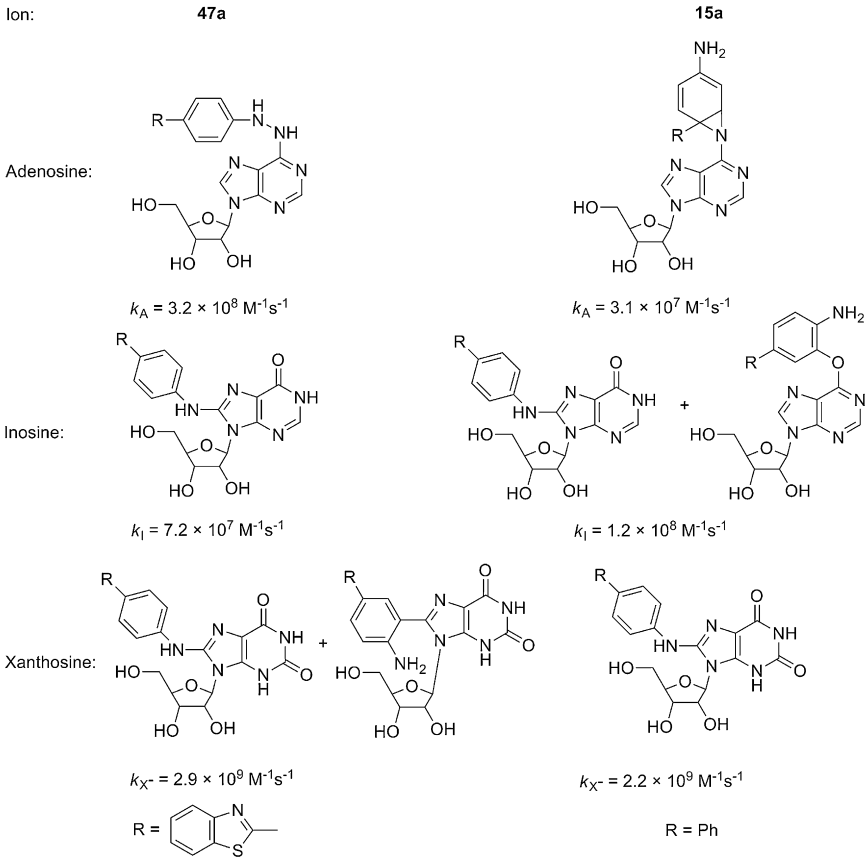

Chart 3.6 Adenosine, inosine, and xanthosine adducts of nitrenium ions **47a** and **15a**.

pyrimidines, with k_C of 1.7×10^8 M^{-1} s^{-1}, so that a reasonable yield of the product could be obtained at cytosine concentrations of 100 mM.[195]

The product with cytosine has a bond between the exocyclic amino group of **47a** and C-5 of the pyrimidine, **53a** (Chart 3.7).[195] Cytosine/cytidine adducts with most carcinogenic AAs and HAAs have not been detected, but the model metabolite of the weakly carcinogenic monocyclic amine 3,5-dimethylaniline, *N*-acetoxy-3,5-dimethylaniline, reacts with calf thymus DNA to form four significant adducts, one of which is an adduct with 2′-deoxycytidine with the analogous structure **54**.[196]

The reactions of **47a** with monomeric purines and pyrimidines are similar to the corresponding reactions of nitrenium ions such as **15a** that are derived from carcinogenic AAs. The reactions of **47a** with adenosine and cytosine are somewhat more efficient than the corresponding reactions of

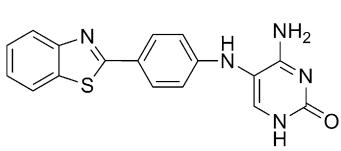

53a

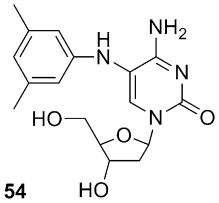

54

Chart 3.7 Comparison of cytosine adduct **53a** and cytidine adduct **54**.

15a, but the general trend of higher selectivity for reaction with **d-G** is a common feature of all of the long-lived nitrenium ions that have been investigated to date, including **47a**.[17–20,83–86,195] The structures of nucleoside–nitrenium ion adducts of **47a** are generally similar to those isolated from the reactions of other *N*-arylnitrenium ions with nucleosides, although there are some differences, particularly in the case of adenosine.[84,195] The results suggest that in vivo, **47a** and similar nitrenium ions derived from ring-substituted derivatives of **3a** will target **d-G** residues within DNA to produce the C-8 adduct as the major product in much the same way that has previously been observed for carcinogenic AAs and HAAs.[195]

Substituent effects have been examined in the series of ions **47a–d** derived from the corresponding acetic acid esters **44a–d** (Chart 3.8).[197] The largest substituent effect is observed in the rate constant for hydrolysis of the ester at neutral pH, k'_o. The 3′-Me substituent increases the hydrolysis rate by ca. 60-fold, while the 5-F substituent decreases the rate by a factor of about 2. Substituent effects on k_{az}/k_s, measured by the 'azide clock' method

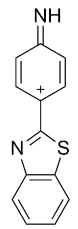

47a

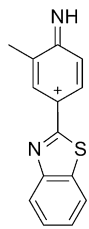

47b

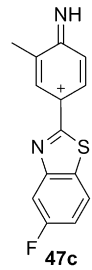

47c

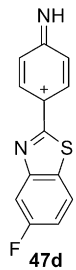

47d

k_o' (s^{-1})	2.3×10^{-3}	1.4×10^{-1}	1.2×10^{-1}	1.2×10^{-3}
k_{az}/k_s (M^{-1})	2.6×10^{3}	4.2×10^{3}	3.0×10^{3}	1.3×10^{3}
$1/k_s$ (ns)	530	850	610	260

Chart 3.8 Kinetic comparisons of substituted benzothiazole nitrenium ions.

are not large, ranging only over a factor of ca. 4 through the four ions. The cation aqueous solution lifetime was estimated by assuming that k_{az} is constant through the series and equal to the value directly measured for **47a**.[29] The 3′-Me cation **47b** has the longest lifetime, 850 ns, but this is less than double the lifetime of the unsubstituted ion **47a**. The 5-F cation **47d** has the shortest lifetime at 250 ns, but, again, the substituent effect is not large. The two effects approximately cancel for **47c**, the cation derived from the drug Phortress, now in clinical trials, so that its lifetime is nearly the same as the unsubstituted cation. None of the substituent effects suggest unusual behavior or a basis for differential biological selectivity that depends on cation lifetimes.

Although the nitrenium ions **47a**, **47b**, and **47c** appear to be responsible for the ultimate cytotoxic effects of the corresponding amines, they do not provide the basis for the selectivity of the drugs. That selectivity is a result of the involvement of cytosolic AhR binding and translocation of the drugs to the nucleus, induction of CYP4501A1 by the AhR–benzothiazole complex, and the resulting oxidative metabolism of the drugs.[27] Cells lacking either cytosolic AhR or the inducible CYP4501A1 are not sensitive to these drugs. Fortunately, many tumor cell lines do exhibit both of these characteristics, making them susceptible to the benzothiazole-derived drugs.[27] It also appears that the estrogen receptor (ER) may be activated by the AhR–benzothiazole complex in some sensitive cell lines, providing a secondary pathway for cytotoxicity.[31]

4.2. Diaminoflavones

In 1996 a series of 5-aminoflavone derivatives were tested for antitumor activity against the MCF-7 breast cancer cell line.[198] The most effective compound in the series was 5,4′-diaminoflavone, **4** (Charts 3.2 and 3.9). The 4′-amino group was found to be essential to activity, and movement of the 5-amino group to positions 6, 7, or 8 led to significantly decreased activity, as did movement of the 4′-amino group to the 3′-position.[198] Although activity was strongly linked to the presence of the ER in the target cells because ER^- cell lines were resistant to the drug, the IC_{50} values for **4** were not sensitive to the presence of estradiol (9.8 nM in the absence of estradiol and 7.2 nM in the presence of 10^{-4} μM estradiol).[198] This indicated that **4** does not bind directly to ER.[198] Subsequent studies showed that the presence of the rat liver homogenate S-9 mix significantly decreased the activity of **4** against MCF-7 cells apparently due to ring hydroxylation.[199]

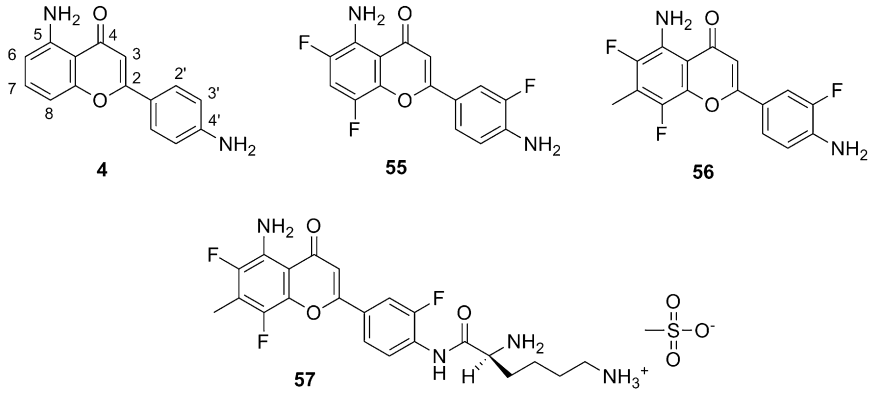

Chart 3.9 Anti-tumor 5,4′-diaminoflavones.

The 6,8,3′-trifluoro derivative, **55** (Chart 3.9), restored activity against MCF-7 cells in the presence of S-9 mix and extended activity to some ER^- cell lines, including ovarian cancer cell lines.[199] In vivo tests in nude mice inoculated with MCF-7 showed that **55** was effective at preventing tumor growth.[199] Additional structure–activity relationships showed that the 7-Me derivative, **56**, had enhanced antitumor activity.[200] Further developments have concentrated on this compound. The water-soluble prodrug, **57**, has reached Phase II clinical trials in the United States.[31]

Initial metabolism studies showed that **56** was converted by rat and human microsomes, by recombinant CYP4501A1 and CYP4501A2, and by sensitive human tumor cell lines to metabolites that bound covalently to DNA and caused DNA, damage responses in the cells.[201,202] Increased protein levels of both CYP4501A1 and CYP4501A2 were found in sensitive MCF-7 cell lines treated with **56**, suggesting that the drug induces the production of these enzymes.[201] Renal cancer cell lines sensitive to **56** were shown to have increased levels of CYP4501A1 and CYP4501B1 messenger RNA, while insensitive cell lines did not.[203] Stable transfection of the SULT1A1 gene into the resistant MDA-MB-231 cell line sensitized these cells to **56**.[204] The drug was also shown to induce expression of the SULT1A1 gene in MCF-7 cells.[204] Chinese Hamster V79 cells transfected with a number of polymorphs of the human CYP4501A1 and SULT1A1 genes exhibited differential metabolism and cytoxicity.[205] The SULT1A1 polymorphs exhibited considerable differences in IC_{50} values (ranging from 0.01 to 4.4 μM) in cells expressing the wild-type CYP4501A1 gene, indicating the importance of the SULT1A1 polymorph to the sensitivity of cells to this drug.[205]

The involvement of AhR in the activation of **56** was probed by a number of experiments. An AhR-deficient variant of the MCF-7 cell line was shown to be resistant to the drug in comparison to the drug-sensitive MCF-7 cells through measurement of total cellular protein levels and apoptosis as a function of drug concentration.[206] Dose-dependent induction of CYP4501A1 was observed in sensitive MCF-7 cells, but did not occur in the AhR-deficient variant.[206] MCF-7 cells and AhR-deficient cells transfected with an XRE-dependent luciferase reporter gene behaved differently upon exposure to **56**. The MCF-7 cells showed a significant increase in luciferase activity in the presence of **56**, but the AhR-deficient cells did not.[206] Drug-dependent AhR translocation to the nuclease was also detected in MCF-7 cells, but in the AhR-deficient cell line a low concentration of AhR was predominately located in the nucleus independent of the concentration of **56**.[206] It appears that the metabolism of **56** and related diaminoflavones follows a similar path to that observed for the 2-(4-aminophenyl)benzothiazoles requiring AhR binding in the cytosol, translocation to the nucleus, induction of CYP4501A1, and oxidative metabolism involving CYP4501A1 and SULT1A1.[31] Involvement of SULT1A1 in the metabolism of the benzothiazole-derived drugs has not been reported, so metabolism of **56** has been established one step further than the benzothiazoles.[27,31]

Phase I (CYP450 induced) metabolism of **56** was probed in mouse microsomes.[207] Five oxidized products were detected by UPLC/MS and tentative structures were assigned based on MS fragmentation patterns. Recombinant human CYP4501A1, 1A2, and 2C19 enzymes were also shown to generate the same five products. Scheme 3.13 summarizes product identities and, where it is possible to make a conclusion, indicates the identity of the human enzyme that appears to be predominately involved in the reaction.[207] Phase II metabolism (including products of SULT activation) was also probed in mouse urine using the UPLC/MS technique.[207] A number of glucuronides were identified, but only the sulfates are shown in Scheme 3.13 because SULT1A1 has been demonstrated to be involved in activation of the drug.[205]

The three monohydroxylated products identified as $N^{4'}$-OH-**56**, **58**, N^{5}-OH-**56**, **59**, and 3-OH-**56**, **60** are predominately produced by different human enzymes.[207] CYP4501A1 is predominately responsible for generation of **58**, while CYP4501A2 is predominately responsible for **60**. Both of these isozymes appear to be responsible for formation of **59**. Two dihydroxylated products, **61** and **62**, were also detected.[207]

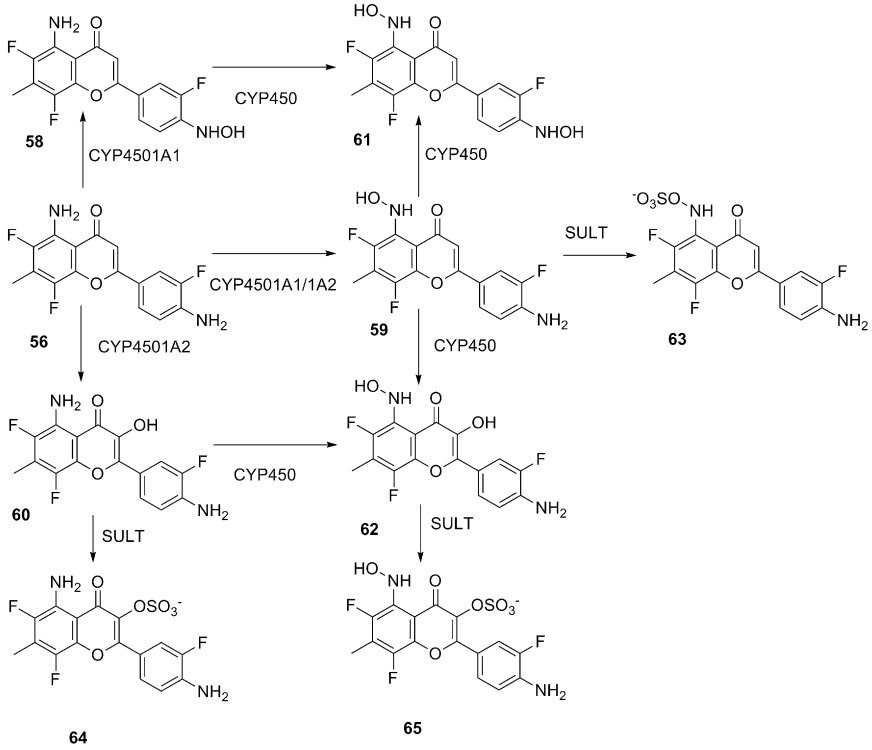

Scheme 3.13 Simplified metabolic scheme for **56** in the mouse.

The sulfates **63**–**65** are necessarily stable materials because they were isolated from mouse urine.[207] It is unlikely that any of them are responsible for DNA damage. The missing sulfate, **66** (Scheme 3.14), or possibly **67** (Scheme 3.14), was suspected to be the likely reactive compound responsible for DNA damage through a nitrenium ion mechanism.[31,207,208] The nitrenium ion **68** does not appear to be a stabilized species, but inductive effects have been shown to be subordinate to resonance stabilization of nitrenium ions, so it is possible that the species has the requisite lifetime to react selectively with DNA bases.[18,20,77,193,194]

Although the nitrenium ion chemistry of **68** has not been explored the metabolic evidence for activation of **56** strongly suggests a pathway very similar to that of the benzothiazole-derived compounds **3a**–**c**. Experiments with precursors of **68** would clearly establish whether the nitrenium ion is generated, and whether it has the required reaction selectivity patterns.

These are the only two examples that the authors are aware of in which a nitrenium ion appears to be directly involved in the mechanism of drug

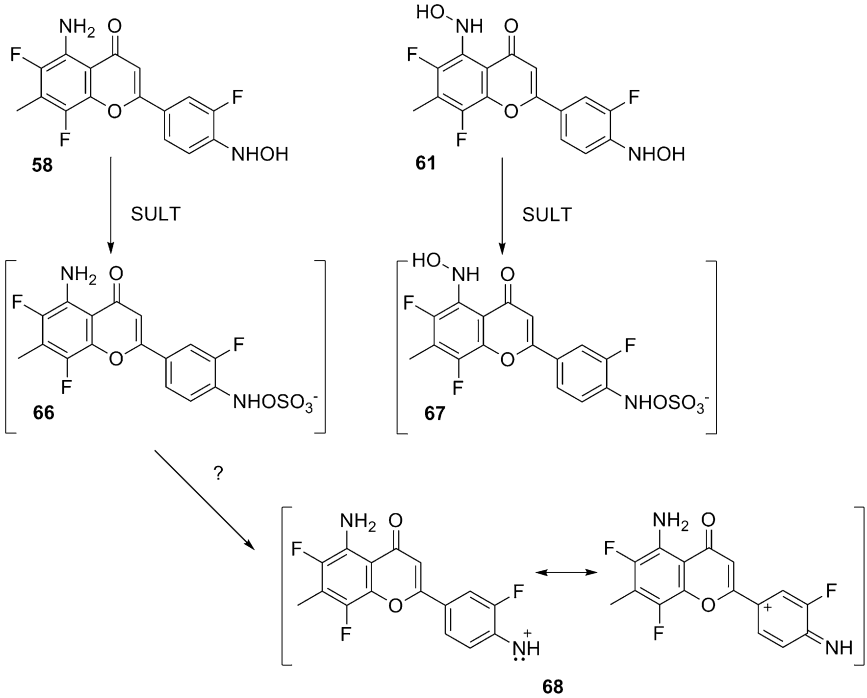

Scheme 3.14 Possible pathway to proposed nitrenium ion **68**.

action. Whether more such drugs are developed in the future will depend on the ultimate success of the two drug candidates that are now undergoing evaluation in clinical trials.

5. CONCLUSION

The importance of *N*-arylnitrenium ion chemistry in biological processes has advanced considerably over the years from a speculative hypothesis with little concrete evidence that proposed the involvement of nitrenium ions in AA carcinogenesis, to the current situation in which that hypothesis has been well established. During that same time frame it has been shown that the same metabolic activation processes that generate carcinogenic and mutagenic nitrenium ion precursors from AAs and HAAs can also metabolize nitrogen-containing drugs to form nitrenium ion precursors, and the nitrenium ions derived from these precursors have been implicated in dangerous side effects of certain drugs. Most recently, the

cytotoxic effects of nitrenium ions have been put to use as the warheads of antitumor drugs that are selectively metabolized by target tumor cells into nitrenium ion precursors. It is gratifying that the knowledge and expertise gained from an understanding of the biological and chemical basis for the deleterious effects of AA carcinogens can be put to therapeutic use to treat the same diseases that AAs and HAAs have been shown to cause. Further developments in this area are anticipated with considerable interest.

REFERENCES

1. Miller JA. Carcinogenesis by chemicals: an overview–G. H. A. Clowes memorial lecture. *Cancer Res*. 1970;30(3):559-576. PubMed PMID: 4915745.
2. Miller EC, Miller JA. Searches for ultimate chemical carcinogens and their reactions with cellular macromolecules. *Cancer*. 1981;47(10):2327-2345. PubMed PMID: 7272889.
3. Beland FA, Beranek DT, Dooley KL, Heflich RH, Kadlubar FF. Arylamine-DNA adducts in vitro and in vivo: their role in bacterial mutagenesis and urinary bladder carcinogenesis. *Environ Health Perspect*. 1983;49:125-134. PubMed PMID: 6339219; PubMed Central PMCID: PMCPMC1569140.
4. Beland FA, Kadlubar FF. Formation and persistence of arylamine DNA adducts in vivo. *Environ Health Perspect*. 1985;62:19-30. PubMed PMID: 4085422; PubMed Central PMCID: PMCPMC1568675.
5. Guengerich FP. *N-hydroxyarylamines*. *Drug Metab Rev*. 2002;34(3):607-623. http://dx.doi.org/10.1081/DMR-120005663. PubMed PMID: 12214670.
6. Vineis P, Pirastu R. Aromatic amines and cancer. *Cancer Causes Control*. 1997;8(3):346-355. PubMed PMID: 9498898.
7. Banoglu E. Current status of the cytosolic sulfotransferases in the metabolic activation of promutagens and procarcinogens. *Curr Drug Metab*. 2000;1(1):1-30. PubMed PMID: 11467078.
8. Hein DW. Molecular genetics and function of NAT1 and NAT2: role in aromatic amine metabolism and carcinogenesis. *Mutat Res*. 2002;506-507:65-77. http://dx.doi.org/10.1016/S0027510702001537 [pii]. PubMed PMID: 12351146.
9. Sim E, Lack N, Wang CJ, Long H, Westwood I, Fullam E, et al. Arylamine N-acetyltransferases: structural and functional implications of polymorphisms. *Toxicology*. 2008;254(3):170-183. http://dx.doi.org/10.1016/S0300-483X(08)00422-8 [pii] 10.1016/j.tox.2008.08.022. PubMed PMID: 18852012.
10. Kim D, Guengerich FP. Cytochrome P450 activation of arylamines and heterocyclic amines. *Annu Rev Pharmacol Toxicol*. 2005;45:27-49. http://dx.doi.org/10.1146/annurev.pharmtox.45.120403.100010. PubMed PMID: 15822170.
11. Cho BP. Dynamic conformational heterogeneities of carcinogen-DNA adducts and their mutagenic relevance. *J Environ Sci Health C Environ Carcinog Ecotoxicol Rev*. 2004;22(2):57-90. http://dx.doi.org/10.1016/K589823086R19X63 [pii]. 10.1081/LESC-200038217. PubMed PMID: 16291518.
12. Sugimura T. Carcinogenicity of mutagenic heterocyclic amines formed during the cooking process. *Mutat Res*. 1985;150(1-2):33-41. PubMed PMID: 3889618.
13. Eisenbrand G, Tang W. Food-borne heterocyclic amines. Chemistry, formation, occurrence and biological activities. A literature review. *Toxicology*. 1993;84(1-3):1-82. PubMed PMID: 8266331.
14. Sugimura T. Overview of carcinogenic heterocyclic amines. *Mutat Res*. 1997; 376(1-2):211-219. PubMed PMID: 9202758.

15. Sugimura T, Wakabayashi K, Nakagama H, Nagao M. Heterocyclic amines: Mutagens/carcinogens produced during cooking of meat and fish. *Cancer Sci*. 2004;95(4):290-299. PubMed PMID: 15072585.
16. Knize MG, Kulp KS, Salmon CP, Keating GA, Felton JS. Factors affecting human heterocyclic amine intake and the metabolism of PhIP. *Mutat Res*. 2002;506-507:153-162. http://dx.doi.org/10.1016/S0027510702001628 [pii]. PubMed PMID: 12351155.
17. McClelland RA, Gadosy TA, Ren D. 1997 Alfred Bader Award Lecture - Reactivities of arylnitrenium ions with guanine derivatives and other nucleophiles. *Can J Chem-Revue Canadienne De Chimie*. 1998;76(10):1327-1337. http://dx.doi.org/10.1139/cjc-76-10-1327. PubMed PMID: WOS:000078002800001.
18. Novak M, Rajagopal S. N-Arylnitrenium ions. *Adv Phys Org Chem*. 2001;Vol 36(36):167-254. http://dx.doi.org/10.1016/S0065-3160(01)36005-7. PubMed PMID: WOS:000173171100004.
19. Novak M, Rajagopal S, Xu L, Kazerani S, Toth K, Brooks M, et al. Chemistry of carcinogenic and mutagenic metabolites of heterocyclic aromatic amines. *J Phys Org Chem*. 2004;17(6-7):615-624. http://dx.doi.org/10.1002/poc.765. |10.1002/poc.765. PubMed PMID: WOS:000222274200022.
20. Novak M, Chakraborty M. N-Arylhydroxylamines and Chemical Carcinogenicity. In: Rappoport Z, Liebman JF, eds. *PATAI'S Chemistry of Functional Groups, The Chemistry of Hydroxylamines, Oximes and Hydroxamic Acids, Vol. 2 Part 2*. Wext Sussex, England: John Wiley & Sons, Ltd; 2010:577-622.
21. Guengerich FP. Cytochrome P450s and other enzymes in drug metabolism and toxicity. *AAPS J*. 2006;8(1):E101-E111. http://dx.doi.org/10.1208/aapsj080112. PubMed PMID: 16584116; PubMed Central PMCID: PMCPMC2751428.
22. Kalgutkar AS, Dalvie DK, O'Donnell JP, Taylor TJ, Sahakian DC. On the diversity of oxidative bioactivation reactions on nitrogen-containing xenobiotics. *Curr Drug Metab*. 2002;3(4):379-424. PubMed PMID: 12093357.
23. Uetrecht J. N-oxidation of drugs associated with idiosyncratic drug reactions. *Drug Metab Rev*. 2002;34(3):651-665. http://dx.doi.org/10.1081/DMR-120005667. PubMed PMID: 12214672.
24. Arlt VM, Stiborova M, Schmeiser HH. Aristolochic acid as a probable human cancer hazard in herbal remedies: a review. *Mutagenesis*. 2002;17(4):265-277. PubMed PMID: 12110620.
25. Zhou SF, Xue CC, Yu XQ, Wang G. Metabolic activation of herbal and dietary constituents and its clinical and toxicological implications: an update. *Curr Drug Metab*. 2007;8(6):526-553. PubMed PMID: 17691916.
26. Stiborová M, Frei E, Arlt VM, Schmeiser HH. Metabolic activation of carcinogenic aristolochic acid, a risk factor for Balkan endemic nephropathy. *Mutat Res*. 2008;658(1-2):55-67. http://dx.doi.org/10.1016/S1383-5742(07)00028-2 [pii] 10.1016/j.mrrev.2007.07.003. PubMed PMID: 17851120.
27. Bradshaw TD, Westwell AD. The development of the antitumor benzothiazole prodrug, Phortress, as a clinical candidate. *Curr Med Chem*. 2004;11(8):1009-1021. PubMed PMID: 15078163.
28. O'Brien SE, Browne HL, Bradshaw TD, Westwell AD, Stevens MF, Laughton CA. Antitumor benzothiazoles. Frontier molecular orbital analysis predicts bioactivation of 2-(4-aminophenyl)benzothiazoles to reactive intermediates by cytochrome P4501A1. *Org Biomol Chem*. 2003;1(3):493-497. PubMed PMID: 12926251.
29. Chakraborty M, Jin KJ, Brewer SC, Peng HL, Platz MS, Novak M. Indirect and direct detection of the 4-(benzothiazol-2-yl)phenylnitrenium ion from a putative metabolite of a model anti-tumor drug. *Org Lett*. 2009;11(21):4862-4865. http://dx.doi.org/10.1021/ol901959z. PubMed PMID: 19788283; PubMed Central PMCID: PMCPMC2783571.

30. Chakraborty M, Jin KJ, Glover SA, Novak M. Characterization of the 4-(benzothiazol-2-yl)phenylnitrenium ion from a putative metabolite of a model antitumor drug. *J Org Chem*. 2010;75(15):5296-5304. http://dx.doi.org/10.1021/jo101275y. PubMed PMID: 20670034; PubMed Central PMCID: PMCPMC2921917.
31. Callero MA, Loaiza-Pérez AI. The role of aryl hydrocarbon receptor and crosstalk with estrogen receptor in response of breast cancer cells to the novel antitumor agents benzothiazoles and aminoflavone. *Int J Breast Cancer*. 2011;2011:923250. http://dx.doi.org/10.4061/2011/923250. PubMed PMID: 22295239; PubMed Central PMCID: PMCPMC3262585.
32. Butler MA, Guengerich FP, Kadlubar FF. Metabolic oxidation of the carcinogens 4-aminobiphenyl and 4,4'-methylene-bis(2-chloroaniline) by human hepatic microsomes and by purified rat hepatic cytochrome P-450 monooxygenases. *Cancer Res*. 1989;49(1):25-31. PubMed PMID: 2908851.
33. Langouët S, Paehler A, Welti DH, Kerriguy N, Guillouzo A, Turesky RJ. Differential metabolism of 2-amino-1-methyl-6-phenylimidazo[4,5-b]pyridine in rat and human hepatocytes. *Carcinogenesis*. 2002;23(1):115-122. PubMed PMID: 11756232.
34. Wakabayashi K, Nagao M, Esumi H, Sugimura T. Food-derived mutagens and carcinogens. *Cancer Res*. 1992;52(7 Suppl):2092s-2098s. PubMed PMID: 1544146.
35. Kato R, Kamataki T, Yamazoe Y. N-hydroxylation of carcinogenic and mutagenic aromatic amines. *Environ Health Perspect*. 1983;49:21-25. PubMed PMID: 6832094; PubMed Central PMCID: PMCPMC1569125.
36. Hammons GJ, Milton D, Stepps K, Guengerich FP, Tukey RH, Kadlubar FF. Metabolism of carcinogenic heterocyclic and aromatic amines by recombinant human cytochrome P450 enzymes. *Carcinogenesis*. 1997;18(4):851-854. PubMed PMID: 9111224.
37. Oda Y, Aryal P, Terashita T, Gillam EM, Guengerich FP, Shimada T. Metabolic activation of heterocyclic amines and other procarcinogens in Salmonella typhimurium umu tester strains expressing human cytochrome P4501A1, 1A2, 1B1, 2C9, 2D6, 2E1, and 3A4 and human NADPH-P450 reductase and bacterial O-acetyltransferase. *Mutat Res*. 2001;492(1-2):81-90. http://dx.doi.org/10.1016/S1383571801001541 [pii]. PubMed PMID: 11377247.
38. Cramer JW, Miller JA, Miller EC. N-Hydroxylation: A new metabolic reaction observed in the rat with the carcinogen 2-acetylaminofluorene. *J Biol Chem*. 1960;235:885-888. PubMed PMID: 13812621.
39. Thorgeirsson SS, Jollow DJ, Sasame HA, Green I, Mitchell JR. The role of cytochrome P-450 in N-hydroxylation of 2-acetylaminofluorene. *Mol Pharmacol*. 1973;9(3):398-404. PubMed PMID: 4122821.
40. Heflich RH, Neft RE. Genetic toxicity of 2-acetylaminofluorene, 2-aminofluorene and some of their metabolites and model metabolites. *Mutat Res*. 1994;318(2):73-114. PubMed PMID: 7521935.
41. DeBaun JR, Miller EC, Miller JA. N-hydroxy-2-acetylaminofluorene sulfotransferase: its probable role in carcinogenesis and in protein-(methion-S-yl) binding in rat liver. *Cancer Res*. 1970;30(3):577-595. PubMed PMID: 5425283.
42. DeBaun JR, Smith JY, Miller EC, Miller JA. Reactivity in vivo of the carcinogen N-hydroxy-2-acetylaminofluorene: increase by sulfate ion. *Science*. 1970;167(3915):184-186. PubMed PMID: 5409643.
43. Weisburger JH, Yamamoto RS, Williams GM, Grantham PH, Matsushima T, Weisburger EK. On the sulfate ester of N-hydroxy-N-2-fluorenylacetamide as a key ultimate hepatocarcinogen in the rat. *Cancer Res*. 1972;32(3):491-500. PubMed PMID: 5061304.
44. Lai CC, Miller JA, Miller EC, Liem A. N-sulfoöxy-2-aminofluorene is the major ultimate electrophilic and carcinogenic metabolite of N-hydroxy-2-acetylaminofluorene in the

livers of infant male C57BL/6J x C3H/HeJ F1 (B6C3F1) mice. *Carcinogenesis*. 1985;6(7):1037-1045. PubMed PMID: 3860305.
45. Lai CC, Miller EC, Miller JA, Liem A. Initiation of hepatocarcinogenesis in infant male B6C3F1 mice by N-hydroxy-2-aminofluorene or N-hydroxy-2-acetylaminofluorene depends primarily on metabolism to N-sulfooxy-2-aminofluorene and formation of DNA-(deoxyguanosin-8-yl)-2-aminofluorene adducts. *Carcinogenesis*. 1987;8(3):471-478. PubMed PMID: 3815742.
46. Walraven JM, Trent JO, Hein DW. Structure-function analyses of single nucleotide polymorphisms in human N-acetyltransferase 1. *Drug Metab Rev*. 2008;40(1):169-184. http://dx.doi.org/10.1016/790483193 [pii] 10.1080/03602530701852917. PubMed PMID: 18259988; PubMed Central PMCID: PMCPMC2265210.
47. Walraven JM, Zang Y, Trent JO, Hein DW. Structure/function evaluations of single nucleotide polymorphisms in human N-acetyltransferase 2. *Curr Drug Metab*. 2008;9(6):471-486. PubMed PMID: 18680467; PubMed Central PMCID: PMCPMC2507886.
48. Minchin RF, Reeves PT, Teitel CH, McManus ME, Mojarrabi B, Ilett KF, et al. N- and O-acetylation of aromatic and heterocyclic amine carcinogens by human monomorphic and polymorphic acetyltransferases expressed in COS-1 cells. *Biochem Biophys Res Commun*. 1992;185(3):839-844. http://dx.doi.org/10.1016/0006-291X(92)91703-S [pii]. PubMed PMID: 1627140.
49. Hein DW, Doll MA, Rustan TD, Gray K, Feng Y, Ferguson RJ, et al. Metabolic activation and deactivation of arylamine carcinogens by recombinant human NAT1 and polymorphic NAT2 acetyltransferases. *Carcinogenesis*. 1993;14(8):1633-1638. PubMed PMID: 8353847.
50. Hein DW, Rustan TD, Ferguson RJ, Doll MA, Gray K. Metabolic activation of aromatic and heterocyclic N-hydroxyarylamines by wild-type and mutant recombinant human NAT1 and NAT2 acetyltransferases. *Arch Toxicol*. 1994;68(2):129-133. PubMed PMID: 8179482.
51. Hein DW, Doll MA, Rustan TD, Ferguson RJ. Metabolic activation of N-hydroxyarylamines and N-hydroxyarylamides by 16 recombinant human NAT2 allozymes: effects of 7 specific NAT2 nucleic acid substitutions. *Cancer Res*. 1995;55(16):3531-3536. PubMed PMID: 7627960.
52. Liu L, Von Vett A, Zhang N, Walters KJ, Wagner CR, Hanna PE. Arylamine N-acetyltransferases: characterization of the substrate specificities and molecular interactions of environmental arylamines with human NAT1 and NAT2. *Chem Res Toxicol*. 2007;20(9):1300-1308. http://dx.doi.org/10.1021/tx7001614. PubMed PMID: 17672512.
53. Kadlubar FF, Miller JA, Miller EC. Hepatic metabolism of N-hydroxy-N-methyl-4-aminoazobenzene and other N-hydroxy arylamines to reactive sulfuric acid esters. *Cancer Res*. 1976;36(7 PT 1):2350-2359. PubMed PMID: 819129.
54. Lindsay J, Wang LL, Li Y, Zhou SF. Structure, function and polymorphism of human cytosolic sulfotransferases. *Curr Drug Metab*. 2008;9(2):99-105. PubMed PMID: 18288952.
55. Glatt H. Sulfotransferases in the bioactivation of xenobiotics. *Chem Biol Interact*. 2000;129(1-2):141-170. http://dx.doi.org/10.1016/S0009-2797(00)00202-7 [pii]. PubMed PMID: 11154739.
56. Turesky RJ. The role of genetic polymorphisms in metabolism of carcinogenic heterocyclic aromatic amines. *Curr Drug Metab*. 2004;5(2):169-180. PubMed PMID: 15078194.
57. Ozawa S, Chou HC, Kadlubar FF, Nagata K, Yamazoe Y, Kato R. Activation of 2-hydroxyamino-1-methyl-6-phenylimidazo[4,5-b] pyridine by cDNA-expressed human and rat arylsulfotransferases. *Jpn J Cancer Res*. 1994;85(12):1220-1228. PubMed PMID: 7852185.

58. Turesky RJ, Garner RC, Welti DH, Richoz J, Leveson SH, Dingley KH, et al. Metabolism of the food-borne mutagen 2-amino-3,8-dimethylimidazo[4,5-f]quinoxaline in humans. *Chem Res Toxicol.* 1998;11(3):217-225. http://dx.doi.org/10.1016/tx9701891 [pii] 10.1021/tx9701891. PubMed PMID: 9544620.
59. Davis CD, Schut HA, Snyderwine EG. Enzymatic phase II activation of the N-hydroxylamines of IQ, MeIQx and PhIP by various organs of monkeys and rats. *Carcinogenesis.* 1993;14(10):2091-2096. PubMed PMID: 8222059.
60. Muckel E, Frandsen H, Glatt HR. Heterologous expression of human N-acetyltransferases 1 and 2 and sulfotransferase 1A1 in Salmonella typhimurium for mutagenicity testing of heterocyclic amines. *Food Chem Toxicol.* 2002;40(8):1063-1068. http://dx.doi.org/10.1016/S0278691502000327 [pii]. PubMed PMID: 12067565.
61. Nagaoka H, Wakabayashi K, Kim SB, Kim IS, Tanaka Y, Ochiai M, et al. Adduct formation at C-8 of guanine on in vitro reaction of the ultimate form of 2-amino-1-methyl-6-phenylimidazo[4,5-b]pyridine with 2'-deoxyguanosine and its phosphate esters. *Jpn J Cancer Res.* 1992;83(10):1025-1029. PubMed PMID: 1452454.
62. Lin D, Kaderlik KR, Turesky RJ, Miller DW, Lay JO, Kadlubar FF. Identification of N-(Deoxyguanosin-8-yl)-2-amino-1-methyl-6-phenylimidazo [4,5-b]pyridine as the major adduct formed by the food-borne carcinogen, 2-amino-1-methyl-6-phenylimidazo[4,5-b]pyridine, with DNA. *Chem Res Toxicol.* 1992;5(5):691-697. PubMed PMID: 1446011.
63. Snyderwine EG, Roller PP, Adamson RH, Sato S, Thorgeirsson SS. Reaction of N-hydroxylamine and N-acetoxy derivatives of 2-amino-3-methylimidazolo[4,5-f]quinoline with DNA. Synthesis and identification of N-(deoxyguanosin-8-yl)-IQ. *Carcinogenesis.* 1988;9(6):1061-1065. PubMed PMID: 3370750.
64. Snyderwine EG, Yamashita K, Adamson RH, Sato S, Nagao M, Sugimura T, et al. Use of the ^{32}P-postlabeling method to detect DNA adducts of 2-amino-3-methylimidazolo [4,5-f]quinoline (IQ) in monkeys fed IQ: identification of the N-(deoxyguanosin-8-yl)-IQ adduct. *Carcinogenesis.* 1988;9(10):1739-1743. PubMed PMID: 3168152.
65. Schut HA, Snyderwine EG. DNA adducts of heterocyclic amine food mutagens: implications for mutagenesis and carcinogenesis. *Carcinogenesis.* 1999;20(3):353-368. PubMed PMID: 10190547.
66. Irving CC, Veazey RA. Persistent binding of 2-acetylaminofluorene to rat liver DNA in vivo and consideration of the mechanism of binding of N-hydroxy-2-acetylaminofluorene to rat liver nucleic acids. *Cancer Res.* 1969;29(10):1799-1804. PubMed PMID: 5823948.
67. Westra JG, Kriek E, Hittenhausen H. Identification of the persistently bound form of the carcinogen N-acetyl-2-aminofluorene to rat liver DNA in vivo. *Chem Biol Interact.* 1976;15(2):149-164. http://dx.doi.org/10.1016/0009-2797(76)90160-5 [pii]. PubMed PMID: 975399.
68. Fuchs RP. Arylamidation and arylation by the carcinogen N-2-fluorenylacetamide: a sensitive and rapid radiochemical assay. *Anal Biochem.* 1978;91(2):663-673. PubMed PMID: 9762153.
69. Turesky RJ, Rossi SC, Welti DH, Lay JO, Kadlubar FF. Characterization of DNA adducts formed in vitro by reaction of N-hydroxy-2-amino-3-methylimidazo[4,5-f]quinoline and N-hydroxy-2-amino-3,8-dimethylimidazo[4,5-f]quinoxaline at the C-8 and N2 atoms of guanine. *Chem Res Toxicol.* 1992;5(4):479-490. PubMed PMID: 1391614.
70. Turesky RJ, Gremaud E, Markovic J, Snyderwine EG. DNA adduct formation of the food-derived mutagen 2-amino-3-methylimidazo[4,5-f]quinoline in nonhuman primates undergoing carcinogen bioassay. *Chem Res Toxicol.* 1996;9(2):403-408. http://dx.doi.org/10.1016/tx950132j [pii] 10.1021/tx950132j. PubMed PMID: 8839042.
71. Novak M, Toth K, Rajagopal S, Brooks M, Hott LL, Moslener M. Reactivity and selectivity of the N-acetyl-Glu-P-1, N-acetyl-Glu-P-2, N-acetyl-MeIQx, and

N-acetyl-IQx nitrenium ions: Comparison to carbocyclic N-arylnitrenium ions. *J Am Chem Soc.* 2002;124(27):7972-7981. http://dx.doi.org/10.1021/ja0121944. |10.1021/ja0121944. PubMed PMID: WOS:000176612400028.

72. Gassman PG. Nitrenium ions. *Acc Chem Res.* 1970;3(1):26-33. http://dx.doi.org/10.1021/ar50025a004. PubMed PMID: WOS: A1970F107700004.
73. Gassman PG, Granrud JE. Synthesis and rearrangement of methenesulfonate esters of N-hydroxyacetanilides -A model for a penultimate carcinogen. *J Am Chem Soc.* 1984;106(5):1498-1499. http://dx.doi.org/10.1021/ja00317a060. PubMed PMID: WOS: A1984SH16500060.
74. Novak M, Pelecanou M, Roy AK, Andronico AF, Plourde FM, Olefirowicz TM, et al. Solvolysis of N-sulfonoxyacetanilides in aqueous and alcohol solutions - Generation of electrophilic species. *J Am Chem Soc.* 1984;106(19):5623-5631. http://dx.doi.org/10.1021/ja00331a036. PubMed PMID: WOS: A1984TJ67200036.
75. Novak M, Roy AK. Hydrolysis of N-(sulfonatooxy)-para-acetotoluidide - Solution chemistry of models for carcinogenic metabolites of aromatic amides. *J Org Chem.* 1985;50(5):571-580. http://dx.doi.org/10.1021/jo00205a006. PubMed PMID: WOS: A1985ADG1400006.
76. Fishbein JC, McClelland RA. Azide ion trapping of the intermediate in the Bamberger rearrangement - Lifetime of a free nitrenium ion in aqueous-solution. *J Am Chem Soc.* 1987;109(9):2824-2825. http://dx.doi.org/10.1021/ja00243a045. PubMed PMID: WOS: A1987H107700044.
77. Novak M, Kahley MJ, Eiger E, Helmick JS, Peters HE. Reactivity and selectivity of nitrenium ions derived from ester derivatives of carcinogenic N-(4-biphenylyl) hydroxylamine and the corresponding hydroxamic acid. *J Am Chem Soc.* 1993;115(21):9453-9460. http://dx.doi.org/10.1021/ja00074a010. PubMed PMID: WOS: A1993MD06900010.
78. Novak M, Helmick JS, Oberlies N, Rangappa KS, Clark WM, Swenton JS. The electrochemical preparation and kinetic and product studies of acylated quinol and quinol ether imines - In search of the hydrolysis products of the ulyimate carcinogen of N-acetyl-2-aminofluorene. *J Org Chem.* 1993;58(4):867-878. http://dx.doi.org/10.1021/jo00056a019. PubMed PMID: WOS: A1993KM22900019.
79. Richard JP, Jencks WP. A simple relationship between carbocation lifetime and reactivity-selectivity relationships for the solvolysis of ring-substituted 1-phenylethyl derivatives. *J Am Chem Soc.* 1982;104(17):4689-4691. http://dx.doi.org/10.1021/ja00381a037. PubMed PMID: WOS: A1982PC82900038.
80. Richard JP, Rothenberg ME, Jencks WP. Formation and stability of ring-substituted 1-phenylethyl carbocations. *J Am Chem Soc.* 1984;106(5):1361-1372. http://dx.doi.org/10.1021/ja00317a032. PubMed PMID: WOS: A1984SH16500032.
81. Davidse PA, Kahley MJ, McClelland RA, Novak M. Flash-photolysis observation and lifetimes of 2-fluorenyl and 4-biphenylylacetylnitrenium ions in aqueous-solution. *J Am Chem Soc.* 1994;116(10):4513-4514. http://dx.doi.org/10.1021/ja00089a065. PubMed PMID: WOS: A1994NM98800065.
82. McClelland RA, Davidse PA, Hadzialic G. Electron-Deficient Strong Bases - Generation of the 4-biphenylylnitrenium and 2-fluorenylnitrenium ions by nitrene protonation in water. *J Am Chem Soc.* 1995;117(14):4173-4174. http://dx.doi.org/10.1021/ja00119a035. PubMed PMID: WOS: A1995QT13200035.
83. Novak M, Kennedy SA. Selective trapping of N-acetyl-N-(4-Biphenylyl)nitrenium and N-acetyl-N-(2-fluorenyl)nitrenium ions by 2'-deoxyguanosine in aqueous-solution. *J Am Chem Soc.* 1995;117(1):574-575. http://dx.doi.org/10.1021/ja00106a083. PubMed PMID: WOS: A1995QC06100083.
84. Kennedy SA, Novak M, Kolb BA. Reactions of ester derivatives of carcinogenic N-(4-biphenylyl)hydroxylamine and the corresponding hydroxamic acid with purine

nucleosides. *J Am Chem Soc.* 1997;119(33):7654-7664. http://dx.doi.org/10.1021/ja970698p. PubMed PMID: WOS: A1997XT03700005.
85. McClelland RA, Kahley MJ, Davidse PA. Reactivity of the 4-biphenylyl and 2-fluorenylnitrenium ions with heterocyclic and carbon nucleophiles. *J Phys Org Chem.* 1996;9(6):355-360. http://dx.doi.org/10.1002/(SICI)1099-1395(199606)9. 6<355::AID-POC792>3.0.CO;2-Q. PubMed PMID: WOS: A1996UW80000008.
86. McClelland RA, Ahmad A, Dicks AP, Licence VE. Spectroscopic characterization of the initial C8 intermediate in the reaction of the 2-fluorenylnitrenium ion with 2 '-deoxyguanosine. *J Am Chem Soc.* 1999;121(14):3303-3310. http://dx.doi.org/10.1021/ja9836702. PubMed PMID: WOS:000079884800008.
87. Novak M, Kennedy SA. Inhibitory effect of DNA structure on the efficiency of reaction of guanosine moieties with a nitrenium ion. *J Phys Org Chem.* 1998;11(1):71-76. http://dx.doi.org/10.1002/(SICI)1099-1395(199801)11. 1<71::AID-POC973>3.0.CO;2-H. PubMed PMID: WOS:000072655300012.
88. Novak M, Xu L, Wolf RA. Nitrenium ions from food-derived heterocyclic arylamine mutagens. *J Am Chem Soc.* 1998;120(7):1643-1644. http://dx.doi.org/10.1021/ja974222h. PubMed PMID: WOS:000072246500051.
89. Novak M, Kazerani S. Characterization of the 2-(alpha-carbolinyl)nitrenium ion and its conjugate base produced during the decomposition of the model carcinogen 2-N-(pivaloyloxy)-2-amino-alpha-carboline in aqueous solution. *J Am Chem Soc.* 2000;122(15):3606-3616. http://dx.doi.org/10.1021/ja993433e. PubMed PMID: WOS:000086729500006.
90. Broyde S, Wang L, Zhang L, Rechkoblit O, Geacintov NE, Patel DJ. DNA adduct structure-function relationships: comparing solution with polymerase structures. *Chem Res Toxicol.* 2008;21(1):45-52. http://dx.doi.org/10.1021/tx700193x. PubMed PMID: 18052109.
91. Ju C, Uetrecht JP. Mechanism of idiosyncratic drug reactions: reactive metabolite formation, protein binding and the regulation of the immune system. *Curr Drug Metab.* 2002;3(4):367-377. PubMed PMID: 12093356.
92. Kalgutkar AS. Handling reactive metabolite positives in drug discovery: What has retrospective structure-toxicity analyses taught us? *Chem Biol Interact.* 2011;192(1-2):46-55. http://dx.doi.org/10.1016/S0009-2797(10)00547-8 [pii] 10.1016/j.cbi.2010.09.003. PubMed PMID: 20833160.
93. Stepan AF, Walker DP, Bauman J, Price DA, Baillie TA, Kalgutkar AS, et al. Structural alert/reactive metabolite concept as applied in medicinal chemistry to mitigate the risk of idiosyncratic drug toxicity: a perspective based on the critical examination of trends in the top 200 drugs marketed in the United States. *Chem Res Toxicol.* 2011;24(9):1345-1410. http://dx.doi.org/10.1021/tx200168d. PubMed PMID: 21702456.
94. Kane J, Honigfeld G, Singer J, Meltzer H. Clozapine for the treatment-resistant schizophrenic. A double-blind comparison with chlorpromazine. *Arch Gen Psychiatry.* 1988;45(9):789-796. PubMed PMID: 3046553.
95. Lindström LH. A retrospective study on the long-term efficacy of clozapine in 96 schizophrenic and schizoaffective patients during a 13-year period. *Psychopharmacology (Berl).* 1989;99(Suppl):S84-S86. PubMed PMID: 2813670.
96. Baldessarini RJ, Clozapine Frankenburg FR. A novel antipsychotic agent. *N Engl J Med.* 1991;324(11):746-754. http://dx.doi.org/10.1056/NEJM199103143241107. PubMed PMID: 1671793.
97. Lieberman JA, Safferman AZ. Clinical profile of clozapine: adverse reactions and agranulocytosis. *Psychiatr Q.* 1992;63(1):51-70. PubMed PMID: 1438605.
98. Safferman A, Lieberman JA, Kane JM, Szymanski S, Kinon B. Update on the clinical efficacy and side effects of clozapine. *Schizophr Bull.* 1991;17(2):247-261. PubMed PMID: 1882209.

99. Lieberman JA, Johns CA, Kane JM, Rai K, Pisciotta AV, Saltz BL, et al. Clozapine-induced agranulocytosis: non-cross-reactivity with other psychotropic drugs. *J Clin Psychiatry*. 1988;49(7):271-277. PubMed PMID: 3391979.
100. Kellner M, Wiedemann K, Krieg JC, Berg PA. Toxic hepatitis by clozapine treatment. *Am J Psychiatry*. 1993;150(6):985-986. PubMed PMID: 8494085.
101. Alvir JM, Lieberman JA. A reevaluation of the clinical characteristics of clozapine-induced agranulocytosis in light of the United States experience. *J Clin Psychopharmacol*. 1994;14(2):87-89. PubMed PMID: 8195462.
102. Alvir JM, Lieberman JA. Agranulocytosis: incidence and risk factors. *J Clin Psychiatry*. 1994;55(Suppl B):137-138. PubMed PMID: 7961558.
103. Gardner I, Zahid N, MacCrimmon D, Uetrecht JP. A comparison of the oxidation of clozapine and olanzapine to reactive metabolites and the toxicity of these metabolites to human leukocytes. *Mol Pharmacol*. 1998;53(6):991-998. PubMed PMID: 9614200.
104. Gardner I, Leeder JS, Chin T, Zahid N, Uetrecht JP. A comparison of the covalent binding of clozapine and olanzapine to human neutrophils in vitro and in vivo. *Mol Pharmacol*. 1998;53(6):999-1008. PubMed PMID: 9614201.
105. Liu ZC, Uetrecht JP. Clozapine is oxidized by activated human neutrophils to a reactive nitrenium ion that irreversibly binds to the cells. *J Pharmacol Exp Ther*. 1995;275(3):1476-1483. PubMed PMID: 8531118.
106. Pirmohamed M, Williams D, Madden S, Templeton E, Park BK. Metabolism and bioactivation of clozapine by human liver in vitro. *J Pharmacol Exp Ther*. 1995;272(3):984-990. PubMed PMID: 7891353.
107. Maggs JL, Williams D, Pirmohamed M, Park BK. The metabolic formation of reactive intermediates from clozapine, a drug associated with agranulocytosis in man. *J Pharmacol Exp Ther*. 1995;275(3):1463-1475. PubMed PMID: 8531117.
108. Williams DP, Pirmohamed M, Naisbitt DJ, Maggs JL, Park BK. Neutrophil cytotoxicity of the chemically reactive metabolite(s) of clozapine: possible role in agranulocytosis. *J Pharmacol Exp Ther*. 1997;283(3):1375-1382. PubMed PMID: 9400013.
109. Uetrecht J, Zahid N, Tehim A, Fu JM, Rakhit S. Structural features associated with reactive metabolite formation in clozapine analogues. *Chem Biol Interact*. 1997;104(2-3):117-129. PubMed PMID: 9212779.
110. Dragovic S, Boerma JS, van Bergen L, Vermeulen NP, Commandeur JN. Role of human glutathione S-transferases in the inactivation of reactive metabolites of clozapine. *Chem Res Toxicol*. 2010;23(9):1467-1476. http://dx.doi.org/10.1021/tx100131f. PubMed PMID: 20849150.
111. Iverson S, Kautiainen A, Ip J, Uetrecht JP. Effect of clozapine on neutrophil kinetics in rabbits. *Chem Res Toxicol*. 2010;23(7):1184-1191. http://dx.doi.org/10.1021/tx100035k. PubMed PMID: 20553052.
112. Ip J, Wilson JX, Uetrecht JP. Testing the hypothesis that vitamin C deficiency is a risk factor for clozapine-induced agranulocytosis using guinea pigs and ODS rats. *Chem Res Toxicol*. 2008;21(4):869-873. http://dx.doi.org/10.1021/tx7004025. PubMed PMID: 18380445.
113. Ip J, Uetrecht JP. Testing the hypothesis that selenium deficiency is a risk factor for clozapine-induced agranulocytosis in rats. *Chem Res Toxicol*. 2008;21(4):874-878. http://dx.doi.org/10.1021/tx7004037. PubMed PMID: 18380444.
114. Dilly S, Liégeois JF. Interaction of clozapine and its nitrenium ion with rat D2 dopamine receptors: in vitro binding and computational study. *J Comput Aided Mol Des*. 2011;25(2):163-169. http://dx.doi.org/10.1007/s10822-010-9407-8. PubMed PMID: 21184252.
115. Chen ZL, Zhu DY. Aristicholia alkaloids. In: Brossi A, ed. *The Alkaloids, Vol. 31*. New York, NY: Academic Press; 1987:29-66.
116. Pailer M, Bergthal P, Schaden G. Uber die isolierung und charakterisierung von vier neun aristolochiasauren (aus Aristolochia clematitis L) - Pflanzliche naturstoffe mit

einer nitrogruppe 4. *Monatshefte Fur Chemie Und Verwandte Teile Anderer Wissenschaften*. 1965;96(3):863-883. http://dx.doi.org/10.1007/BF00919160. PubMed PMID: WOS: A19656648800014.
117. Kumar V, Poonam Prasad AK, Parmar VS. Naturally occurring aristolactams, aristolochic acids and dioxoaporphines and their biological activities. *Nat Prod Rep*. 2003;20(6):565-583. PubMed PMID: 14700200.
118. Kupchan SM, Doskotch RW. Tumor inhibitors. I. Aristolochic acid, the active principle of Aristolochia indica. *J Med Pharm Chem*. 1962;91:657-659. PubMed PMID: 14056399.
119. Kupchan SM, Wormser HC. Tumor inhibitors. X. Photochemical synthesis of phenanthrenes. Synthesis of aristolochic acid and related compounds. *J Org Chem*. 1965;30(11):3792-3800. PubMed PMID: 5846158.
120. Mengs U, Lang W, Poch J. The carcinogenic action of aristolochic acid in rats. *Arch Toxicol*. 1982;51(2):107-119. http://dx.doi.org/10.1007/BF00302751. PubMed PMID: WOS: A1982PT88800001.
121. Mengs U. Tumour induction in mice following exposure to aristolochic acid. *Arch Toxicol*. 1988;61(6):504-505. PubMed PMID: 3190449.
122. Schmeiser HH, Pool BL, Wiessler M. Mutagenicity of the two main components of commercially available carcinogenic aristolochic acid in Salmonella typhimurium. *Cancer Lett*. 1984;23(1):97-101. PubMed PMID: 6378360.
123. Cosyns JP, Jadoul M, Squifflet JP, Wese FX. van Ypersele de Strihou C. Urothelial lesions in Chinese-herb nephropathy. *Am J Kidney Dis*. 1999;33(6):1011-1017. http://dx.doi.org/10.1016/S0272-6386(99)70136-8 [pii] 10.1016/S0272-6386(99)70136-8. PubMed PMID: 10352187.
124. Lord GM, Cook T, Arlt VM, Schmeiser HH, Williams G, Pusey CD. Urothelial malignant disease and Chinese herbal nephropathy. *Lancet*. 2001;358(9292):1515-1516. http://dx.doi.org/10.1016/S014067360106576X [pii]. PubMed PMID: 11705569.
125. Ioset JR, Raoelison GE, Hostettmann K. Detection of aristolochic acid in Chinese phytomedicines and dietary supplements used as slimming regimens. *Food Chem Toxicol*. 2003;41(1):29-36. http://dx.doi.org/10.1016/S0278691502002193 [pii]. PubMed PMID: 12453725.
126. Nortier JL, Martinez MC, Schmeiser HH, Arlt VM, Bieler CA, Petein M, et al. Urothelial carcinoma associated with the use of a Chinese herb (Aristolochia fangchi). *N Engl J Med*. 2000;342(23):1686-1692. http://dx.doi.org/10.1056/NEJM200006083422301. PubMed PMID: 10841870.
127. Schwetz BA. From the Food and Drug Administration. *JAMA*. 2001;285(21):2705. http://dx.doi.org/10.1016/jfd10005-1 [pii]. PubMed PMID: 11386912.
128. Schmeiser HH, Schoepe KB, Wiessler M. DNA adduct formation of aristolochic acid I and II in vitro and in vivo. *Carcinogenesis*. 1988;9(2):297-303. PubMed PMID: 3338114.
129. Pfau W, Schmeiser HH, Wiessler M. Aristolochic acid binds covalently to the exocyclic amino group of purine nucleotides in DNA. *Carcinogenesis*. 1990;11(2):313-319. PubMed PMID: 2302759.
130. Pfau W, Schmeiser HH, Wiessler M. ^{32}P-postlabelling analysis of the DNA adducts formed by aristolochic acid I and II. *Carcinogenesis*. 1990;11(9):1627-1633. PubMed PMID: 2401053.
131. Pfau W, Schmeiser HH, Wiessler M. N^6-adenyl arylation of DNA by aristolochic acid II and a synthetic model for the putative proximate carcinogen. *Chem Res Toxicol*. 1991;4(5):581-586. PubMed PMID: 1665354.
132. Stiborová M, Fernando RC, Schmeiser HH, Frei E, Pfau W, Wiessler M. Characterization of DNA adducts formed by aristolochic acids in the target organ (forestomach) of rats by ^{32}P-postlabelling analysis using different chromatographic procedures. *Carcinogenesis*. 1994;15(6):1187-1192. PubMed PMID: 8020154.

133. Fernando RC, Schmeiser HH, Scherf HR, Wiessler M. Formation and persistence of specific purine DNA adducts by ^{32}P-postlabelling in target and non-target organs of rats treated with aristolochic acid I. *IARC Sci Publ.* 1993;(124):167-171. PubMed PMID: 8225480.
134. Schmeiser HH, Bieler CA, Wiessler M. van Ypersele de Strihou C, Cosyns JP. Detection of DNA adducts formed by aristolochic acid in renal tissue from patients with Chinese herbs nephropathy. *Cancer Res.* 1996;56(9):2025-2028. PubMed PMID: 8616845.
135. Bieler CA, Stiborova M, Wiessler M, Cosyns JP, van Ypersele de Strihou C, Schmeiser HH. ^{32}P-post-labelling analysis of DNA adducts formed by aristolochic acid in tissues from patients with Chinese herbs nephropathy. *Carcinogenesis.* 1997;18(5):1063-1067. PubMed PMID: 9163697.
136. Yun BH, Rosenquist TA, Sidorenko V, Iden CR, Chen CH, Pu YS, et al. Biomonitoring of aristolactam-DNA adducts in human tissues using ultra-performance liquid chromatography/ion-trap mass spectrometry. *Chem Res Toxicol.* 2012;25(5):1119-1131. http://dx.doi.org/10.1021/tx3000889. PubMed PMID: 22515372.
137. Krumbiegel G, Hallensleben J, Mennicke WH, Rittmann N, Roth HJ. Studies on the metabolism of aristolochic acids I and II. *Xenobiotica.* 1987;17(8):981-991. http://dx.doi.org/10.3109/00498258709044197. PubMed PMID: 3673113.
138. Chan W, Luo HB, Zheng Y, Cheng YK, Cai Z. Investigation of the metabolism and reductive activation of carcinogenic aristolochic acids in rats. *Drug Metab Dispos.* 2007;35(6):866-874. http://dx.doi.org/10.1016/dmd.106.013979 [pii] 10.1124/dmd.106.013979. PubMed PMID: 17344338.
139. Schmeiser HH, Frei E, Wiessler M, Stiborova M. Comparison of DNA adduct formation by aristolochic acids in various in vitro activation systems by ^{32}P-post-labelling: evidence for reductive activation by peroxidases. *Carcinogenesis.* 1997;18(5):1055-1062. PubMed PMID: 9163696.
140. Stiborová M, Frei E, Breuer A, Wiessler M, Schmeiser HH. Evidence for reductive activation of carcinogenic aristolochic acids by prostaglandin H synthase – (32)P-postlabeling analysis of DNA adduct formation. *Mutat Res.* 2001;493(1-2):149-160. http://dx.doi.org/10.1016/S1383571801001711 [pii]. PubMed PMID: 11516724.
141. Stiborová M, Frei E, Wiessler M, Schmeiser HH. Human enzymes involved in the metabolic activation of carcinogenic aristolochic acids: evidence for reductive activation by cytochromes P450 1A1 and 1A2. *Chem Res Toxicol.* 2001;14(8):1128-1137. http://dx.doi.org/10.1016/tx010059z [pii]. PubMed PMID: 11511187.
142. Stiborová M, Frei E, Sopko B, Wiessler M, Schmeiser HH. Carcinogenic aristolochic acids upon activation by DT-diaphorase form adducts found in DNA of patients with Chinese herbs nephropathy. *Carcinogenesis.* 2002;23(4):617-625. PubMed PMID: 11960915.
143. Stiborová M, Frei E, Sopko B, Sopková K, Marková V, Lanková M, et al. Human cytosolic enzymes involved in the metabolic activation of carcinogenic aristolochic acid: evidence for reductive activation by human NAD(P)H:quinone oxidoreductase. *Carcinogenesis.* 2003;24(10):1695-1703. http://dx.doi.org/10.1016/bgg119 [pii] 10.1093/carcin/bgg119. PubMed PMID: 12869422.
144. Stiborová M, Frei E, Hodek P, Wiessler M, Schmeiser HH. Human hepatic and renal microsomes, cytochromes P450 1A1/2, NADPH:cytochrome P450 reductase and prostaglandin H synthase mediate the formation of aristolochic acid-DNA adducts found in patients with urothelial cancer. *Int J Cancer.* 2005;113(2):189-197. http://dx.doi.org/10.1002/ijc.20564. PubMed PMID: 15386410.
145. Levová K, Moserová M, Kotrbová V, Sulc M, Henderson CJ, Wolf CR, et al. Role of cytochromes P450 1A1/2 in detoxication and activation of carcinogenic aristolochic

acid I: studies with the hepatic NADPH:cytochrome P450 reductase null (HRN) mouse model. *Toxicol Sci*. 2011;121(1):43-56. http://dx.doi.org/10.1016/kfr050 [pii] 10.1093/toxsci/kfr050. PubMed PMID: 21362632.
146. Arlt VM, Levová K, Bárta F, Shi Z, Evans JD, Frei E, et al. Role of P450 1A1 and P450 1A2 in bioactivation versus detoxication of the renal carcinogen aristolochic acid I: studies in Cyp1a1-/-, Cyp1a2-/-, and Cyp1a1/1a2-/- mice. *Chem Res Toxicol*. 2011;24(10):1710-1719. http://dx.doi.org/10.1021/tx200259y. PubMed PMID: 21932800.
147. Schmeiser HH, Pool BL, Wiessler M. Identification and mutagenicity of metabolites of aristolochic acid formed by rat liver. *Carcinogenesis*. 1986;7(1):59-63. PubMed PMID: 3510750.
148. Stiborová M, Frei E, Breuer A, Bieler CA, Schmeiser HH. Aristolactam I a metabolite of aristolochic acid I upon activation forms an adduct found in DNA of patients with Chinese herbs nephropathy. *Exp Toxicol Pathol*. 1999;51(4-5):421-427. PubMed PMID: 10445409.
149. Priestman TJ. *Cancer Chemotherapy: An Introduction*. 3rd ed.). Berlin: Springer; 1989. 3–26.
150. Shi DF, Bradshaw TD, Wrigley S, McCall CJ, Lelieveld P, Fichtner I, et al. Antitumor benzothiazoles. 3. Synthesis of 2-(4-aminophenyl)benzothiazoles and evaluation of their activities against breast cancer cell lines in vitro and in vivo. *J Med Chem*. 1996;39(17):3375-3384. http://dx.doi.org/10.1016/jm9600959 [pii] 10.1021/jm9600959. PubMed PMID: 8765521.
151. Tzanopoulou S, Pirmettis IC, Patsis G, Paravatou-Petsotas M, Livaniou E, Papadopoulos M, et al. Synthesis, characterization, and biological evaluation of $M(I)(CO)_3(NNO)$ complexes ($M = Re^{99m}Tc$) conjugated to 2-(4-aminophenyl)benzothiazole as potential breast cancer radiopharmaceuticals. *J Med Chem*. 2006;49(18):5408-5410. http://dx.doi.org/10.1021/jm0606387. PubMed PMID: 16942013.
152. Tzanopoulou S, Sagnou M, Paravatou-Petsotas M, Gourni E, Loudos G, Xanthopoulos S, et al. Evaluation of Re and ^{99m}Tc complexes of 2-(4'-aminophenyl) benzothiazole as potential breast cancer radiopharmaceuticals. *J Med Chem*. 2010;53(12):4633-4641. http://dx.doi.org/10.1021/jm1001293. PubMed PMID: 20518489.
153. Henriksen G, Hauser AI, Westwell AD, Yousefi BH, Schwaiger M, Drzezga A, et al. Metabolically stabilized benzothiazoles for imaging of amyloid plaques. *J Med Chem*. 2007;50(6):1087-1089. http://dx.doi.org/10.1021/jm061466g. PubMed PMID: 17319654.
154. Wang Y, Klunk WE, Debnath ML, Huang GF, Holt DP, Shao L, et al. Development of a PET/SPECT agent for amyloid imaging in Alzheimer's disease. *J Mol Neurosci*. 2004;24(1):55-62. http://dx.doi.org/10.1016/JMN:24:1:055 [pii] 10.1385/JMN:24:1:055. PubMed PMID: 15314250.
155. Wu C, Cai L, Wei J, Pike VW, Wang Y. Lipophilic analogs of thioflavin S as novel amyloid-imaging agents. *Curr Alzheimer Res*. 2006;3(3):259-266. PubMed PMID: 16842103.
156. Wu C, Wei J, Gao K, Wang Y. Dibenzothiazoles as novel amyloid-imaging agents. *Bioorg Med Chem*. 2007;15(7):2789-2796. http://dx.doi.org/10.1016/S0968-0896(06)00950-3 [pii] 10.1016/j.bmc.2006.11.022. PubMed PMID: 17293116.
157. Serdons K, Verduyckt T, Cleynhens J, Terwinghe C, Mortelmans L, Bormans G, et al. Synthesis and evaluation of a ^{99m}Tc-BAT-phenylbenzothiazole conjugate as a potential in vivo tracer for visualization of amyloid beta. *Bioorg Med Chem Lett*. 2007;17(22):6086-6090. http://dx.doi.org/10.1016/S0960-894X(07)01098-0 [pii] 10.1016/j.bmcl.2007.09.055. PubMed PMID: 17904367.
158. Ra C, Jung B, Park G. The fungicidal benzothiazole methoxyacrylates: Synthesis, conformational analysis and fungicidal activity. *Heterocycles*. 2004;62:793-802. PubMed PMID: WOS:000188256600064.

159. Yildiz-Oren I, Yalcin I, Aki-Sener E, Ucarturk N. Synthesis and structure-activity relationships of new antimicrobial active multisubstituted benzazole derivatives. *Eur J Med Chem*. 2004;39(3):291-298. http://dx.doi.org/10.1016/S0223523404000029 [pii] 10.1016/j.ejmech.2003.11.014. PubMed PMID: 15051178.
160. Zhou Y, Sun Z, Froelich JM, Hermann T, Wall D. Structure-activity relationships of novel antibacterial translation inhibitors: 3,5-diamino-piperidinyl triazines. *Bioorg Med Chem Lett*. 2006;16(20):5451-5456. http://dx.doi.org/10.1016/S0960-894X(06)00828-6 [pii] 10.1016/j.bmcl.2006.07.052. PubMed PMID: 16890435.
161. Tasler S, Müller O, Wieber T, Herz T, Krauss R, Totzke F, et al. N-substituted 2'-(aminoaryl)benzothiazoles as kinase inhibitors: hit identification and scaffold hopping. *Bioorg Med Chem Lett*. 2009;19(5):1349-1356. http://dx.doi.org/10.1016/S0960-894X(09)00071-7 [pii] 10.1016/j.bmcl.2009.01.054. PubMed PMID: 19211246.
162. Weekes AA, Westwell AD. 2-Arylbenzothiazole as a privileged scaffold in drug discovery. *Curr Med Chem*. 2009;16(19):2430-2440. PubMed PMID: 19601790.
163. Bradshaw TD, Wrigley S, Shi DF, Schultz RJ, Paull KD, Stevens MF. 2-(4-Aminophenyl)benzothiazoles: novel agents with selective profiles of in vitro anti-tumour activity. *Br J Cancer*. 1998;77(5):745-752. PubMed PMID: 9514053; PubMed Central PMCID: PMCPMC2149949.
164. Bradshaw TD, Shi DF, Schultz RJ, Paull KD, Kelland L, Wilson A, et al. Influence of 2-(4-aminophenyl)benzothiazoles on growth of human ovarian carcinoma cells in vitro and in vivo. *Br J Cancer*. 1998;78(4):421-429. PubMed PMID: 9716022; PubMed Central PMCID: PMCPMC2063080.
165. Chua MS, Kashiyama E, Bradshaw TD, Stinson SF, Brantley E, Sausville EA, et al. Role of Cyp1A1 in modulation of antitumor properties of the novel agent 2-(4-amino-3-methylphenyl)benzothiazole (DF 203, NSC 674495) in human breast cancer cells. *Cancer Res*. 2000;60(18):5196-5203. PubMed PMID: 11016648.
166. Kashiyama E, Hutchinson I, Chua MS, Stinson SF, Phillips LR, Kaur G, et al. Antitumor benzothiazoles. 8. Synthesis, metabolic formation, and biological properties of the C- and N-oxidation products of antitumor 2-(4-aminophenyl)benzothiazoles. *J Med Chem*. 1999;42(20):4172-4184. http://dx.doi.org/10.1016/jm990104o [pii]. PubMed PMID: 10514287.
167. Loaiza-Pérez AI, Trapani V, Hose C, Singh SS, Trepel JB, Stevens MF, et al. Aryl hydrocarbon receptor mediates sensitivity of MCF-7 breast cancer cells to antitumor agent 2-(4-amino-3-methylphenyl) benzothiazole. *Mol Pharmacol*. 2002;61(1):13-19. PubMed PMID: 11752201.
168. Trapani V, Patel V, Leong CO, Ciolino HP, Yeh GC, Hose C, et al. DNA damage and cell cycle arrest induced by 2-(4-amino-3-methylphenyl)-5-fluorobenzothiazole (5F 203, NSC 703786) is attenuated in aryl hydrocarbon receptor deficient MCF-7 cells. *Br J Cancer*. 2003;88(4):599-605. http://dx.doi.org/10.1016/6600722 [pii] 10.1038/sj.bjc.6600722. PubMed PMID: 12592376; PubMed Central PMCID: PMCPMC2377159.
169. Bradshaw TD, Trapani V, Vasselin DA, Westwell AD. The aryl hydrocarbon receptor in anticancer drug discovery: friend or foe? *Curr Pharm Des*. 2002;8(27):2475-2490. PubMed PMID: 12369945.
170. Janosek J, Hilscherová K, Bláha L, Holoubek I. Environmental xenobiotics and nuclear receptors–interactions, effects and in vitro assessment. *Toxicol In Vitro*. 2006;20(1):18-37. http://dx.doi.org/10.1016/S0887-2333(05)00110-4 [pii] 10.1016/j.tiv.2005.06.001. PubMed PMID: 16061344.
171. Hutchinson I, Chua MS, Browne HL, Trapani V, Bradshaw TD, Westwell AD, et al. Antitumor benzothiazoles. 14. Synthesis and in vitro biological properties of fluorinated 2-(4-aminophenyl)benzothiazoles. *J Med Chem*. 2001;44(9):1446-1455. http://dx.doi.org/10.1016/jm001104n [pii]. PubMed PMID: 11311068.

172. Hutchinson I, Jennings SA, Vishnuvajjala BR, Westwell AD, Stevens MF. Antitumor benzothiazoles. 16. Synthesis and pharmaceutical properties of antitumor 2-(4-aminophenyl)benzothiazole amino acid prodrugs. *J Med Chem.* 2002;45(3):744-747. http://dx.doi.org/10.1016/jm011025r [pii]. PubMed PMID: 11806726.
173. Bradshaw TD, Bibby MC, Double JA, Fichtner I, Cooper PA, Alley MC, et al. Preclinical evaluation of amino acid prodrugs of novel antitumor 2-(4-amino-3-methylphenyl)benzothiazoles. *Mol Cancer Ther.* 2002;1(4):239-246. PubMed PMID: 12467219.
174. Bradshaw TD, Chua MS, Browne HL, Trapani V, Sausville EA, Stevens MF. In vitro evaluation of amino acid prodrugs of novel antitumor 2-(4-amino-3-methylphenyl) benzothiazoles. *Br J Cancer.* 2002;86(8):1348-1354. http://dx.doi.org/10.1038/sj.bjc.6600225. PubMed PMID: 11953897; PubMed Central PMCID: PMCPMC2375326.
175. Hose CD, Hollingshead M, Sausville EA, Monks A. Induction of CYP1A1 in tumor cells by the antitumor agent 2-[4-amino-3-methylphenyl]-5-fluoro-benzothiazole: a potential surrogate marker for patient sensitivity. *Mol Cancer Ther.* 2003;2(12):1265-1272. PubMed PMID: 14707267.
176. Monks A, Harris E, Hose C, Connelly J, Sausville EA. Genotoxic profiling of MCF-7 breast cancer cell line elucidates gene expression modifications underlying toxicity of the anticancer drug 2-(4-amino-3-methylphenyl)-5-fluorobenzothiazole. *Mol Pharmacol.* 2003;63(3):766-772. PubMed PMID: 12606787.
177. Brantley E, Patel V, Stinson SF, Trapani V, Hose CD, Ciolino HP, et al. The antitumor drug candidate 2-(4-amino-3-methylphenyl)-5-fluorobenzothiazole induces NF-kappaB activity in drug-sensitive MCF-7 cells. *Anticancer Drugs.* 2005;16(2):137-143. http://dx.doi.org/10.1016/00001813-200502000-00004 [pii]. PubMed PMID: 15655410.
178. Wallqvist A, Connelly J, Sausville EA, Covell DG, Monks A. Differential gene expression as a potential classifier of 2-(4-amino-3-methylphenyl)-5-fluorobenzothiazole-sensitive and -insensitive cell lines. *Mol Pharmacol.* 2006;69(3):737-748. http://dx.doi.org/10.1016/mol.105.017061 [pii] 10.1124/mol.105.017061. PubMed PMID: 16332985.
179. Martinez JM, Sali T, Okazaki R, Anna C, Hollingshead M, Hose C, et al. Drug-induced expression of nonsteroidal anti-inflammatory drug-activated gene/macrophage inhibitory cytokine-1/prostate-derived factor, a putative tumor suppressor, inhibits tumor growth. *J Pharmacol Exp Ther.* 2006;318(2):899-906. http://dx.doi.org/10.1016/jpet.105.100081 [pii] 10.1124/jpet.105.100081. PubMed PMID: 16714403.
180. Mukherjee A, Martin SG. In vitro cytotoxicity of Phortress against colorectal cancer. *Int J Oncol.* 2006;29(5):1287-1294. PubMed PMID: 17016663.
181. Hutchinson I, Bradshaw TD, Matthews CS, Stevens MF, Westwell AD. Antitumor benzothiazoles. Part 20: 3'-cyano and 3'-alkynyl-substituted 2-(4'-aminophenyl) benzothiazoles as new potent and selective analogues. *Bioorg Med Chem Lett.* 2003;13(3):471-474. http://dx.doi.org/10.1016/S0960894X02009307 [pii]. PubMed PMID: 12565953.
182. Mortimer CG, Wells G, Crochard JP, Stone EL, Bradshaw TD, Stevens MF, et al. Antitumor benzothiazoles. 26. (1) 2-(3,4-dimethoxyphenyl)-5-fluorobenzothiazole (GW 610, NSC 721648), a simple fluorinated 2-arylbenzothiazole, shows potent and selective inhibitory activity against lung, colon, and breast cancer cell lines. *J Med Chem.* 2006;49(1):179-185. http://dx.doi.org/10.1021/jm050942k. PubMed PMID: 16392802.
183. Aiello S, Wells G, Stone EL, Kadri H, Bazzi R, Bell DR, et al. Synthesis and biological properties of benzothiazole, benzoxazole, and chromen-4-one analogues of the potent antitumor agent 2-(3,4-dimethoxyphenyl)-5-fluorobenzothiazole (PMX 610, NSC

721648). *J Med Chem*. 2008;51(16):5135-5139. http://dx.doi.org/10.1021/jm800418z. PubMed PMID: 18666770.

184. Akhtar T, Hameed S, Al-Masoudi NA, Loddo R, La Colla P. In vitro antitumor and antiviral activities of new benzothiazole and 1,3,4-oxadiazole-2-thione derivatives. *Acta Pharm*. 2008;58(2):135-149. http://dx.doi.org/10.1016/X517Q7H577174482 [pii] 10.2478/v10007-008-0007-2. PubMed PMID: 18515224.
185. Brantley E, Trapani V, Alley MC, Hose CD, Bradshaw TD, Stevens MF, et al. Fluorinated 2-(4-amino-3-methylphenyl)benzothiazoles induce CYP1A1 expression, become metabolized, and bind to macromolecules in sensitive human cancer cells. *Drug Metab Dispos*. 2004;32(12):1392-1401. http://dx.doi.org/10.1016/dmd.104.001057 [pii] 10.1124/dmd.104.001057. PubMed PMID: 15355884.
186. Brantley E, Antony S, Kohlhagen G, Meng L, Agama K, Stinson SF, et al. Anti-tumor drug candidate 2-(4-amino-3-methylphenyl)-5-fluorobenzothiazole induces single-strand breaks and DNA-protein cross-links in sensitive MCF-7 breast cancer cells. *Cancer Chemother Pharmacol*. 2006;58(1):62-72. http://dx.doi.org/10.1007/s00280-005-0127-z. PubMed PMID: 16331501.
187. Leong CO, Gaskell M, Martin EA, Heydon RT, Farmer PB, Bibby MC, et al. Antitumor 2-(4-aminophenyl)benzothiazoles generate DNA adducts in sensitive tumour cells in vitro and in vivo. *Br J Cancer*. 2003;88(3):470-477. http://dx.doi.org/10.1016/6600719 [pii] 10.1038/sj.bjc.6600719. PubMed PMID: 12569393; PubMed Central PMCID: PMCPMC2747538.
188. Leong CO, Suggitt M, Swaine DJ, Bibby MC, Stevens MF, Bradshaw TD. In vitro, in vivo, and in silico analyses of the antitumor activity of 2-(4-amino-3-methylphenyl)-5-fluorobenzothiazoles. *Mol Cancer Ther*. 2004;3(12):1565-1575. http://dx.doi.org/10.1016/3/12/1565 [pii]. PubMed PMID: 15634650.
189. Hilal R, Abdel Khalek A, Elroby S. DFT-investigation of nitrenium ions derived from metabolism of antitumor 2-(4-aminophenyl)benzothiazoles. *Journal of Molecular Structure-Theochem*. 2005;731(1-3):115-121. http://dx.doi.org/10.1016/j.theochem.2005.04.017. 10.1016/j.theochem.2005.04.017. PubMed PMID: WOS:000232847400015.
190. Stevens M, Shi D, Castro A. Antitumor benzothiazoles 2. Formation of 2,2'-diaminobiphenyls from the decomposition of 2-(4-azidophenyl)benzazoles in trifluoromethanesulfonic acid. *J Chem Soc-Perkin Trans 1*. 1996;(1):83-93. http://dx.doi.org/10.1039/p19960000083. PubMed PMID: WOS: A1996TQ68100012.
191. Bystrov VF, Belaya ZN, Gruz BE, Syrova GP, Tolmachev AI, Shulezhko LM, et al. Reactivity constants of some 2-hetaryls. *Zh Obshch Khim*. 1968;38(5):1001-1005. PubMed PMID: WOS: A1968C522600012.
192. Durmis J, Karvas M, Manasek Z. 2-Aryl derivatives of condensed five-membered N-heterocyclic compounds. I. Dissociation constants of 2- and 4-substituted phenols and naphthols. *Collect Czech Chem Commun*. 1973;38(1):215-223. PubMed PMID: WOS: A1973O550900026.
193. Novak M, Kahley MJ, Lin J, Kennedy SA, Swanegan LA. Reactivity patterns of N-arylnitrenium ions-Lack of correlation with sigma(+). *J Am Chem Soc*. 1994;116(25):11626-11627. http://dx.doi.org/10.1021/ja00104a076. PubMed PMID: WOS: A1994PX38600076.
194. Ren D, McClelland RA. Carbocation-like reactivity patterns in X '-substituted-4-biphenylylnitrenium ions. *Canadian Journal of Chemistry-Revue Canadienne De Chimie*. 1998;76(1):78-84. http://dx.doi.org/10.1139/cjc-76-1-78. PubMed PMID: WOS: 000072999600010.
195. Novak M, Chakraborty M. Reactions of a putative metabolite of the model antitumor drug 2-(4-aminophenyl) benzothiazole with purines and pyrimidines. *J Phys Org Chem*. 2011;24(10):960-968. http://dx.doi.org/10.1002/poc. 1905. PubMed PMID: WOS:000295429500014.

196. Cui L, Sun H-L, Wishnok JS, Tannenbaum SR, Skipper PL. Identification of Adducts Formed by Reaction of N-Acetoxy-3,5-dimethylaniline with DNA. *Chem Res Toxicol.* 2007;20(11):1730-1736.
197. Novak M, Chakraborty M, Zhang Y, Cerda-Smith C. *to be submitted to J Org Chem.* 2012.
198. Akama T, Shida Y, Sugaya T, Ishida H, Gomi K, Kasai M. Novel 5-aminoflavone derivatives as specific antitumor agents in breast cancer. *J Med Chem.* 1996;39(18):3461-3469. http://dx.doi.org/10.1016/jm950938g [pii] 10.1021/jm950938g. PubMed PMID: 8784443.
199. Akama T, Ishida H, Shida Y, Kimura U, Gomi K, Saito H, et al. Design and synthesis of potent antitumor 5,4'-diaminoflavone derivatives based on metabolic considerations. *J Med Chem.* 1997;40(12):1894-1900. http://dx.doi.org/10.1016/jm9700326 [pii] 10.1021/jm9700326. PubMed PMID: 9191967.
200. Akama T, Ishida H, Kimura U, Gomi K, Saito H. Structure-activity relationships of the 7-substituents of 5,4'-diamino-6,8,3'-trifluoroflavone, a potent antitumor agent. *J Med Chem.* 1998;41(12):2056-2067. http://dx.doi.org/10.1016/jm970728z [pii] 10.1021/jm970728z. PubMed PMID: 9622547.
201. Kuffel MJ, Schroeder JC, Pobst LJ, Naylor S, Reid JM, Kaufmann SH, et al. Activation of the antitumor agent aminoflavone (NSC 686288) is mediated by induction of tumor cell cytochrome P450 1A1/1A2. *Mol Pharmacol.* 2002;62(1):143-153. PubMed PMID: 12065765.
202. Pobst LJ, Ames MM. CYP1A1 activation of aminoflavone leads to DNA damage in human tumor cell lines. *Cancer Chemother Pharmacol.* 2006;57(5):569-576. http://dx.doi.org/10.1007/s00280-005-0075-7. PubMed PMID: 16096788.
203. Loaiza-Pérez AI, Kenney S, Boswell J, Hollingshead M, Hose C, Linehan WM, et al. Sensitivity of renal cell carcinoma to aminoflavone: role of CYP1A1. *J Urol.* 2004;171(4):1688-1697. http://dx.doi.org/10.1016/S0022-5347(05)62391-9 [pii] 10.1097/01.ju.0000108860.03389.1b. PubMed PMID: 15017268.
204. Meng LH, Shankavaram U, Chen C, Agama K, Fu HQ, Gonzalez FJ, et al. Activation of aminoflavone (NSC 686288) by a sulfotransferase is required for the antiproliferative effect of the drug and for induction of histone gamma-H2AX. *Cancer Res.* 2006;66(19):9656-9664. http://dx.doi.org/10.1016/66/19/9656 [pii] 10.1158/0008-5472.CAN-06-0796. PubMed PMID: 17018623.
205. Zheng Q, Sha X, Liu J, Heath E, Lorusso P, Li J. Association of human cytochrome P450 1A1 (CYP1A1) and sulfotransferase 1A1 (SULT1A1) polymorphisms with differential metabolism and cytotoxicity of aminoflavone. *Mol Cancer Ther.* 2010;9(10):2803-2813. http://dx.doi.org/10.1016/1535-7163.MCT-10-0597 [pii] 10.1158/1535-7163.MCT-10-0597. PubMed PMID: 20713530.
206. Loaiza-Pérez AI, Kenney S, Boswell J, Hollingshead M, Alley MC, Hose C, et al. Aryl hydrocarbon receptor activation of an antitumor aminoflavone: basis of selective toxicity for MCF-7 breast tumor cells. *Mol Cancer Ther.* 2004;3(6):715-725. http://dx.doi.org/10.1016/3/6/715 [pii]. PubMed PMID: 15210858.
207. Chen C, Meng L, Ma X, Krausz KW, Pommier Y, Idle JR, et al. Urinary metabolite profiling reveals CYP1A2-mediated metabolism of NSC686288 (aminoflavone). *J Pharmacol Exp Ther.* 2006;318(3):1330-1342. http://dx.doi.org/10.1016/jpet.106.105213 [pii] 10.1124/jpet.106.105213. PubMed PMID: 16775196; PubMed Central PMCID: PMCPMC1551906.
208. Patterson AD, Gonzalez FJ, Idle JR. Xenobiotic metabolism: a view through the metabolometer. *Chem Res Toxicol.* 2010;23(5):851-860. http://dx.doi.org/10.1021/tx100020p. PubMed PMID: 20232918; PubMed Central PMCID: PMCPMC2872059.

SUBJECT INDEX

Note: Page numbers with "f" denote figures; "t" tables.

N

AUTHOR INDEX

C

D

E

F

G

H

I

J

K

L

M

N

O

P

Q

R

S

T

U

V

Z

CUMULATIVE INDEX OF TITLES

D

E

F

G

H

I

K

L

M

N

O

P

R

S

T

CUMULATIVE INDEX OF AUTHORS